University of Tennessee, Knoxville
TRACE: Tennessee Research and Creative Exchange

Doctoral Dissertations | Graduate School

5-2020

Uncovering Process Challenges and Performance Differences for Complex Substrate Utilization in Microbial Electrolysis Cells

Scott Jason Satinover
University of Tennessee, ssatinov@vols.utk.edu

Follow this and additional works at: https://trace.tennessee.edu/utk_graddiss

Recommended Citation

Satinover, Scott Jason, "Uncovering Process Challenges and Performance Differences for Complex Substrate Utilization in Microbial Electrolysis Cells. " PhD diss., University of Tennessee, 2020.
https://trace.tennessee.edu/utk_graddiss/5808

This Dissertation is brought to you for free and open access by the Graduate School at TRACE: Tennessee Research and Creative Exchange. It has been accepted for inclusion in Doctoral Dissertations by an authorized administrator of TRACE: Tennessee Research and Creative Exchange. For more information, please contact trace@utk.edu.

To the Graduate Council:

I am submitting herewith a dissertation written by Scott Jason Satinover entitled "Uncovering Process Challenges and Performance Differences for Complex Substrate Utilization in Microbial Electrolysis Cells." I have examined the final electronic copy of this dissertation for form and content and recommend that it be accepted in partial fulfillment of the requirements for the degree of Doctor of Philosophy, with a major in Energy Science and Engineering.

Abhijeet P. Borole, Major Professor

We have read this dissertation and recommend its acceptance:

Terry C. Hazen, Brian Davison, Kimberly Carter

Accepted for the Council:

Dixie L. Thompson

Vice Provost and Dean of the Graduate School

(Original signatures are on file with official student records.)

Uncovering Process Challenges and Performance Differences for Complex Substrate Utilization in Microbial Electrolysis Cells

A Dissertation Presented for the

Doctor of Philosophy

Degree

The University of Tennessee, Knoxville

Scott Jason Satinover

May 2020

Copyright © 2020 by Scott Jason Satinover

All rights reserved.

DEDICATION

To my parents, Ira and Luisa, for convincing me to keep persevering despite the many challenges I encountered along the way. To my brother, Mike, I imagine you will love that this document will grant me the credentials required to make our upcoming book seem even more legitimate. Finally, to Uncle Joe. Through all the tribulations, I did it. I hope I've made you proud.

ACKNOWLEDGEMENTS

I'd like to acknowledge Dr. Abhijeet Borole for introducing me to the fascinating world of bioelectrochemical systems and showing me their potential to change the world. This field has inspired me to pursue scientific knowledge in disciplines that I firmly believed I would never study. Aided with his feedback, the knowledge and skills this dissertation required me to learn has been immeasurably valuable for my personal growth. I'd like to thank the Bredesen Center for accepting me into the program and providing me with this opportunity. I would also like to acknowledge Dr. Terry Hazen, who provided a lab space and an ability to continue the work discussed in this dissertation. I would also like to thank Dr. Brian Davison, who also provided essential support while the equipment was moved from Oak Ridge National Laboratory to the University of Tennessee. I'd also like to thank the biosciences division at Oak Ridge National Laboratory, and in particular, Dr. Anthony Palumbo, who aided my projects and supported my work while at the national lab. I'd also like to thank Dr. Kim Carter, for being available for ideas, discussions, and the assurance she provided along the way. I'd also like to thank Miguel Rodriguez Jr., Dr. Raynella Connatser, and Dr. Adrian Gonzalez, whose assistance with analytical chemistry was essential towards the pursuit of this dissertation. Finally, I'd like to acknowledge Dr. Hazen's graduate students and staff: Dr. Maria Campa, Emma Dixon, Isis Fukai, Zabrenna Griffiths, Dominique Joyner, Erin Kelly, Ye Li, Ann-Marie Harik, J. Izaak Miller, Andrew Putt, and Sa'ad Abd Ar Rafie. You all shared your lab without reservation when I most needed it, and I consider you all my scientific family. This dissertation would not be possible without the contributions of those listed here.

ABSTRACT

This dissertation investigated the use of nine complex waste streams, or substrates, in an engineered lab scale flow-through Microbial Electrolysis Cell (MEC). Of the nine wastes tested, seven had not been demonstrated in MECs previously. The wastes included five biomass pyrolysis aqueous fractions, oil and gas produced water, a corn stover fermentation product, and two aqueous fractions from hydrothermal liquefaction process. Produced water created the most process challenges, including calcium-related fouling, precipitate formation, deposit formation that prevented anode fluid flow, and poor COD conversion. Pretreatment effectively alleviated precipitation but did not prevent the formation of deposit. None of the other substrates required pretreatment or created the aforementioned problems. Four of the seven complex feedstocks when fed to MECs generated average current densities of approximately 5 A/m^2 at organic loading rates of 10 grams of COD per liter of anode per day (g/L-day), which resulted in high conversion of organic acids and sugars detected by High-Performance Liquid Chromatography. Two wastes were more poorly converted due to recalcitrance (below 4 A/m^2) despite showing high conversion percentages of these same compounds. Corn stover fermentation products produced the highest performance of the complex feedstocks, which exceeded 7 A/m^2 at 10 g/L-day. The highest performing substrate occurred using a simple substrate, acetate. Mass transfer limitations appeared for all substrates, indicated by rising whole cell voltages and pH polarization between the anode and cathode. A deposit was visible on the anode when MECs were fed produced water that prevented anode liquid flow. Adsorption of phenol was also observed. COD degradation will not directly correspond to current production if adsorption is occurring. Therefore, this mechanism may be more important than otherwise assumed. Finally, correlations between MEC performance and microbial community developed using different

substrates showed only a weak association. Electrochemical performance metrics proved to be much more closely related to organic loading rate and substrate composition. This indicates that chemical characteristics may be more effective at predicting MEC performance than biology. Communities in MECs are therefore shown to express a variety of phenotypes. Understanding these changes in community behavior will require various ‘omics techniques.

TABLE OF CONTENTS

LIST OF TABLES

LIST OF FIGURES

INTRODUCTION

Microbial Fuel Cells (MFCs), Microbial Electrolysis Cells (MECs), and the general class of Bioelectrochemical systems (BESs) have ushered in a new wave of waste recycling alternatives that has exploded in scientific interest. The ability to generate green products via this technology makes it of great interest to the sustainable economy needed for 21st century. BES function primarily by oxidizing organic molecules using a microbial catalyst at an electrode (anode), followed by a migration of charge. The charged species recombines with the electrons at another electrode, the cathode, where they are reduced. BESs use this oxidation-reduction (redox) reaction created in the whole cell to perform electrical work. Depending on the redox reaction desired, the reaction can be spontaneous (in the case of an MFC) or may require additional energy (in the case of a MEC). Like all electrochemical cells, this thermodynamic feasibility is theoretically represented by the Nernst equation:

$$E_{cell} = E^{\ominus}_{cell} - \frac{RT}{zF}\ln(Q_r)$$

E_{cell} is the whole cell potential, $E^{\ominus}_{cell}$ is the cell potential at standard conditions, F is Faraday's constant, z is the number of electrons transferred in the redox reaction, R is the universal gas constant, T is temperature, and Q_r is the reaction quotient. The reaction quotient, Q_r, represents the ratio of the multiplication of the products' activities over the multiplication of the reactants' activities.

Proper development of electrically active biofilms on the anode is central to an MEC's performance. The performance is governed by a set of parameters including system design, operational and biological parameters [1]. In all scenarios, a community of fermenters and anode respiring bacteria (also known as exoelectrogens) is needed to degrade efficiently the largest

quantity of organics possible and convert them into electrons and protons. Together, these microbes degrade organics and respire on the anode. There are several ways microbes can respire, including via mediators and direct contact with the electrode [2]. Mediators act as chemical conduits which reduce via microbes and oxidize at the electrode, while directly contacted microbes can transfer charge often through the use of conductive structures, such as nanowires. Anode respiration is most practically accomplished when the community forms a self-assembled biofilm directly on the anode surface, which helps prevent microbial washout that would otherwise occur when the microbes are planktonic. Using exoelectrogens in the biofilm introduces a caveat. While fermenters may not need external potential to convert organics, exoelectrogens are not so fortunate, and are only able to respire on an anode if the whole cell reaction is energetically favorable. Using acetate as an example electron donor, the half reaction and oxidation potential at standard conditions (Pressure = 1 bar, T = 25 °C, pH = 0) is:

$$CH_3COO^- + 2H_2O \rightarrow 2CO_2 + 7H^+ + 8e^- \quad (-0.09\,V\ vs\ SHE)$$

For an MEC, the reduction half reaction to produce hydrogen at standard conditions is:

$$2H^+ + 2e^- \rightarrow H_2\ (0.0\,V)$$

The whole reaction is therefore:

$$CH_3COO^- + H^+ + 2H_2O \rightarrow 2CO_2 + 4H_2 \quad (-0.09\,V\ vs\ SHE)$$

The change in Gibbs free energy at standard conditions can also be calculated from this, using 8 electrons transferred and Faraday constant (F):

$$\Delta G^o = -nF\Delta E^o = 17.1\frac{kcal}{mol}$$

Whether this electrochemical reaction will occur or not is dictated by chemical equilibrium. This value is not at biological conditions, so the Gibbs free energy must be adjusted. The products

concentrations are unknown, however the pH is approximately neutral, so that can be used. At standard biological conditions, the above reaction is also not spontaneous. Chemical equilibrium for the reaction at standard biological conditions (products and reactants = 1M, and pH = 7) is described by the following:

$$\Delta G = \Delta G^o + RTln\left(\frac{P_{CO_2}^2 P_{H_2}^4}{[CH_3COO^-][H^+]}\right) = 17.1 + 9.55 = 26.6\frac{kcal}{mol}$$

Where R is the universal gas constant, and T is the temperature. At other product and reactant concentrations, the product concentrations dominate equilibrium, and the whole reaction is not spontaneous. There is an important distinction; this is only true if the cathode is configured to produce hydrogen as described in the overall reaction above. Other electron acceptors, such as oxygen, can be used at the cathode side to make this reaction spontaneous and therefore promote exoelectrogenic growth. Using oxygen as an electron acceptor at the cathode for acetate oxidation at the anode promotes the following overall reaction at standard conditions:

$$CH_3COO^- + H^+ + 2O_2 \rightarrow 2CO_2 + 2H_2O \quad (+1.14\,V\ vs\ SHE)$$

This is spontaneous at standard conditions. However, oxygen is not available at the electrode in an MEC (and no hydrogen is produced in this reaction either). Therefore, an applied potential is required under normal operation conditions. MECs also have limitations like all electrochemical cells, and they usually require more energy than what is minimally required in theory even at non-standard conditions. Additional electrical potential, called an overpotential, is often needed as the additional energy. Overpotentials can also vary as the MEC operates. To assure that the microbes have a consistent electron sink, and that changes in MEC overpotential do not prevent the reaction from occurring, the anode can be poised to a fixed potential. This allows the whole cell potential to vary and therefore maintain the reaction. This strategy has been shown to

increase MEC productivity and inhibit methanogen activity [3]. Under these conditions, if the starting inoculum has been selectively enriched, exoelectrogenic populations can thrive in optimized devices, capitalizing on the syntrophies with fermenters present in the biofilm that degrade other compounds towards carbon sources exoelectrogens can consume. However, once the correct potential is reached, finding the "ideal" whole cell voltage is not always easy. The extent by which exoelectrogenic communities can respire in favorable redox conditions using complex feedstocks turns out to be broad. As shown by Lewis and Borole, the biofilm composition can adapt to a wide range of different applied anode potentials in order to effectively oxidize complex carbon sources, as long as the applied potential is sufficiently above theoretical limits [4]. Other strategies used to improve MEC performance include closing the distance between electrodes [5], feeding MECs by continuous addition instead of batch [6], actively harvesting H_2 at the cathode by applying a vacuum at the cathode [7], and by inducing liquid shear at the anode [8]. The design and operation of the MEC used in this study incorporates these concepts in its design to assure that high performance is reached.

Demonstrations on BESs have a long and rich history that started more than a century ago. H. Potter first demonstrated the potential for microbes to create electrical energy by several microorganisms, including *E. Coli* and *Saccharomyces cerevisiae*, fed glucose in a galvanostatic cell in 1911 [9]. Several reviews, either directly or indirectly, have contextualized the historical framework in more detail [10-12]. Most of these sources suggest that the popularity of BESs, either as a device that could solve engineering challenges or as a tool for scientific inquiry, resurged within the last two decades, though the attribution of the exact catalyst in interest is difficult to pinpoint. There are a few highly cited studies that may shed light on why these devices became popular. One of the earliest studies by Kim et al. (2002) determined that MFCs could be operated

without the use of externally provided mediators, coining the device as a, "mediator-less microbial fuel cell" [13]. This study ushered in the widespread use of electrically active biofilms for BES applications, paving the way for the other studies that rely on biofilm formation in BESs. Demonstrating direct respiration to electrodes for a variety of microbes has also been a key interest for BES development. Kim et al. (1999) demonstrated that *Shewanella putrefaciens* IR-1 could respire on an electrode without mediators [14]. Bond and Lovley followed this research and were the first to confirm that *G. sulfurreducens,* a species commonly found in BESs, could respire and produce electricity using an electrode that they were directly attached [15]. Reguera et al. then determined one of the mechanisms for direct electron transfer by identifying the electrically conductive pili known as nanowires created by *G. sulfurreducens* [16]. Since then, BESs like MECs have been used as a platform for studying further microbial respiration. Process controls designed to improve performance and reduce cost also continued to be published. One of the most cited studies was conducted by Liu et al., who were responsible for demonstrating that cathodes in MFCs could be operated using air rather than needing liquid based cathodes [17]. This study was also impactful because it was one of the first that successfully fed wastewater to an MFC. In that sense, that study can be credited as being one of the first to use a complex feedstock in a BES. Since then, many different designs and substrates have been used to operate BESs [18-20], and the focus on complex feedstocks remains a point of inquiry.

There is an expanding catalog of potential substrates which may all be useful in BESs. However, only a few studies have compared different complex feedstocks in a single BES configuration to understand the effect of feedstock composition [21-26]. These studies mostly compared diversity of microbial community and the BES performance, but rarely attributed substrate composition and compound transformation of individual compounds that might be

affiliated with performance. The findings of these studies are more thoroughly discussed in Chapter VI of the dissertation. Several of these studies used methods discussed in a dissertation by Lesnik [27]. Lesnik et al. compared the community structure of many different MFCs operating and used a machine learning algorithm to predict the performance and community structure as a result of substrate composition used, while Cai et al. performed the reverse process by predicting the substrate that was responsible for creating the community structure [24, 25]. These studies are critical for practical predictions in performance. Another approach, using exploratory statistics rather than machine learning, may further assist in visualizing the correlations between input and output variables. Further, MECs have not had this kind of investigation applied to them when fed complex feedstocks, and using uncharacterized complex feedstocks for comparisons will improve the value of further study

Simple substrate metabolism in non-BES fermenter cultures has also been compared by microbial characterization using 16S rRNA sequencing and chemical analysis by Miceli et al. [28]. The authors indicated that community structure was dependent on substrate type as well as substrate concentration, an idea that has been supported in MFCs by Shao et al [29]. Miceli et al.'s work may be appropriate for BES understanding, as the microcosms generated volatile fatty acids (VFAs), which are commonly used as substrates in BESs. These compounds appear critical to the performance of MECs, but their tracking across multiple complex substrates is rare.

Motives for Research

Producing hydrogen using a high performing MEC will have practical implications as well as more deeper reaching understanding. From a practical perspective, hydrogen functions as an essential compound for many applications in energy and chemical industries. As outlined by

the H2@Scale initiative by the Department of Energy, hydrogen is used for upgrading oils from biomass, creating ammonia/fertilizers, or aiding in synthetic fuel creation [30]. Currently, hydrogen is produced largely by natural gas steam reforming, a process that is comparatively mature and inexpensive, though it is not sustainable. MEC technology, while currently not commercialized, appears to be a promising sustainable alternative. Further, waste remediation is important for establishing a sustainable and environmentally friendly energy network, as leftover organics associated with energy products can be toxic if not properly disposed. The added benefit of MECs in the context of this work is therefore two-fold; they simultaneously increase the value of the wastes by making hydrogen out of them, while also treating the wastes. Using pyrolysis products as an example, MECs can be used to increase the value of the fuels created by biomass pyrolysis by producing the hydrogen necessary to create low oxygen fuels using those same pyrolysis oils, while also treating the resultant effluent wastewater [31-33]. Ideally, the wastes used in MECs do not have much value, which applies to the wastes used throughout this dissertation. This is largely contingent on MECs ability to adapt. If MECs require a specially tailored inoculum for every substrate type, they may struggle to find widespread commercial adoption.

Beyond the motive for producing hydrogen due to its value, there are several additional pieces of information that can be extracted from substrate degradation that may improve MEC development in the future. Substrates, especially complex ones, are not equivalent and can cause different problems to MEC performance. They may contain high levels of inhibitory organics (phenolics and furans for instance) [34], which would prevent degradation of other compounds. The substrates may simply be recalcitrant, where even if they can degrade, their degradation speed is slow.

Even if substrates are biodegradable, substrates can also be broken down and result in product inhibition. This is commonly observed as pH imbalances in the anode and cathode. Substrate transformation may also result in the creation of other undesirable products, such as ammonia, precipitates, inorganic acids, or films. MEC performance may be adversely affected as a result of these differences in substrate. Ultimately there are many variables that can affect performance based solely on the substrate type used. It can be easy to fixate on all of the issues associated with one substrate, and to build solutions around the problems that single substrate poses. However, this can divert efforts away from developing robust MECs that can handle a wide variety of complex feedstocks if done in exclusion. This does not mean that working with new substrates should be done with little rigor either. Identifying general criteria that influence MEC performance requires one to rigorously test a variety of substrates first. Only then can identifying common criteria affecting performance across complex substrates be conducted. Once this is accomplished future designs aimed at treating complex wastes can be made.

In addition to chemical composition of substrates, biological response as a result of substrate composition also plays a critical role in understanding the conversion of organics to hydrogen in MECs. The communities in MECs, by virtue of being alive, change due to stimulus. Demonstrating MEC substrate dexterity to a variety of complex feedstocks is essential, but also understanding how these communities change to feedstocks will illuminate some of the limitations found in MECs. For instance, if certain community members dominate, or do not, as a result of feedstock type, it may indicate which microbes are most important for improved MEC performance. That may allow for targeted anode community development and supplementation for improved performance. Alternatively, community roles may be more flexible. If they are very flexible, then perhaps community structure is less important than identifying the conversion

pathways they express. Finally, if this flexibility is present, then the focus can be driven more towards identifying the cause of this flexibility, which may expand on it in future communities in MECs. A diverse biofilm introduces a remarkably complex series of interactions that result in compound degradation and hydrogen production. Understanding the biofilm response in a high performing MEC to being fed complex substrates at a taxonomical level will provide an introductory understanding on just what kind of flexibility these communities demonstrate. Thus, the problem statement can be written as follows:

To further enable the advancement of MEC technology, understanding changes in performance resulting from exposure to different complex feedstocks is essential. It is also important to understand the most important underlying causes of performance variations in hydrogen production from complex feedstocks. General impactful criteria, including chemical and biological information, that affect MECs regardless of the complex substrates they are fed must be explored.

To limit variability in the experiments that follow, the reactor design remained mostly consistent throughout the dissertation, though reactor designs will certainly need improving in the future. A broad range of substrates is then tested under controlled organic loading conditions, process conditions, and starting microbial consortia to understand the most important capability and limitations high performing MECs have when fed complex substrates. The unique challenges to each substrate are identified in each chapter, and then general observations across substrates are determined.

Hypotheses of Dissertation

The substrate that initially inspired this work was derived from oil and gas produced water, but the motive to pursue this waste's treatment wasn't necessarily due to MEC development and characterization. Oil and gas wells produced a significant fraction of

wastewater along with the hydrocarbons they produce. Proper oil and gas wastewater disposal is still a problem, and MECs could be used to mitigate the issues with its handling. Even reusing produced water at surface can result in complications, as H_2S can evolve in the water, and salts can be plentiful. This problem with H_2S compromised a prior hydraulic fracturing job I had worked on. There, H_2S was not observed at the surface of the pond our crew had been using for their hydraulic fracturing water source. However, hydraulic fracturing crews do not pull water from the top of the pond, they pull it from the bottom, which can become anaerobic quickly. The most traditional route for removing H_2S involves the use of chemicals, which also kill microbes. Because they do not remove the organics causing the growth of H_2S producing microbes, these are only temporary solutions, often requiring consistent monitoring of water quality to avoid contaminating equipment with H_2S that has been produced despite treatment. I have since been curious about deploying preventative methods. By removing the organics present in produced water, one might be able to effectively prevent the evolution of H_2S by sulfate reducing bacteria, which was suspected to H_2S evolution over time. By removing the organics that promote H2S reaction, an MEC would therefore be a more permanent solution that would also recover energy as hydrogen. Previous work using BESs fed with produced water has been conducted [35-40], but they often have poor Coulombic efficiency and performance (current density, power density, hydrogen productivity). Using some of the concepts regarding high performance discussed earlier, the hypothesis was that microbial electrolysis cells could have increased performance if those concepts were employed. It is formally stated as:

If anode microbial consortia are adapted to high salinity, and the microbial electrolysis cell is configured for high-performance, then the microbial electrolysis cells will be able to accept high salinity waste streams such as produced water from oil and gas wells and generate current and hydrogen at similar rates to when they are fed model substrates.

The findings from Chapter I indicated that complex substrates could create many different problems that were not observed with the simple substrates. Comparison between acetate and produced water could not translate to observations and correlations that may appear for other substrates. The causes for the differences between performance and substrate selection might be more obvious if the substrates compared were similar. Chapter II expanded on this idea by taking pyrolysis aqueous products from two different feedstocks, guayule and willow, and investigated their conversion in MECs using the same motives that were outlined for bio-oil aqueous phase (BOAP) described by Lewis et al. [31]. The hypothesis for Chapter II is formally stated as:

If a microbial electrolysis cell has an established biofilm that had successfully shown to degrade a specific complex feedstock, e.g. BOAP, then it should be able utilize other complex substrates with similar characteristics, e.g. BOAPs derived from other feedstocks, with similar productivities.

Because the organic loading rates were identical across substrates, comparisons could be made. However, this experiment was limited to only pyrolysis aqueous phases, a substrate type that had been tested in MECs previously. One substrate type that had not been tested previously was derived from algae sources using a process called hydrothermal liquefaction (HTL). Similar to pyrolysis, HTL can be used on biomass to create energy products, and it also creates an aqueous phase waste with no current value. HTL effluents had been used in MECs previously, but the feedstock for HTL had never been demonstrated in MECs prior. Chapter III uses an algal based aqueous phase from two different algae strains but conducted a similar comparison study to Chapter II. HTL products from algae were suspected to contain high concentrations of ammoniacal nitrogen. Because of the high amounts of ammoniacal nitrogen in the effluents,

ammonium might be driven to the cathode like other positive ions when MECs use a cation exchange membrane. The first hypothesis for Chapter III is:

If algal HTL wastewater containing N-compounds is used in an MEC, then, degradation of the N-compounds may result in ammonia production, which can assist in charge transfer.

Because of the nitrogen and organic content of spent MEC effluent, it was hypothesized that the effluent could also be used to regrow more algae as a source of nitrogen and organics. The second hypothesis of Chapter III was therefore:

If MECs can be used to convert some of the residual organics to hydrogen and if spent substrate in MECs contains residual organics and nutrients derived from biomass, then the remaining content can be used to grow additional biomass such as algae, demonstrating the potential for a circular bio-economy that can produce energy products with minimal waste output.

In the previous chapters, current production and hydrogen productivity seemed to be dictated more prominently by substrate recalcitrance than by proton transfer. If proton transfer limitations did not impede performance, then selecting the right complex feedstock for this model of MEC should improve current densities and hydrogen productivity. By feeding a less recalcitrant complex substrate to a biofilm that had been selectively enriched on these more troublesome substrates, better performance might be more obtainable. A corn stover fermentation product described previously [6] proved to be a promising contender for this substrate, so it was used. The hypothesis for Chapter IV was therefore:

If an established electro-active biofilm is evolved to tolerate inhibitory compounds, removing the compounds or use of waste streams without those compounds should result in much higher productivities.

To expand the pool of demonstrated substrates, additional substrates were also tested using the same hypothesis described in Chapter II, including a neutralized bio-oil aqueous phase

and a red oak bio-oil aqueous phase. However, without the same level of rigor shown in Chapter II, and because the substrates were processed differently, only the neutralize bio-oil aqueous phase -fed MEC results were published as part of a publication [41]. The findings assisted in the later analysis conducted.

The prior work created the bulk of the data for MECs fed nine substrates, seven of which had never been demonstrated in MECs before. Next, the community and their roles in MECs fed with these substrates needed to be better understood. Evidence suggested that the robust community used throughout the experiments had rapidly adapted throughout the years of testing on these substrates quickly to stabilized performance. However, there was little data to show just how robust a given starting community was, or how it would change. To more thoroughly test this idea, the community response to multiple substrates using rapid adaptation one week was tested. This was tested by feeding multiple substrates to an MEC, and transitioning from one substrate to the other, rather than inoculating new MECs each time a carbon source was tested. From there, the performance was tracked after an adaptation time of one week. It was suspected that this would correspond with a loss or increase in microbial diversity depending on the performance observed. The first hypothesis of Chapter VI is:

If Microbial Electrolysis Cells are fed complex feedstocks, then their community structure diversity will inversely relate to the accumulation and degradation of acetate for any substrate.

We also noticed that many of the substrates contained acetate. Acetate, being a model substrate for MECs, was suspected to be a key component in microbial electrolysis cell performance, either as an intermediate product or as a product that was directly delivered to MECs. It was unsure how acetate accumulation and degradation occurred in each substrate was, however it was

possible that it could be used to predict performance on MECs. Thus, the second hypothesis of Chapter VI was:

If Microbial Electrolysis Cells are fed complex feedstocks that contain inhibitory and recalcitrant compounds as part of their substrates, then the creation and degradation rates of acetate within MECs should correlate to the performance observed with that complex substrate.

Once the correlations between substrate performance and biology were made, it was possible to expand the analysis to the substrates tested in this dissertation. Unfortunately, without the biology data for the other substrates, those correlations could not be made. However, with chemical data of the substrates and electrochemical performance data, those correlations could be explored across multiple substrates. The comparison tools used included Principal Component Analysis, specifically the loading plot that was produced from the analysis. This tool formed the basis of the exploratory statistics found in Chapter VII. Two analysis using data from continuous and batch experiments were conducted here. From this analysis, the relationship between substrate composition and performance was made, indicating relationships between composition and performance that could be expanded to any type of substrate used in MECs.

References

1. Borole, A.; Reguera, G.; Ringeisen, B.; Wang, Z.-W.; Feng, Y.; Hong Kim, B., Electroactive biofilms: Current status and future research needs. *Energy & Environmental Science* **2011,** *4*, (12), 4813-4834.
2. Logan, B. E., Exoelectrogenic bacteria that power microbial fuel cells. *Nat Rev Micro* **2009,** *7*, (5), 375-381.
3. Nam, J.-Y.; Tokash, J. C.; Logan, B. E., Comparison of microbial electrolysis cells operated with added voltage or by setting the anode potential. *International Journal of Hydrogen Energy* **2011,** *36*, (17), 10550-10556.
4. Lewis, A. J.; Borole, A. P., Adapting microbial communities to low anode potentials improves performance of MECs at negative potentials. *Electrochimica Acta* **2017,** *254*, 79-88.
5. Cheng, S.; Liu, H.; Logan, B. E., Increased Power Generation in a Continuous Flow MFC with Advective Flow through the Porous Anode and Reduced Electrode Spacing. *Environmental Science & Technology* **2006,** *40*, (7), 2426-2432.
6. Pannell, T. C.; Goud, R. K.; Schell, D. J.; Borole, A. P., Effect of fed-batch vs. continuous mode of operation on microbial fuel cell performance treating biorefinery wastewater. *Biochemical Engineering Journal* **2016,** *116*, 85-94.
7. Lu, L.; Hou, D.; Wang, X.; Jassby, D.; Ren, Z. J., Active H2 Harvesting Prevents Methanogenesis in Microbial Electrolysis Cells. *Environmental Science & Technology Letters* **2016,** *3*, (8), 286-290.
8. Pham, H. T.; Boon, N.; Aelterman, P.; Clauwaert, P.; De Schamphelaire, L.; Van Oostveldt, P.; Verbeken, K.; Rabaey, K.; Verstraete, W., High shear enrichment improves the performance of the anodophilic microbial consortium in a microbial fuel cell. *Microb. Biotechnol.* **2008,** *1*, (6), 487-496.
9. Potter, M. C.; Waller Augustus, D., Electrical effects accompanying the decomposition of organic compounds. *Proceedings of the Royal Society of London. Series B, Containing Papers of a Biological Character* **1911,** *84*, (571), 260-276.
10. Seviour, T. W.; Hinks, J., Bucking the current trend in bioelectrochemical systems: a case for bioelectroanalytics. *Critical Reviews in Biotechnology* **2018,** *38*, (4), 634-646.
11. Pant, D.; Singh, A.; Van Bogaert, G.; Irving Olsen, S.; Singh Nigam, P.; Diels, L.; Vanbroekhoven, K., Bioelectrochemical systems (BES) for sustainable energy production and product recovery from organic wastes and industrial wastewaters. *RSC Adv.* **2012,** *2*, (4), 1248-1263.
12. Santoro, C.; Arbizzani, C.; Erable, B.; Ieropoulos, I., Microbial fuel cells: From fundamentals to applications. A review. *Journal of Power Sources* **2017**.
13. Kim, H. J.; Park, H. S.; Hyun, M. S.; Chang, I. S.; Kim, M.; Kim, B. H., A mediator-less microbial fuel cell using a metal reducing bacterium, Shewanella putrefaciens. *Enzyme and Microbial Technology* **2002,** *30*, (2), 145-152.
14. Kim, B.-H.; Kim, H.-J.; Hyun, M.-S.; Park, D.-H., Direct electrode reaction of Fe (III)-reducing bacterium, Shewanella putrefaciens. *Journal of Microbiology and Biotechnology* **1999,** *9*, 127-131.
15. Bond, D. R.; Lovley, D. R., Electricity Production by Geobacter sulfurreducens Attached to Electrodes. *Appl Environ Microbiol* **2003,** *69*, (3), 1548-1555.

16. Reguera, G.; McCarthy, K. D.; Mehta, T.; Nicoll, J. S.; Tuominen, M. T.; Lovley, D. R., Extracellular electron transfer via microbial nanowires. *Nature* **2005,** *435*, (7045), 1098-1101.
17. Liu, H.; Ramnarayanan, R.; Logan, B. E., Production of Electricity during Wastewater Treatment Using a Single Chamber Microbial Fuel Cell. *Environmental Science & Technology* **2004,** *38*, (7), 2281-2285.
18. Pandey, P.; Shinde, V. N.; Deopurkar, R. L.; Kale, S. P.; Patil, S. A.; Pant, D., Recent advances in the use of different substrates in microbial fuel cells toward wastewater treatment and simultaneous energy recovery. *Applied Energy* **2016,** *168*, 706-723.
19. Bajracharya, S.; Sharma, M.; Mohanakrishna, G.; Dominguez Benneton, X.; Strik, D. P. B. T. B.; Sarma, P. M.; Pant, D., An overview on emerging bioelectrochemical systems (BESs): Technology for sustainable electricity, waste remediation, resource recovery, chemical production and beyond. *Renewable Energy* **2016,** *98*, 153-170.
20. Kadier, A.; Simayi, Y.; Kalil, M. S.; Abdeshahian, P.; Hamid, A. A., A review of the substrates used in microbial electrolysis cells (MECs) for producing sustainable and clean hydrogen gas. *Renewable Energy* **2014,** *71*, 466-472.
21. Chae, K.-J.; Choi, M.-J.; Lee, J.-W.; Kim, K.-Y.; Kim, I. S., Effect of different substrates on the performance, bacterial diversity, and bacterial viability in microbial fuel cells. *Bioresource Technology* **2009,** *100*, (14), 3518-3525.
22. Sun, G.; Thygesen, A.; Meyer, A. S., Acetate is a superior substrate for microbial fuel cell initiation preceding bioethanol effluent utilization. *Applied Microbiology and Biotechnology* **2015,** *99*, (11), 4905-4915.
23. Kiely, P. D.; Cusick, R.; Call, D. F.; Selembo, P. A.; Regan, J. M.; Logan, B. E., Anode microbial communities produced by changing from microbial fuel cell to microbial electrolysis cell operation using two different wastewaters. *Bioresource Technology* **2011,** *102*, (1), 388-394.
24. Lesnik, K. L.; Liu, H., Predicting Microbial Fuel Cell Biofilm Communities and Bioreactor Performance using Artificial Neural Networks. *Environmental Science & Technology* **2017,** *51*, (18), 10881-10892.
25. Cai, W.; Lesnik, K. L.; Wade, M. J.; Heidrich, E. S.; Wang, Y.; Liu, H., Incorporating microbial community data with machine learning techniques to predict feed substrates in microbial fuel cells. *Biosensors and Bioelectronics* **2019,** *133*, 64-71.
26. Marone, A.; Ayala-Campos, O. R.; Trably, E.; Carmona-Martínez, A. A.; Moscoviz, R.; Latrille, E.; Steyer, J.-P.; Alcaraz-Gonzalez, V.; Bernet, N., Coupling dark fermentation and microbial electrolysis to enhance bio-hydrogen production from agro-industrial wastewaters and by-products in a bio-refinery framework. *International Journal of Hydrogen Energy* **2017,** *42*, (3), 1609-1621.
27. Lesnik, K. Consider the Community : Developing Predictive Linkages between Community Structure and Performance in Microbial Fuel Cells. Oregon State University, Corvallis, OR, 2017.
28. Miceli, J. F., III; Torres, C. I.; Krajmalnik-Brown, R., Shifting the balance of fermentation products between hydrogen and volatile fatty acids: microbial community structure and function. *FEMS Microbiol. Ecol.* **2016,** *92*, (12).
29. Shao, Q.; Li, J.; Yang, S.; Sun, H., Effects of different substrates on microbial electrolysis cell (MEC) anodic membrane: biodiversity and hydrogen production performance. *Water Science and Technology* **2019,** *79*, (6), 1123-1133.

30. Pivovar, B., H2@Scale Overview. In *2018 DOE Hydrogen and Fuel Cells Program Review*, National Renewable Energy Laboratory: 2018.
31. Lewis, A. J.; Ren, S.; Ye, X.; Kim, P.; Labbe, N.; Borole, A. P., Hydrogen production from switchgrass via an integrated pyrolysis–microbial electrolysis process. *Bioresource Technology* **2015,** *195*, 231-241.
32. Satinover, S. J.; Elkasabi, Y.; Nuñez, A.; Rodriguez, M.; Borole, A. P., Microbial electrolysis using aqueous fractions derived from Tail-Gas Recycle Pyrolysis of willow and guayule. *Bioresource Technology* **2019,** *274*, 302-312.
33. Brooks, V.; Lewis, A. J.; Dulin, P.; Beegle, J. R.; Rodriguez, M.; Borole, A. P., Hydrogen production from pine-derived catalytic pyrolysis aqueous phase via microbial electrolysis. *Biomass and Bioenergy* **2018,** *119*, 1-9.
34. Zeng, X.; Borole, A. P.; Pavlostathis, S. G., Inhibitory Effect of Furanic and Phenolic Compounds on Exoelectrogenesis in a Microbial Electrolysis Cell Bioanode. *Environmental Science & Technology* **2016,** *50*, (20), 11357-11365.
35. Monzon, O.; Yang, Y.; Kim, J.; Heldenbrand, A.; Li, Q.; Alvarez, P. J. J., Microbial fuel cell fed by Barnett Shale produced water: Power production by hypersaline autochthonous bacteria and coupling to a desalination unit. *Biochemical Engineering Journal* **2017,** *117, Part A*, 87-91.
36. Roustazadeh Sheikhyousefi, P.; Nasr Esfahany, M.; Colombo, A.; Franzetti, A.; Trasatti, S. P.; Cristiani, P., Investigation of different configurations of microbial fuel cells for the treatment of oilfield produced water. *Applied Energy* **2017,** *192*, 457-465.
37. Stoll, Z. A.; Forrestal, C.; Ren, Z. J.; Xu, P., Shale gas produced water treatment using innovative microbial capacitive desalination cell. *J. Hazard. Mater.* **2015,** *283*, 847-855.
38. Ghasemi Naraghi, Z.; Yaghmaei, S.; Mardanpour, M. M.; Hasany, M., Produced Water Treatment with Simultaneous Bioenergy Production Using Novel Bioelectrochemical Systems. *Electrochimica Acta* **2015,** *180*, 535-544.
39. Zhang, X.; Zhang, D.; Huang, Y.; Zhang, K.; Lu, P., Simultaneous removal of organic matter and iron from hydraulic fracturing flowback water through sulfur cycling in a microbial fuel cell. *Water Research* **2018,** *147*, 461-471.
40. Shrestha, N.; Chilkoor, G.; Wilder, J.; Ren, Z. J.; Gadhamshetty, V., Comparative performances of microbial capacitive deionization cell and microbial fuel cell fed with produced water from the Bakken shale. *Bioelectrochemistry* **2018,** *121*, 56-64.
41. Park, L. K.-E.; Satinover, S. J.; Yiacoumi, S.; Mayes, R. T.; Borole, A. P.; Tsouris, C., Electrosorption of organic acids from aqueous bio-oil and conversion into hydrogen via microbial electrolysis cells. *Renewable Energy* **2018,** *125*, 21-31.

CHAPTER I

COMPARING PERFORMANCE AND MICROBIAL COMPOSITION OF ACETATE AND OIL WELL PRODUCED WATER-FED MICROBIAL ELECTROLYSIS CELLS AT VARYING SALINITIES

This chapter has been derived from a manuscript in preparation for publication. Satinover, S. conducted the microbial electrolysis work, DNA extractions, 16S rRNA sequencing, as well as performed the analysis and wrote the chapter, making revisions suggested by coauthors. Campa, M.F. aided with DNA extraction, ion chromatography, and sequencing. Hazen, T. provided guidance and equipment for 16S rRNA sequencing. Borole A. provided guidance and feedback on experiments, planning, data analysis, assisted in manuscript preparation and editing the drafts.

Abstract

This study compared MECs fed with a pretreated produced water to MECs fed with acetate at three different anode liquid conductivities, corresponding to three organic loading rates. The current density, hydrogen productivity, and Coulombic efficiency were the largest reported for any produced water fed MEC so far. Coulombic efficiencies for produced water-fed MECs sharply declined as organic loading decreased, while acetate-fed MECs consistently outperformed produced water-fed MECs. 16S rRNA sequencing of anode communities showed higher diversity in MECs fed with produced water vs. MECs fed with acetate. The anode communities differed significantly from the raw produced water. The MECs fed with produced water developed significantly different communities compared with the MEC fed with acetate. The genus *Geobacter* dominated both MECs. To enable treatment of produced water in MECs, additional designs will need to be developed that can manage fouling, and clogging while efficiently degrading organics in produced water.

Introduction

Wastewaters created by oil and gas wells during hydrocarbon production are the most prevalent waste sources of oil and gas activity. Perhaps the most troubling issue associated with underground injection comes from its role in induced seismic activity. The United States Geological Survey (USGS) has linked the recent rise in seismic activity to underground injection [1, 2], with maximum earthquakes being observed as large as a 5.6 on the moment scale [3]. This practice is not to be confused with hydraulic fracturing, in that the phrase "underground injection" or "saltwater disposal" typically only refers to wastewater injection. Induced seismic activity, while alarming, does not always occur. Several statements made on behalf of the USGS contend that most wells are operated without being linked to earthquakes at all [1, 2], and most earthquakes are not on the same order of intensity as the earthquakes observed in Oklahoma. Still, the potential for induced earthquakes, even if uncommon, warrants concern. This issue could easily be alleviated if a cost-effective treatment method was available to repurpose the water recovered. Any sort of water recycle would not only curb industry water demand but would also alleviate induced seismic activity.

The amount of water recovered is large and can be difficult to manage. Satinover and Borole have outlined some of the problems associated with produced water recovery and treatment in a forthcoming book chapter [4], which has been described and adapted below to provide context. The Ground Water Protection Counsel (GWPC) estimated that the U.S. produced roughly 21.2 billion barrels of produced water in 2012 from oil and gas wells [5]. Handling this amount of water has been a point of contention amongst environmentalists and well operators for some time now. Today, the dominant disposal method involves injecting this wastewater back into the subsurface. Regulated under Class II well injection protocols by the

EPA [6], the GWPC report claims that, “about 93% of produced water from onshore wells and about 91% of the produced water from all wells was injected underground” [5]. These volumes and costs are not trivial. Chesapeake energy, along with the EPA, has quoted disposal costs at 0.25 cents per barrel [7]. Using this value and the produced water volume previously described, the total cost to industry for disposal would equal approximately $4.82 Billion, and this cost is a significant undershoot. It is likely far more expensive due to additional transportation, storage, and pretreatment costs.

Oil and gas wastewater can have significant variability in its composition, but some of the content is common. High salinity, water hardness, suspended solids, emulsified oils and greases, and some dissolved organic content are traditionally found, with salinities being higher than that of sea water at later production phases [8]. Salinity and organic content has been found to change with time as the well produces [9]. The chemical composition used at the surface of hydraulic fractured wells can vary considerably [10], adding additional complexity to treatability of oil and gas wastewaters as early time waters are recovered. Systems that can treat these waters must have adaptability and a capacity to degrade multiple compounds in an energy efficient manner.

It may be tempting to argue for desalinating produced water, however desalination technology currently comes with its own drawbacks. First, desalination requires pretreatment before it can be conducted. As an example, pretreatment for Reverse Osmosis (RO) is required in order to prevent membrane fouling [11, 12]. Other desalination techniques may not suffer from fouling but may only be effective within certain salinity ranges. Capacitive Deionization (CDI), for instance, is primarily useful for brackish waters, where RO is otherwise significantly more efficient at salt concentrations above 2 g/L [13]. Additionally, efficiency losses occur with

desalination as salinities increase. Theil et al. discussed this concept, and found that for a system with 50% water recovery using seawater as the input fluid (35g/kg NaCl), treating fluid with output brine that had NaCl at saturation would result in operating pressures equal 379.2 bar, or nearly 5500 psi, compared to 60.1 bar used for a doubled salinity brine output [14]. The authors conclude that because produced water often already has high salinity, operating pressures will likely be very high for produced water using RO. By contrast, thermal evaporation systems, such as vapor compression expansion, are typically only used for high saline fluids due to their high energy consumption, but can be efficient for high salinity fluids [12, 14]. Newer technologies have been proposed for desalination, including gas hydrate utilization. This technology has been demonstrated for saline sources including produced water and sea water [15, 16], but has not realized commercial deployment yet. Current technology requires significant energy that may be cost prohibitive and expanding new desalination technology to function effectively on highly saline sources like produced water remains a point of interest.

Based on the background provided, produced water desalination will only be attractive if energy efficient technologies are created. New technologies may accomplish this by extracting energy from the feed source. One possible method of extracting energy from wastewater is with bioelectrochemical systems (BESs), which were first demonstrated on wastewaters in the 2000s [17, 18] . Bioelectrochemical systems are devices that convert aqueous organics into valuable end products, such as current, hydrogen, or other chemicals. These devices have found particular appeal because they have been used to treat a variety of wastewaters [19, 20]. A BES contains an anode where chemical species are oxidized, and a cathode where other species are reduced. In BESs, a microcosm of bacteria and/or archaea colonize a conductive material generating electrons from organic molecules at the anode. The cathode can either be abiotic or biotic. Many

different configurations exist [21], the most common of which is a microbial fuel cell (MFC), which creates current as the end product. A microbial electrolysis cell (MEC), creates hydrogen by reducing protons at the cathode. Cathode colonizing microbes in BESs may be used to make other products like methane [22]. Another unique BES is the microbial desalination cell (MDC), which uses the energy created to drive a desalination unit, often contained within the same device. For any of the BESs listed, produced water is also potentially valuable because it has a common contaminant that may be useful in BESs. Organic acids can be present in produced waters, which are known to cause corrosion in oil and gas handling systems [8, 23] and are therefore a problem for normal produced water management. These organic acids typically result from the oxidation of hydrocarbons under anaerobic conditions [24, 25], or from the use of pH buffers used in injection. Acetate is commonly used as a model substrate for BESs and serves as an easily degradable substrate along with other organic acids in BESs.

Produced water use in BESs and saline BESs have been investigated previously, although saline BESs that are fed simple carbon sources are significantly more common [26-36]. Additional studies have been comprehensively reviewed by Grattieri et al.[37]. BESs fed with produced water come with their own drawbacks and design problems. Salinity has been shown to be inhibitor in BESs. One study showed that MFC performance declined after salinity increased past 20 g/L [33], which is the case for most produced waters. However, microbial communities capable of tolerating much higher concentrations p to 60 g/L have also been reported [38]. Additionally, produced water energy production in BESs is significantly lower than acetate at the same carbon loading. Roustazadeh et al. found that produced water operated cells had an order of magnitude less peak voltage than acetate-fed MFCs under the same organic loading conditions, and lower Coulombic efficiency despite similar COD removal [27]. Monzon et al. was able to achieve higher

operating voltages and power densities, but did not compare other substrate performance directly within the same reactor [26].

The effect of salinity on BES performance using a complex feedstock compared to BESs using acetate at equivalent organic and saline conditions is unknown. Currently, there are no studies that compare the performance of BESs at varying salinities using produced water as a substrate. Additionally, the salinity may change the microbial composition after an acclimation period. As suggested by Satinover and Borole [4], performance may be improved using more sophisticated enrichment and BES designs. MECs may also find themselves advantageous for handing produced water by providing hydrogen necessary for petroleum processing. Thus, this study attempts to investigate the performance and microbial community differences that occur when MECs are exposed to varying salinities and substrates, using produced water and acetate as a complex and simple substrate, respectively. Community differences can be determined by use of 16S rRNA sequencing, and by adjusting the carbon source type and concentration, the community should be more complex when being fed produced water than with acetate. Further, because salinity can have an adverse effect on MEC performance up to a point, it is possible that the community will change as a function of salinity and organic loading as well. Finally, the community should more rapidly and effectively consume acetate than produced water, and this study will determine if salinity affects the differences between both substrate performances.

Materials and Methods

Produced Water Source, Characterization, and Pretreatment

Produced water at any stage of production can have salinity above 100,000 ppm [39], however according to findings by Cluff et al. [9], early time produced water should have the largest

organic content and lowest salinity of the water produced by a given well. Lower salinity would limit inhibition due to salt, and higher organic concentrations would mean MECs would have more available carbon source. These factors could assist in generating higher performance. To maximize the potentially high organic content and lower salt content early time produced water may have, early time produced water (often referred to as "flowback water") was acquired from a hydraulically fractured well in West Texas. The produced water samples were filtered by 0.20 µm filter and characterized by pH measurement, chemical oxygen demand (COD), conductivity, and ion chromatography (IC). For IC, samples were filtered again by 0.20 µm and stored at 4°C until analysis. Anion and cation samples were then diluted 500-fold based on chlorides present. Samples for anion (fluoride, chloride, bromide, nitrate, sulfate) and organic acid (propionate, formate, butyrate) detection used A Dionex Seven Anion Standard II (ThermoFisher Scientific, Waltham, MA) and in-house organic acid standards (0.5-200 µM). Samples were measured on a Dionex ICS 5000+ series with Dual Pump, Dual Column system (ThermoFisher Scientific, Waltham, MA) using an AS11HC column at 35 °C with a KOH effluent gradient of 0-60 mM at 1.3 mL/min. Samples for cation (lithium, sodium, ammonium, potassium, magnesium, calcium, and strontium) detection were acidified using 0.1 M HCl, and stored at 4 °C until analysis. A Dionex Six Cation-II Standard (ThermoFisher Scientific, Waltham, MA), was used to establish calibration curves (5µg/L – 500mg/L). Samples were measured on a Dionex ICS 5000+ series with Dual Pump, Dual Column system (ThermoFisher Scientific, Waltham, MA) using a CS12-A column at 35 °C with 20 mM methanesulfonic acid effluent at 1 mL/min.

MEC Design, Enrichment, and Operation

MECs were created as previously described [40] with slight modification. The cation exchange membrane was replaced with an anion exchange membrane to prevent Ca^{2+} and Mg^{2+}

precipitation and membrane fouling, which ultimately led to rupture without pretreatment (See the Appendix of this chapter for more information). Additionally, phosphate buffer in the cathode was replaced with 12 mL of sterile nitrogen sparged deionized water was used as a conduit for ion migration and was injected into the cathode from a bottom stopcock. Otherwise, the MECs were constructed identically to those referenced earlier [40]. Briefly, anode and cathode chambers were made of PVC pipe with 1.5 in labeled inner diameter, measured at 1.57 in, for a total anode and cathode volume of 16 mL each. Carbon felt was used as the anode electrode and filled the entire 16ml volume, creating a total anode volume of 83% of the 16 mL. Projected surface area was estimated at 12.56 cm^2. A carbon rod was inserted into the anode and used to collect current. An Ag/AgCl electrode was used as the reference electrode and was also inserted in the side of the anode. 0.5 mg/cm^2 platinum deposited carbon was used as the catalyst, which was pressed against stainless steel mesh, together acting as the cathode. 12 mL of anaerobic deionized water was used as a conduit for ion migration and was injected into the cathode from a bottom stopcock. Cells were operated electrochemically by a Bio-Logic potentiostat (Bio-Logic USA, Knoxville, TN) by poising the anode at -0.2 V with the reference electrode in a three electrode set up. Whole MEC voltage was recorded with a DataQ DI-1100 (DataQ Instruments, Akron, Ohio). Two duplicate MECs were used for the experiments conducted.

Anode nutrient medium was created as previously described [40] with slight modification. When MECs were fed produced water, the produced water was pretreated using 150 mM of Na_2HPO_4 in order to precipitate Ca^{2+} before use in MECs. BES fouling using oil and gas wastewater has been reported in the past [36], and Na_2HPO_4 addition helped avoid this problem. The water this process created is referred to as pretreated produced water (PPW). COD, pH, and conductivity were then measured before and after Na_2HPO_4 pretreatment. MECs were then fed

exclusively with PPW that had been diluted with anode nutrient until conductivities of 40, 30, and 20 mS/cm were reached. Total anode liquid volume was 180 mL for all experiments. For acetate experiments, NaCl was added to anode nutrient media until the same conductivities used in produced water experiments were reached, which required 20.6, 14.1, and 7.5 g/L of NaCl respectively. For both acetate and produced water, experiments used 0.58, 0.40, and 0.21 g-COD/L for 40, 30, and 20 mS/cm salinities respectively, reflected by the organic content of the PPW.

MECs were inoculated using three inoculum sources. The first was from reactors developed previously [41]. Then, 5 mL samples from an anaerobic digester wastewater treatment plant in Knoxville, Tennessee, and 5 mL samples of raw unfiltered produced water were injected into the bottom of the MEC. MECs were fed initially a 1:1 mix of glucose and acetate and were progressively weaned off glucose and acetate to produced water over the span of two months until produced water became the sole carbon source. This procedure was followed because enrichment of communities using simple substrates at the beginning has been shown to improve performance in MFCs according to Sun et al. [42]. Unfortunately, stocks of raw produced water were limited. To conserve the amount of produced water used, acetate, glucose, and hydrated guar gum were fed in batches along with PPW until experiments. MECs were operated under these conditions for 1 year.

MEC conductivity was gradually increased by providing additional batches of PPW to anode nutrient media without changing the anode liquid media until a conductivity of 40 mS/cm was reached. Anode liquid media was recirculated through the anode at a flow rate of 3.5 mL/min, where recycled anode liquid media was stored using a sterile glass bottle. Cells were run for 72, 48, and 24 h, resulting in organic loadings of 0.58, 0.40, and 0.21 g-COD/L

respectively, which were the time scales determined when current in MECs reached a minimum after batch addition of acetate (less than 0.7 mA). Anode liquid media samples were acquired at the start of the experiment and every 24 h after.

Gases in the anode and cathode were analyzed using Gas Chromatography (GC). A Focus GC (ThermoFisher Scientific, Waltham, MA) was used to identify hydrogen, oxygen, nitrogen, and methane by sampling from a port in the anode and cathode. This GC was outfitted with a HP Plot Molecular Sieve 5A (Agilent technologies Santa Clara, CA) as the column, and used ultra-high purity helium as the carrier gas. The oven temperature was set to 30 °C, held here at 1 minute, and then ramped to 72 ºC in 7 minutes, where it was then held for 30 seconds. Inlet, block, and transfer temperatures were all 50 ºC throughout the entire sampling period. 100 µl of anode and cathode gas samples were taken every 24 h for GC measurements using a gas tight glass syringe.

MEC Electrochemical Analysis

MECs were analyzed using metrics previously described [40]. The performance metrics calculated included current density, hydrogen productivity, anode Coulombic efficiency, cathode conversion efficiency, hydrogen recovery, electrical efficiency, and overall energy efficiency. These metrics were calculated from the average current generated, the time of the experiments conducted, geometry of the MECs used in this study, and the average voltage applied to the MECs. Current density is the average current (I_{avg}) over the projected surface area (A):

$$CD = \frac{I_{avg}}{A}$$

Hydrogen productivity is defined as the volume of hydrogen produced (V_H) over the anode volume and time of the experiment (t):

$$H_{prod} = \frac{V_H}{V_{ano} t}$$

Anode Coulombic efficiency, often referred to throughout here as Coulombic efficiency, is described as the average current over the expected current released from the removed COD (I_e):

$$CE_{anode} = \frac{I_{avg}}{I_e}$$

Cathode conversion efficiency is the ratio of hydrogen produced over the amount of hydrogen that would be theoretically possible based on the charge delivered. It is defined by:

$$CCE = \left(\frac{PV_H/RT}{\frac{I_{avg} t}{2F}} \right)$$

Where P, T are the pressure and temperature of the experiment. R and T are the universal gas constant and Faraday constant, respectively. Hydrogen recovery is the multiplication of the Coulombic efficiency and the cathode conversion efficiency:

$$Y_{H2} = \frac{PV_H/RT}{2\Delta nCOD}$$

Where ΔnCOD is the number of moves of COD removed. Electrical efficiency is defined as the ratio of the combustion energy of hydrogen (W_{H2}) over the electrical energy delivered over the course of the experiment (W_E):

$$\eta_E = \frac{-W_{H_2}}{W_E}$$

Overall energy efficiency includes the energy stored in the substrate delivered (W_s), and creates the following expression:

$$\eta_{E+S} = \frac{W_{H_2}}{W_s - W_E}$$

The energy content of the substrate was assumed to be 14.955 kJ/g-COD based on what had been used previously [26]. The operating temperature and pressure was 23 ºC and 1 atmosphere,

respectively. The energy content of the substrate was assumed to be 15.0 kJ/g-COD, and the hydrogen combustion value used was 285.8 kJ/mol-H_2, as used earlier [40, 43].

Produced water COD was determined by first diluted 25 and 50-fold using deionized water. COD was recorded using Hach high range COD vials (Hach Company, Loveland, CO). 0.5 g of mercuric sulfate was added to each vial and vortexed for 10 seconds before produced water samples were added to COD vials. Samples were diluted 4-fold to prevent chloride interference. Samples were digested for 2 h in a Hach DRB 200 thermostat at 150 C. COD concentration was then determined by measuring the absorbance of the digested vials using a Spectronic Genesys 20 spectrophotometer (ThermoFisher Scientific, Waltham, MA) at 620 nm. Despite the use of mercuric sulfate, chlorides still appeared to interfere. Other methods, including ferrous ammonium sulfate titration described in Standard Methods [44], did not appear to remove this interference. To work around this, a modified COD standard curve was used that accounted for the residual interference caused by chlorides. Additional details are available in the Appendix of the chapter.

MEC Microbial Community Characterization and Correlations

To characterize the microbial communities that were active in the MEC anode, 16S rRNA sequencing was carried out on the raw produced water and felt samples from MECs that had be run on to two substrates Raw produced water was filtered by 0.2 um before extraction, which was then cut open and used for DNA extraction. Anode felt samples were removed from the anode at 30 and 40 mS/cm conductivity after an acclimation period to either PPW or acetate of no more than two weeks. This was performed by opening the MEC in an anaerobic chamber. Upon opening the reactors, a deposit was found on the exterior of the felt cylinder, accumulating at the anode electrode exterior. The deposit accumulated between the anode enclosure wall and

the anode liquid media entrance and exit ports. This film appeared to have clogged the MECs and prevented anode liquid media flow. The film was not characterized, but once the anode surface where the film was deposited was scrapped with a sterile spatula, the flow through the felt was restored. This film only occurred when MECs were run on PPW and guar gum and was scrapped intermittently to assure good flow through the felt occurred after experiments. Felt samples were removed using a flame sterilized coring bit in the anaerobic chamber, where the removed felt was replaced with sterile felt. Felt samples were stored in -80 ℃ before DNA extraction. DNA extraction was conducted by thawing felt samples, chopping them into four pieces with a sterile blade, and then using a QIAGEN (Qiagen, Venlo, Netherlands) Powersoil Pro DNA extraction kit. A Nanodrop Spectrophotometer (ThermoFisher Scientific, Waltham, MA) was used to initially quantify the extracted DNA using 1 µl of sample for each measurement prior to PCR, scanning between a wavelength of 220 and 350 nm. PCR was applied to extracted DNA to amplify the 16S rRNA gene using the protocol described previously [45-47]. Briefly, 1-2 µl of DNA was used per amplification. The size of the amplicons was visualized using a 1% agarose electrophoresis gel at 60V for 30 minutes. An Agilent Bioanalyzer (Agilent Technologies, Santa Clara, CA) was then used to further characterize the quality of the amplicons. Excess primer dimers were removed using a Zymo Select-a-Size DNA Clean and Concentrator Kit (Zymo Research, Irvine, CA) removing fragments smaller than 200 bp. Samples were then quantified by using a Qubit fluorometer (ThermoFisher Scientific, Waltham, MA). DNA was then sequencing by an Illumina MiSeq (Illumina, San Diego, CA). Operational taxonomic units (OTUs) from 16S sequencing were analyzed using Qiime2 software [48] and taxonomies were classified using the Silva database [49-51]. Alpha diversity metrics where calculated also using Qiime2 and included Shannon, Simpson, and Chao1 indices. Principle

Component Analysis (PCA) was conducted using the results from 40 and 30 mS/cm experiments. The components were determined using current density, hydrogen productivity, Coulombic efficiency, cathode conversion efficiency, electrical efficiency, and dominant genera detected by 16S rRNA sequencing. PCA was performed using SPSS software (IBM Corporation, Armonk, NY), using Oblimin rotation with Kaiser normalization.

Results and Discussion

Produced Water Chemical Characterization

The untreated produced water contained a total detected cation and anion concentration of 21 g/L and 61 g/L, respectively. Na^+ was the dominant cation (18.1 g/L), and Cl^- was the dominant anion (59.1 g/L). Pretreatment of the produced water via $Na_2 HPO_4$ addition resulted in Na^+ increasing to 22.2 g/L, and Cl^- increasing to 61.8 g/L. Table 1 shows the differences in ion composition before and after pretreatment.

Table 1: Results of Ion Chromatography on 0.22 µm filtered untreated produced water (PW) and produced water after introduction of phosphates (PPW). The later was used exclusively in MECs, and concentrations of compounds shown are in mg/L. Compounds that were below detection are abbreviated as "BD". Key includes: Lactate (Lact.) Acetate (Acet.), Propionate (Prop.), Formate (Form.), Butyrate (Buty.), Pyruvate (Pyru.), Succinate (Succ.), Oxalate (Oxal.), Fumarate (Fuma.), and Citrate (Citr.)

Cations (mg/L)						
	Li^+	**Na^+**	**NH_4^+**	**K^+**	**Mg^{2+}**	**Ca^{2+}**
PW	BD	18079.8	567.9	394.2	227.6	1647.7
PPW	BD	22243.7	520.6	421.6	133.3	61.6

Anions (mg/L)									
	F^-	**Cl^-**	**NO_2^-**	**Br^-**	**NO_3^-**	**SO_4^{2-}**	**PO_4^{3-}**	**Lact.**	**Acet.**
PW	BD	59100.1	BD	405.8	122.8	675.9	0.0	227.9	453.4
PPW	BD	61790.5	BD	430.7	117.0	645.9	708.9	280.1	416.2
	Prop.	**Form.**	**Buty.**	**Pyru.**	**Succ.**	**Oxal.**	**Fuma.**	**Citr.**	
PW	BD	272.0	BD	BD	BD	BD	BD	BD	
PPW	BD	255.6	BD	BD	BD	BD	BD	BD	

Ca^{2+} and Mg^{2+} were significantly removed by Na_2HPO_4 addition, resulting in lowering Ca^{2+} concentration by 96.3%, and Mg^{2+} by 41.4%. NH_4^+ also decreased after addition of PO_4^{3-} by 4.1%. This could be caused by the formation of other complexes, such as struvite, as a result of Na_2HPO_4 addition. Na^+ and PO_4^{3-} ion concentration increased, which was expected given the addition of Na_2HPO_4. Cl^- increased after pretreatment, however the mechanism was not determined. Anion composition was dominated by Cl^-, but also included organics such as lactic, acetic, and formic acids. Lactic acid presence is unusual, as it is not traditionally found in produced waters as often as acetic and formic acid [8]. However, lactic acid bacteria have been found previously in produced water microbial communities, who found that *Lactococcus* and *Enterococcus* were found in produced water samples from wells drilled in the Bakken formation [39]. Lactic acid can also form from hydrolysis of polylactide polymers, which have

been studied as a hydraulic fracturing fluid loss additive [52], an additive that is used to prevent fracturing fluids from exiting the fracture and bleeding off into the formation. Ultimately, these organic acids accounted for more than 0.8 g-COD/L for both untreated produced water and PPW. Because of these concentrations, it was expected that the produced water used here would contain a significant fraction of easily convertible COD that would result in high current densities and hydrogen productivities.

After Na_2HPO_4 pretreatment, total COD dropped from 2.66 ± 0.19 g/L to 2.34 ± 0.28 g/L, pH dropped from 7.06 to 6.36, and conductivity increased from 131.2 mS/cm to 143.1 mS/cm. These bulk properties are shown in Table 4 in the Appendix of this chapter. Na_2HPO_4 pretreatment retained a substantial amount of organic material in the produced water, while only causing a marginal drop in pH and a slight increase in conductivity, making the product still useable as a substrate in MECs. However, Na_2HPO_4 pretreatment is unlikely to be used as a pretreatment method for produced water in MECs. Phosphorus is a limited resource, and its use here may contribute to reaching the earth's hypothetical "peak phosphate" production and consumption. Other Ca^{2+} removal methods, such as by using ion exchange resins, will not be effective at salinities present in produced water. Rather, new configurations of MECs that lack a membrane will need to be considered in order to operate without the worry of Ca^{2+} precipitation on membranes or electrodes, or the necessity of pretreatment. Unfortunately, MECs without membranes suffer additional problems, such as hydrogen scavenging by methanogens [53].

Electrochemical Results

Prolonged exposure to untreated produced water ultimately resulted in membrane rupture. Use of an anion exchange membrane with untreated produced water did not result in membrane rupture but did cause precipitation and voltage rise much like with cation exchange

membranes (data not shown). Acid cleaning using 1 M HCl decreased operating voltage, which would continue to rise when using untreated produced water. By contrast, PPW did not contribute to an irreversible rise in voltage. All data shown in the main body of the text therefore used PPW. Figure 1 illustrates the electrochemical data investigated for each of the experimental conditions and substrates tested on the MECs. Each of the following subsections summarize the findings uncovered under the conditions tested. For emphasis, lower salinity experiments correspond to decreasing organic content, however organic loading rates were equivalent for both substrates.

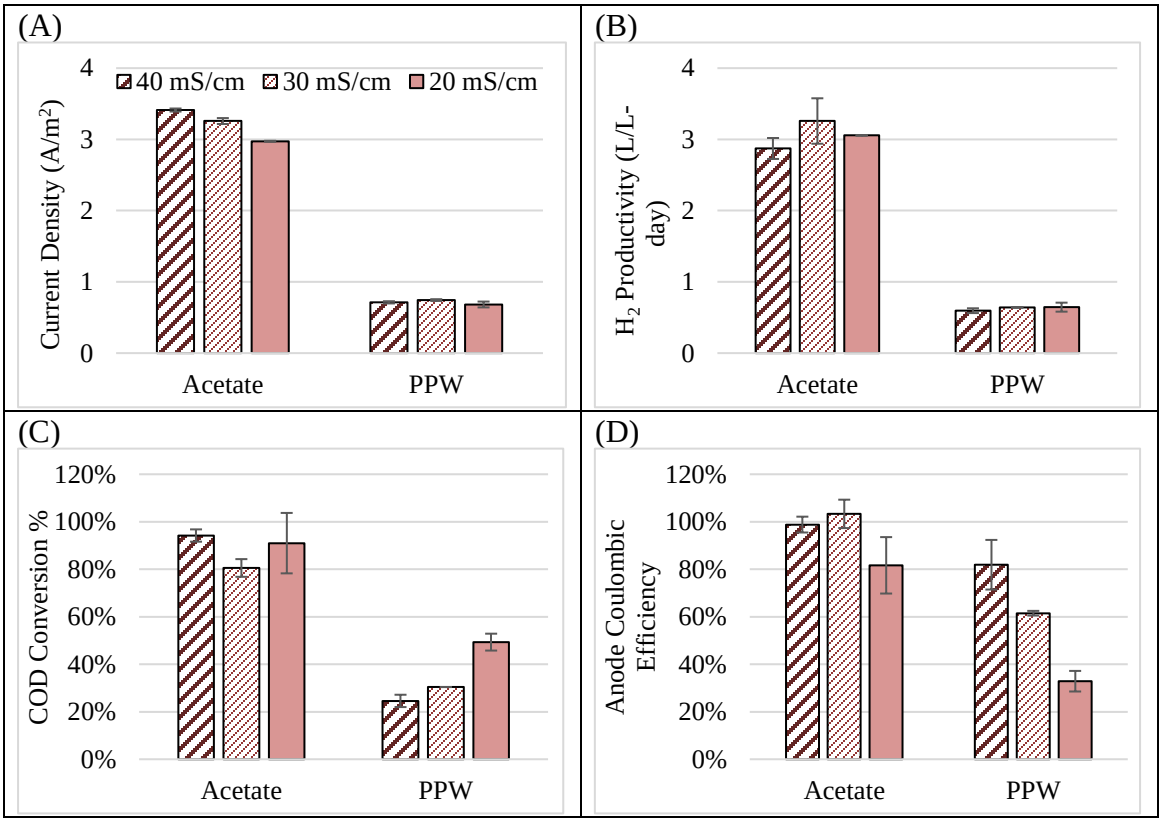

Figure 1: Electrochemical performance and efficiencies of MECs at 20, 30 and 40 mS/cm using acetate and PPW. Current densities, hydrogen productivities, and COD removal percentages were much lower across all trials, however efficiency metrics were much more comparable across substrates.

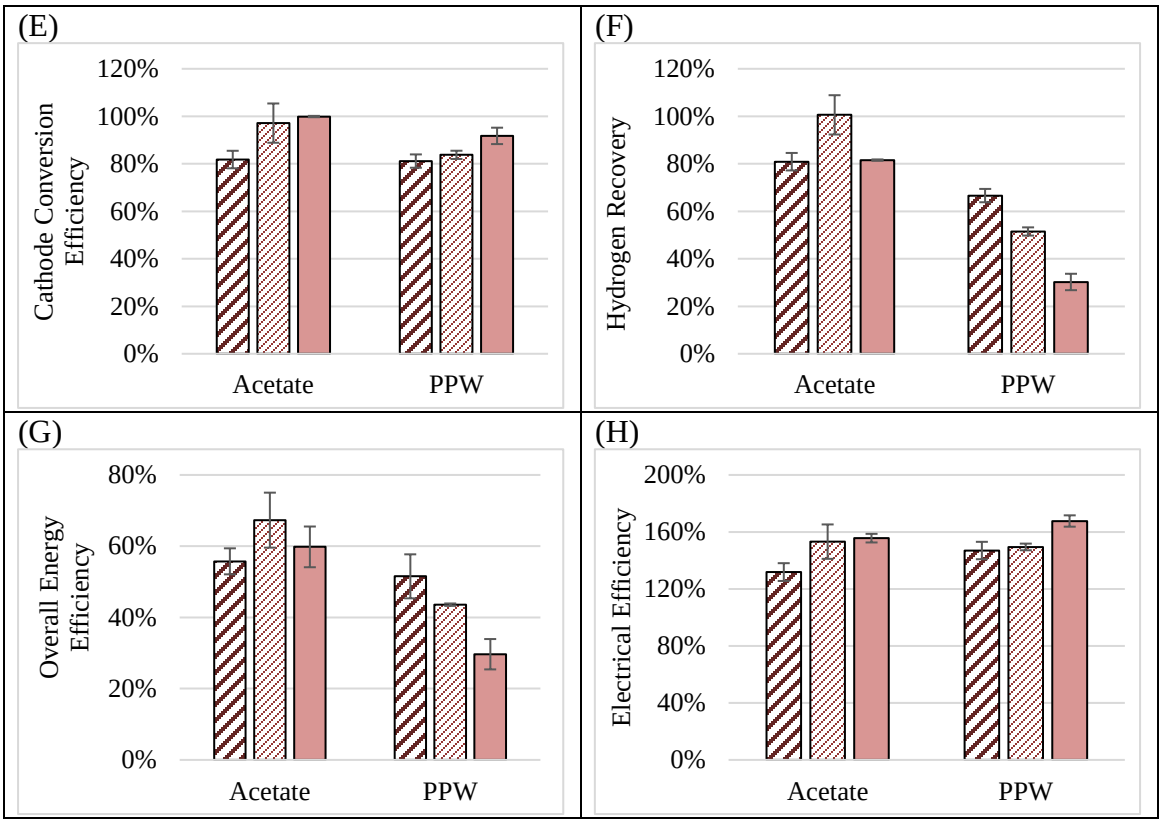

Figure 1 continued

Current Density, Hydrogen Productivity, and COD Removal

The highest average current density observed in the MECs was 3.4 ± 0.002 A/m^2, obtained when MECs were fed acetate at a conductivity of 40 mS/cm. At the same loading, the PPW only achieved a current density of 0.7 ± 0.02 A/m^2. Shown in Figure 1A, PPW achieved relatively consistent average current densities across all organic loadings and associated conductivities. The findings reported here represent the best performance of any MEC reported to date for treatment of produced water. For instance, the highest observed maximum current density reported previously was no greater than 0.57 A/m^2 [36] which used an MFC with much higher organic loading in batch-fed reactors (10 g-COD/L). Sheikhyousefi et al., reported current densities that were lower than demonstrated here, calculated at 0.32 A/m^2 from information

provided by the authors [27], and Monzon et al. reached a maximum power density calculated at 0.34 A/m^2 [26]. Naraghi et al. performed MEC experiments, but normalized current density to volume, reporting a volumetric current density of 0.31 A/m^3 [29]. For equivalent comparison, the current density presented here in the same units is approximately 66 A/m^3. Table 2 compares BES performances of other studies fed with acetate and produced water with the MECs used in this study.

Table 2: Literature comparison between saline BESs that use either acetate or produced water, comparing microbial fuel cells (MFC), microbial electrolysis cell (MEC) and microbial osmotic desalination cell (MODC). To date, the MECs used here that were fed produced water have demonstrated the highest Coulombic efficiency, and the highest performing BESs that by hydrogen productivity and current density compared to other BESs fed produced water.

Reactor Type	**Substrate**	**Salinity/ Conductivity**	**Average Current Density (A/m^2)**	**Coulombic Efficiency**	**Hydrogen Productivity (L/L-day)**	**COD Removal %**	**Reference**
MFC	acetate	45 g/L NaCl	85	22.7%			[54]
MFC	acetate	132 mS/cm	1.5	10.71 - 0.67%		95.5 - 97.0%	[27]
MFC	acetate	50 g/L NaCl	<2.64	38		10-38%	[35]
MEC	acetate	25% salinity	6.8				[31]
MEC	acetate	40 mS/cm	3.4 ± 0.02	98.8 ± 3.33%	2.87 ± 0.15	94.2 ± 2.6%	this work
MFC	produced water		<0.34	10%		68%	[26]
MFC	produced water	132 mS/cm	0.32	0.88 - 1.85%		94.4 - 95.9%	[27]
MFC	produced water	200000 ppm	3.26 mA/m^3	0.20%		90%	[29]
MEC	produced water	200000 ppm	310 mA/m^3		0.0004	81%	[29]
MFC	produced water		< 0.57	6-40%		96%	[36]
MEC	produced water	40 mS/cm	0.71 ± 0.02	81.9 ± 10.4%	0.59 ± 0.033	24.6 ± 2.59%	this work

Hydrogen productivity was also much higher for acetate-fed reactors than for PPW-fed reactors under the same organic loading conditions. The largest average hydrogen productivity occurred at 30 mS/cm while being fed with acetate, yielding 3.3 ± 0.32 L/L-day averaged over the length of the experiment (Figure 1B). PPW, by contrast, only reached 0.64 ± 0.03 L/L-day under the same conditions. The only MEC to use any kind of produced water was from Naraghi et al., who achieved a hydrogen productivity of 0.0004 L/L-day [29]. This makes the MECs used here the highest performing MECs operating on produced water of any kind to date, though they are not the highest performing MECs using acetate. MEC design and pre-enrichment of anode microbial consortia can drastically affect MEC performance, which was a likely factor responsible for these differences.

We expected high conversion percentages of COD at high conversion rates due to the high levels of organic acids. However, this was not found to be the case. If complete removal of the organic acids present in PPW was achieved, it would represent a COD removal of 36%. This was not achieved by the MECs at 40 mS/cm or 30 mS/cm. By contrast, COD removal was high for all acetate-fed experiments. The maximum COD removal for the PPW-fed MECs was 49.3 ± 3.55% at 20 mS/cm, whereas 94.2 ± 2.59% of COD was removed in acetate-fed MECs at 40 mS/cm. Otherwise, the produced water fed MEC removal percentages were lower than others. Monzon et al. was closer to the results shown here, having a removal percentage 68% [26]. Other studies exceeded COD removal percentages than what was demonstrated here. These included Naraghi et al, who achieved a COD removal percentage of 89% [29], 96.6% from Sheikhyousefi et al. [27], and 88% by Shrestha et al. [36]. Some of these differences may be attributed to the potential inaccuracy of the modified COD method, which may not have accounted for saline interference as demonstrated in this study. Additionally, the discrepancies could be the result of reactor

configuration, starting inoculum, hydraulic retention time, or substrate type. Sheikhyousefi et al. attributes the removal of organic material to oxygen diffusion into the cathode, allowing for aerobic degradation of organics that may otherwise not have been possible [27]. Aerobic degradation of hydrocarbons is generally agreed upon to promote faster growth of microbes than anaerobic hydrocarbon degraders [55], resulting in quicker hydrocarbon degradation when oxygen is present assuming equivalent biomass yields per mole of substrate. Here, because organic acids contributed to a large fraction of the PPW's COD, it was expected that larger conversion efficiencies than demonstrated. Rather, adsorption of substrate may be playing a larger role in affecting this removal percentage, which will be further discussed later.

Conversion Efficiency

While the conversion of COD was not as high as reported in other studies, the efficiency metrics were higher that other systems for both acetate and PPW-fed MECs. Acetate-fed MECs reached a maximum anode Coulombic efficiency of 103.3 ± 5.98% at 30 mS/cm, while PPW-fed MECs reached an anode Coulombic efficiency of 81.9 ± 10.4% at 40 mS/cm. Coulombic efficiency exceeded 30% for all conditions tested. This efficiency exceeded those reported in prior studies that used produced water as a substrate. Of the studies that reported Coulombic efficiency, Monzon et al. achieved a Coulombic efficiency of only 10% [26], Sheikhyousefi et al. reached a Coulombic efficiency no larger than 1.85% [27], and Naraghi et al. did not reach Coulombic efficiencies higher than 0.2% [29]. The lowest recorded Coulombic efficiency here at 20 mS/cm when MECs were fed with PPW, at 32.9 ± 4.34%, with Coulombic efficiency reaching 81.9 ± 10.4% when MECs were fed with PPW under 40 mS/cm conditions. In this regard, these MECs have outperformed prior BESs using oil and gas produced water. The apparent loss of Coulombic efficiency in PPW-fed MECs compared to those fed with acetate has

also been reported previously. Sheikhyousefi et al. demonstrated a comparison between acetate-fed and real produced water-fed MFCs and found that the maximum Coulombic efficiency for acetate-fed MFCs was nearly an order of magnitude larger than for produced water-fed MFCs [27]. With other complex feedstocks, this trend is also true. Lewis et al. showed that acetate-fed MECs had higher Coulombic efficiencies at the same organic loading rates in the same time intervals that a complex feedstock derived from switchgrass did [56]. This phenomenon makes sense conceptually. Fermentable substrates require additional steps before conversion to electricity, resulting in slower conversion rates. These compounds also create a diversion for electrons by being partially utilized to create biomass, required for fermenter metabolism. Even with this in mind, the results are still surprising, as the amount of substrate COD attributed to acetate should have been easily convertible and reflected in high Coulombic efficiencies. However, one phenomenon that may have contributed to lower Coulombic efficiencies is the observed film that formed during operation discussed in the Methods section. As mentioned in the Methods section of this chapter, the anode chamber was found to clog when the MECs were fed with PPW. While biomass can accumulate and increase the resistance to flow through the felt, this problem did not occur when MECs were fed with acetate. It may be possible that compounds in PPW were removed by adsorption and precipitation rather than biological degradation. Characterizing the deposited organics, as well as testing new anode materials, will further improve MEC designs used to treat oil and gas produced water. Compounds that deposited instead of degraded would represent a significant fraction of removed COD without contributing to electron production or methane creation and may also prevent anode biofilm access to more carbon source as substrate deposits. MECs run at higher conductivities had larger organic loading and operating time, and these MECs had more time to degrade compounds. However, because the film prevented flow,

additional organics delivered to the MEC were not adequately degraded, resulting in the lower COD conversion observed. Both adsorption and retention time in the MECs would have contributed to Coulombic efficiency and COD conversion in ways that would be challenging to quantify.

Cathode conversion efficiency, by contrast, was above 80% for all substrates and conductivities tested, with the highest values appearing at 20 mS/cm, for both substrates. For batch operated MECs using the same reactor configuration, cathode conversion efficiency has been shown to either marginally decrease or be unaffected by organic loading using a non-saline complex waste varying between 0.1 and 0.3 g/L [43], or increased when organic loading conditions were increased from 0.2 to 0.5 g/L [40]. Cathode conversion efficiency is therefore dependent on substrate type and organic loading, where the differences in this metric will be more pronounced at larger differences in organic loading conditions. In saline MECs, Carmona-Martinez et al. showed that cathode efficiency increased as organic loading increased in an anode growth media of constant salinity (35 g/L)[57]. Additionally, at equal organic loading, cathode conversion efficiencies have been shown to be marginally lower at higher conductivity [58]. Thus, conductivity, organic loading, and substrate characterization play a role in affecting this efficiency metric, the extent of which is not necessarily quantified individually here. Mechanistically, increased conductivity may obstruct proton transfer that would otherwise be absent if protons were the only cations present in MECs, an impossibility in real systems. Losses in proton transfer rates were reported in MECs when the salt concentration in the anode liquid media was increased from 0 to 10 g/L[59]. The results demonstrated here may indicate a scenario where cathode conversion efficiency decreased due to conductivity more than the larger organic loading increased cathode conversion efficiency. Because cathode conversion efficiency was

high for MECs fed either substrate, hydrogen recovery of PPW-fed MECs was largely driven by changes in anode Coulombic efficiency. The highest hydrogen recovery obtained for PPW-fed MECs was 66.6 ± 10.8% at a conductivity of 30 mS/cm, while it was 100.6 ± 14.4% for acetate-fed MECs at the same conductivity. Hydrogen recovery was consistent for acetate-fed MECs across loadings, but the same was not true for PPW-fed MECs.

Electrical efficiency exceeded 100% for all trials and substrates, as shown in Figure 1H, with the highest efficiencies being 167.7 ± 3.98% using PPW at 20 mS/cm loading. MECs fed with acetate reached a maximum electrical efficiency of 155.6 ± 3.02% at the same conductivity. Electrical efficiency was lower for MECs fed with acetate due to the higher operating voltages despite similar cathode conversion efficiencies. As loading and conductivity increased, electrical efficiency dropped for both substrates. Cathode conversion efficiency decreased for both substrates as conductivity and organic loading increased, and operating voltage was consistent across substrates used and organic loading rates, causing losses in electrical efficiency.

Overall energy efficiency was much lower for PPW-fed MECs than for acetate-fed MECs. This is likely because of the relative complex nature of PPW compared to acetate. Because the electrical efficiencies were similar across substrates and salinities, overall energy efficiency is primarily driven by the anode's inability to convert the organics found in PPW efficiently into electrons. Unfortunately, there are no prior studies that explain what mechanisms cause this difference in overall energy efficiency between produced water and acetate fed MECs. However, one study that fed a complex feedstock to MECs attributed the diversion of electrons towards biomass production, polymer formation, and fermentation, but not methanogenesis, and justified this position by using an electron balance[60]. It is likely that the same phenomenon is occurring here. The MECs showed negligible amounts of methane in the cathode, and less than

1% of the anode headspace was identified as methane. An electron balance (see the Appendix of this chapter) showed that methane production used less than 1.6% of electrons released by COD conversion under all of the conditions tested. Methanogenesis was therefore not the primary electron sink. Adsorption discussed earlier would contribute to lower overall energy efficiencies and higher electron losses by removing substrate without contributing to energy production.

Microbial Characterization Results

In all of the conditions tested, the communities were dominated by bacteria, while archaea represented a significantly small percent (< 1%) of the total microbial population. Figure 2 shows the 16S rRNA relative OTU abundance results from the untreated produced water, and anode communities from acetate-fed MECs, and PPW-fed MECs.

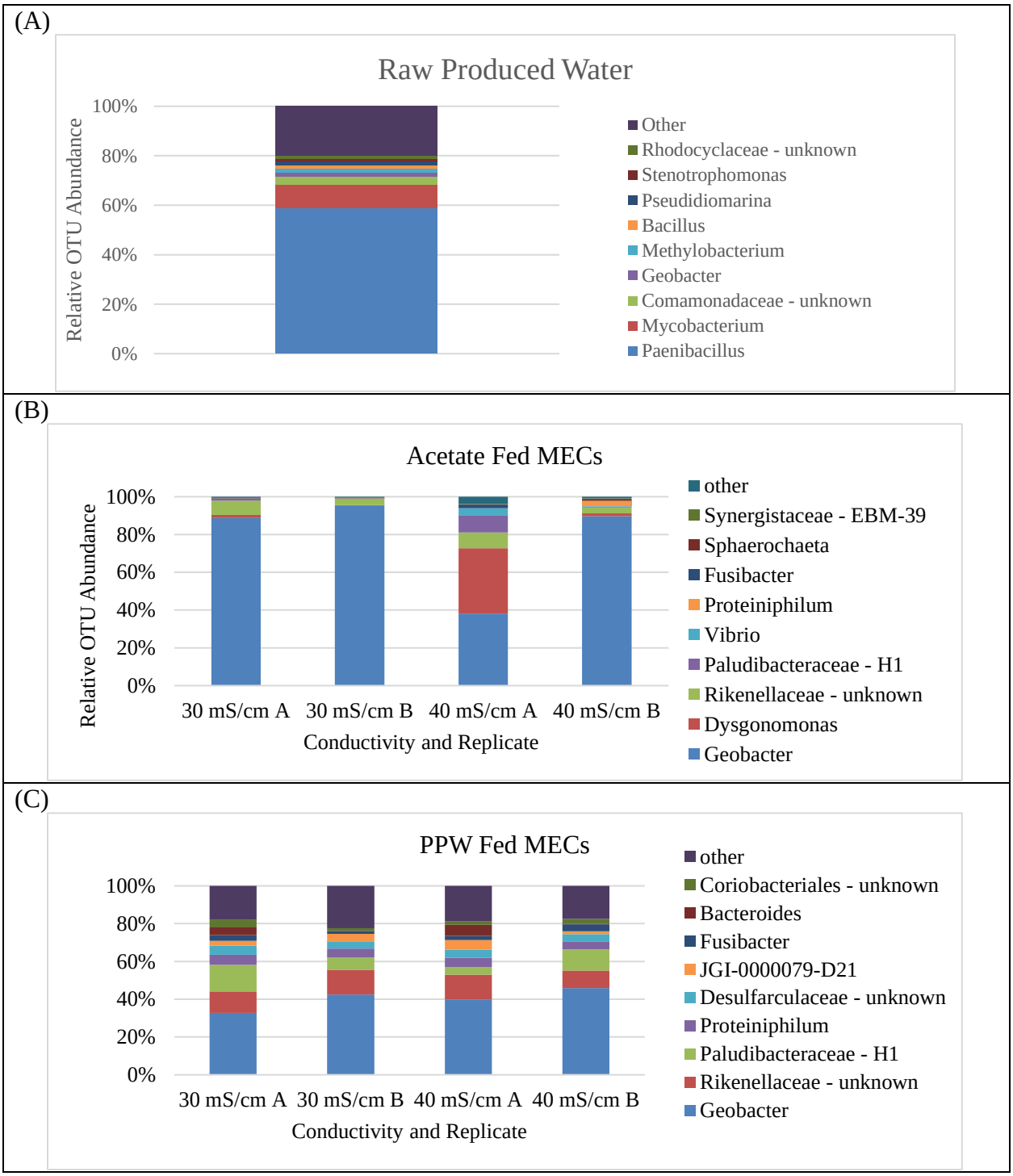

Figure 2: 16S rRNA results of raw produced water (A), Acetate fed MECs (B) and PPW fed MECs (C). Microbes present in produced water varied considerably from microbes found in MECs that were fed either substrate.

The findings of the 16S rRNA sequencing support the quantification of methane via GC, which found very small quantities of the gas in the anode, and negligible amounts in the cathode (see Figure 6 in the Appendix of this chapter). This also suggests that methanogenic populations were not enriched in either PPW or acetate fed MECs. The most dominant microbe genus in produced water was *Paenibacillus,* which is a facultative anaerobe. It has been reported to degrade a number of hydrocarbons[61]. *Paenibacillus* sp. has also been shown to produce the enzymes required to degrade the hydraulic fracturing fluid additive, guar gum [62]. Being a facultative anaerobe, it would be unlikely to thrive in the severely anaerobic conditions that are present in hydrocarbon bearing formations. An explanation for its proliferation comes from how produced fluid is often handled. Traditionally, oil and gas produced waters are stored in ponds or tanks at the surface before reinjection, which inadvertently incorporates oxygen into the water. Additionally, because guar gum is a very common fracturing additive, it may have been used as part of the hydraulic fracturing operations used on the well the produced water was retrieved from. Guar gum's residues are easily biodegradable given that guar gum is primarily composed of β 1-4 linked mannose with α 1-6 branched galactose. Guar gum was not explicitly detected in PPW, but its prevalence in the area where the well was fractured, and information provided by the well owner and operator (whom have chosen to remain anonymous), supports this possibility. By introducing oxygen at the surface and by having fermentable compounds present in the produced water, *Paenibacillus* may have flourished. This microbe has, however, not been reported extensively in produced water. Cluff et al. tracked the microbial composition of three horizontally fractured wells as they produced water over time and found very small or no amounts of *Paenibacillus* at any stage of production [9]. In fact, the overall microbial composition of their produced water was very different than what was determined here. Wang et al.

performed a geographically widespread 16S rRNA sequence analysis recently on produced waters from wells drilled in shales in Colorado, Texas, and North Dakota, and did not find significant presence of *Paenibacillus* [39]. Dominant microbes reported include *Rhodococcus* sp. in the Denver-Julesburg formation produced water in Colorado, and *Bradyrhizobium* sp. and *Geobacter* sp. in the early time produced water from Texas and North Dakota.

Exoelectrogens are of high interest in this study as the primary contributors towards energy production in MECs. Several were found in the raw produced water at small percentages. Those genera included *Geobacter* and *Halanaerobium*. Of the exoelectrogens documented in BESs, *Geobacter* has been found in saline MFCs and raw produced water[32, 39, 63], but has also been shown to decrease rapidly in abundance at NaCl concentrations above 0.1 M [64]. *Geobacter* is a well-studied exoelectrogenic genus that first illustrated the capability to respire on electrically conductive surfaces using a conductive pili known as a nanowire, discovered by Reguera et al. in 2005 [65]. *Geobacter* is the model exoelectrogen in many studies investigating biofilm activity and respiration without the use of electron mediators, typically using acetate as the carbon source. *Geobacter* was found in the produced water used in this study at 1.8% of the relative OTUs documented. The other exoelectrogenic genus, *Halanaerobium*, was expected in the MECs used in this study, although it represented only 0.05% of the OTUs detected in the raw produced water. Paul et al. attributed exoelectrogenic activity to this microbe by operating an MFC that was inoculated using only a culture of *H. hydrogeniformans* [66]. Further, it had been previously found in MFCs fed with produced water [26], and was found in high abundance in produced waters recovered by Cluff et al.[9] and Daly et al.[67]. *Halanaerobium* also contains fermentative species that can thrive in high pressure environments such as *H. coglenese* [68], which suggests that the *Halanaerobium* found in produced waters could fit either fermentative or

exoelectrogenic roles in produced water MECs. Another commonly identified genus found in MFCs [26, 27] and in produced waters [9, 69] is *Marinobacter*, but it has not been identified as an exoelectrogen. Some of the species of *Marinobacter*, most notably *M. hydrocarbonoclasticus*, have been demonstrated to degrade hydrocarbons in saline environments [70]. Monzon et al. showed that *M. hydrocarbonoclasticus* represented 70% of the community biofilm in their produced water fed MFCs [26]. By contrast, Sheikhyousefi et al. had only 0.4% of its MFC community represented by *Marinobacter* in working MFCs, while *Marinobacter* represented more than 27.5% of the community in non-working MFCs [27].Thus, *Marinobacter* is likely a fermenter in BESs, not an exoelectrogen. Because of its existence in the produced water used in this study, and its prevalence in other MFCs, the MECs used here were suspected to have enriched that microbe before sequencing.

Microbial communities found in the MEC anode differed significantly from those in the untreated produced water. Several of the genera present in produced water discussed earlier, *Paenibacillus*, *Halanaerobium*, or *Marinobacter* were not found in any of the MEC anode felt samples sequenced in this study. This suggests that these microbes were either never alive prior to use in the reactors or could not compete with the existing consortia in MECs. Additionally, there may be some functional limitations of these microbes that prevented their enrichment. As an example, the isolate of *H. hydrogeniformans* used in an MFC by Paul et al. formed limited biofilms [66]. It is possible that the species present in the produced water were washed out as a result of the multiple changes of nutrient medium that the MECs were subjected to during the experiments. As a result, other microbes would be better suited to form biofilms and degrade produced water in MECs. Further, not all highly saline BESs have dominant populations containing *Halanaerobium*. Sheikhyousefi et al. did not find *Halanaerobium* as the dominant

microbe in their MFCs [27], and neither did Naraghi et al. [29]. Thus, several unique starting inoculum can be used to enrich BESs that successfully degrade produced water.

Geobacter was identified as the dominant genus in all our MEC samples. *Geobacter* was not the only exoelectrogen present in our reactors, but it was the dominant genus, with a relative abundance reaching up to 90% in most of the acetate-fed MECs. Other exoelectrogenic genera such as *Desulfuromonas* was found in small abundances (<0.1%). Thus, species belonging to *Geobacter* likely functioned as the primary exoelectrogen in these reactors for both substrates. The other microbes found were likely enriched using the other compounds exoelectrogens did not use. *Paludibacteraceae – H1* was found in large abundance on PPW-fed MECs. *Paludibacteraceae,* contains mainly strict anaerobes, and some of the genera, such as *Paludibacter,* have been documented as saccharolytic fermenters [71].

Using multiple inoculum sources may have contributed to enriching a unique group of microbes found in MECs that would not be present in any of the sources individually. Some microbes may have been derived from the anaerobic digester inoculum, such as the unknown genus of Rikenellaceae detected. Rikenellaceae is a family that has been found in gut microflora [72] and an undetermined genera was found in relative abundances above 9% for all produced water fed MECs. Some Rikenellaceae genera may have also come from the produced water, as several genera of this phylum were present in the produced water used in this study. Others were likely to have originated from produced water exclusively, such as *Proteinphilum* It was found in very small quantities in produced water, (<0.01%) and made up more than 4% of the community, while it is not regularly reported in MECs. It is likely that degradation products from compounds added in fracturing fluid and the anaerobic conditions in MECs, contributed to their enrichment.

While the known functionality of the microbes can lead to some insight, a mechanistic understanding can only be obtained via use of rigorous ‘omics techniques or investigations using pure cultures. However, the evidence supports the conclusion that the electro-active biofilm enrichment obtained via use of a compact, flow-through MEC design and process conditions allowed for better performance than observed previously with produced water. Further study will help understand the role of these microbes in MECs. To maximize performance of MECs operating on complex feedstocks like produced water, a selectively enriched community derived from multiple sources being fed simple and complex carbon sources is more effective than relying on single inoculum, an unenriched consortia, or being fed only one complex carbon source.

The diversity of the PPW-fed MECs was larger than the acetate-fed ones across all replicates. *Geobacter* represented much larger percentages of the community structure when the MECs were fed with acetate than when the MECs were fed with produced water. The one exception being replicate A at 40 mS/cm. Table 3 shows the alpha diversity metrics calculated amongst the samples using Shannon, Simpson, and Chao1 diversity indices for each of the samples.

Table 3: Alpha diversity of 16S rRNA sequencing using Chao1, Shannon, and Simpson indices based on reactor Replicate (A or B), MEC anode liquid media conductivity, and substrate type. Raw Produced Water alpha diversity has also been included for comparison. Diversity indices have been rarified to the lowest sample count observed

Reactor Replicate	Conductivity (mS/cm)	Substrate	Chao1 index	Shannon index	Simpson index
A	40	PPW	159	3.75	0.79
B	40	PPW	130	3.47	0.76
A	30	PPW	143	3.95	0.85
B	30	PPW	162	3.95	0.82
A	40	Acetate	47	2.51	0.73
B	40	Acetate	45	0.98	0.24
A	30	Acetate	31	0.88	0.25
B	30	Acetate	31	0.55	0.15
Raw Produced Water	131	N/A	422	3.64	0.68

As shown in Figure 2(C), the second most abundant microbe genus in this replicate was *Dysgonomonas*, which is a known saccharolytic fermenter that does not use acetate [71]. One may think its appearance was an error, however, it was found in all MEC samples, albeit at low (<2%) relative abundances. As mentioned in the methods section; glucose, acetate, and guar gum were used for initial growth along with PPW, which may have allowed for some enrichment of this microbe. However, once the experiments were conducted, glucose and guar gum addition stopped, which should have prevented the enrichment of fermenters. Substrate adsorption may have played a role in locally enriching this microbe between experiments, further supporting the need to study the effect of deposited complex wastes and polymers on MEC community structure and function.

In most BES studies, identified microbial communities are assumed to represent the community structure of the entire anode. That is, samples acquired from one portion of the anode will have the same community structure as another. The accumulation of deposits observed, and

the community structure results shown here suggest that such uniformity may not be true in all cases. Both replicates operating on acetate at 40 mS/cm performed similarly, as shown by the standard deviation of the results in Figure 1, however the communities were very different at 40 mS/cm. While it is possible that the smaller fraction of *Geobacter* in replicate A contributed to the same amount of current production as shown replicate B's more *Geobacter* dominant population while being fed with acetate, this explanation may not be true. Replicates ran on 30 mS/cm with acetate both showed an overwhelming dominance of *Geobacter*, and there is no evidence that the microbes present in replicate A at 40 mS/cm during acetate feeding are typically enriched using acetate as a carbon source. Another reasonable explanation that can be drawn here is that the first scrapping and flushing did not remove all of the added carbon that was provided from the PPW. Even though film scrapping should have removed microbes and compounds entrained in the deposit, residual that could not be seen by eye may have been left on the anode felt. This is especially true for porous materials like carbon felt, where physical scrapping of the exterior does not remove any deposit organics on the interior of the felt. This may have allowed for the local enrichment other microbes, and therefore promoted larger diversity, where residual deposit was insufficiently removed.

The possibility of an unequally distributed community in MEC anodes may have an important impact on device design and operation, especially for insoluble substrates or those that form deposits. For larger MECs, community structure, and therefore community diversity, may change more prominently in larger systems with low hydraulic retention times. This has been shown to occur in long tubular MFCs by Kim et al [73]. For complex feedstocks, additional intermediates will be present at different concentrations from the entry to the exit of the anode in cross flow systems. With complex feedstocks that require a consortium, where rates of

degradation, intermediate products, and the associated activity of microbes remain unclassified, a location-dependent community structure may be an inevitability.

Principle Component Analysis

PCA indicated that *Geobacter* populations were grouped together with performance metrics including hydrogen productivity, current density, and Coulombic efficiency, while other genera, including an unknown genus of Rikenellaceae, and the H1 genus of Paludibacteraceae were not. Because there were only eight samples with taxonomical data and electrochemical data, only 8 variables were allowed for analysis. Thus, the top three most represented OTUs were selected for PCA. Figure 3 illustrates these results visually with the two most representative components.

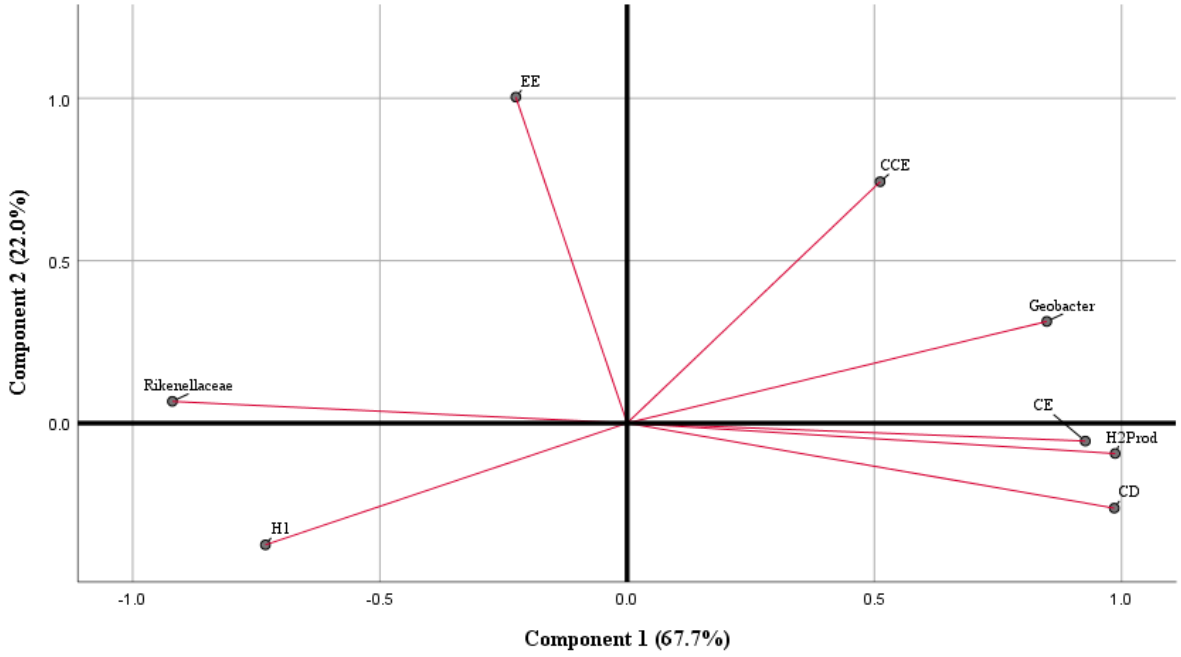

Figure 3: Principle Component Analysis of MECs using commonly identified genera *Geobacter*, Rikenellaceae – *unknown*, and Paludibacteraceae – *H1* (*H1*) and independent electrochemical performance metrics across all substrates and loading conditions. Key going counterclockwise: coulombic efficiency (CE), current density (CD), hydrogen productivity (H2Prod), cathode conversion efficiency (CCE), and electrical efficiency (EE).

Rikenellaceae -*unknown* and Paludibacteraceae – *H1* are not known exoelectrogenic genera and most likely contribute to more complex molecule degradation, which were found in higher abundances in MECs fed with PPW than while fed with acetate. Additionally, these two genera were not grouped with performance efficiency, being virtually at the end of component 1. It might be tempting to assume that this analysis implies that Rikenellaceae - *unknown* and Paludibacteraceae – *H1* would be present only in poorly operating MECs, however this observation is only appropriate when comparing the two substrates tested. These two genera do not consume acetate, and as a result should not be enriched in acetate-fed MECs, which happened to outperform PPW-fed MECs. Rather, the two species likely contribute to performance of PPW-fed MECs by aiding in additional organic compound degradation. If they

were not present in MECs, performance would decline unless another microbe could functionally replace the role these two microbes played. This analysis therefore does not entirely describe all of the relationships these microbes will have on performance and efficiency for other substrates in MECs. To improve the understanding of the relationships associated with these microbes and performance, additional independent substrates will need to be tested to determine if these microbes, and others, contribute to reactor efficiency in more meaningful ways. Electrical efficiency, by contrast, was shown to not be similar to either of the groups, suggesting that operating voltage may be more similar to other metrics not documented in the PCA plot. More importantly, electrical efficiency is not grouped with microbial characterization in the PCA plot. Thus, it is likely that electrical efficiency is more closely related to reactor design than anode communities. Reactor design continues to play a critical role in the commercial potential for MECs, and this study further supports the idea that certain performance metrics are more reliant on system configuration than microbial composition. The extent of this interplay for a given reactor configuration is not often documented. BES design has been known to rely on optimizing not only biology, but also system design and operational parameters that may or may not affect one another [21]. Determining the extent of these relationships amongst parameters across substrates will be key for future device design. While the known functionality of microbes can lead to some insight, a mechanistic understanding can only be obtained via use of rigorous 'omics techniques or investigations using pure cultures. However, we can conclude that the electro-active biofilm enrichment obtained via use of a compact, flow-through MEC design and process conditions allowed for better performance than observed previously with produced water. Further study will help understand the role of these microbes in MECs, as well as how reactor design affects them and vice versa.

Conclusions

MECs have become a highly investigated technology for wastewater treatment and reuse. Prior studies have struggled to yield high current densities, hydrogen productivities, or Coulombic efficiencies from BESs being fed produced water. While current densities and hydrogen productivities for PPW-fed MECs were still lower than for the MECs fed with acetate, this study achieved the highest Coulombic efficiencies and current densities reported using produced water. However, membrane fouling and substrate adsorption continued to occur, requiring substrate pretreatment and regular anode felt maintenance. Despite these issues, the performance documented is promising. If issues related to fouling and adsorption can be overcome, then MECs may be able to efficiently treat produced water. Developing new MEC designs that do not require Na_2HPO_4 pretreatment of substrate may improve the value of this technology. 16S rRNA sequencing showed distinctive differences in community structure between acetate-fed and produced water-fed MECs, and less differences due to salinity or organic loading. Acetate-fed MECs were less diverse than produced water MECs, and also contained higher populations of *Geobacter*. However, this does not explain why, or if, other genera aided or prevented effective conversion of organics to current. Identifying meaningful correlations will require studying additional complex substrates using the same reactor and anode biofilm. This study shows that such investigations of community structure could lead to meaningful understanding of the community dynamics at work if additional substrates are tested. These could include additional sources of produced water, which may produce noticeable differences in performance and community structure and need to be tested in high performing BESs.

References

1. Petersen, M. D.; Mueller, C. S.; Moschetti, M. P.; Hoover, S. M.; Llenos, A. L.; Ellsworth, W. L.; Michael, A. J.; Rubinstein, J. L.; McGarr, A. F.; Rukstales, K. S. *2016 one-year seismic hazard forecast for the Central and Eastern United States from induced and natural earthquakes*; 2016-1035; Reston, VA, 2016.
2. USGS Induced Earthquakes. https://earthquake.usgs.gov/research/induced/overview.php
3. Ellsworth, W. L., Injection-Induced Earthquakes. *Science* **2013,** *341*, (6142), 1225942.
4. Satinover, S.; Borole, A., Hydrogen and Electricity Production from Oil and Gas Wastes. In *Hydrocarbon Biotechnology - Challenges and future Trends*, Ismail, W. A.; Hamme, J. V., Eds. Apple Academic Press: forthcoming 2020; Vol. 1.
5. GWPC *U.S. Produced Water Volumes and Management Practices in 2012*; Ground Water Protection Council: April 2015, 2015.
6. Class II Oil and Gas Related Injection Wells. *US EPA* **2017**.
7. Underground Injection Wells for Produced Water Disposal. In Chesapeake Energy Corporation.
8. Neff, J.; Lee, K.; DeBlois, E. M., Produced Water: Overview of Composition, Fates, and Effects. In *Produced Water*, Lee, K.; Neff, J., Eds. Springer New York: 2011; pp 3-54.
9. Cluff, M. A.; Hartsock, A.; MacRae, J. D.; Carter, K.; Mouser, P. J., Temporal Changes in Microbial Ecology and Geochemistry in Produced Water from Hydraulically Fractured Marcellus Shale Gas Wells. *Environmental Science & Technology* **2014,** *48*, (11), 6508-6517.
10. Stringfellow, W. T.; Camarillo, M. K.; Domen, J. K.; Shonkoff, S. B. C., Comparison of chemical-use between hydraulic fracturing, acidizing, and routine oil and gas development. *PLOS ONE* **2017,** *12*, (4), e0175344.
11. Fakhru'l-Razi, A.; Pendashteh, A.; Abdullah, L. C.; Biak, D. R. A.; Madaeni, S. S.; Abidin, Z. Z., Review of technologies for oil and gas produced water treatment. *J. Hazard. Mater.* **2009,** *170*, (2), 530-551.
12. Igunnu, E. T.; Chen, G. Z., Produced water treatment technologies. *Int J Low-Carbon Tech* **2014,** *9*, (3), 157-177.
13. Zhao, R.; Porada, S.; Biesheuvel, P. M.; van der Wal, A., Energy consumption in membrane capacitive deionization for different water recoveries and flow rates, and comparison with reverse osmosis. *Desalination* **2013,** *330*, 35-41.
14. Thiel, G. P.; Tow, E. W.; Banchik, L. D.; Chung, H. W.; Lienhard V, J. H., Energy consumption in desalinating produced water from shale oil and gas extraction. *Desalination* **2015,** *366*, 94-112.
15. Fakharian, H.; Ganji, H.; Naderifar, A., Desalination of high salinity produced water using natural gas hydrate. *Journal of the Taiwan Institute of Chemical Engineers* **2017,** *72*, 157-162.
16. Kang, K. C.; Linga, P.; Park, K.-n.; Choi, S.-J.; Lee, J. D., Seawater desalination by gas hydrate process and removal characteristics of dissolved ions (Na+, K+, Mg2+, Ca2+, B3+, Cl−, SO42−). *Desalination* **2014,** *353*, 84-90.
17. Liu, H.; Ramnarayanan, R.; Logan, B. E., Production of Electricity during Wastewater Treatment Using a Single Chamber Microbial Fuel Cell. *Environmental Science & Technology* **2004,** *38*, (7), 2281-2285.

18. Wagner, R. C.; Regan, J. M.; Oh, S.-E.; Zuo, Y.; Logan, B. E., Hydrogen and methane production from swine wastewater using microbial electrolysis cells. *Water Research* **2009,** *43*, (5), 1480-1488.
19. Pandey, P.; Shinde, V. N.; Deopurkar, R. L.; Kale, S. P.; Patil, S. A.; Pant, D., Recent advances in the use of different substrates in microbial fuel cells toward wastewater treatment and simultaneous energy recovery. *Applied Energy* **2016,** *168*, 706-723.
20. Kadier, A.; Simayi, Y.; Kalil, M. S.; Abdeshahian, P.; Hamid, A. A., A review of the substrates used in microbial electrolysis cells (MECs) for producing sustainable and clean hydrogen gas. *Renewable Energy* **2014,** *71*, 466-472.
21. Borole, A.; Reguera, G.; Ringeisen, B.; Wang, Z.-W.; Feng, Y.; Hong Kim, B., Electroactive biofilms: Current status and future research needs. *Energy & Environmental Science* **2011,** *4*, (12), 4813-4834.
22. Van Eerten-Jansen, M. C. A. A.; Heijne, A. T.; Buisman, C. J. N.; Hamelers, H. V. M., Microbial electrolysis cells for production of methane from CO2: long-term performance and perspectives. *International Journal of Energy Research* **2012,** *36*, (6), 809-819.
23. Joosten, M. W.; Kolts, J.; Hembree, J. W.; Ach, M. In *Organic Acid Corrosion In Oil And Gas Production*, CORROSION 2002, 2002/01/01/, 2002; NACE International: 2002.
24. Skaare, B. B.; Kihle, J.; Torsvik, T., Biodegradation of Crude Oil as Potential Source of Organic Acids in Produced Water. In *Produced Water*, Springer, New York, NY: 2011; pp 115-126.
25. Dolfing, J.; Larter, S. R.; Head, I. M., Thermodynamic constraints on methanogenic crude oil biodegradation. *The ISME Journal* **2007,** *2*, (4), 442-452.
26. Monzon, O.; Yang, Y.; Kim, J.; Heldenbrand, A.; Li, Q.; Alvarez, P. J. J., Microbial fuel cell fed by Barnett Shale produced water: Power production by hypersaline autochthonous bacteria and coupling to a desalination unit. *Biochemical Engineering Journal* **2017,** *117, Part A*, 87-91.
27. Roustazadeh Sheikhyousefi, P.; Nasr Esfahany, M.; Colombo, A.; Franzetti, A.; Trasatti, S. P.; Cristiani, P., Investigation of different configurations of microbial fuel cells for the treatment of oilfield produced water. *Applied Energy* **2017,** *192*, 457-465.
28. Stoll, Z. A.; Forrestal, C.; Ren, Z. J.; Xu, P., Shale gas produced water treatment using innovative microbial capacitive desalination cell. *J. Hazard. Mater.* **2015,** *283*, 847-855.
29. Ghasemi Naraghi, Z.; Yaghmaei, S.; Mardanpour, M. M.; Hasany, M., Produced Water Treatment with Simultaneous Bioenergy Production Using Novel Bioelectrochemical Systems. *Electrochimica Acta* **2015,** *180*, 535-544.
30. Zhang, X.; Zhang, D.; Huang, Y.; Zhang, K.; Lu, P., Simultaneous removal of organic matter and iron from hydraulic fracturing flowback water through sulfur cycling in a microbial fuel cell. *Water Research* **2018,** *147*, 461-471.
31. Shehab, N. A.; Ortiz-Medina, J. F.; Katuri, K. P.; Hari, A. R.; Amy, G.; Logan, B. E.; Saikaly, P. E., Enrichment of extremophilic exoelectrogens in microbial electrolysis cells using Red Sea brine pools as inocula. *Bioresource Technology* **2017,** *239*, 82-86.
32. Miyahara, M.; Kouzuma, A.; Watanabe, K., Effects of NaCl concentration on anode microbes in microbial fuel cells. *AMB Express* **2015,** *5*.
33. Lefebvre, O.; Tan, Z.; Kharkwal, S.; Ng, H. Y., Effect of increasing anodic NaCl concentration on microbial fuel cell performance. *Bioresource Technology* **2012,** *112*, 336-340.

34. Ismail, Z. Z.; Ibrahim, M. A., Desalination of oilfield produced water associated with treatment of domestic wastewater and bioelectricity generation in microbial osmotic fuel cell. *Journal of Membrane Science* **2015,** *490*, 247-255.
35. Tapia-Tussell, R.; Valle-Gough, R. E.; Peraza-Baeza, I.; Domínguez-Maldonado, J.; Gonzalez-Muñoz, M.; Cortes-Velazquez, A.; Leal-Baustista, R. M.; Alzate-Gaviria, L., Influence of two polarization potentials on a bioanode microbial community isolated from a hypersaline coastal lagoon of the Yucatan peninsula, in México. *Science of The Total Environment* **2019,** *681*, 258-266.
36. Shrestha, N.; Chilkoor, G.; Wilder, J.; Ren, Z. J.; Gadhamshetty, V., Comparative performances of microbial capacitive deionization cell and microbial fuel cell fed with produced water from the Bakken shale. *Bioelectrochemistry* **2018,** *121*, 56-64.
37. Grattieri, M.; Minteer, S. D., Microbial fuel cells in saline and hypersaline environments: Advancements, challenges and future perspectives. *Bioelectrochemistry* **2018,** *120*, 127-137.
38. Rousseau, R.; Santaella, C.; Achouak, W.; Godon, J.-J.; Bonnafous, A.; Bergel, A.; Délia, M.-L., Correlation of the Electrochemical Kinetics of High-Salinity-Tolerant Bioanodes with the Structure and Microbial Composition of the Biofilm. *CHEMELECTROCHEM* **2014,** *1*, (11), 1966-1975.
39. Wang, H.; Lu, L.; Chen, X.; Bian, Y.; Ren, Z. J., Geochemical and microbial characterizations of flowback and produced water in three shale oil and gas plays in the central and western United States. *Water Research* **2019,** *164*, 114942.
40. Satinover, S. J.; Elkasabi, Y.; Nuñez, A.; Rodriguez, M.; Borole, A. P., Microbial electrolysis using aqueous fractions derived from Tail-Gas Recycle Pyrolysis of willow and guayule. *Bioresource Technology* **2019,** *274*, 302-312.
41. Beegle, J. R.; Borole, A. P., An integrated microbial electrolysis-anaerobic digestion process combined with pretreatment of wastewater solids to improve hydrogen production. *Environmental Science: Water Research & Technology* **2017,** *3*, (6), 1073-1085.
42. Sun, G.; Thygesen, A.; Meyer, A. S., Acetate is a superior substrate for microbial fuel cell initiation preceding bioethanol effluent utilization. *Applied Microbiology and Biotechnology* **2015,** *99*, (11), 4905-4915.
43. Lewis, A. J.; Ren, S.; Ye, X.; Kim, P.; Labbe, N.; Borole, A. P., Hydrogen production from switchgrass via an integrated pyrolysis–microbial electrolysis process. *Bioresource Technology* **2015,** *195*, 231-241.
44. *Standard Methods for the Examination of Water & Wastewater*. 23rd ed. edition ed.; American Water Works Association: Washington, D.C., 2017.
45. Ritalahti, K. M.; Amos, B. K.; Sung, Y.; Wu, Q.; Koenigsberg, S. S.; Löffler, F. E., Quantitative PCR Targeting 16S rRNA and Reductive Dehalogenase Genes Simultaneously Monitors Multiple Dehalococcoides Strains. *Appl Environ Microbiol* **2006,** *72*, (4), 2765-2774.
46. Campa, M. F.; Techtmann, S. M.; Gibson, C. M.; Zhu, X.; Patterson, M.; Garcia de Matos Amaral, A.; Ulrich, N.; Campagna, S. R.; Grant, C. J.; Lamendella, R.; Hazen, T. C., Impacts of Glutaraldehyde on Microbial Community Structure and Degradation Potential in Streams Impacted by Hydraulic Fracturing. *Environmental Science & Technology* **2018,** *52*, (10), 5989-5999.
47. Harms, G.; Layton, A. C.; Dionisi, H. M.; Gregory, I. R.; Garrett, V. M.; Hawkins, S. A.; Robinson, K. G.; Sayler, G. S., Real-Time PCR Quantification of Nitrifying Bacteria in a

Municipal Wastewater Treatment Plant. *Environmental Science & Technology* **2003,** *37*, (2), 343-351.
48. Bolyen, E.; Rideout, J. R.; Dillon, M. R.; Bokulich, N. A.; Abnet, C.; Al-Ghalith, G. A.; Alexander, H.; Alm, E. J.; Arumugam, M.; Asnicar, F.; Bai, Y.; Bisanz, J. E.; Bittinger, K.; Brejnrod, A.; Brislawn, C. J.; Brown, C. T.; Callahan, B. J.; Caraballo-Rodríguez, A. M.; Chase, J.; Cope, E.; Da Silva, R.; Dorrestein, P. C.; Douglas, G. M.; Durall, D. M.; Duvallet, C.; Edwardson, C. F.; Ernst, M.; Estaki, M.; Fouquier, J.; Gauglitz, J. M.; Gibson, D. L.; Gonzalez, A.; Gorlick, K.; Guo, J.; Hillmann, B.; Holmes, S.; Holste, H.; Huttenhower, C.; Huttley, G.; Janssen, S.; Jarmusch, A. K.; Jiang, L.; Kaehler, B.; Kang, K. B.; Keefe, C. R.; Keim, P.; Kelley, S. T.; Knights, D.; Koester, I.; Kosciolek, T.; Kreps, J.; Langille, M. G. I.; Lee, J.; Ley, R.; Liu, Y.-X.; Loftfield, E.; Lozupone, C.; Maher, M.; Marotz, C.; Martin, B. D.; McDonald, D.; McIver, L. J.; Melnik, A. V.; Metcalf, J. L.; Morgan, S. C.; Morton, J.; Naimey, A. T.; Navas-Molina, J. A.; Nothias, L. F.; Orchanian, S. B.; Pearson, T.; Peoples, S. L.; Petras, D.; Preuss, M. L.; Pruesse, E.; Rasmussen, L. B.; Rivers, A.; Robeson, I. I. M. S.; Rosenthal, P.; Segata, N.; Shaffer, M.; Shiffer, A.; Sinha, R.; Song, S. J.; Spear, J. R.; Swafford, A. D.; Thompson, L. R.; Torres, P. J.; Trinh, P.; Tripathi, A.; Turnbaugh, P. J.; Ul-Hasan, S.; van der Hooft, J. J. J.; Vargas, F.; Vázquez-Baeza, Y.; Vogtmann, E.; von Hippel, M.; Walters, W.; Wan, Y.; Wang, M.; Warren, J.; Weber, K. C.; Williamson, C. H. D.; Willis, A. D.; Xu, Z. Z.; Zaneveld, J. R.; Zhang, Y.; Zhu, Q.; Knight, R.; Caporaso, J. G., QIIME 2: Reproducible, interactive, scalable, and extensible microbiome data science. *PeerJ Preprints* **2018,** *6*, e27295v2.
49. Quast, C.; Pruesse, E.; Yilmaz, P.; Gerken, J.; Schweer, T.; Yarza, P.; Peplies, J.; Glöckner, F. O., The SILVA ribosomal RNA gene database project: improved data processing and web-based tools. *Nucleic Acids Research* **2012,** *41*, (D1), D590-D596.
50. Yilmaz, P.; Parfrey, L. W.; Yarza, P.; Gerken, J.; Pruesse, E.; Quast, C.; Schweer, T.; Peplies, J.; Ludwig, W.; Glöckner, F. O., The SILVA and "All-species Living Tree Project (LTP)" taxonomic frameworks. *Nucleic Acids Research* **2013,** *42*, (D1), D643-D648.
51. Glöckner, F. O.; Yilmaz, P.; Quast, C.; Gerken, J.; Beccati, A.; Ciuprina, A.; Bruns, G.; Yarza, P.; Peplies, J.; Westram, R.; Ludwig, W., 25 years of serving the community with ribosomal RNA gene reference databases and tools. *J Biotechnol* **2017,** *261*, 169-176.
52. Yoshimura, K.; Matsui, H.; Morita, N., Development of Polyglycolic- and Polylactic-Acid Fluid-Loss-Control Materials for Fracturing Fluids. *SPE-168179-PA* **2016,** *30*, (04), 295-309.
53. Lee, H.-S.; Torres, C. I.; Parameswaran, P.; Rittmann, B. E., Fate of H2 in an upflow single-chamber microbial electrolysis cell using a metal-catalyst-free cathode. *Environmental Science & Technology* **2009,** *43*, (20), 7971-7976.
54. Rousseau, R.; Dominguez-Benetton, X.; Délia, M.-L.; Bergel, A., Microbial bioanodes with high salinity tolerance for microbial fuel cells and microbial electrolysis cells. *Electrochemistry Communications* **2013,** *33*, 1-4.
55. Widdel, F.; Knittel, K.; Galushko, A., Anaerobic Hydrocarbon-Degrading Microorganisms: An Overview. In *Handbook of Hydrocarbon and Lipid Microbiology*, Timmis, K. N., Ed. Springer Berlin Heidelberg: Berlin, Heidelberg, 2010; pp 1997-2021.
56. Lewis, A. J.; Campa, M. F.; Hazen, T. C.; Borole, A. P., Unravelling biocomplexity of electroactive biofilms for producing hydrogen from biomass. *Microb. Biotechnol.* **2018,** *11*, (1), 84-97.

57. Carmona-Martínez, A. A.; Trably, E.; Milferstedt, K.; Lacroix, R.; Etcheverry, L.; Bernet, N., Long-term continuous production of H2 in a microbial electrolysis cell (MEC) treating saline wastewater. *Water Research* **2015,** *81*, 149-156.
58. Call, D.; Logan, B. E., Hydrogen Production in a Single Chamber Microbial Electrolysis Cell Lacking a Membrane. *Environmental Science & Technology* **2008,** *42*, (9), 3401-3406.
59. Borole, A. P.; Lewis, A. J., Proton transfer in microbial electrolysis cells. *Sustainable Energy Fuels* **2017,** *1*, (4), 725-736.
60. Lewis, A. J.; Borole, A. P., Microbial electrolysis cells using complex substrates achieve high performance via continuous feeding-based control of reactor concentrations and community structure. *Applied Energy* **2019,** *240*, 608-616.
61. Grady, E. N.; MacDonald, J.; Liu, L.; Richman, A.; Yuan, Z.-C., Current knowledge and perspectives of Paenibacillus: a review. *Microb Cell Fact* **2016,** *15*, (1), 203-203.
62. Li, Y.-F.; Calley, J. N.; Ebert, P. J.; Helmes, E. B., Paenibacillus lentus sp. nov., a β-mannanolytic bacterium isolated from mixed soil samples in a selective enrichment using guar gum as the sole carbon source. *International Journal of Systematic and Evolutionary Microbiology* **2014,** *64*, (Pt 4), 1166-1172.
63. Nevin, K. P.; Zhang, P.; Franks, A. E.; Woodard, T. L.; Lovley, D. R., Anaerobes unleashed: Aerobic fuel cells of Geobacter sulfurreducens. *Journal of Power Sources* **2011,** *196*, (18), 7514-7518.
64. Miyahara, M.; Kouzuma, A.; Watanabe, K., Sodium chloride concentration determines exoelectrogens in anode biofilms occurring from mangrove-grown brackish sediment. *Bioresource Technology* **2016,** *218*, 674-679.
65. Reguera, G.; McCarthy, K. D.; Mehta, T.; Nicoll, J. S.; Tuominen, M. T.; Lovley, D. R., Extracellular electron transfer via microbial nanowires. *Nature* **2005,** *435*, (7045), 1098-1101.
66. Paul, V. G.; Minteer, S. D.; Treu, B. L.; Mormile, M. R., Ability of a haloalkaliphilic bacterium isolated from Soap Lake, Washington to generate electricity at pH 11.0 and 7% salinity. *Environmental Technology* **2014,** *35*, (8), 1003-1011.
67. Daly, R. A.; Borton, M. A.; Wilkins, M. J.; Hoyt, D. W.; Kountz, D. J.; Wolfe, R. A.; Welch, S. A.; Marcus, D. N.; Trexler, R. V.; MacRae, J. D.; Krzycki, J. A.; Cole, D. R.; Mouser, P. J.; Wrighton, K. C., Microbial metabolisms in a 2.5-km-deep ecosystem created by hydraulic fracturing in shales. *Nature Microbiology* **2016,** *1*, 16146.
68. Booker, A. E.; Hoyt, D. W.; Meulia, T.; Eder, E.; Nicora, C. D.; Purvine, S. O.; Daly, R. A.; Moore, J. D.; Wunch, K.; Pfiffner, S. M.; Lipton, M. S.; Mouser, P. J.; Wrighton, K. C.; Wilkins, M. J., Deep-Subsurface Pressure Stimulates Metabolic Plasticity in Shale-Colonizing Halanaerobium spp. *Appl Environ Microbiol* **2019,** *85*, (12), e00018-19.
69. Murali Mohan, A.; Hartsock, A.; Bibby, K. J.; Hammack, R. W.; Vidic, R. D.; Gregory, K. B., Microbial Community Changes in Hydraulic Fracturing Fluids and Produced Water from Shale Gas Extraction. *Environmental Science & Technology* **2013,** *47*, (22), 13141-13150.
70. Gauthier, M. J.; Lafay, B.; Christen, R.; Fernandez, L.; Acquaviva, M.; Bonin, P.; Bertrand, J.-C., Marinobacter hydrocarbonoclasticus gen. nov., sp. nov., a New, Extremely Halotolerant, Hydrocarbon-Degrading Marine Bacterium. *International Journal of Systematic and Evolutionary Microbiology* **1992,** *42*, (4), 568-576.
71. *Bergey's Manual of Systematics of Archaea and Bacteria*. John Wiley & Sons: 2015; p 1-2.

72. Hakansson, A.; Molin, G., Gut microbiota and inflammation. *Nutrients* **2011,** *3*, (6), 637-682.
73. Kim, J. R.; Beecroft, N. J.; Varcoe, J. R.; Dinsdale, R. M.; Guwy, A. J.; Slade, R. C. T.; Thumser, A.; Avignone-Rossa, C.; Premier, G. C., Spatiotemporal development of the bacterial community in a tubular longitudinal microbial fuel cell. *Applied Microbiology and Biotechnology* **2011,** *90*, (3), 1179-1191.

Chapter I Appendix

Cation exchange membranes were replaced with anion exchange membranes in order to prevent membrane rupture, as shown in Figure 4. This was successful, however additional deposits accumulated on anion exchange membranes, causing rises in over potential. This was remedied by introducing phosphate pretreatment, which prevented the membrane fouling observed.

Figure 4: Cation exchange membrane fouling associated with Ca^{2+} and pH gradients in bicarbonate buffered media. Left image is a new membrane, the right image is a damaged one. The reactors, which regularly encounter pH imbalances in the anode and cathode, facilitated Ca^{2+} precipitation on both cation and anion exchange membranes. Submersion in 1 M HCl temporarily relieved observed operating voltage rise but did not fix ruptured membranes.

COD modified measurement method

To adjust for the residual interference, a standard curve was created by varying the chloride concentration and COD concentration in Hach COD vials using a modified version of the same method described earlier in this section. Conductivities of 13.7, 20, 25, 30, 35, and 40 mS/cm were made by adding NaCl until the desired conductivity was reached to 1 L of anode liquid media. Saline COD standards were created using potassium hydrogen phthalate at 0, 0.15,

0.5, and 0.8 g-COD/L, which was suspended in concentrated anode liquid media by taking 5X concentrated version of the anode liquid media, and diluting with potassium hydrogen phthalate solution and DI until the COD concentrations desired were reached. Standards were vortexed for 5 seconds to mix thoroughly. These standards were then diluted 4 times before use in COD vials with 0.5 g additional mercuric sulfate, where the samples were digested as described earlier in this section. This process was replicated at the all of the conductivities mentioned to find the relationship between conductivity, baseline interference, and standard curve slope. PPW COD was determined using a 25- and 50-fold dilution using deionized water, and used the slope determined from the standards to find the COD of the substrate.

Figure 5 shows the resultant conductivity relationship used to determine the COD of a saline solution using deionized water as the blank. From there, the equation used to describe COD for all saline samples was determined to be the following by multiplying the slope and intercepts determined by the dilution factor used, which was 4 for samples, and 25 or 50 for produced water samples:

$$COD = 2.631(dillution\ factor)(abs.) - 0.043\left(\frac{cond.}{dillution\ factor}\right)$$

Where abs. represents the absorbance of the high range COD vial, and cond. is the measured conductivity of the sample before dilution in mS/cm.

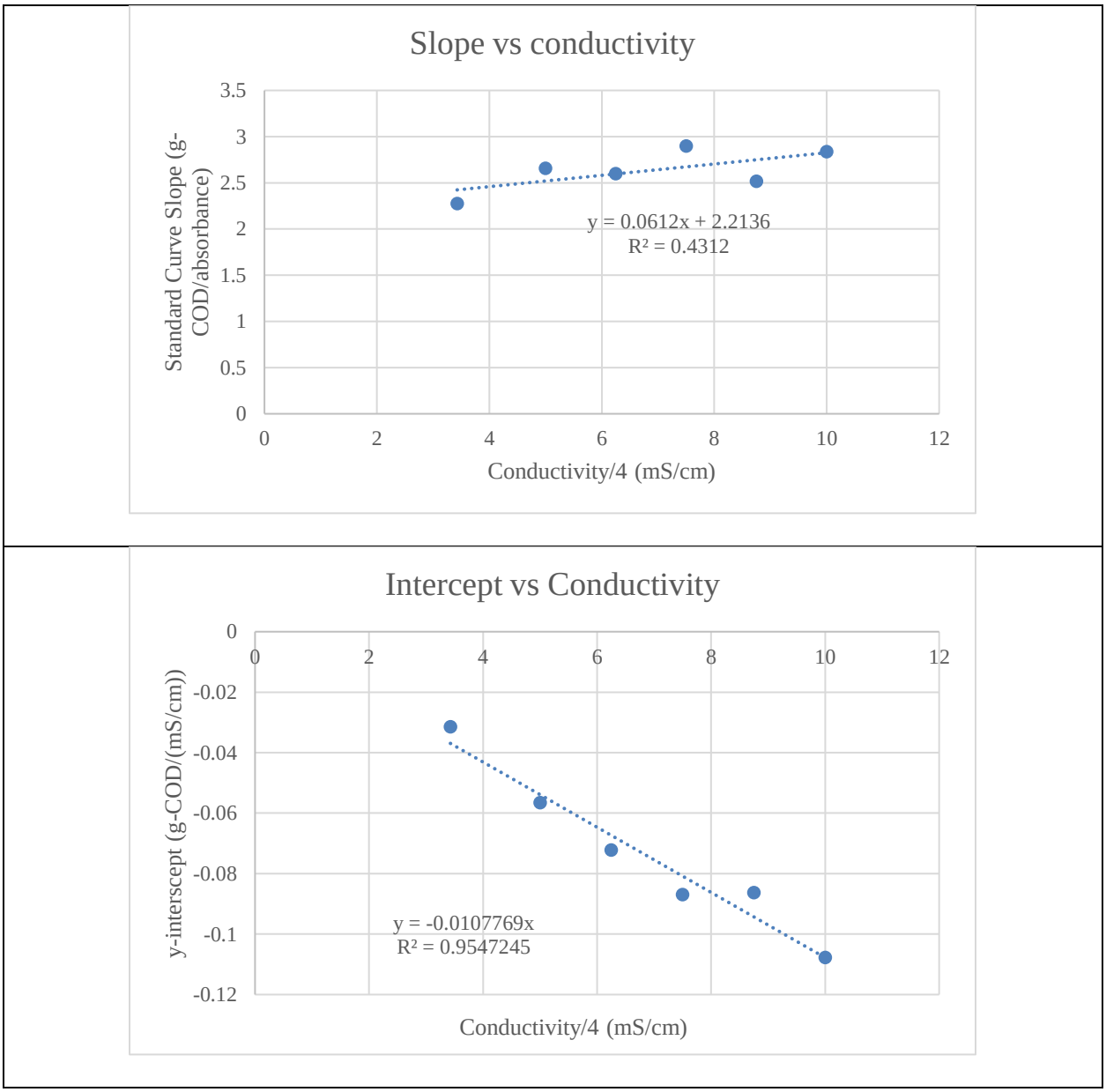

Figure 5: COD standard curve intercept associated with saline COD measurements in 4X diluted samples and y intercept for linear interpolation. Linear regression poorly fit Slope vs Conductivity date ($R^2 < 0.5$) but fit intercept data much better. Thus, an average for the slope was taken instead.

Bulk Properties of Untreated Produced Water and PPW

Table 4: Bulk properties of the produced water before and after treatment.

	Untreated Produced Water	**PPW**
COD (g/L)	2.66 ± 0.19	2.34 ± 0.28
Conductivity (mS/cm)	131.2	143.1
pH	7.06	6.36

Electron Balance

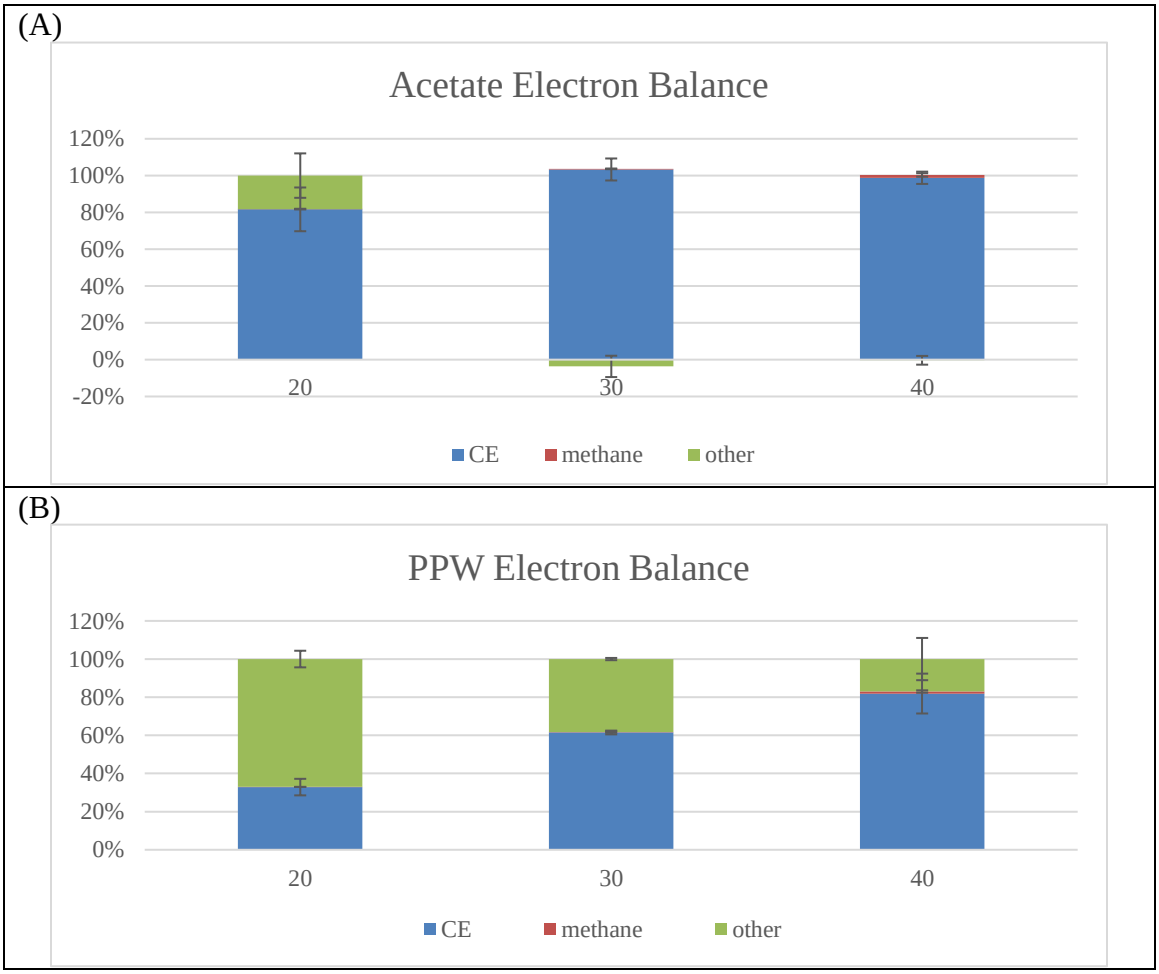

Figure 6: Electron balance of all the sinks, including electrons contributed to current as anode Coulombic efficiency (CE), methane, and other sinks, for both acetate and produced water fed MECs at different conductivities tested. Note, less than 1.6% of all conditions had electrons diverted to methane, indicating that sinks were present elsewhere other than methanogenesis.

Cyclic Voltammetry

Cyclic Voltammetry (CV) was performed on all tested conditions during batch addition. CV was performed starting at an anode applied potential of -0.5V and ramped to 0.1 V and back to -0.5 V at a sweep rate of 1 V/s. During the time CV was performed (20 minutes) this had negligible

effect on the performance and efficiency of the MECs. In all conditions tested, the CV showed maximum currents were created using acetate as the substrate rather than PPW.

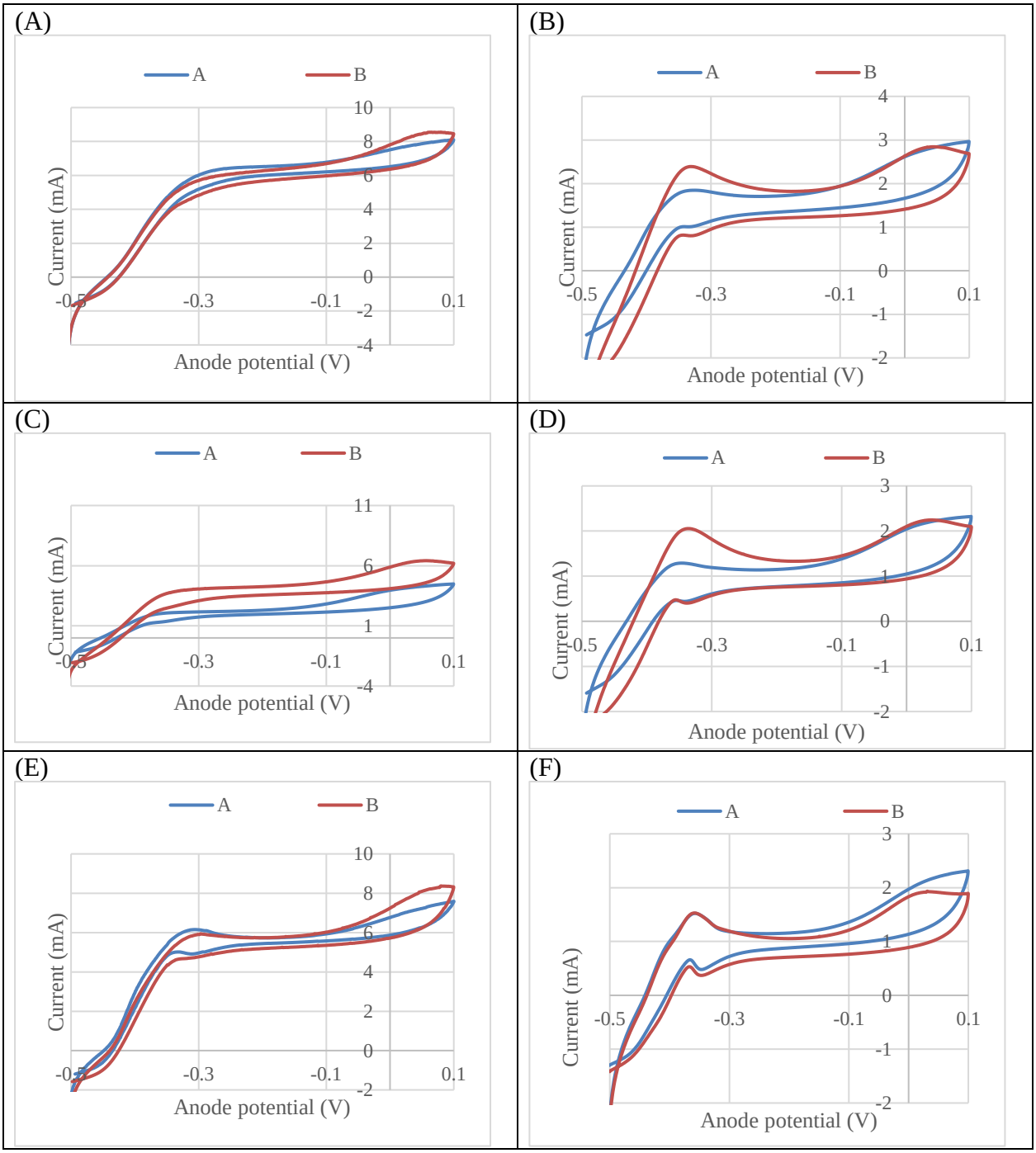

Figure 7: Cyclic voltammetry (CV) associated with MECs operating on PPW and acetate for each replicate (A and B). CV curves are averaged from both replicates. (A) and (B) are for 40 mS/cm for acetate and PPW respectively, (C) and (D) are for 30 mS/cm for acetate and PPW respectively, and (E) and (F) are for 20 mS/cm for acetate and PPW respectively.

CHAPTER II

MICROBIAL ELECTROLYSIS USING AQUEOUS FRACTIONS DERIVED FROM TAIL-GAS RECYCLE PYROLYSIS OF WILLOW AND GUAYULE

This chapter was originally published by:

Satinover, S. J.; Elkasabi, Y.; Nuñez, A.; Rodriguez, M.; Borole, A. P., Microbial electrolysis using aqueous fractions derived from Tail-Gas Recycle Pyrolysis of willow and guayule. *Bioresource Technology* **2019,** *274*, 302-312.

4-hydroxybenzoic acid was incorrectly mentioned in the publication, when it was actually 4-hydroxybenzaldehyde. Additionally, some of the phrasing in the Appendix of this chapter had been adjusted for accuracy. An erratum has been sent to the publisher to address these changes, though it does not affect the most important conclusions. Otherwise, minor grammatical and formatting changes have been made to this chapter from the version in print. Satinover, S. conducted the microbial electrolysis work and High-Performance Liquid Chromatography (HPLC), as well as performed the analysis and wrote the chapter, making revisions suggested by coauthors. Elkasabi Y produced the pyrolysis aqueous products used in the experiments. Nuñez A performed the Ultra High-Performance Liquid Chromatography and Mass Spectrometry on the samples provided by Satinover, S. Rodriguez Jr. M assisted with HPLC of samples provided by Satinover, S. Borole A. provided guidance and feedback on experiments, data analysis, manuscript preparation, editing the drafts, and submitted the final version for journal publication.

Abstract

This study investigated microbial electrolysis of two aqueous phase waste products derived from guayule and willow generated from tail gas recycle pyrolysis (TGRP). The highest average current density achieved was 5.0 ± 0.7 A/m^2 and 1.8 ± 0.2 A/m^2 for willow and guayule respectively. Average hydrogen productivity was 5.0 ± 1.0 L/L-day from willow and 1.5 ± 0.2 L/L-day for guayule. Willow also generated higher Coulombic efficiency, anode conversion

efficiency, and hydrogen recovery than guayule. Compounds investigated exceeded 80% degradation, which included organic acids, sugar derivatives, and phenolics. Mass spectrometric analysis demonstrated the accumulation of a long chain amine not present in either substrate before treatment, and the persistence of several peptide residues resulting from the TGRP process. New biorefineries may one day capitalize on this otherwise discarded byproduct of TGRP, further improving the potential applications and value of microbial electrolysis towards energy production.

Introduction

The United States generates a large quantity of biomass which can be used for production of biofuels and bioproducts. The Department of Energy's, "2016 Billion-Ton Report", suggests that the US could sustainably create 1 billion tons of biomass without adversely affecting supplies of feedstocks and materials to other industries [1]. Of this biomass, a significant portion is generated as unused waste production with no economic value. The report estimates that 123 to 155 million dry tons of unused biomass waste are produced per year [1].

One frequently cited technology used to convert such unused feedstocks into energy products is pyrolysis, where the feedstock is elevated to a high temperature in an anoxic environment for a short period of time. Depending on the exposure time and temperature, the pyrolysis may be characterized as slow, intermediate, or fast. Fast pyrolysis, for instance, traditionally creates a product that is primarily liquid (up to 80 wt%) while slow pyrolysis produces a larger quantity of solid product known biochar [2, 3]. The oil phase, known as bio-oil, is a flammable liquid, which has potential to be converted into hydrocarbon fuels. Fast pyrolysis

can be used to create a high yield of oil from renewable biomass, making it a valuable candidate for renewable fuel creation.

Bio-oil, however, often requires other treatments to become a suitable product, like as a substitute for refined crude oil products. Bio-oil contains a high weight percentage of oxygen compared to traditional hydrocarbons, resulting in low stability and insufficient heating value [4]. Treatments such as hydrocracking and hydrodeoxygenation are used to improve quality of the bio-oil or upgrade it, requiring a consistent source of high purity hydrogen gas. Combining these constraints, upgrading bio-oil becomes prohibitively energy intensive and expensive [5]. Additionally, the hydrogen used is often produced by nonrenewable processes like natural gas via steam reforming [6], which contributes to greenhouse gas emissions. These problems make pyrolysis products economically and, in some cases, environmentally less attractive than conventionally extracted hydrocarbons. To solve these challenges, finding a cheaper and renewable source of hydrogen is essential.

One technology that may solve this challenge is microbial electrolysis, which has been used to generate hydrogen efficiently from unconventional resources. Microbial electrolysis cells (MECs) are bioelectrochemical systems (BES)s [7], closely related to microbial fuel cells (MFCs), but require an external potential to generate hydrogen. In BESs, the bacteria degrade organic materials and externally reduce chemical species or deposit electrons to conductive surfaces, generating current from the stored chemical energy of the organics [8]. While MECs require energy to create hydrogen, their operation is theoretically less energy intensive than standard water electrolysis cells, as the microbial metabolism of organics allows for the catalysis of products that leads to a smaller redox potential gap for hydrogen production. In the past, BESs have been demonstrated to convert a diverse number of biodegradable organics such as volatile

organic acids, sugars, and phenolics [9-12], which represent significant fractions of more complex waste streams. Complex waste products derived from renewable sources therefore represent a potential asset for renewable hydrogen generation.

Pyrolysis processing produces a waste byproduct that may be suitable for use as a substrate in MECs [13]. The water phase and water-soluble products of pyrolysis, known here as pyrolysis aqueous phase (PyAP), contain high organic content and represents a loss if it is not valorized. PyAP derived from biomass contains lignin-derived subunits such as methoxylated phenolics and other phenolic acids, aldehydes and ketones, as well as pyrolysis sugar derivatives like levoglucosan [14, 15], which together make up a significant fraction of the total organic content found in PyAP. Some of these components are relatively toxic to humans, their composition is complex, and in many cases PyAPs are not fully characterized. Total organic carbon (TOC) of PyAP can also be quite high, varying from tens of and up to more than one hundred g/L [16, 17]. The extracted TOC concentration depends on how the PyAP is processed; TOC can be extracted by adding deionized water to the bio-oil, however other extraction techniques using pretreatment of PyAP have been investigated [18]. Pretreatment methods should try to separate the compounds which are unnecessary or detrimental to downstream operations so that they can be valorized via other methods. Hydrogen production via MEC technology therefore may be able to use many different PyAPs, owning its viability to the biodiversity of the biofilm which allows high flexibility in adapting to a wide range of organic compounds.

One method recently employed within the biomass pyrolysis framework is Tail-Gas Recycle Pyrolysis (TGRP), which recycles the end gas products of the pyrolysis reactor to supplement the energy required. While the TGRP process produces smaller oil yields (15 - 35 wt%,), it produces an oil phase of an improved quality by means of a lower oxygen content (8 -

25 wt%) [19-21], depending on feedstock and the specific conditions used. At the same time, the volume of produced PyAP increases due to increased water production in the process. Hence, the TGRP process offers a means for producing distillable usable oils. Complex aqueous wastes like PyAPs from TGRP thus represent a potential feedstock for sustainable hydrogen production through use of MECs. However, comparisons between complex feedstocks for hydrogen production using a single reactor configuration are rare, and do not exist for PyAPs. PyAP and other pyrolysis aqueous waste streams, being slightly more specific than industrial and municipal wastewaters traditionally discussed, have received less attention. Comparisons between BES performance amongst different biomasses have been done before, though these comparisons commonly rely on sources from multiple different studies, feedstocks, and reactors [11, 22], which makes differences less attributable to feedstock alone. Performance comparisons of a specific BES in a known configuration using complex feedstocks from similar sources will elucidate the challenges of operating BESs with real waste products as a potential technology in biorefineries and extend the application further to a wider range of waste streams.

For complex substrates, the significant differences between potential substrates introduces an added challenge, that BESs must be able to convert a wide variety of substrates without too large an adaptation period. These criteria will dictate how viable this technology will be for commercialization. Additionally, work using mature biofilms is important for obtaining commercially relevant process data. As of this publication, no studies have been conducted using and comparing the performance of a fully developed MEC anode using multiple PyAP sources. This study thus compared the performance of an MEC using PyAP streams derived from the same pyrolysis treatment from two different feedstocks: willow and guayule. By adjusting the concentration of substrate delivered to the system within each experiment, any discrepancies in

performance as a function of concentration are tracked over time. In addition, individual compound concentrations were measured for predominant compounds and tracked to understand the conversion efficiency of easily degradable as well as recalcitrant chemical species.

Source of Biomass and Substrate

This study used PyAPs from two biomass sources: willow and guayule. These two substrate sources are markedly different in composition and traditional use. Willow has had a long and rich history as an agricultural product and building material because of its ability to grow quickly in moist soils. By contrast, guayule shrubs are notable for their ability to grow in arid conditions, making them more resilient to drought than willow, and being primarily a source of hypoallergenic rubber. The rubber accounts for a small percentage of the total biomass, and interest in utilizing the remaining biomass has grown. Recently, it has been found that the post-rubber extracted biomass of guayule, called bagasse, could be used to create high energy dense bio-oils from fast pyrolysis [23]. Willow, on the other hand, has been cultivated for the creation of biomass to be used for energy and has been used for production of biogas/syngas production. Production of hydrogen has been investigated in pre and post processing using torrefaction [24, 25], however, the product is not of high purity and is generally not the only intended product of torrefaction. By contrast, MECs are commonly configured to produce hydrogen gas at high purity.

No study has used willow or guayule as a substrate in MECs to produce hydrogen to date. Therefore, this study expands the prior work done on pyrolysis-based biomass substrates in MECs [26, 27] by using guayule- and willow-derived PyAPs and comparing the two feedstocks with each other as well as with previously published literature on switchgrass-based MECs. By using a pre-grown anode, the biofilm growth phase associated with most BES experiments was

minimized. The effect of substrate loading and mode of operation (batch vs. continuous supply) were investigated. Typical MEC parameters including hydrogen productivity, recovery, and current densities were determined to understand the potential of MECs to treat the aqueous phase generated from willow and guayule.

Materials and Methods

TGRP of Willow and Guayule

Pyrolysis products were produced at the Eastern Regional Research Center, according to previously-published methods [19-21]. Briefly, ground biomass of choice was fed into a fluidized bed reactor (500 ^{o}C) at 2 - 3 kg/hr, with a residence time of approximately 0.5 - 2 s. A cyclone separated solid char particles from the hot vapors, and a series of cold-water condensers condensed the vapors into liquid. Experiments used the aqueous phases from the first two condenser fractions. Electrostatic precipitation was used to remove the remaining organics of the resulting non-condensable gases after the last condenser. Leftover gases were recycled back into the reactor to account for 50−70% of the pyrolysis reactor gas using a preheater and gas blower, while the remaining gas was additional nitrogen. For guayule pyrolysis, a mixture of 70% guayule bagasse and 30% guayule leaves were used. The willow substrate was made from stems, which were chipped and ground prior to TGRP.

MEC Design, Enrichment, and Set Up

MECs were used from experiments previously described, using the matured biofilm established [28]. Just before experiments, the MECs were operated on PyAP derived from red oak for several weeks, which resulted in well-established biofilms. No inoculation procedure or preparation were therefore used, and the anode was not mechanically or chemically altered in

any way before use in experiments. The anode chamber was made from a 3.81 cm (1.5 in) inner diameter PVC pipe with a thickness of 1.27 cm (0.5 in) and a total volume of 16 mL. The anode contained two 0.635 in (0.25 in) thick pieces of carbon felt (Alfa Aesar, Tewksbury, MA) sandwiched over a thin stainless steel rod, used as the current collector. A membrane electrode assembly (MEA) (Sainergy Tech, Inc., Marrieta, GA) was used as the cation exchange membrane, and was made out of Nafion 115 and 0.5 mg Pt/cm^2 deposited carbon. These materials served as the separator and the cathode catalyst respectively. The cathode chamber was constructed from an equally sized PVC pipe, and used a circular stainless streel mesh interfaced with the Pt-deposited carbon, attached to a stainless-steel wire, as the current collector. Two grooved polycarbonate end plates served as the cell enclosure. A central grooved plate served as a support for the MEA and ensured contact between surfaces. Two rubber gaskets on each end of the anode chamber were used to ensure a liquid tight anode that could be regularly opened for maintenance. In addition to the anode and cathode, an Ag/AgCl reference electrode (Basi Inc, West Lafayette, IN) was inserted into a port drilled on the side of the anode chamber. Each experiment was run using two MECs to ascertain reproducibility, and the same MECs were used for each organic loading condition. Experiments were conducted on the two PyAPs in sequence, allowing for one week of adaptation time with each new substrate. The first substrate used was the guayule-derived PyAP, followed by the willow-derived PyAP. The aqueous streams were filtered before use in the reactors using a 0.2 μm nylon filter.

Mode of MEC Operation – Batch vs. Continuous Feeding

The MECs were operated using the protocol reported previously [26]. To summarize, 12 mL of 200 mM potassium phosphate buffer to a pH of 7 was used in the cathode and replaced before each experiment via an inlet port at the bottom of the cathode enclosure. Fresh cathode

buffer was sparged with nitrogen for 15 minutes before each experiment. A tube from the top of the cathode was inserted into an inverted graduated cylinder immersed in water to record cathode gas accumulation and ensure a negative pressure on the cathode, which has been shown to improve hydrogen production and inhibit methanogenesis [29]. A tee with a septum was installed in the cathode gas line allow for cathode gas sample collection. Gas volumes were recorded every 24 h. The anode liquid medium included monobasic and dibasic sodium phosphate, ammonium chloride, potassium chloride, and trace minerals and vitamins, as reported previously [26, 30]. A graduated cylinder was used to measure out 200 mL of medium, which was sparged for 30 minutes before circulation. After sparging, 40 mL of media was used to flush the anode chamber and lines prior to each run. Substrate was added via a septum inlet approximately 4 inches below the inlet of the anode chamber. A syringe pump (Cole-Parmer, Vernon Hills, Il) was used to control the substrate delivery rate. Cells were operated at a liquid flow rate of 3.5 mL/min. Liquid flowrate was controlled by a peristaltic pump (Cole Parmer, Vernon Hills, Il). Figure 8 shows a schematic for the MEC experimental set up.

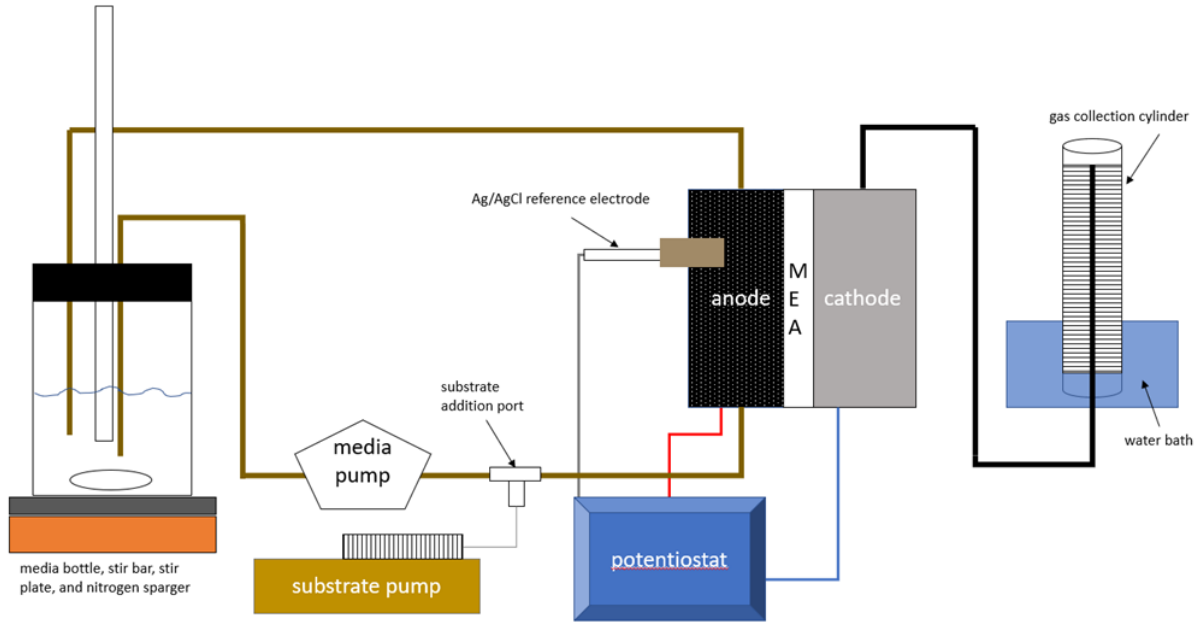

Figure 8: Schematic diagram used for investigating TGRP PyAP conversion to hydrogen using an MEC.

The cells were operated using a three-electrode setup and by poising the anode potential at -0.2 V relative to the reference electrode. Three organic loading rates were investigated for continuous experiments: 2, 4, and 10 grams of chemical oxygen demand (COD) per liter anode volume per day (g/L-day) for a period of 48 to 72 h. Filtered substrate was diluted from the originally measured COD to 4, 8, and 20 g of COD per liter (g/L) using deionized water, which was then injected at a rate of 275 µL/hr, to achieve the desired substrate delivery rate. For batch experiments, 0.2 and 0.5 g/L was conducted for both substrates, where the substrate was added directly to the media bottle containing fresh media. Batch experiments ran for 24 h. A Bio-Logic VSP potentiostat (Bio-Logic USA, Knoxville, TN) was used to apply the anode potential and record current. A DataQ DI-1100 (DataQ Instruments, Akron, Ohio) along with WinDaq software was used to record the operating voltage of the cells. During experiments, MECs were measured for COD every 24 h.

Compound Identification via High-Performance Liquid Chromatography and Ultra High-Performance Liquid Chromatography-Mass Spectrometry (UHPLC-MS)

Compounds of interest and methods were established based on prior work [26, 27, 31]. To summarize, samples were acquired for High-Performance Liquid Chromatography (HPLC) at the end of the 10 g/L-day experiment. The run with the highest loading was used since it would have the greatest change in the individual compounds as a result of the MEC treatment. HPLC was done with two detectors: (1) a photo diode array (PDA) and (2) a refractive index detector (RID) (SPD-M20A and RID-20A respectively, Shimadzu, Torrance, CA). The detectors were operated at a temperature of 50°C. The spectra collected by the PDA detector over the range a range of 190-800 nm was used to determine maximum absorbance, and the corresponding retention time and area were recorded. This was used to designate the identity of the compounds based on standards and then used to determine concentrations in samples from the MEC runs. The column used for the analysis was an Aminex HPX-87H by Bio-Rad (Bio-Rad, Hercules, CA), and it was run at 60°C. Samples were run using a 5 mM H_2SO_4 mobile phase for two h at a flow rate of 0.5 mL/min. Ten compounds were quantified including furfural, 5-hydroxymethylfurfural, acetic acid, vanillic acid, syringic acid, catechol, phenol, levoglucosan, propionic acid, and 4-hydroxybenzoic acid. Standards of these compounds were prepared at concentrations of 1, 0.1, and 0.02 g/L, and run along with PyAP and blank samples. Both PyAPs were diluted to 1 g/L and 0.1 g/L to quantify the compounds, after acidification with 5 mM H_2SO_4. In addition to the ten compounds quantified by HPLC, Ultra-High-Performance Liquid Chromatography-Mass Spectrometry (UHPLC-MS) was used to identify unknown peaks in the samples. This analysis was conducted on samples collected from the 10 g/L-day run. The analysis was performed using a Nano-Acquity UHPLC (Waters Co. Milford, MA) with an Atlantis C18, 1.7 µm, 150 x 1 mm column (Waters) using a gradient based on two solvents: water with 0.1% formic acid as solvent

A and acetonitrile with 0.1% formic acid as solvent B. The flow rate was 60µl/min with the following elution profile: 95% A and 5% B at initial time, followed by a linear gradient to 50% A and 50% B at 40 minutes, finished by a column wash at 45 with 15% A and 85% B. The water and acetonitrile were mass spectrometry grade (Optima LC/MS grade, Fisher Scientific, Fair Lawn, NJ). The UHPLC effluent was directed to a Q-Exactive Plus Orbitrap mass spectrometer (Thermo Electron America LLC. Madison, WI) operated with an ESI-HESI-II probe set to scan with a resolution of 140,000 (at 200 Da) between the mass range of 90 to 1500 Da and using the polysiloxane peak at *m/z* 391.28429 as internal to obtain the minimal error ($\Delta M/M_{Calculated}$) in the mass determination (>1 ppm). The probe was set at 300 ^{o}C with a capillary voltage to 2.5 kV. Tandem mass spectrometry (MS/MS) data was obtained at a normalized energy of 30 eV and a resolution of 70,000 (at 200 Da). Protonated compounds ion formulas for the monoisotopic mass of $[M+H]^+$ were determined with the mass spectrometer software Xcalibur (Thermo), using C, N, O, and S as possible element components of the ions eluting under the chromatographic peaks of the corresponding sample. The isotopic pattern of the $[M+H]^+$ was compared with the simulated model predicted by the software using a resolution of 140,000 (at 200Da). This alternative allowed the verification of the reported composition of molecular formulas with great accuracy in compounds with $[M+H]^+$ below *m/z* 400. For larger $[M+H]^+$ ions, the calculated formulas were confirmed by the resulting MS/MS fragments and the calculated composition.

COD Analysis and Calculations

Current density, hydrogen productivity, Coulombic efficiency, hydrogen recovery, cathode conversion efficiency, electrical efficiency, and overall energy efficiency were calculated using the electrochemical and chemical data generated in this study. Calculations were performed as described previously [26]. To summarize, current density (A/m^2) is described by:

$$CD = \frac{I_{avg}}{A}$$

I_{avg} is the observed average current, and A is the projected surface area of the anode. In this set of experiments, the projected surface area of the anode was found to be 12.83 cm^2. Hydrogen productivity (L/L-day) is defined as:

$$H_{prod} = \frac{V_H}{V_{ano}t}$$

Where V_H is the volume of hydrogen observed, V_{ano} is the anode volume, and t is the time that the hydrogen was produced in. Here, the anode volume remaining was approximated to be 83% of the 16 mL anode enclosure volume. Anode Coulombic efficiency was determined by:

$$CE_{anode} = \frac{I_{avg}}{I_e}$$

Where I_e represents the theoretical current that could be derived from the system, which is determined by the amount of charge available due to the amount of COD converted in the reactor, divided by the time of the experiment. Cathode conversion efficiency was found by the following expression:

$$CCE = \left(\frac{PV_H/RT}{\frac{I_{avg}t}{2F}} \right)$$

Where F is Faraday's constant. Cathode conversion efficiency is used as an alternative metric to hydrogen recovery to measure cell performance because it relies on the moles of electrons generated in the cell as function of current, versus using the COD converted, to determine how effectively current produced translates to hydrogen production. Hydrogen recovery was calculated using:

$$Y_{H2} = \frac{PV_H/RT}{2\Delta nCOD}$$

Where the numerator is used to estimate the moles of hydrogen collected in the cylinder based on the pressure (P), volume of hydrogen recorded, the universal gas constant (R), and the temperature of the experiment (T). Conditions used for these calculations were assumed to be at room temperature and pressure (P = 101.325 kPa, T = 296.15 K). The denominator represents the equivalent amount of hydrogen that could be theoretically produced based on the moles of COD converted (ΔnCOD).

Voltage data was used in conjunction with electrochemical and chemical data to calculate two metrics, electrical efficiency and overall energy efficiency. Electrical efficiency is defined as:

$$\eta_E = \frac{-W_{H_2}}{W_E}$$

Where W_{H2} is the combustion energy of hydrogen and W_E is the electrical energy determined by the time, the average current, and voltage applied to the cell. To determine the combustion energy, the heating value of hydrogen was assumed to be 285.8 kJ/mol. Overall energy efficiency builds on electrical efficiency by incorporating the energy stored in the substrate, and is calculated by:

$$\eta_{E+S} = \frac{W_{H_2}}{W_s - W_E}$$

The energy content of the substrate was assigned a value of 14.955 kJ/g-COD, also used by Lewis et al. [26].

COD was determined using high range Hach COD vials and a Hach DRB 200 instrument (Hach Company, Loveland, CO). Absorbance of samples at 620 nm were measured via a Spectronic 20 Genesys colorimeter (Millipore Sigma, St. Louis, MO) to observe oxidized chromate ions. A set of standards from known COD concentration, ranging from 50 to 1000 mg-

COD/L were created using a Hach standard containing 1000 mg-COD/L. Two measurements of COD were used for each PyAP and averaged to determine COD of substrate used for experiments.

Results and Discussion

Characterization of Aqueous Phase

The COD of guayule and willow-derived PyAP was determined to be 89.0 ± 4.1 g/L and 76.8 ± 0.3 g/L, respectively. Switchgrass PyAP was also reanalyzed for comparison and was found to have a COD of 133.9 ± 3.4 g/L. Compared to the COD of the switchgrass PyAP, the COD of the two substrates used in this study was considerably lower. Nevertheless, organic content was sufficiently high that a dilution was necessary prior to use in MECs. Municipal wastewater, which has almost two orders of magnitude lower COD, is typically used directly in MECs. The COD of the substrates used here also indicates the high chemical energy content of the aqueous phase, suggesting potential for high hydrogen recovery.

HPLC analysis of the two feedstocks resulted in detection of nine individual compounds. These compounds were acetic acid, 5-hydroxymethylfurfural, vanillic acid, syringic acid, catechol, phenol, levoglucosan, propionic acid, and 4-hydrobenzoic acid. HPLC determined that the willow PyAP's COD resulted from larger quantities of identifiable organics compared to the guayule sample. Specifically, 65.0% of the COD present in the willow substrate was attributed to the compounds identified by HPLC, while only 9.4% of the COD of the guayule sample was accounted for by HPLC. Of the ten compounds detected, only vanillic acid and catechol were found to be at higher percentages in guayule. Table 6 in the Appendix of this chapter shows this data in more detail. While not all organic compounds were detected in the substrates, this

proposes a compelling possibility that the convertible compounds detected in willow contributed to current and hydrogen production much more easily than the other organics in guayule, which were most likely recalcitrant.

While a few compounds were identified by UHPLC-MS, they could not be quantified due to lack of standards. However, the similarities and differences between the two substrates can be investigated using available data. UHPLC-MS was run for 40 minutes per sample, sample products indicated here were eluting between 2 and 20 minutes with no product detected after that time. All the compounds identified were nitrogenated, and no sulfur derived compounds were found. While the HPLC was configured to detect primarily polar and soluble compounds, the UHPLC-MS used a C18 column, enabling detection of less soluble compounds, further providing an insight into novel molecules present in the substrates. Also, the UHPLC-MS identified heavier molecular weight compounds than those found in HPLC due to a cutoff point of 150 Da used to assure data accuracy. Further, compounds containing nitrogen often ionize well by electrospray, the technique used here for UHPLC-MS. Thus, the large nitrogen containing compounds observed are expected. Observing the resultant retention times and proposed mass compositions, many of the compounds present are not found in nature and are not easily identifiable. As a result, standards were not available for analysis and their conversion could not be quantified in the reactors. There are some differences in the species identified in the two samples, which could be due to the different sources of biomass. Some similarities were also observed, which could be due to the similar treatment (TGRP) of the feedstocks. In general, guayule PyAP had more observed species than willow within the retention time window observed. While there are several discrepancies between the two substrates, several compounds are common. Specifically, the peaks eluting at approximately 5.8, 9.8, and 12.4 min with MS/MS

spectra are related to unnatural peptide residues resulting from the TGRP treatment, which correspond to $C_{12}H_{23}O_2N_2$, $C_{24}H_{45}O_4N_4$ and $C_{36}H_{67}O_6N_6$ respectively. From MS/MS analysis, all three of these compounds appeared to have a cyclohexylamine, (public database compound #7281 https://www.mzcloud.org). From the analysis, it is likely that these residues were created by the TGRP process, as cyclohexanes are not found in naturally occurring amino acids and peptides. However, the rest of the residues appear to be composed of either lysine, followed by one to three leucine or isoleucine amino acids, which all occur naturally. An associated structure for the other compounds in raw substrates was not determined because of insufficient mass spectrometric data.

Current Density, Total COD Conversion, H_2 Production, and Energy Efficiency from Willow and Guayule-derived Aqueous Phase

Figure 9 shows the average current density, maximum current density, hydrogen productivity, anode Coulombic efficiency, cathode conversion efficiency, and hydrogen recovery associated with each substrate at 2, 4, and 10 g/L-day loading, and batch experiments at 0.2 and 0.5 g/L, which are labeled and oriented from left to right on each figure.

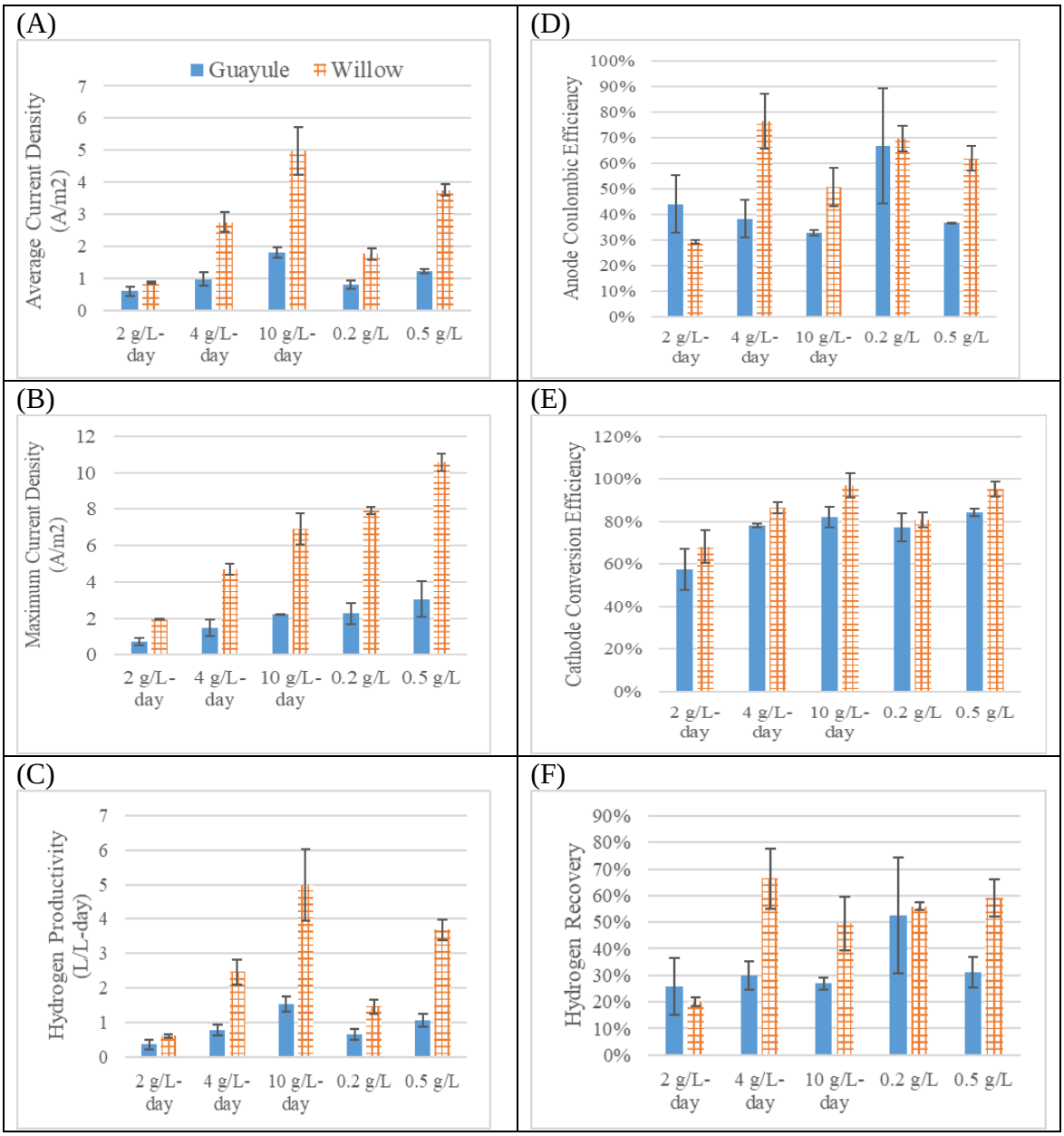

Figure 9: Performance of MECs during conversion of pyrolysis aqueous phase from willow and guayule sources. Average (A) and maximum (B) current density, A/m^2, hydrogen productivity in L-H_2/L-anode volume-day (L/L-day) (C), anode Coulombic efficiency (D) cathode conversion efficiency (E) and hydrogen recovery (F) from guayule and willow-derived pyrolysis aqueous phase using MEC. Continuous experiments (2,4, and 10 g/L-day) were analyzed every 24 h for 48 -72 h, and batch experiments (0.2 and 0.5 g/L) were run for 24 h. Error bars represent the standard deviation associated with the replicates.

The maximum current density was achieved by the willow substrate under 0.5 g/L-day loading conditions at 10.6 ± 0.5 A/m^2, however this was short lived, as the average over the 24-h period

was only 3.8 ± 0.2 A/m^2. By contrast, the continuous runs had a much narrower margin of difference between maximum and average current densities, where the maximum current density observed for willow was 6.9 ± 0.9 A/m^2 at 10 g/L-day, and the average at the same loading was 5.0 ± 0.7 A/m^2. Other studies that utilized a pyrolysis derived aqueous substrate, and the same reactor configuration, yielded similar results. Lewis et al. reported an average current density of 4.5 ± 0.2 A/m^2 at 10 g/L-day [26], and Park et al. reported an average current density of 5.3 ± 0.2 A/m^2 under the same loading conditions [27]. Thus, the willow's current density was similar to those of previously studied similar substrates. By contrast, guayule-derived PyAP substrate underperformed compared to the willow-derived substrate for both hydrogen production rates and current density. The maximum current density was also achieved at 0.5 g/L batch experiments, at only 3.1 ± 1.0 A/m^2, which was less than a third of what was observed with the willow substrate. Observing the relative acetate concentration alone should rectify this discrepancy, as acetate is traditionally the model substrate for exoelectrogens and is used commonly in BES studies for this reason. The willow substrate, having nearly 30% of its COD contributed to by acetate, should produce more current and hydrogen than an equivalent substrate delivery rate where all the other compounds were only detected to account for 10% of the measured COD. While it is possible that other easily fermentable compounds not detected by HPLC exist, the performance of the cells combined with the discovered composition suggests otherwise, resulting in a significantly underperforming cell compared to those run on other substrates as previously discussed.

Total COD conversion was also different between the two substrates, as shown in Table 5.

Table 5: COD conversion percentage by loading and substrate. For all trials, more COD was degraded using the willow and guayule PyAP. This was partially reflected in performance differences.

Substrate	Organic Loading	COD removal (%)
Guayule	2 g/L-day	45.2 ± 0.4%
	4 g/L-day	43.0 ± 1.1%
	10 g/L-day	39.5 ± 2.3%
	0.2 g/L	24.5 ± 4.0%
	0.5 g/L	31.4 ± 0.6%
Willow	2 g/L-day	70.7 ± 3.2%
	4 g/L-day	61.5 ± 1.6%
	10 g/L-day	66.8 ± 0.2%
	0.2 g/L	57.0 ± 3.9%
	0.5 g/L	60.2 ± 5.3%

MECs using the willow substrate converted more overall COD in all trials than MECs running on guayule PyAP. This partially indicates the relative recalcitrance of the guayule compared to the willow substrate within our system, but it also explains in part why the current density was lower than the willow PyAP. Without degrading as many of the available organics, not as many electrons would have become available to be used for generating current. However, this difference in degradation does not appear proportional to performance, indicating that other inhibitions using the guayule substrate are preventing organics from being converted effectively to electrons.

The willow substrate achieved a maximum hydrogen productivity of 5.0 ± 1.0 L/L-day at an organic loading of 10 g/L-day, while the guayule substrate produced only 1.5 ± 0.2 L/L-day at the same loading. By comparison with other pyrolysis derived aqueous streams, Lewis et al. reported a maximum hydrogen production rate of 4.3 L/L-day [26], and Park et al. reported 4.3 L/L-day [27]. Thus, the results produced by the willow substrate are in line with prior experiments, however the guayule substrate underperformed. Given the composition of the guayule PyAP, this

result is expected, as with less or slower converted organic substrate it can be expected that less hydrogen productivity will occur due to fewer available electrons produced. Pyrolysis aqueous products like those used in this study can be fermentation limiting [31], and in conjunction with the COD degradation information, it is possible that this limitation holds true with guayule. The contribution of acetate to COD found in willow (31.0%) compared to guayule (3.0%) supports the idea that the willow PyAP should be a more quickly and easily converted substrate. However, the added complexity of the substrates and the inability to identify all the organics present in this study impedes a more detailed level of understanding that would more strongly confirm this possibility.

These performance metrics are not the highest observed for simple substrates. Jeremiasse et al. was able to achieve a current density of 22.8 A/m^2 and a hydrogen productivity of over 50 L/L-day with acetate as the carbon source [32], although the concentration of the carbon used was much higher, calculated here at 491 g- $NaCH_3COO \cdot 3H_2O$ /L-day approximated with their described anode volume, which is equal to roughly 231 g/L-day by COD, while ours was only provided 10 g/L-day. Thus, it may be possible to increase the loading beyond 10 g/L-day to achieve higher hydrogen productivity and current densities than demonstrated in this study. However, to do so practically, pH adjustment must be kept at a minimum, which was performed daily at 10 g/L-day for the systems used here. Another limitation comes from the length of these experiments. In our study, current stability was observed for no more than three days, however long-term experiments on the order of weeks will be necessary to confirm cell stability and performance for other substrates like PyAPs. Ultimately, high performing cells will need to maintain pH neutrality for many days without excessive reliance on buffered media solutions,

while also preventing cathodes from being colonized by hydrogenotrophic methanogens or methanogens that can operate via electron transfer, both of which have been found in BESs [33, 34].

Anode Coulombic efficiencies were not correlated to loading conditions necessarily, however cathode conversion efficiency increased as substrate delivery increased. Shown in Figure 2(D), the highest anode Coulombic efficiency was produced by the willow substrate at 4 g/L, at 76.4 ± 10.6%, while the anode Coulombic efficiency for the guayule was observed at 66.9 ± 22.5% at 0.2 g-COD/L. Anode Coulombic efficiency has been previously reported to decrease with increasing loading rate. Lewis et al. reported the anode Coulombic efficiency dropped from 96% to 54% with increased loading from 2 to 10 g/L-day for the switchgrass pyrolysis aqueous product [26]. The demonstrated anode Coulombic efficiencies have room for improvement, though there may be some potential explanations that were not investigated directly. While the willow PyAP created Coulombic efficiencies that were similar to prior work using the same reactor configuration [26, 27], guayule PyAP did not. The guayule-fed MEC produced an insoluble material that appeared to build up in the nutrient reservoir. Conversion of COD into this material may have reduced the Coulombic efficiency. Further characterization of this observed insoluble material would be useful but was beyond the scope of this study. The guayule substrate is a small demonstration of this potential limitation for various biomass streams. Further decomposition may be achieved through other means not performed here, such as using acidic, basic, thermal, or other chemical pretreatments not used for these waste streams. pH neutralization of pyrolysis aqueous phase products similar to the PyAPs discussed in this study has been shown to remove significant fractions of organic acids present in the oil phase of the pyrolysis products, which were then used in microbial electrolysis reactors [27]. Such investigation may provide useful for optimizing future MEC feedstocks for hydrogen production.

Prior work has shown that cathode efficiency increased as substrate concentration increased [26, 27], which is consistent with the results shown here. However, an increased loading under batch conditions was also reported to decrease cathode conversion efficiency [26], which was not shown here as seen in figure 2(E). Cathode conversion efficiency was consistently higher for willow substrate than for guayule for all loading conditions, also shown in Figure 2(E). The highest cathode conversion efficiency was observed with continuous experiments at an organic loading of 10 g-COD/L using willow, which reached 97.1 ± 5.6%. By contrast, guayule operated MECs had their highest cathode conversion efficiency during the 0.5 g/L batch experiment at 84.4 ± 11.4%. In general, these values agree with previous findings on other pyrolysis aqueous products. Lewis et al. reported a cathode conversion efficiency of 94 ± 5.5% [26], and Park et al. reported a conversion efficiency that exceeded 80% for 10 g/L-day experiments [27].

Combining anode and cathode efficiencies, hydrogen recovery was calculated as shown in Figure 2(F). For the willow substrate, hydrogen recovery was highest in the continuous experiment at 4 g/L-day, reaching a recovery of 66.3 ± 11.2%, while the guayule substrate demonstrated its largest average hydrogen recovery at 0.2 g/L for a recovery of 52.5 ± 21.9%. The hydrogen recovery of guayule was lower than willow in all experiments except for the 2 g/L-day experiment. However, the total hydrogen produced for the guayule was still much lower than willow for all cases, and a recovery below 30% is significantly less than other studies using pyrolysis aqueous products as substrates. Lewis et al. reported a hydrogen recovery (also referred to as percent hydrogen yield) as high as 72 ± 1.8% in batch experiments, and was no less than 50% for all experiments [26]. Park et al. also reported hydrogen recoveries of approximately 50% for all runs [27]. Thus, while the willow substrate experiments are similar to other MECs utilizing pyrolysis derived aqueous products, guayule was not. Few studies have made comparisons

between batch, fed-batch, or continuous performance of MECs for complex substrates, but there is some evidence worth discussing. Lewis et al. was perhaps the first paper to compare the performance of MECs in batch vs continuous experiments using a pyrolysis aqueous product. The authors concluded that continuous and batch experiments lost anode Coulombic efficiency as loading was increased in both cases, which was only supported for the guayule substrate [26]. Another study using a microbial desalination cell found that the cells lost Coulombic efficiency in batch experiments (from 94% - 74%) whereas continuous experiments retained a stable Coulombic efficiency (45%), indicating some loss in overall performance while operating in batch over time [35]. Pannell et al. has also made this comparison using MFCs treating a corn stover derived fermentation product, where anode conversion efficiency dropped as cells were operated in fed-batch mode, while continuously fed cells remained stable [36].

The average cell voltage measured for the MECs ranged from 0.8 to 1.1 V. For the willow PyAP, the maximum voltage was 1.1 ± 0.08 V, observed at an organic loading of 10 g/L-day, and the minimum was 0.8 ± 0.001 V at a loading of 2 g/L-day. For the guayule PyAP, the maximum and minimum voltage was 1.0 ± 0.001 V and 0.8 ± 0.05 V at 10 g/L-day and 2 g/L-day, respectively. Electrical efficiency was largest for the 0.5 g/L batch experiments for both substrates, at 144.4 ± 3.4% and 144.1 ± 23.7% for the willow and guayule PyAP, respectively. Compared to water electrolysis, this is a two-fold higher efficiency further demonstrating the advantage of MECs beyond valorization of waste compounds. Overall energy efficiency was much lower, with a maximum of 47%, obtained for willow PyAP at 4 g/L-day continuous operation. Additional data on overall energy efficiency is included in the Appendix of this chapter. Thus, this technology and the substrates show promise and the performance can be improved via further investigations.

HPLC Results

Figure 10(A) shows the percent removal of individual compounds detected in the MECs, and Figure 10(B) shows the average rate of removal of these compounds over the length of the experiment as compared to switch grass PyAP from prior experiments [26]. All of the compounds investigated had a positive net degradation except for 5-hydroxymethylfurfural, which accumulated.

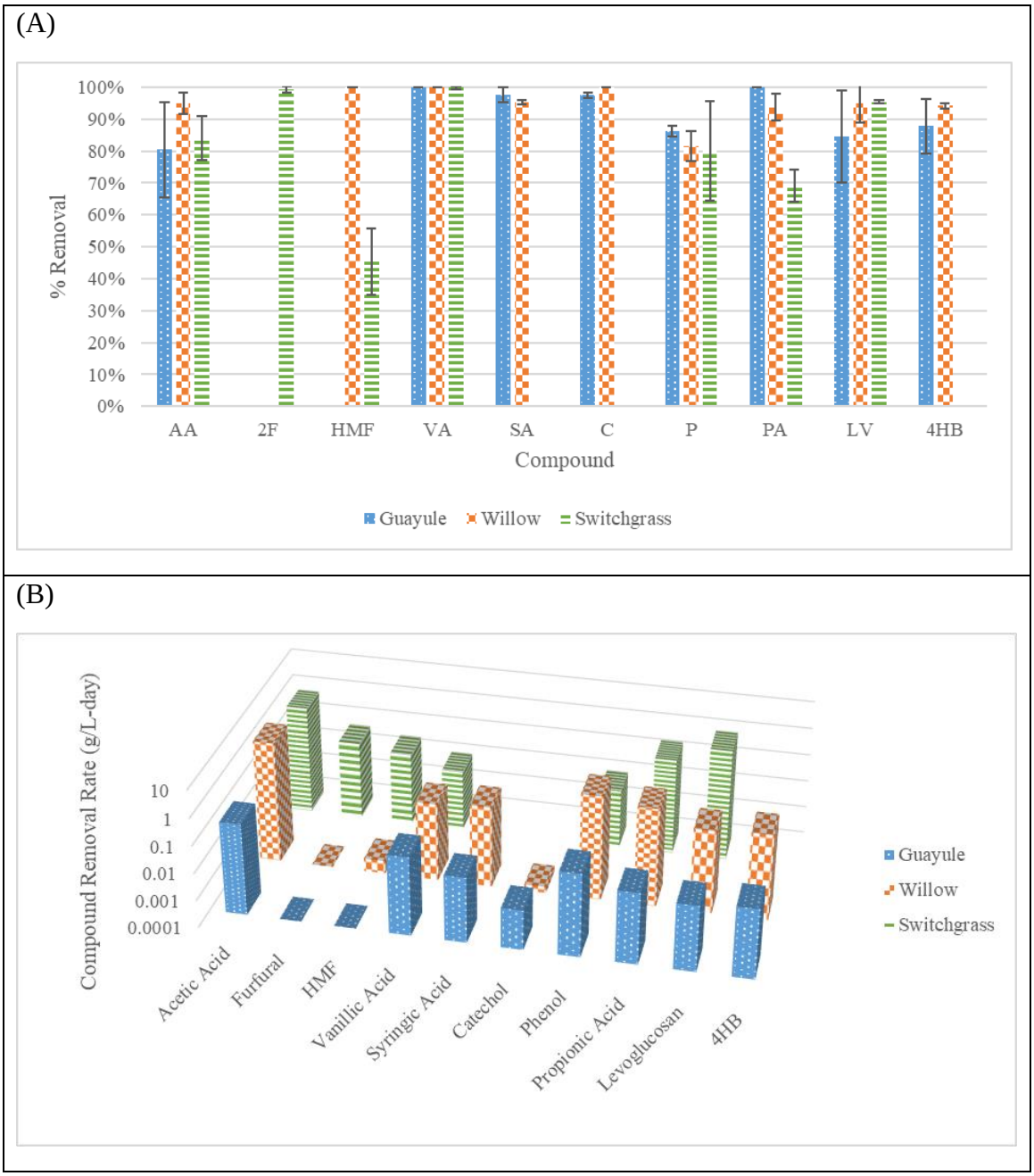

Figure 10: Percentage removal of compounds from aqueous phase during 10 g/L-day for guayule and willow substrates (A) and rate of removal of the same phase during hydrogen production in MEC at substrate loading 10 g/L-day (B). The results shown for switchgrass are also at the same loading rate [26]. The abbreviations are: acetic acid (AA), furfural (2F), 5-hydroxymethylfurfural (HMF), vanillic acid (VA), syringic acid (SA), catechol (C), phenol (P), levoglucosan (LV), propionic acid (PA), and 4-Hydroxybenzaldehyde (4HB). Not shown are accumulated chemicals, which only occurred for 5-hydroxymethylfurfural in the guayule trial. Error bars represent the standard deviation associated with the replicates.

Transformation of Furanic Compounds

The furanic compounds examined here are furfural and 5-hydroxymethylfurfural (HMF). Furanic compounds have been demonstrated to inhibit MEC performance and fermenter metabolism [9, 37]. These inhibitory effects only occur above a certain threshold, as illustrated by Zeng et al. therefore conversion of such compounds can still occur in MECs at lower concentrations [10]. Here, only HMF was detected in the willow PyAP at a concentration of 0.03 mg/L. Additionally, while HMF appeared to be below detectable limits in the untreated guayule PyAP, it accumulated in small quantities when the MECs were run on the guayule substrate, where less than 0.04 mg/L was detected. HMF is not often a biological byproduct, but more well known as a byproduct of thermal treatment of biomass like pyrolysis. Thus, it is unlikely that the MECs created the HMF as an intermediate in MEC operation. Most likely, the amount present in the guayule was below detectable limits but accumulated enough to exceed the detectable limit in the final sample. For both substrates, the amount of HMF was less than any of the other compounds investigated. Additionally, the concentrations detected are still substantially lower than what was has been tested earlier and it is unlikely these small quantities of HMF affected performance. Zeng et al. reported a 50% decrease in performance using a concentration 3.0 g/L HMF [9], more than four orders of magnitude above the concentrations detected in this study. Given the small quantities of HMF detected and the complete absence of furfural, it is unlikely that furanic compounds played a significant role in inhibition or hydrogen production for either PyAP tested here.

Transformation of Phenolic Compounds

Like furanic compounds, phenolic compounds have also been demonstrated to be inhibitory to exoelectrogenic populations in MECs at high concentrations, exhibiting conversion

at lower concentration [9, 10]. Here, the phenolics investigated are phenol, catechol, syringic acid, vanillic acid, and 4-hydroxybenzaldehyde acid. Despite the inhibition potentially created by these compounds, the MECs were able to consume significant fractions of all phenolics recorded. For example, vanillic acid presence was observed to be below detectable limits for both treated substrates. Catechol conversion must be taken with some additional context. Assessment of catechol degradation is slightly difficult, since it is a potential intermediate of degradation of other phenolic compounds [9, 10]. More specifically, catechol has been demonstrated as an intermediate product associated with the degradation of substituted benzoic acids by *Streptomyces* [38]. While the two substrates had similar proportions of vanillic acid, any additional catechol that was created must have been partially consumed as part of the substrate delivery. The same conclusions can be drawn for phenol. Phenol and catechol have been shown to be a transformation products in MECs from more complex phenolics [9]. While no benzoic acids were directly quantified here, a precursor was identified. 4-hydroxybenzaldehyde is regularly converted to 4-hydroxybenzoic acid via p-hydroxybenzaldehyde dehydrogenase. This enzyme is created by several types of organisms, including microbes. One notable microbe is *P. putida* [39], which has been found in BESs in the past [40]. However, 4-hydroxybenzoic acid may not be created during MEC operation. The exoelectrogen G. *metallireducens* has also been suggested to degrade this compound by channeling it to benzoyl-CoA [41]. Additionally, 4-hydroxybenzaldehyde has been previously degraded when added to MFCs as part of a mixture of other fermentation inhibitors [42]. Thus, it may not necessarily be inhibitory to exoelectrogenic activity as much as other phenolic compounds. Because 4-hydroxybenzaldehyde had high degradation percentages in our reactors (above 80%), it is likely that inhibition that would have been observed by accumulation did not occur. At the concentrations provided, none of the

phenolics appeared to be toxic, though their relative complexity may require more complex biochemical pathways to degrade than model substrates like acetate.

Conversion of Organic Acids and Sugar Derivatives

Carbonyl/carboxyl groups analyzed here include propionate, acetate, and the sole sugar derivative included levoglucosan. Acetate and levoglucosan were converted more readily in willow substrate run MECs than on guayule. Propionate was significantly converted for both substrates, as more than 90% of propionic acid that was delivered was converted in both substrates. Propionic acid is traditionally difficult to degrade compared to other substrates, and can accumulate rather than degrade in anaerobic digesters but is not necessarily inhibitory [43]. Since, 2005, MFCs have been used to demonstrate propionate degradation and generation as the sole carbon source and a part of wastewater [44]. Recently, propionic acid degradation in MECs has been shown at high concentrations using selectively enriched communities. Hari et al. recently demonstrated a comparison between acetate and propionate as the sole carbon sources for MECs, tracking the community structure as a function of carbon source and time, at difference concentrations for each substrate. Using concentrations up to 4 g-COD/L for both substrates, the authors found that cells consumed more acetate than propionate, and that *Geobacter* was a dominant genus for all concentrations of substrate [45]. For more complex substrates like those used in this study, the interactions between microbes utilized to degrade compounds is less understood. Even with just propionate, the transportation and flow of electrons can vary solely based on concentration of substrate used [46]. However, in comparison to the study using only propionate and acetate, the removal percentage demonstrated in this study was higher than what was found for high concentrations experiments by Hari et al. (75 ± 14% for high concentration reactors at 4 g-COD/L, where ours was 93.8 ± 4.1% for willow, and 100 ±

0.0% for guayule). Correctly identifying the source of these differences is challenging, it could be the result of different community structure, process control, or simply a function of concentration. The propionate concentrations delivered over 72 h the 10 g/L-day experiments were conducted was significantly less for both willow (88 mg/L) and guayule (8 mg/L) PyAPs than what was added by Hari et al. (2607 mg/L) [45].

UHPLC/MS Product Degradation

From the samples collected after 10 g/L-day runs for both substrates. several compounds showed significant degradation or accumulation. Compared to the raw substrates, several compounds were below detectable limits. In particular, compounds $C_{10}H_{11}O_2N_2$ and $C_{11}H_{18}N_3$ appeared to have degraded significantly, if not entirely. Much like the raw substrates, many other structures could not be determined here, however there is one exception. $C_{10}H_{24}N$ appears to be the only compound that accumulated from both substrates. This compound appears at 13.61 minutes and produced a spectra consistent with decylamine. The compound structures can be found in Figure 11 in the Appendix. The process by which decylamine is produced is unclear. However, it is unlikely that it is derived from the peptide residues or organics detected by HPLC. This compound is likely a cleavage product from a more complex molecule that the UHPLC/MS did not detect due to its large molecular weight, most likely composing a larger bulk molecule. The peptide residues do not have a long enough straight carbon chain in any part of their composition, and no amino acid groups found in nature have this structure as part of their side chain group either. Biochemically, other rearrangements of molecules would be unlikely. Still, decylamine is not unique to biomass TGRP. Although decylamine appeared to accumulate in both reactors, this compound can be degraded. At least one strain of *Pseudomonas* has been shown to degrade several saturated long chain amines, ranging from C_3 to C_{18} [47]. Other

compounds accumulated were substrate specific, such as $C_{13}H_{14}N_3$ from the willow substrate. However, without a metric to compare quantities, and without more sophisticated omics techniques identifying the community behavior more closely, the pathway that chemicals identified here were either generated or degraded from could not be determined. Such investigation will unravel the necessary individual microbes, their syntrophies, and explanations for limitations associated with complex feedstock degradation, a necessity for further optimizing MEC performance on complex feedstocks, and PyAPs in particular.

Future Prospects of MEC—Integrated Technologies

MECs can convert a wide array of diverse substrates, while simultaneously creating very valuable end products. With the findings discussed here and the substrates used in other studies referenced earlier [26, 27], pyrolysis waste products are becoming an increasingly viable waste stream that can be generated from multiple sources, including switchgrass, guayule, and willow plants. Future biorefineries may capitalize on this substrate ambivalence by quickly adapting MECs to produce hydrogen for newly created biofuels regardless of source. As more pretreated biomass aqueous byproducts become generated, MEC technology will become more popular, ushering in unique combinations of pretreatment. For instance, Shen et al. recently reported successful MEC operation using an aqueous product from hydrothermal liquefaction treated swine manure [48]. Dark fermentation has also been coupled with MEC operation in the past for treating industrial wastewater [49]. Concurrent treatment steps may also be necessary for energy recovery, as one study by Beegle and Borole investigated the effect of thermal and pH modification on substrates for use in an anaerobic digestor coupled MEC [50], while another study by Park et al. combined anaerobic digestion with an MEC for improved methane generation in a standard anaerobic digester [51]. Because of this diversity of applications, MECs may find

themselves easily integrated in many unique biorefinery and wastewater treatment processes that can be readily supplemented with prior or concurrent treatment mechanisms. Biogas creation and utilization can vary based on the source of the substrate. For aqueous products like PyAPs, the hydrogen could be used onsite for fuel upgrading, but excess hydrogen may also be useful for other applications like for use in onsite fuel cells or as part of a growing market for hydrogen use as fuel for transportation. This study therefore contributes to a growing body of work that shows a significant amount of potential in unconventional waste streams for hydrogen production. To continue this work, more substrates derived from biomass, and pyrolysis aqueous products in particular, must be conducted to ensure MEC viability. However, although new substrates continue to be demonstrated in MECs, they are not without their limitations. Several challenges outside of using certain substrates need to be addressed before MECs become commercially feasible. The biggest will be to improve sustained hydrogen production rates, which may be accomplished by higher organic loading and adequately scaling up technology. MEC scale up has historically been a significant challenge that remains an open field of inquiry. Performance must also be achieved without inhibition caused by unconverted organics, anode product inhibition, or the necessity to use costly processes to ensure continued cell operation, such as real time pH adjustment, media sparging, precipitate/scale removal, etc. Many of these issues may be alleviated by improving mass transfer from the anode to the cathode, limitations commonly found in MECs [52], however finding the ideal method to improve mass transfer remains an open question that will not necessarily be limited by biology. MEC viability will also be improved by reducing reactor costs, which may be accomplished by replacing the cathode catalyst and the MEAs used with cheaper alternatives, and by reducing energy requirements such as reducing flow rates and applied cell voltages. Any number of these changes may impede performance.

Finding a compromise between cost and performance will be a challenge for the foreseeable future. New technological advancements will require an interdisciplinary perspective, borrowing elements from not only biological sciences and biosystems engineering, but chemical, mechanical, materials, and electrical engineering, among other applied sciences.

Conclusions

This study investigated and compared the performance of MECs operating on two PyAPs from willow and guayule plants from the same pyrolysis process and MEC configuration. In general, the willow substrate had a significant fraction of more easily convertible organic compounds and generally outperformed the guayule-fed MECs. MECs using the willow PyAP were comparable in performance to other MECs using biomass reported in literature. HPLC confirmed significant degradation of organic acids, sugar derivatives, and phenolics, many of which are inhibitory. UHPLC/MS also confirmed the degradation of several new nitrogenous compounds, not reported previously. Future biorefinery and bio-oil upgrading feasibility will require demonstration of efficient hydrogen production at larger scales.

References

1. DOE, 2016 Billion-Ton Report | Department of Energy. **2016**.
2. Bridgwater, T.; Meier, D.; Radlein, D., *An Overview of Fast Pyrolysis of Biomass*. 1999; Vol. 30, p 1479.
3. Ronsse, F.; van Hecke, S.; Dickinson, D.; Prins, W., Production and characterization of slow pyrolysis biochar: influence of feedstock type and pyrolysis conditions. *GCB Bioenergy* **2013,** *5*, (2), 104-115.
4. Mortensen, P. M.; Grunwaldt, J. D.; Jensen, P. A.; Knudsen, K. G.; Jensen, A. D., A review of catalytic upgrading of bio-oil to engine fuels. *Applied Catalysis A: General* **2011,** *407*, (1), 1-19.
5. Czernik, S.; Bridgwater, A. V., Overview of Applications of Biomass Fast Pyrolysis Oil. *Energy Fuels* **2004,** *18*, (2), 590-598.
6. Ogden, J. M., Prospects for building a hydrogen energy infrastructure. *Annu. Rev. Energy. Environ.* **1999,** *24*, (1), 227-279.
7. Borole, A.; Reguera, G.; Ringeisen, B.; Wang, Z.-W.; Feng, Y.; Hong Kim, B., Electroactive biofilms: Current status and future research needs. *Energy & Environmental Science* **2011,** *4*, (12), 4813-4834.
8. Logan, B. E., Exoelectrogenic bacteria that power microbial fuel cells. *Nat Rev Micro* **2009,** *7*, (5), 375-381.
9. Zeng, X.; Borole, A. P.; Pavlostathis, S. G., Inhibitory Effect of Furanic and Phenolic Compounds on Exoelectrogenesis in a Microbial Electrolysis Cell Bioanode. *Environmental Science & Technology* **2016,** *50*, (20), 11357-11365.
10. Zeng, X.; Borole, A. P.; Pavlostathis, S. G., Biotransformation of Furanic and Phenolic Compounds with Hydrogen Gas Production in a Microbial Electrolysis Cell. *Environmental Science & Technology* **2015,** *49*, (22), 13667-13675.
11. Pandey, P.; Shinde, V. N.; Deopurkar, R. L.; Kale, S. P.; Patil, S. A.; Pant, D., Recent advances in the use of different substrates in microbial fuel cells toward wastewater treatment and simultaneous energy recovery. *Applied Energy* **2016,** *168*, 706-723.
12. Pant, D.; Van Bogaert, G.; Diels, L.; Vanbroekhoven, K., A review of the substrates used in microbial fuel cells (MFCs) for sustainable energy production. *Bioresource Technology* **2010,** *101*, (6), 1533-1543.
13. Pandey, M. P.; Kim, C. S., Lignin Depolymerization and Conversion: A Review of Thermochemical Methods. *Chem. Eng. Technol.* **2011,** *34*, (1), 29-41.
14. P. Vispute, T.; W. Huber, G., Production of hydrogen , alkanes and polyols by aqueous phase processing of wood-derived pyrolysis oils. *Green Chemistry* **2009,** *11*, (9), 1433-1445.
15. Black, B. A.; Michener, W. E.; Ramirez, K. J.; Biddy, M. J.; Knott, B. C.; Jarvis, M. W.; Olstad, J.; Mante, O. D.; Dayton, D. C.; Beckham, G. T., Aqueous Stream Characterization from Biomass Fast Pyrolysis and Catalytic Fast Pyrolysis. *ACS Sustainable Chemistry & Engineering* **2016,** *4*, (12), 6815-6827.
16. Fan, J.; Matharu, A.; Zhang, Z.; Macquarrie, D.; Clark, J.; Hunt, A.; Shuttleworth, P.; Gronnow, M.; De bruyn, M.; Budarin, V., Low-temperature microwave-assisted pyrolysis of waste office paper and the application of bio-oil as an Al adhesive. *Green Chemistry* **2014,** *17*.

17. Sınağ, A.; Uskan, B.; Gülbay, S., Detailed characterization of the pyrolytic liquids obtained by pyrolysis of sawdust. *Journal of Analytical and Applied Pyrolysis* **2011,** *90*, (1), 48-52.
18. Park, L. K.-E.; Ren, S.; Yiacoumi, S.; Ye, X. P.; Borole, A. P.; Tsouris, C., Separation of Switchgrass Bio-Oil by Water/Organic Solvent Addition and pH Adjustment. *Energy Fuels* **2016,** *30*, (3), 2164-2173.
19. Boateng, A. A.; Elkasabi, Y.; Mullen, C. A., Guayule (Parthenium argentatum) pyrolysis biorefining: Fuels and chemicals contributed from guayule leaves via tail gas reactive pyrolysis. *Fuel* **2016,** *163*, 240-247.
20. Mullen, C. A.; Boateng, A. A.; Goldberg, N. M., Production of Deoxygenated Biomass Fast Pyrolysis Oils via Product Gas Recycling. *Energy Fuels* **2013,** *27*, (7), 3867-3874.
21. Boateng, A. A.; Mullen, C. A.; Elkasabi, Y.; McMahan, C. M., Guayule (Parthenium argentatum) pyrolysis biorefining: Production of hydrocarbon compatible bio-oils from guayule bagasse via tail-gas reactive pyrolysis. *Fuel* **2015,** *158*, 948-956.
22. Zhen, G.; Lu, X.; Kumar, G.; Bakonyi, P.; Xu, K.; Zhao, Y., Microbial electrolysis cell platform for simultaneous waste biorefinery and clean electrofuels generation: Current situation, challenges and future perspectives. *Progress in Energy and Combustion Science* **2017,** *63*, 119-145.
23. Boateng, A. A.; Mullen, C. A.; Goldberg, N. M.; Hicks, K. B.; McMahan, C. M.; Whalen, M. C.; Cornish, K., Energy-dense liquid fuel intermediates by pyrolysis of guayule (Parthenium argentatum) shrub and bagasse. *Fuel* **2009,** *88*, (11), 2207-2215.
24. Prins, M. J.; Ptasinski, K. J.; Janssen, F. J. J. G., More efficient biomass gasification via torrefaction. *Energy* **2006,** *31*, (15), 3458-3470.
25. Woytiuk, K.; Campbell, W.; Gerspacher, R.; Evitts, R. W.; Phoenix, A., The effect of torrefaction on syngas quality metrics from fluidized bed gasification of SRC willow. *Renewable Energy* **2017,** *101*, 409-416.
26. Lewis, A. J.; Ren, S.; Ye, X.; Kim, P.; Labbe, N.; Borole, A. P., Hydrogen production from switchgrass via an integrated pyrolysis–microbial electrolysis process. *Bioresource Technology* **2015,** *195*, 231-241.
27. Park, L. K.-E.; Satinover, S. J.; Yiacoumi, S.; Mayes, R. T.; Borole, A. P.; Tsouris, C., Electrosorption of organic acids from aqueous bio-oil and conversion into hydrogen via microbial electrolysis cells. *Renewable Energy* **2018,** *125*, 21-31.
28. Lewis, A. J.; Borole, A. P., Understanding the impact of flow rate and recycle on the conversion of a complex biorefinery stream using a flow-through microbial electrolysis cell. *Biochemical Engineering Journal* **2016,** *116*, (Supplement C), 95-104.
29. Lu, L.; Hou, D.; Wang, X.; Jassby, D.; Ren, Z. J., Active H2 Harvesting Prevents Methanogenesis in Microbial Electrolysis Cells. *Environmental Science & Technology Letters* **2016,** *3*, (8), 286-290.
30. Borole, A. P.; Hamilton, C. Y.; Vishnivetskaya, T. A.; Leak, D.; Andras, C.; Morrell-Falvey, J.; Keller, M.; Davison, B., Integrating engineering design improvements with exoelectrogen enrichment process to increase power output from microbial fuel cells. *Journal of Power Sources* **2009,** *191*, (2), 520-527.
31. Lewis, A. J.; Campa, M. F.; Hazen, T. C.; Borole, A. P., Unravelling biocomplexity of electroactive biofilms for producing hydrogen from biomass. *Microb. Biotechnol.* **2018,** *11*, (1), 84-97.

32. Jeremiasse, A.; Hamelers, H.; Saakes, M.; Buisman, C., Ni foam cathode enables high volumetric H2 production in a microbial electrolysis cell. *International Journal of Hydrogen Energy* **2010,** *35*, (23), 12716-12723.
33. Lee, H.-S.; Torres, C. I.; Parameswaran, P.; Rittmann, B. E., Fate of H2 in an upflow single-chamber microbial electrolysis cell using a metal-catalyst-free cathode. *Environmental Science & Technology* **2009,** *43*, (20), 7971-7976.
34. Villano, M.; Aulenta, F.; Ciucci, C.; Ferri, T.; Giuliano, A.; Majone, M., Bioelectrochemical reduction of CO2 to CH4 via direct and indirect extracellular electron transfer by a hydrogenophilic methanogenic culture. *Bioresource Technology* **2010,** *101*, (9), 3085-3090.
35. Ebrahimi, A.; Najafpour, G.; Kebria, D., Effect of batch vs. continuous mode of operation on microbial desalination cell performance treating municipal wastewater. *Iranian Journal of Hydrogen & Fuel Cell* **2016,** *3*, (4), 281-290.
36. Pannell, T. C.; Goud, R. K.; Schell, D. J.; Borole, A. P., Effect of fed-batch vs. continuous mode of operation on microbial fuel cell performance treating biorefinery wastewater. *Biochemical Engineering Journal* **2016,** *116*, 85-94.
37. Klinke, H. B.; Thomsen, A. B.; Ahring, B. K., Inhibition of ethanol-producing yeast and bacteria by degradation products produced during pre-treatment of biomass. *Applied Microbiology and Biotechnology* **2004,** *66*, (1), 10-26.
38. Sutherland, J. B.; Crawford, D. L.; Pometto, A. L., Catabolism of substituted benzoic acids by streptomyces species. *Appl Environ Microbiol* **1981,** *41*, (2), 442-8.
39. Cronin, C. N.; Kim, J.; Fuller, J. H.; Zhang, X.; McIntire, W. S., Organization and Sequences of p-Hydroxybenzaldehyde Dehydrogenase and Other Plasmid-Encoded Genes for Early Enzymes of the p-Cresol Degradative Pathway in Pseudomonas Putida NCIMB 9866 and 9869. *DNA Sequence* **1999,** *10*, (1), 7-17.
40. Majumder, D.; Maity, J. P.; Tseng, M.-J.; Nimje, V. R.; Chen, H.-R.; Chen, C.-C.; Chang, Y.-F.; Yang, T.-C.; Chen, C.-Y., Electricity Generation and Wastewater Treatment of Oil Refinery in Microbial Fuel Cells Using Pseudomonas putida. *Int J Mol Sci* **2014,** *15*, (9), 16772-16786.
41. Butler, J. E.; He, Q.; Nevin, K. P.; He, Z.; Zhou, J.; Lovley, D. R., Genomic and microarray analysis of aromatics degradation in Geobacter metallireducens and comparison to a Geobacter isolate from a contaminated field site. *BMC Genomics* **2007,** *8*, (1), 180.
42. Borole, A. P.; Mielenz, J. R.; Vishnivetskaya, T. A.; Hamilton, C. Y., Controlling accumulation of fermentation inhibitors in biorefinery recycle water using microbial fuel cells. *Biotechnology for biofuels* **2009,** *2*, (1), 7-7.
43. Pullammanappallil, P. C.; Chynoweth, D. P.; Lyberatos, G.; Svoronos, S. A., Stable performance of anaerobic digestion in the presence of a high concentration of propionic acid. *Bioresource Technology* **2001,** *78*, (2), 165-169.
44. Oh, S.; Logan, B. E., Hydrogen and electricity production from a food processing wastewater using fermentation and microbial fuel cell technologies. *Water Research* **2005,** *39*, (19), 4673-4682.
45. Hari, A. R.; Venkidusamy, K.; Katuri, K. P.; Bagchi, S.; Saikaly, P. E., Temporal Microbial Community Dynamics in Microbial Electrolysis Cells – Influence of Acetate and Propionate Concentration. *Front Microbiol* **2017,** *8*, (1371).

46. Hari, A. R.; Katuri, K. P.; Gorron, E.; Logan, B. E.; Saikaly, P. E., Multiple paths of electron flow to current in microbial electrolysis cells fed with low and high concentrations of propionate. *Applied Microbiology and Biotechnology* **2016,** *100*, (13), 5999-6011.
47. van Ginkel, C. G.; Louwerse, A.; van der Togt, B., Substrate specificity of a long-chain alkylamine-degrading Pseudomonas sp isolated from activated sludge. *Biodegradation* **2008,** *19*, (1), 129-136.
48. Shen, R.; Jiang, Y.; Ge, Z.; Lu, J.; Zhang, Y.; Liu, Z.; Ren, Z. J., Microbial electrolysis treatment of post-hydrothermal liquefaction wastewater with hydrogen generation. *Applied Energy* **2018,** *212*, 509-515.
49. Marone, A.; Ayala-Campos, O. R.; Trably, E.; Carmona-Martínez, A. A.; Moscoviz, R.; Latrille, E.; Steyer, J.-P.; Alcaraz-Gonzalez, V.; Bernet, N., Coupling dark fermentation and microbial electrolysis to enhance bio-hydrogen production from agro-industrial wastewaters and by-products in a bio-refinery framework. *International Journal of Hydrogen Energy* **2017,** *42*, (3), 1609-1621.
50. Beegle, J. R.; Borole, A. P., An integrated microbial electrolysis-anaerobic digestion process combined with pretreatment of wastewater solids to improve hydrogen production. *Environmental Science: Water Research & Technology* **2017,** *3*, (6), 1073-1085.
51. Park, J.; Lee, B.; Tian, D.; Jun, H., Bioelectrochemical enhancement of methane production from highly concentrated food waste in a combined anaerobic digester and microbial electrolysis cell. *Bioresource Technology* **2018,** *247*, 226-233.
52. Popat, S. C.; Torres, C. I., Critical transport rates that limit the performance of microbial electrochemistry technologies. *Bioresource Technology* **2016,** *215*, (Supplement C), 265-273.

Chapter II Appendix

Moles of H_2 per Mole of COD Removed

The product yield of H_2 per mole of COD removal (mol H_2/mol COD) ranged from 0.4 to 1.32 mol H_2/mol COD for the willow substrate. The lowest ratio observed occurred at 2 g/L-day at 0.4 ± 0.04, while the highest observed ratio was at 4 g/L-day at 1.3 ± 0.2 mol H_2/mol COD. Batch experiments exceeded a ratio of 1 for both 0.2 and 0.5 g/L experiments. For the guayule substrate, this ratio ranged from 0.5 to 1.0 mol H_2/mol COD. The lowest observed was during the 2 g/L-day continuous experiment at 0.5 ± 0.2 mol H_2/mol COD, and the highest was observed at the 0.2 g/L batch experiment at 1.0 ± 0.43 mol H_2/mol COD. Overall, the willow ratios were higher in all experiments than the guayule trials except for the 2 g/L-day experiment. These results agree with the hydrogen recovery values calculated. Hydrogen recovery can also be calculated by dividing the mol H_2/mol COD ratios described here by two.

Other Conversions Observed

While the conversion of only ten compounds was quantified by mass removal using chemical standards, relative compound degradation could be identified for many more compounds detected, even though the chemical names were not specified. Over the course of the HPLC run (2-h long elution), 52 individual peaks were recorded. Of those peaks, most of them degraded for both substrates, however the reactors using guayule accumulated more product peaks that the willow. Specifically, peaks for 12 compounds increased in the guayule PyAP-fed MECs, while only 6 increased in the willow PyAP-fed MECs. Similarly, willow operated MECs degraded more of the unknown compounds than guayule operated MECs. A reduction in peak area was observed for 23 peaks identified in willow vs. only 20 peaks from the guayule sample. This confirms the higher degradation potential of the willow PyAP compared to guayule PyAP.

Figures and Captions

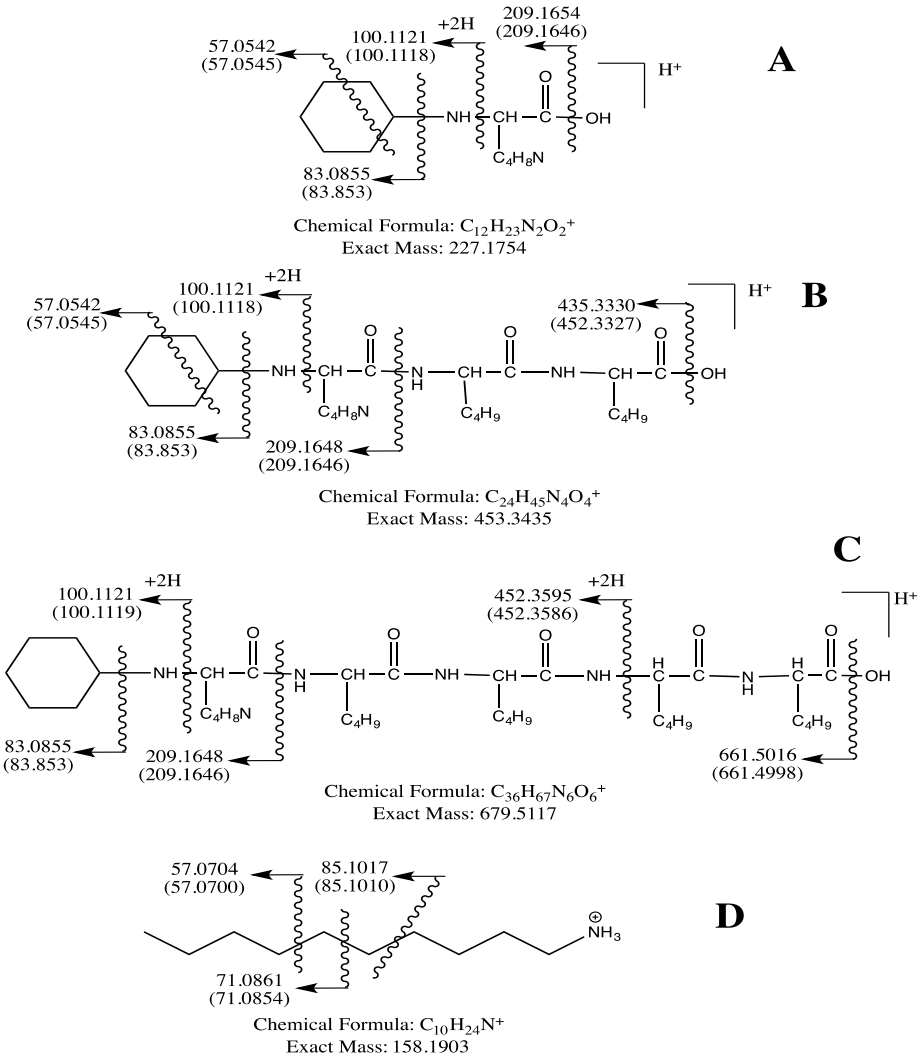

Figure 11: Proposed molecular structures, exact mass, and chemical formulas of several notable compounds identified from UHPLC-MS that were found in both substrates. Arrows represent the division of fragments observed by MS/MS analysis. The MS/MS fragments with the calculated and experimental mass are included in the parentheses. For the peaks eluting at A) 5.8 min, B) 9.8 min, C) 12.4 min, and D)13.3 min. $C_{12}H_{23}O_2N_2$, $C_{24}H_{45}O_4N_4$, $C_{36}H_{67}O_6N_6$, resemble peptide residues, while $C_{10}H_{24}N$ is a saturated long chain amine that appeared to accumulate as the MEC was operated on both substrates.

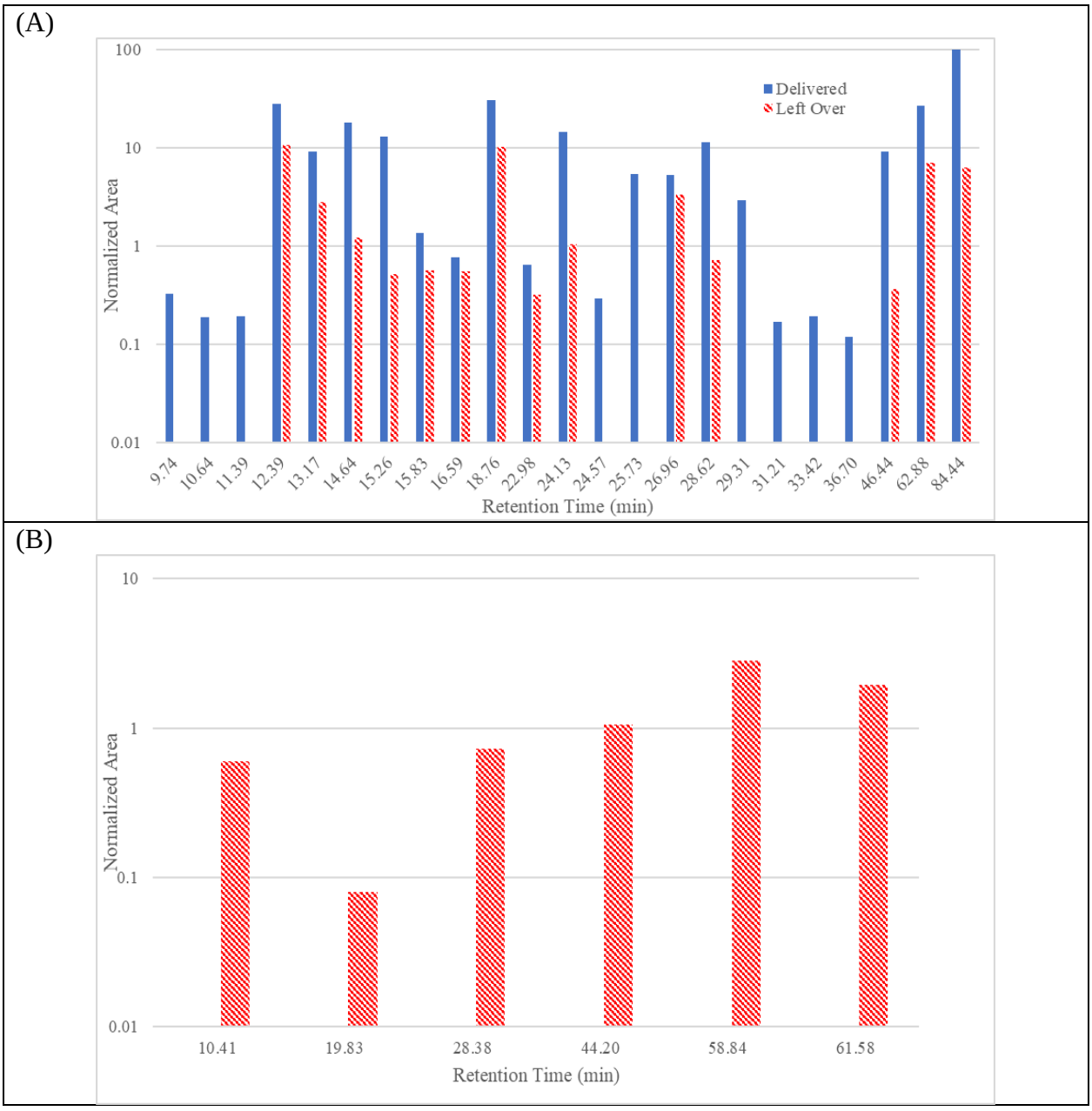

Figure 12: Delivered and remaining values of unknown compounds presented in this study normalized to the largest observed peak area for each untreated substrate. The investigated compounds are excluded here. (A) and (C) represent willow and guayule substrate compounds that decreased in the reactors, while (B) and (D) represent compounds that increased.

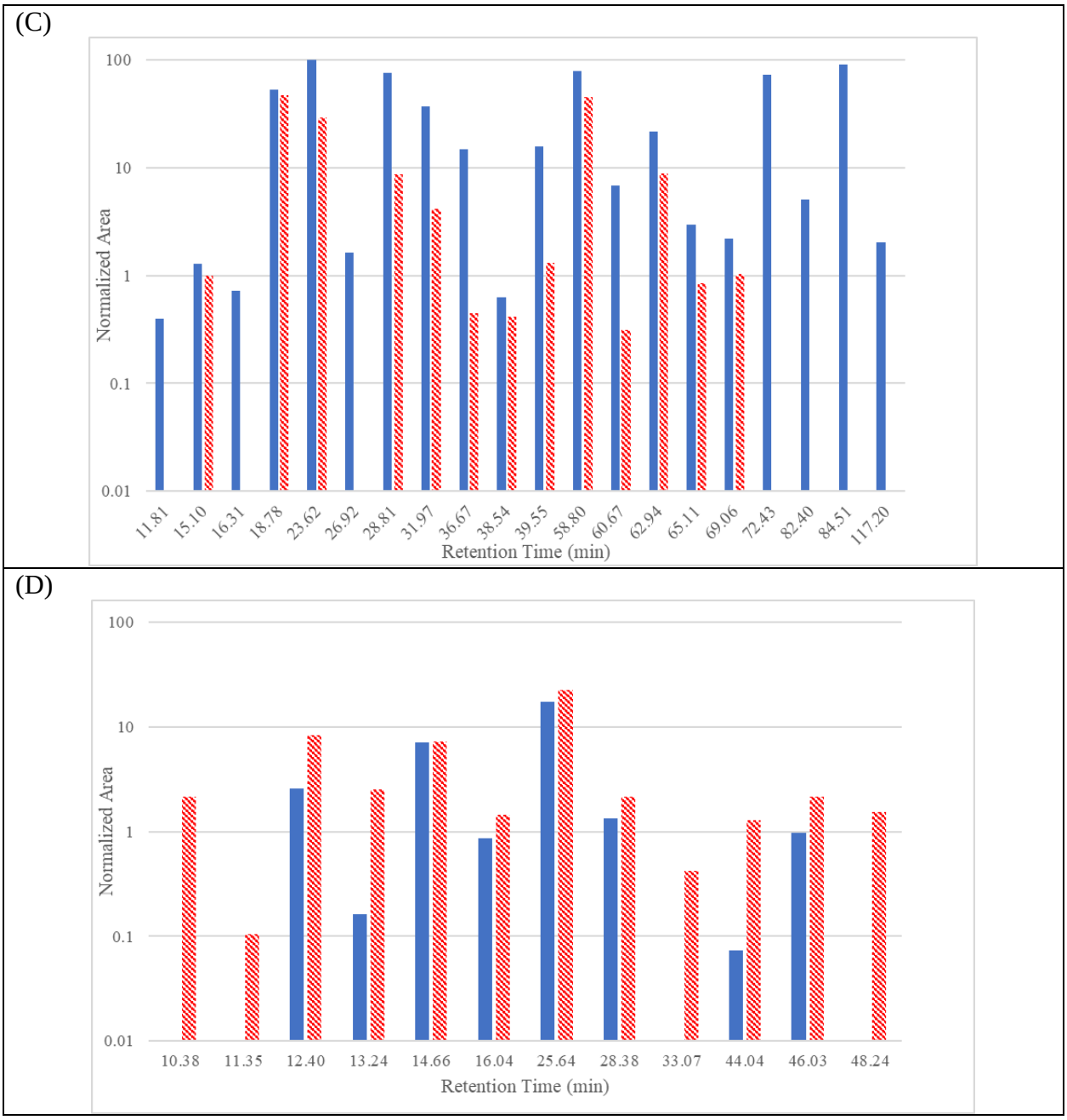

Figure 12 continued

(A)

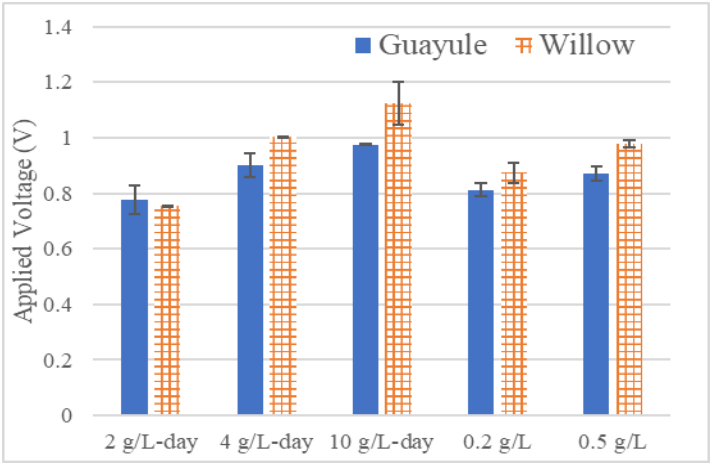

(B)

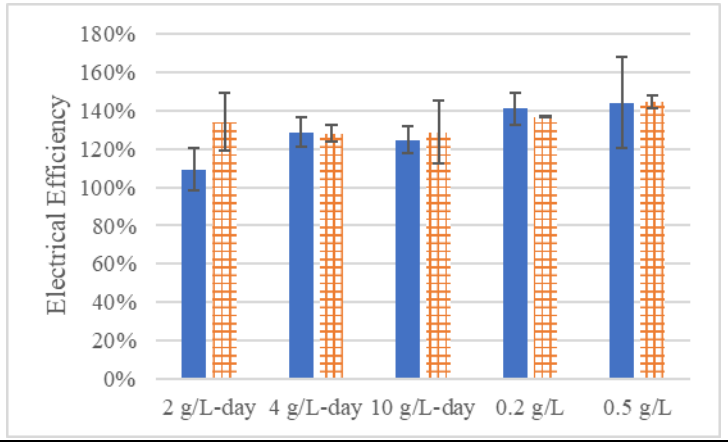

(C)

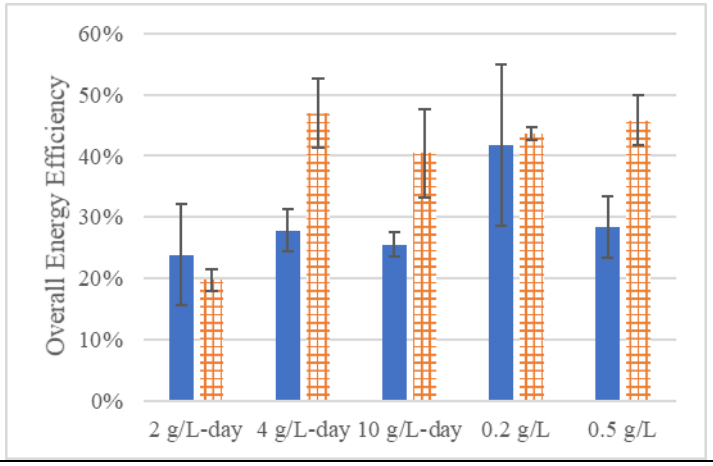

Figure 13: Applied voltage (A), electrical efficiency (B), and overall energy efficiency (A) of the experiments.

Table 6: Calculated COD contributions from each compound detected in PyAP substrates. Notice that the Willow contributed significantly more of its organic content to the compounds measured.

Compound	**Guayule**	**Willow**
acetic acid	2.98%	31.00%
furfural	0.00%	0.00%
hydroxymethylfurfural	0.00%	0.00%
vanillic acid	1.18%	1.09%
syringic acid	0.37%	1.43%
catechol	0.06%	0.0032%
phenol	3.05%	20.45%
propionic acid	0.61%	6.71%
levoglucosan	0.36%	1.40%
4-hydroxybenzaldehyde	0.79%	2.93%
total COD	9.39%	65.02%

Table 7: identified ions of compounds in untreated substrates from Willow (A) and Guayule (B). Considerable compound diversity was observed, however some compounds overlapped. A more diverse collection of nitrogenated compounds were identified in the guayule substrate than in the willow substrate. Several peptide residues were also identified with MS/MS, highlighted in grey.

(A)

Retention time (min)	Detected Mass $[M+H]^+$ (Da)	Error (ppm)	Ion Formula
2.89	167.118	0.89	$C_9H_{15}ON_2$
3.29	181.1336	0.07	$C_{10}H_{17}ON_2$
4.26	195.1493	0.56	$C_{11}H_{19}ON_2$
5.29	227.1753	0.28	$C_{12}H_{23}O_2N_2$
5.76	191.0816	0.22	$C_{10}H_{11}O_2N_2$
6.96	217.1336	0.07	$C_{13}H_{17}ON_2$
8.95	231.1492	0.10	$C_{14}H_{19}ON_2$
9.81	453.3432	0.73	$C_{24}H_{45}O_4N_4$
12.44	679.5117	0.09	$C_{36}H_{67}O_6N_6$

(B)

Retention time (min)	Detected Mass $[M+H]^+$ (Da)	Error (ppm)	Ion Formula
2.82	195.1494	1.30	$C_{11}H_{19}ON_2$
3.25	209.165	0.39	$C_{12}H_{21}ON_2$
3.65	153.1024	0.78	$C_8H_{13}ON_2$
4.00	208.181	0.64	$C_{12}H_{22}N_3$
4.77	223.1804	0.24	$C_{13}H_{23}ON_2$
5.08	234.1237	0.23	$C_{12}H_{16}O_2N_3$
5.38	227.1753	0.07	$C_{12}H_{23}O_2N_2$
5.76	191.0816	0.56	$C_{10}H_{11}O_2N_2$
6.2	178.1339	0.43	$C_{10}H_{16}N_3$
6.7	248.1393	0.01	$C_{12}H_{18}O_2N_3$
7.73	153.1387	0.42	$C_9H_{17}N_2$
8.43	192.1494	0.23	$C_{11}H_{18}N_3$
9.82	453.3431	0.13	$C_{24}H_{45}O_4N_4$
10.61	206.1653	0.90	$C_{12}H_{20}N_3$
11.59	228.1382	0.40	$C_{15}H_{18}ON$
12.44	679.5116	0.10	$C_{36}H_{67}O_6N_6$

Table 8: identified compounds in MEC treated substrates from Willow (A) and Guayule (B). Shaded cells indicate compounds that were not detected in untreated substrates.

(A)

Retention time (min)	Detected Mass [M+H$^+$] (Da)	Error (ppm)	Formula
2.9	167.1181	0.99	$C_9H_{15}ON_2$
3.31	181.1336	0.41	$C_{10}H_{17}ON_2$
5.31	227.1754	0.01	$C_{12}H_{23}O_2N_2$
9.8	453.3433	0.43	$C_{24}H_{45}O_4N_4$
12.44	679.5114	0.41	$C_{36}H_{67}O_6N_6$
13.61	158.1904	0.63	$C_{10}H_{24}N$

(B)

Retention time (min)	Detected Mass [M+H$^+$] (Da)	Error (ppm)	Formula
2.86	195.1494	1.07	$C_{11}H_{19}ON_2$
3.28	209.165	0.88	$C_{12}H_{21}ON_2$
3.68	153.1024	0.89	$C_8H_{13}ON_2$
4.06	152.1183	0.51	$C_8H_{14}N_3$
5.31	227.1754	0.11	$C_{12}H_{23}O_2N_2$
7.92	212.1183	0.22	$C_{13}H_{14}N_3$
8.48	192.1496	0.22	$C_{11}H_{18}N_3$
9.85	453.3433	0.46	$C_{24}H_{45}O_4N_4$
12.47	679.5112	0.72	$C_{36}H_{67}O_6N_6$
13.61	158.1904	0.65	$C_{10}H_{24}N$

CHAPTER III

BIOELECTROCHEMICAL HYDROGEN PRODUCTION, CHARGE TRANSFER MODELING, AND MICROALGAE REGROWTH USING HYDROTHERMAL LIQUEFACTION AQUEOUS PRODUCTS FROM CHLORELLA AND TETRASELMIS

This chapter has been derived from a manuscript in preparation for publication. Satinover, S. conducted the microbial electrolysis work as well as performed the data analysis and wrote the chapter, making revisions suggested by coauthors. Billing, J. created the aqueous fraction wastes used in this chapter. Rodriguez, M. Jr. performed the High-Performance Liquid Chromatography used in this chapter. Connatser, R. and Lewis S. performed the Gas Chromatography – Mass Spectrometry used in this chapter. Mathews, T. and Mandal, S. performed the algae regrowth experiments. Borole A. provided guidance and feedback on experiments, data analysis, manuscript preparation, editing the drafts, and creating subsequent versions.

Abstract

Hydrothermal liquefaction (HTL) has proven to be a promising technology for algae-based biofuel production. However, it creates an aqueous waste product that has little use. Microbial Electrolysis Cells (MECs) were fed HTL aqueous phase (HAP) from two types of algae, *Tetraselmis* sp. and *Chlorella* sp. The spent effluent was reused to grow algae of the same strain type, potentially leading to development of a circular biofuel production system. Electrochemical performance, chemical degradation, and charge transfer were investigated to understand and improve HAP recycle. Average current density of 5.1 ± 0.19 A/m^2 and 3.8 ± 0.08 A/m^2 was reached for *Chlorella* and *Tetraselmis* HAP-fed MECs, respectively. HAP components including acetic acid, propionic acid, ethanol, and glycerol were removed effectively, while acetone and pyridine showed marginal removal. Pyridine was detected in both HAPs but represented less than 1% of the total organic content. Proton and charge transfer analysis showed that proton transfer contributed to the majority of the electrical charge delivered to the cathode,

with ammonium ion transfer contributing 15.4 – 34.4%. Algae regrowth studies using MEC effluent showed nearly complete removal of total organic carbon, but significantly less removal of total nitrogen. *Tetraselmis* sp. growth occurred with *Tetraselmis* sp. MEC effluent, however it was less than the control regrowth nutrient media without effluent. The findings here support the possibility of a circular biofuel framework, but additional constraints, including removal of inorganic contaminants, must be realized for stable circular systems.

Introduction

Climate change has been widely regarded in the global scientific community as one of the most pressing environmental problems facing the world, with much of the concern being driven by the use of greenhouse gas emitting nonrenewable fuel sources. New substitutes must be created from renewable carbon-neutral sources, which must then be effectively scaled to meet commercial demand in a cost-effective manner. This challenge has yet to be met by any source over nonrenewable fossil fuels, and the race to find new or improved technologies, continues in the hopes of finding a solution to the climate change challenge.

Of the feedstocks studied for producing liquid fuels, microalgae represent a promising option. However, this feedstock has many challenges, including the cost of feedstock production and nutrient requirements. A techno-economic analysis reported by Davis et al. in 2011 determined that best case scenario using a 10% return would result in a cost of $8.52 per gallon using open raceways to grow microalgae to produce algal oils directly, and upgrading the algal oil to bio-diesel using hydrotreating [1]. More recently, another techno-economic analysis that investigated the cost of catalytic pyrolysis of microalgae for bio-fuel production found that these microalgae-based biofuels could be feasible at a selling price as low as $5.61 per gallon [2].

Today's costs of conventional fuels are much lower, suggesting that microalgae based fuels are not cost competitive.

While improving biomass growth rates is intuitively one strategy to limit costs, new practices have attempted to either increase fuel yields from algal biomass or develop new and more valuable products. Thermochemical processing via hydrothermal liquefaction (HTL) is a process where an aqueous phase containing biomass substrate is heated and pressurized, typically above 250 C, catalyzing a chemical breakdown of biomass polymers into simple subunits, and separation of the lipids as an oil phase. HTL provides several advantages over other thermochemical treatment processes, in that it can be used on wet biomass and often does not require other chemical or thermal preprocessing. Many different biomass feedstocks have been used in hydrothermal liquefaction, ranging from agricultural waste products from livestock, plant residues and, most importantly for this study algae [3, 4]. Algae's popularity as a feedstock for HTL has been noticed only recently, making it a popular avenue of further research. Process conditions and strain development are two avenues being pursued [5].

Despite its appeals, HTL still has many more hurdles before it sees mainstream adoption. One major deterrent is the waste generated from HTL. The aqueous phase made by HTL is a waste product that has little reuse, and this is also true for algal feedstocks. HTL aqueous phase (HAP) can contain high concentrations of total organics. One study that analyzed the chemical makeup of HAP samples from *Tetraselmis* sp. and *Chlorella* sp. found the chemical oxygen demand (COD) of HAP to be between 43.8 and 84.9 g-COD/L [6]. To minimize the loss of carbon and energy via this fraction, HAP recycling has been proposed [7-10]. When HAP is recycled, organics continue to accumulate in the aqueous phase as it is reused in HTL. Thus, while recycling prevents the immediate need for disposal, it is a temporary solution. More recently, a

study by Davidson et al. compared several methods of HAP treatment, including condensed phase ketonization and dual-bed steam reforming [11]. Davidson et al. first ran the HAP through a multistep cleanup process before energy recovery to minimize catalyst inactivation caused by untreated HAP, suggesting that contaminant removal prior to HAP conversion is essential.

For a complex waste like HAP, another intuitive means of treatment involves biochemical mechanisms. Biller et al. proposed anaerobic digestion as a means of consuming the organics present in the HAP after recycle [7]. Anaerobic degradability was also supported by a study conducted by Tommaso et al. that suggested that HAP could have an anaerobic degradability up to 84% when algae was treated at 320 °C [12]. Other approaches have been outlined in a review by Gu et al [13]. One technology that has not been tested using HAPs are Microbial Electrolysis Cells (MECs). These devices work by using a microbially colonized surface that produces electrons while degrading organics. The electrons are shuttled to a cathode, where they are combined with protons to form hydrogen. This positions MECs as a novel technology that can repurpose unconventional wastes for energy recovery and simultaneously treat waste. Some HTL products have already been demonstrated in MECs, including HTL treated cornstalk [14] and swine manure [15].

For protein-rich feedstocks like algae, ammoniacal nitrogen (NH_3-N) is a typical compound generated by HTL under a wide range of temperatures and residence times from different algal strains [12, 16]. Presence of ammonia in an aqueous stream requires treatment prior to disposal. Concentration and separation of ammonia can result in production of valuable products such as fertilizers and cleaners. Today's method of ammonia production is not sustainable, which is primarily via the Haber process. The Haber process requires a source of hydrogen, which is typically produced by natural gas steam reforming [17]. Renewable means of acquiring NH_3-N will

therefore be necessary in the future. NH_3-N separation is possible using MECs due to the formation of a conjugate acid, ammonium, at neutral pH. In MECs that use a cation exchange membrane, ammonium can migrate from the anode to the cathode, where hydrogen evolution at the cathode increases the cathode pH. The increase in pH deprotonates the ammonium ion, preventing back diffusion through the membrane. NH_3-N removal has already been demonstrated in BESs of other types [15, 18-21], and its presence in BESs has been shown to be inhibitory to current and power production [22]. However, no NH_3-N removal studies have been conducted using algal feedstocks. Additionally, because ammonium is a positive ion, it may aid in charge transfer in MECs, which is a primary factor limiting current in high performance BESs [23, 24].

Several microalgae strains can grow via photosynthesis and can be grown by heterotrophic means, functioning mixotrophically [25]. One study used wastewater from Microbial Fuel Cells (MFCs) and found that *C. vulgaris* could grow in MFC effluent at a maximum growth rate of 4.7 g/L [26], and doubled biomass yields when $NaNO_3$ was added to improve nitrogen availability in the growth media. NO_3^- and NH_3-N are common nitrogen sources for algae regrowth [25], so either source could be useful. If nitrogen availability is a problem for algae growth in BES effluents, HAPs may be a valuable nutrient source. Using microalgae to further degrade HAP has also been studied previously [27]. One of the earliest reports by Jena et al. showed that *C. minutissima* could grow on an aqueous co-product of HTL from *S. platensis*, but biomass regrowth was slower using the co-product than the control media [28]. This trend was supported later by Biller et al., who showed that larger concentrations of HTL effluent diluted less than 400 fold were inhibitory to growth of algae [16]. HAP was shown more recently to be useful for growing microalgae by Das et al., where they showed that *Tetraselmis* sp. could be regrown using 50% of the nutrients it needed from HAP [29]. More recently, Kumar et al. showed

that four microalgae strains represented in harmful algae blooms, *C. minutissima*, *C. sorokiniana* UUIND6, *C. singularis* UUIND5 and *S. abundans,* could be grown in HAP from low temperature HTL (270 ℃) on microalgae [30]. However, the authors also showed that control growth media without HAP generally grew more biomass than the diluted streams. The findings from these previous studies suggest that algae growth in HAP is not ideal. Some of the nutrients found in HAP may still be useable for growth. Edmundson et al. extracted nutrients, including phosphorus and nitrogen, from HTL filter solids and used it as the sole source of those nutrients for algae growth [31]. The authors were able to grow *S. obliquus* at maximum specific growth rates that were nearly the same when using recycled phosphorus as the control media, but this was not true for the recycled nitrogen (which had 74% of the nitrogen attributed to NH_3-N). The limitations to algae growth in HAP are therefore most likely due to a combination of organic and inorganic composition. MECs function by removing a substantial part of the organics and NH_3-N that might otherwise inhibit algae regrowth but may provide enough nitrogen needed for algae growth. Thus, it may be possible to maintain or improve algae regrowth using effluent from MECs recycling nutrients and water in HAP.

This study focusses on using HAP as a source of renewable energy production. HAP conversion was investigated in MECs using two different sources, *Chlorella* sp. and *Tetraselmis* sp. *Chlorella* sp. and *Tetraselmis* sp. were selected based on their availability, their potential to be grown at scale, and the ability of the species to grow heterotrophically [16, 29]. Changes in key chemical species and electrochemical performance were compared for the two substrates. Charge transfer facilitated by proton and ammonium ions was also tracked to determine the efficiency of proton transfer and the contribution of ammonium ion. Evaluating the percentage of cation migration that is attributed to ammonium transfer using NH_3-N rich complex substrates in MECs

has yet to be accomplished, and is needed to determine the separation efficiency that occurs in MECs being fed complex wastes. The HAP treated in MECs was then used to regrow algae, demonstrating the potential for a circular biofuel process. Together, these technologies may aid in establishing the foundation for a circular economy.

Materials and Methods

Formation of HAP products

HAP was generated from algal biomass in Pacific Northwest National Laboratory's (PNNL) bench scale continuous flow hydrothermal reactor. The reactor system is made of 316 L stainless steel and is comprised of high-pressure syringe pumps, tube-in-tube heat exchangers, an inline solids separation vessel, and liquid product collection vessels that also serve as liquid-gas separators. Details of the reactor system are described in earlier publications [32, 33]. The average operating temperature, pressure, and liquid hourly space velocity was 340 °C / 20.4 MPa / 4.1 h^{-1} and 342 °C / 20.2 MPa / 2.1 h^{-1} for the *Chlorella* sp. and *Tetraselmis* sp., respectively. The products of hydrothermal liquefaction are an aqueous liquid phase, an organic liquid phase (biocrude), a gas phase, and a solid phase comprised of precipitated inorganics and char. In the PNNL reactor system, the solid phase is continually separated at reaction conditions to take advantage of the decreased solubility of many inorganic species in near-critical water and facilitate a cleaner liquid-liquid phase separation upon cooling and depressurization. The aqueous phase is separated from the organic phase by gravity separation in a separatory funnel. Maddi et al. reported a detailed characterization of the HAP from microalgae including the species used in the present study: marine samples SW1 to SW4 are from *Tetraselmis* sp. and

fresh water sample FW4 is from *Chlorella* sp. [6]. However, characterization was performed once HAPs were delivered for use in MECs.

Microbial Electrolysis Cell Operation and Start Up

Two replicate MECs were inoculated using a startup community and operational set up from previously described reactors [34, 35]. Briefly, the anode was composed of a sterilized carbon felt, and the cathode was a 0.5 mg/cm^2 platinum deposited carbon pressed to a stainless steel mesh, enclosed in 1.5 in PVC pipe. Both anode and cathode chambers were press fit between polycarbonate plates. The chambers were separated by a Nafion membrane electrode assembly (Sainergy Tech Inc, Marietta, GA). Reactors were operated in a 3-electrode set up using a potentiostat, model VSP (Bio-Logic USA, Knoxville, TN). The MEC anode potential was controlled by poising the anode at -0.2V versus Ag/AgCl electrode. The reference electrode was an Ag/AgCl electrode. Whole cell voltage was recorded using a DataQ DI-1100 and the associated software (DataQ Instruments, Akron, Ohio). Anode liquid media was used to recycle substrate through the anode reactors and was sparged for 30 minutes before operation. Nutrient media was composed of 50 mM phosphate buffer set to an initial pH of 7.2 with the addition of 0.13 g/L KCl added to deionized water. 195 mL of nutrient media was measured out along with 2.5 mL of Wolfe's vitamin and 2.5 mL mineral solutions described previously to create the anode liquid media [36]. For all media changes, 50 mL of anode liquid media was flushed through the anode chamber and recycle lines. Anode liquid media was cycled through the anode at a rate of 3.5 mL/min for all experiments. Cathodes were sparged with nitrogen for 15 minutes before experiments and were rinsed with anaerobic deionized water before being operated. After experiments, deionized water was added to the cathode until the cathode was full before removal and filtration for NH_3-N analysis. The cathode has an empty volume of 16 mL.

Reactors were initially started on 0.2 g/L of glucose and acetate, and fed by continuous addition using a syringe pump at an organic loading rate of 2 grams of chemical oxygen demand (COD) per liter of anode volume per day (g/L-day) using the Chlorella-based HAP (HAP-C) for one week. Media was changed after one week of growth, and then HAP-C delivery was ramped from 2 to 10 g/L-day in increments of 2 g/L-day every 24 h. Once this was complete, a progressive evolution where 4 core samples were removed from mature felt were then used to inoculate new sterile carbon felt in MECs every 2 weeks using the same growth procedure to increase the performance of the MECs. This process was repeated for a total time of two months. Results of progressive evolution are shown in the Appendix of this chapter. MECs were transitioned from being fed HAP-C to the *Tetraselmis* based HAP (HAP-T), and vice versa, using an acclimation period that lasted 1 week, feeding at a rate of 2 g/L-day, influenced from timelines established earlier [37].

Continuous experiments for MECs were conducted over the span of 72 h, and batch fed experiments were conducted for 24 h. Continuously fed experiments used 2, 4, and 10 g/L-day organic loading rates for both substrates, and 0.2 and 0.5 g/L loading was used for batch addition experiments. Hydrogen produced was captured by inverted graduated cylinder in a water batch, capitalizing on a small amount of active H_2 harvesting to increase yields [38]. Anode media samples were collected at the beginning of each experiment and every 24 h until the experiment was concluded for further analysis.

Electrochemical Analysis, NH_3-N and Proton Transfer Tracking model

MEC electrochemical performance metrics were conducted using methods that have been previously described [37]. Metrics calculated included current density, which was normalized to the projected surface area of the MEC (12.56 cm^2), hydrogen productivity in liters H_2 per liter of

anode volume per day (L/L-day) using an anode volume of 13.28 mL, anode Coulombic efficiency, cathode conversion efficiency, hydrogen recovery, electrical efficiency, and overall energy efficiency. Metrics were calculated for all short-term experiments. Anode and cathode gas samples were collected for analysis by gas chromatography (GC) using a Thermo Focus GC (ThermoFisher, Waltham, MA). The GC method was performed with a starting oven temperature at 30 °C, which was held for 1 minute, followed by a ramp to 72 °C at a rate of 5 °C/min. 72 °C was then held for 30 seconds. The inlet, block, and transfer temperature for each run were held at 50 °C for all GC runs. The carrier gas used was helium, which was held at an operating pressure of 30 kPA. Gases detected included hydrogen, methane, oxygen, and nitrogen. An HP Plot Molecular Sieve 5A (Agilent technologies Santa Clara, CA) was used as the column for all GC runs. Liquid samples bulk properties tested included COD, NH_3-N, pH, and total inorganic carbon (TIC). COD of anode media was recorded using Hach high range COD vials (Hach Company, Loveland, CO), which were digested using a Hach DRB 200 at 150 °C for 2 h. Absorbance was measured at 620 nm to determine COD concentration of samples using a Genesys 20 Spectrophotometer (ThermoFisher, Waltham, MA). NH_3-N was measured from samples using a High Range Hach Nitrogen-Ammonia Reagent test kit (Hach Company, Loveland, CO), and absorbance was read at 655 nm using the same spectrophotometer used for COD analysis. Total inorganic (TIC) and organic carbon (TOC) was determined by using a Shimadzu TOC-L (Shimadzu, Torrance, CA). The furnace was operated at 680 °C for all samples, and injection volumes were 2 mL. Samples were diluted with deionized water 20-fold for all samples except samples from 0.2 g/L batch experiments, which were diluted 10-fold. Standards for total inorganic carbon (TIC) were prepared using sodium carbonate and

bicarbonate solutions, while total carbon was standardized using potassium hydrogen phthalate solutions.

Analytical Chemistry of MEC Samples

High-Performance Liquid Chromatography (HPLC) was used to identify five compounds: acetic acid, propionic acid, acetone, ethanol, and glycerol. A Shimadzu refractive index was used (RID-20A) (Shimadzu, Torrance, CA) to detect compounds, along with an Aminex HPX-87H by Bio-Rad (Bio-Rad, Hercules, CA). Samples were run using a 5 mM H_2SO_4 mobile phase for 30 minutes. Samples were acidified by addition of 2 M H_2SO_4 prior to analysis. Additional compounds were identified by Gas Chromatography – Mass Spectrometry (GC-MS). Several classes of semi-volatile organic compounds were detected using liquid-liquid phase extraction. Methylene chloride was used as the extracting solvent which was then analyzed by liquid injection onto an Agilent 6890 gas chromatograph with a Phenomenex (Phenomenex, Torrance, CA) Zebron DB-5MS column and detected via electron ionization mass spectrometry on an Agilent 5975 mass spectrometer. A 20 mg/L pyridine standard was prepared in methylene chloride and injected into the GC-MS prior to each sample injection day. Agilent's ChemStation software was used for major constituent identity assignment and integration.

NH_3-N and Proton Transfer Tracking

Proton accumulation in the anode and cathode was tracked by measuring the accumulated NH_3-N in the anode and cathode, the initial phosphate buffer concentration, the pH in the anode and cathode, and the inorganic carbon of the anode before and after experiments. Because a cation exchange membrane was used, negligible carbonate or phosphate was assumed to diffuse from the anode to the cathode. Samples of catholyte were taken at the end of experiments and diluted to 16 mL using anaerobic deionized water. Anode samples were collected before and

after all short-term experiments. The proton balance was therefore carried out by using alpha notation described by Snoeyink and Jenkins [39], and accounted for protons being carried by inorganic carbon, phosphate, free protons, and ammonium ions. Cathode composition was assumed to have NH_3-N as the only buffer that transferred due to the presence of the cation exchange membrane between the chambers. Ionic strength was assumed to have an negligible impact on species concentrations in the anode based on the theory described by Snoeyink and Jenkins [39]. The pH of the anode liquid medium and catholyte was measured and used to calculate fractions of proton bound species. Using the measured concentration of phosphate, pH, NH_3-N, and carbonate, the protons present in the anode and cathode were tracked before and after experiments. The pH and NH_3-N were measured for all samples, while inorganic carbon was assumed to be negligible in the cathode and negligible at the beginning of the experiment for both anode and cathode. Accounting for all of the species, including NaOH added for pH adjustment, the protons in the anode and cathode was determined by the following equation:

$$H^+ = (3[H_3PO_4] + 2[H_2PO_4^{1-}] + [HPO_4^{2-}] + 2[H_2CO_3^*] + [HCO_3^-] + [NH_4^+] + [H^+] + [NaOH]_{added})(liquid\ volume) \quad (1)$$

Where species in brackets are in molar units. Total proton, phosphate, carbonate, and NH_3-N concentration at the cathode was assumed to be negligible before experiments due to the rinsing and drying of the cathode prior to use. In addition to calculating proton and NH_3-N transfer rates, several efficiency metrics were also determined from the charge accounting. The ratio of total protons transferred ($H^+_{transferred}$) over the amount of charge produced by the MEC in moles ($n_{moles\ e^-}$) called the proton charge ratio, was:

$$\eta_{p-f} = \frac{H^+_{transferred}}{n_{moles\ e^-}} \quad (2)$$

The same metric for charge balanced with NH_3-N transfer, called the NH_3-N-charge ratio, was also determined by measuring the NH_3-N that transferred ($(NH_3\text{-}N)_{transferred}$) over the moles of electrons produced as current:

$$\eta_{NH_3-f} = \frac{(NH_3 - N)_{transferred}}{n_{moles\ e^-}} \qquad (3)$$

The ratio that can be attributed to just proton transfer is therefore the difference between the two ratios. Total proton transfer efficiency was determined as the ratio of protons that transferred over the net protons added to the system:

$$\eta_{p-p} = \frac{H^+_{transferred}}{H^+_f - H^+_i} \qquad (4)$$

Where H_i^+ and H_f^+ represent the moles of protons present in the entire system at the beginning and the end of the experiment, respectively. Proton concentrations were determined based on a proton balance carried out in both chambers, and considered major proton carrying species, including phosphates, carbonates, ammonium, and free protons. The same calculation was performed for NH_3-N exclusively with:

$$\eta_{NH_3-NH_3} = \frac{(NH_3 - N)_{transferred}}{(NH_3{-}N)_f - (NH_3 - N)_i} \qquad (5)$$

Where $(NH_3\text{-}N)_i$ and $(NH_3\text{-}N)_f$ represent the moles of NH_3-N before and after the experiment, respectively. Additional details and the mathematical expressions used to determine NH_3-N and proton transfer at each time point can be found in the Appendix of this chapter.

Algae Regrowth Using MEC Effluent

To create the spent effluent for regrowth, MECs were run on 10 mM phosphate buffered anode media, and substrate was added to continuously feed the reactors at a minimum of 10 g/L-day. MECs were fed until the nutrient media volume had increased to a point where 25% of it

was composed of HAP effluent. The new media mixture was then filter sterilized by 0.2 µm filter and was stored in sterile centrifuge tubes for later use in regrowth studies. This process was repeated twice for each HAP type, where HAP-T was fed into reactors first followed by HAP-C after a 1-week acclimation period. HAP-T was used to grow *Tetraselmis* and HAP-C was used to grow *Chlorella*. Species of these microalgae have been shown to uptake NH_3-N as a nitrogen source [40, 41], suggesting that the NH_3-N found in HAP could be used as the sole nitrogen source for algae growth if organics could be sufficiently removed. Growth of the algae species used methods that have been previously described [42]. *Tetraselmis* sp. UTEX LB 2767 and *Chlorella vulgaris* (UTEX 395) were obtained from the University of Texas at Austin collection of cultures. These species have been shown to be high biofuel yielding strains [43]. Cultures were maintained in a control growth medium (WC) described previously [44]. The HAP effluents were diluted with deionized water to 0.25, 1.25 and 2.5% by volume. The pH of each diluted HAP effluent was adjusted to 8 and steam sterilized by autoclave for 15 minutes before use as a growth medium. 100 mL of diluted HAP effluent for each algae HAP and their associated strain was placed in a 250 mL Erlenmeyer flask. Each algal species was centrifuged separately at 5000 rpm for 10 minutes and washed with sterile nitrogen deplete WC medium five times before inoculation. The algae were inoculated into flasks at a biovolume of 1.74×109 μm^3/mL. The cultures were shaken daily to keep algae suspended. Media were exchanged at 20% volume twice a week. Flasks were placed in an incubator at 25 °C with a 14:10 h (light : dark) photoperiod using 100 100 µmol/m^2-s photosynthetically active radiation (PAR). Algae grown in the control medium was provided a total nitrogen concentration similar to 0.25% HAP effluent. Algal growth was approximated by monitoring the optical density at 750 nm every 2 days for a total of 12 days. Optical density was measured using a Multiskan FC Microplate Photometer

(ThermoFisher Scientific, Waltham, MA, USA). By the end of experiment, 30 mL of algal suspension media was filtered through Whatman GF/F filter and filtrate was analyzed for TOC and total nitrogen (TN). TOC and TN were analyzed using the same protocol described earlier.

Results and Discussion

MEC Short Term Experimental Performance

The two algae-derived substrates were characterized by measuring pH, NH_3-N concentration, and COD concentration. HAP-C was found to have a pH of 8.82, with 6.6 ± 0.1 g-NH_3-N/L, and 79.3 ± 0.17 g-COD/L, while HAP-T was found to have a pH of 8.69, containing 2.6 ± 0.05 g-NH_3-N/L, and 43.2 ± 0.17 g-COD/L. These characteristics of the HAPs proved to have some operational advantages over other substrates, notably that the reactors required limited pH adjustment. This can be attributed to the slightly basic pH of the substrates, buffering capacity provided by ammonium, and the presence of phosphate in the anode nutrient medium. Only one set of experiments with organic loading conditions of 10 g/L-day required pH adjustment, which may have been due to the higher rate of proton production.

For all the tests performed, MECs fed with HAP-C outperformed the reactors fed with HAP-T. Figure 14 shows the current density (A), hydrogen productivity (B), hydrogen recovery (C), and electrical efficiency (D) of the reactors at different organic loading rates under batch and continuous feeding conditions.

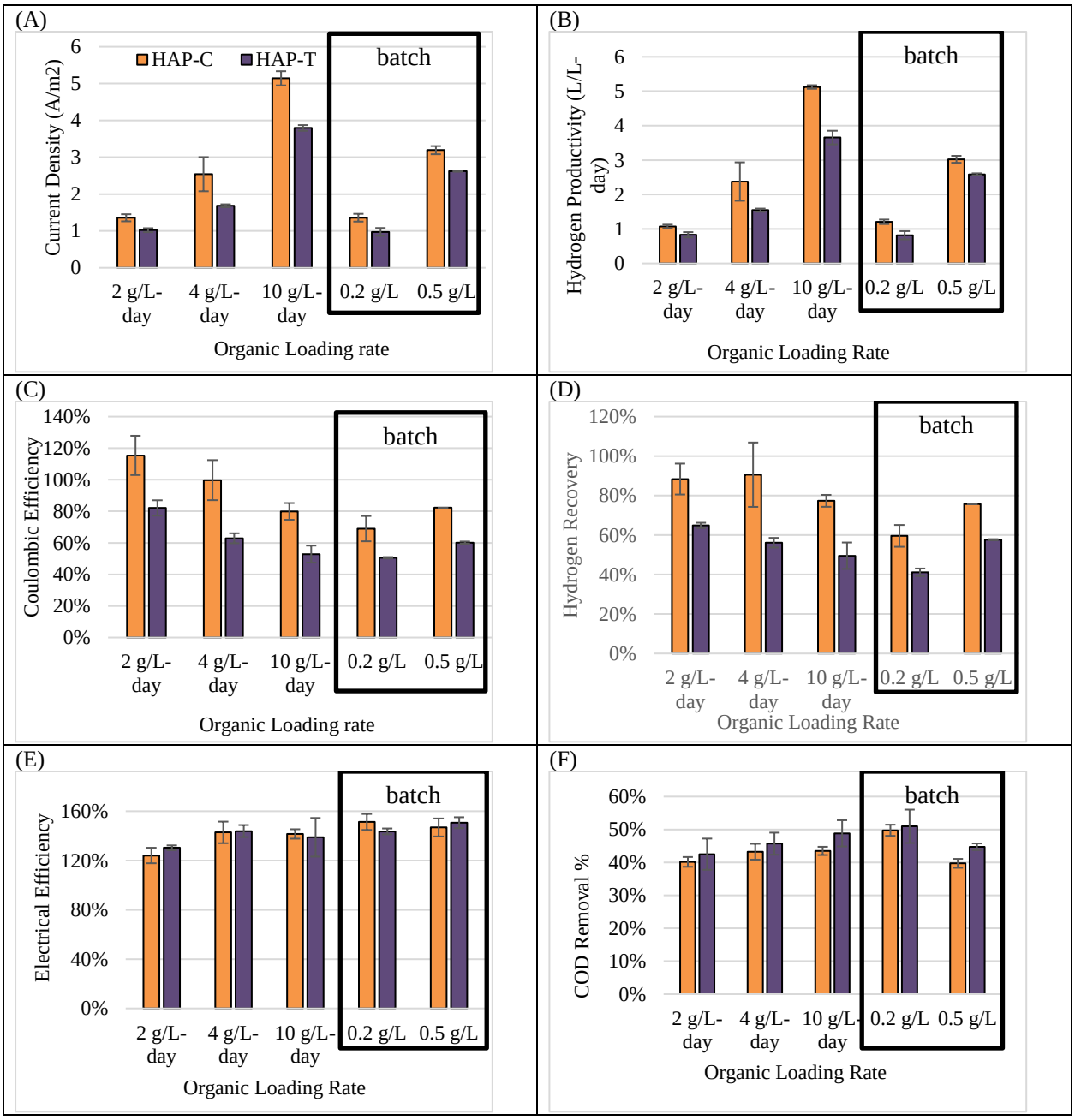

Figure 14: Electrochemical performance of MECs fed with HTL effluent from *Chlorella* sp. (HAP-C) and *Tetraselmis* sp. HTL (HAP-T) under continuous and batch addition. Batch addition results are boxed. The plots show the average current density (A), hydrogen productivity (B), Coulombic efficiency (C), hydrogen recovery (D), electrical efficiency (E), and COD removal percent (F), at the organic loading rates tested. In general, HAP-T-fed MECs appeared to underperform compared to MECs fed with HAP-C.

The largest average current density was reached when the reactors were operated at 10 g/L-day of continuous feeding, producing 5.1 ± 0.19 A/m^2 and 3.8 ± 0.08 A/m^2, when MECs were fed

HAP-C and HAP-T respectively. Current densities observed with HAP-C-fed MECs are comparable to that reported for liquid waste streams derived from other biomass feedstocks such as switchgrass [34], pine [45], and willow [37] in studies conducted using the same reactor configuration. The highest COD removal occurred when MECs were operated under batch-fed conditions, at a loading of 0.2 g/L, reaching a percent removal of 49.8 ± 1.7% for HAP-C-fed MECs, and 51.0 ± 5.1% for HAP-T-fed MECs. For both substrates, Coulombic efficiencies were high, however; at the lower substrate loading rate (2 g/L-day for HAP-C-fed MECs) the Coulombic efficiency was above 100%. This may be explained by the oxidation of inorganic nitrogen species in HAP-fed MECs, namely NH_3-N. NH_3-N has been used in abiotic electrolysis cells for hydrogen production at cell voltages below those used here [46]. Also, NH_3-N has been demonstrated as an energy source in MFCs where it has been either coupled with organic oxidation or where BESs use NH_3-N as the only electron source [19-21]. In the MECs used in this study, NH_3-N is present in the HTL along with the organic carbon delivered. At lower organic rates, it may be possible that current produced by NH_3-N oxidation resulted in a proportionally larger contribution to current generation that was solely generated from organic carbon degradation. The mechanism for NH_3-N oxidation in the MECs used here is not well understood, however, based on a framework proposed by Jadhav and Ghangrekar for MFCs [19]. The authors propose that, in MFCs being fed NH_3-N, the Anammox process occurs, which is described by the following equation:

$$NH_4^+ + NO_2^- \rightarrow N_2 + 2H_2O \qquad (6)$$

In this reaction, no current is produced, as this is not a half reaction. The authors propose that part of the NH_3-N is oxidized to nitrate, which is then reduced to nitrite. The potentials at standard biological conditions (P = 1 bar, T = 25 ºC, and pH = 7) were calculated here:

$$NH_4^+ + 3H_2O \rightarrow NO_3^- + 8e^- + 10H^+ \qquad \Delta E^{o\prime} = -0.36\,V\ vs\ SHE \qquad (7a)$$

$$NO_3^- + 2H^+ + 2e^- \rightarrow NO_2^- + H_2O \qquad \Delta E^{o\prime} = +0.43\,V\ vs\ SHE \qquad (7b)$$

Accordingly, the overall half reaction that creates nitrite from NH_3-N would therefore be:

$$NH_4^+ + 2H_2O \rightarrow NO_2^- + 6e^- + 8H^+ \qquad \Delta E^{o\prime} = -0.34\,V\ vs\ SHE \qquad (7c)$$

Only the reaction described by equation 6a or equation 7 needs to occur for NH_3-N to be removed from the system. Referring to Snoeyink and Jenkins [39], other ammonium oxidation reactions may also be possible. One specific example would be:

$$2NH_4^+ \rightarrow N_{2(g)} + 8H^+ + 6e^- \qquad \Delta E^{o\prime} = +0.28\,V\ vs\ SHE \qquad (7d)$$

Regardless of the reaction taking place, each mole of NH_3-N would produce 6 moles of electrons and 8 moles of protons. The additional two moles of protons that would not be able to balance with the electrons at the cathode would cause a drop in pH despite the above neutral pHs of the substrates. While proton transfer is imperfect in virtually all two chamber BESs, the half reactions proposed could contribute to an additional drop in pH that would be greater than what would be produced by imperfect proton transfer.

Complicating the framework here is the nitro-organic composition of the substrate, in addition to the NH_3-N. Because NH_3-N may be generated by microbial metabolism in addition to being delivered through the substrate, it is difficult to tell how much NH_3-N is being generated or oxidized. Biological NH_3-N generation from organics is commonly known from the degradation of amino acids via Stickland fermentation [47]. NH_3-N generation can also occur during microbial oxidation of other nitrogen containing organics. One example of a compound identified in the HAPs used here is pyridine, which can be oxidized by *Bacillus* sp. and *Nocardia* sp., releasing NH_3-N [48]. Because nitrogen was used as the sparging gas, it was not possible to determine if nitrogen accumulated using the chromatographs from GC. Tracking NH_3-N and other nitrogen

compounds has been performed to an extent previously in BESs. Joicy et al. determined the rate of NH_3-N oxidation using anode respiring bacteria in a BES without organic carbon, and the fractions of nitrite as nitrogen being removed (NO_2-N) [21]. They found that the average removal rate stabilized to 57 mg-NH_3-N/L-day, while NO_2-N varied from 40-80 mg-NO_2-N/L-day. This removal rate could be occurring in our MECs, however with the addition of the nitrogenated compounds and their potential degradation products, NH_3-N removal was not as easily quantified.

Hydrogen recovery was considerably higher for HAP-C-fed MECs than for HAP-T-fed MECs due to the larger Coulombic efficiencies demonstrated, as cathode conversion efficiency was similar across the MECs for both substrates at each organic loading rate (see the Appendix of this chapter). In the case of the HAPs fed to these MECs, hydrogen recovery is largely contingent on the efficiency of the anode to convert organics to electrons, which may be artificially increased by the conversion of NH_3-N at lower organic loading rates. Previous studies using the same reactor configuration have not shown losses in hydrogen recovery due to increased organic loading up to 10 g/L-day [34, 37, 49]. However, these results are largely affected by the sharply declining anode Coulombic efficiencies. In contrast, the batch additions caused hydrogen recovery to increase with organic loading, rather than decrease. This was also driven by the increase in Coulombic efficiencies observed. NH_3-N oxidation may have played a larger role with batch addition than other substrates.

Chemical Characteristics of Substrates

The substrates used here contained organic acids and nitrogenated compounds, as previously reported [6]. Table 9 shows the compounds identified in the feedstocks.

Table 9: Chemical analysis of compounds detected by HPLC and GC-MS based on class and notable individual species. For compounds detected by GC-MS only concentrations of pyridine were available due to availability of standards.

Compound Class/Name	**Detection Method**	**Substrate**	**Detected (Yes/No)**	**Concentration (mg/L)**
Glycerol	HPLC	HAP-C	Yes	3781.5
Acetic Acid	HPLC	HAP-C	Yes	2980.9
Propionic Acid	HPLC	HAP-C	Yes	11693.2
Acetone	HPLC	HAP-C	Yes	655.9
Ethanol	HPLC	HAP-C	Yes	416.5
Pyrizine	GC-MS	HAP-C	No	
Pyridine	GC-MS	HAP-C	Yes	0.395
Phenol	GC-MS	HAP-C	No	
Methylated Pyrizines	GC-MS	HAP-C	Yes	
alkanes (decane or dimethylheptane)	GC-MS	HAP-C	Yes	
pyrrolidinones	GC-MS	HAP-C	Yes	
benzaldehyde	GC-MS	HAP-C	Yes	
methyl piperidine	GC-MS	HAP-C	Yes	
dianhydromannitol	GC-MS	HAP-C	Yes	
hexadecanoic acid, methyl ester	GC-MS	HAP-C	Yes	
Glycerol	HPLC	HAP-T	Yes	1218.7
Acetic Acid	HPLC	HAP-T	Yes	3609.2
Propionic Acid	HPLC	HAP-T	Yes	2499.6
Acetone	HPLC	HAP-T	Yes	739.0
Ethanol	HPLC	HAP-T	No	
Pyrizine	GC-MS	HAP-T	No	
Pyridine	GC-MS	HAP-T	Yes	0.285
Phenol	GC-MS	HAP-T	Yes	
Methylated Pyrizines	GC-MS	HAP-T	Yes	
alkanes (decane or dimethylheptane)	GC-MS	HAP-T	No	
pyrrolidinones	GC-MS	HAP-T	Yes	
benzaldehyde	GC-MS	HAP-T	No	
methyl piperidine	GC-MS	HAP-T	Yes	
dianhydromannitol	GC-MS	HAP-T	Yes	
hexadecanoic acid, methyl ester	GC-MS	HAP-T	Yes	

Both substrates had significant fractions of acetic acid, propionic acid, and glycerol, with smaller concentrations of acetone and pyridine. Ethanol was only detected in HAP-C. The unquantified compounds determined by GC-MS varied more considerably between the substrates. HAP-T contained phenol, while HAP-C did not. Alkanes included decane and dimethylheptane, and were only present in HAP-C. Assessment of the individual compounds contributing to total COD removal showed that HAP-C had more of its COD attributed to the compounds identified and quantified by HPLC and GC-MS than HAP-T. The largest represented compounds in both substrates were acetic acid, glycerol, and propionic acid, as shown in Table 11 in the Appendix of this chapter. Normalized to 1 gram of COD per liter, HAP-C had a concentration 47.7 mg/L per gram of COD (mg/L-gCOD) and 37.6 mg/L-gCOD, and 147.5 mg/L-gCOD for glycerol, acetic acid, and propionic acid respectively. HAP-T had a concentration of 28.2 mg/L-gCOD, 83.6 mg/L-gCOD, and 57.9 mg/L-gCOD for glycerol, acetic acid, and propionic acid respectively.

The presence of propionate being greater in HAP-C than in HAP-T despite the higher performance of HAP-C-fed MECs is unexpected. Hari et al. showed that propionate degradation was not only slower than acetate, but also resulted in lower performances that reactors fed with acetate [50]. Concentrations of propionic acid found in HAP represent a larger percentage of the substrate's COD than other complex feedstocks, such as those described by Satinover et al. (2019) [37] where propionate contributed to less than 8% of their substrate's COD. Pathways used to convert propionic acid and other compounds to current may not be as efficient as model substrates, contributing to losses in performance. Propionate has been shown to be metabolized and result in multiple paths of electron transfer regardless of concentration, and contributes less directly to current than acetate [50, 51]. Further, undetected organics were underrepresented in

measurements. HAP-C had only 35% of its organics as COD identified by both analytical techniques, and only 24.9% were identified for HAP-T. The remaining unquantified organic materials may be more recalcitrant than the organics detected by HPLC. Without standards for the compounds identified by GC-MS, quantifying their removal was not possible. While propionic acid may have contributed to performance losses, the potential impacts unquantified compounds had on performance may also be substantial.

Degradation of Compounds

Of the compounds detected by HPLC, only acetone accumulated under any of the conditions tested, while the other compounds (excluding pyradine) had higher removal percentages and removal rates than acetone. Figure 15 shows the removal percentages and rates of removal for detected compounds at 2, 4, and 10 g/L-day.

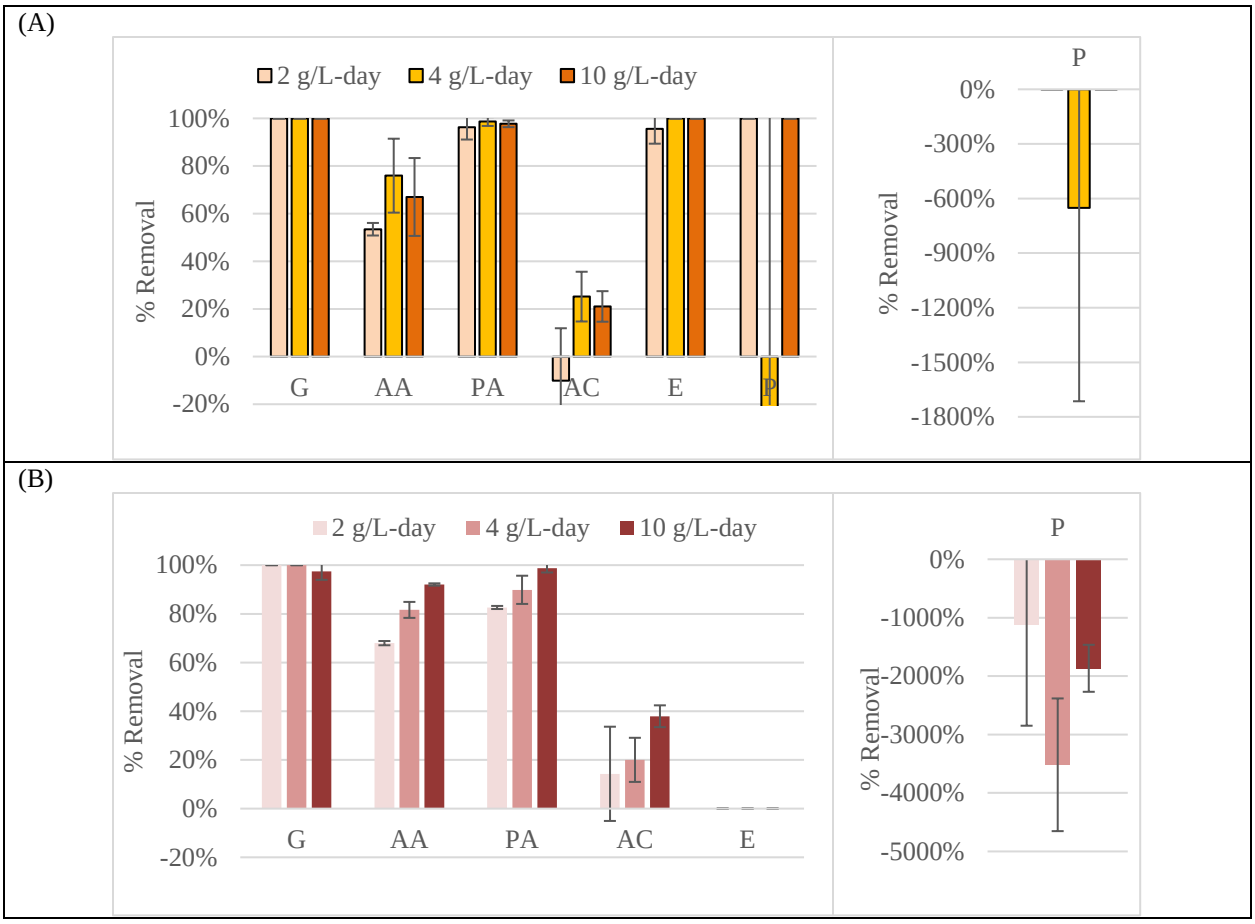

Figure 15: Compound degradation as attributed by HPLC and GC-MS. Compounds shown include glycerol (G), acetic acid (AA), propionic acid (PA), acetone (AC), ethanol (E), and pyridine (P). Figure(A) and Figure(B) show the degradation percentage of each compound identified for MECs fed with HAP-C and HAP-T respectively, and Figure(C) and Figure(D) show the rate of removal of these compounds for MECs fed with HAP-C and HAP-T respectively.

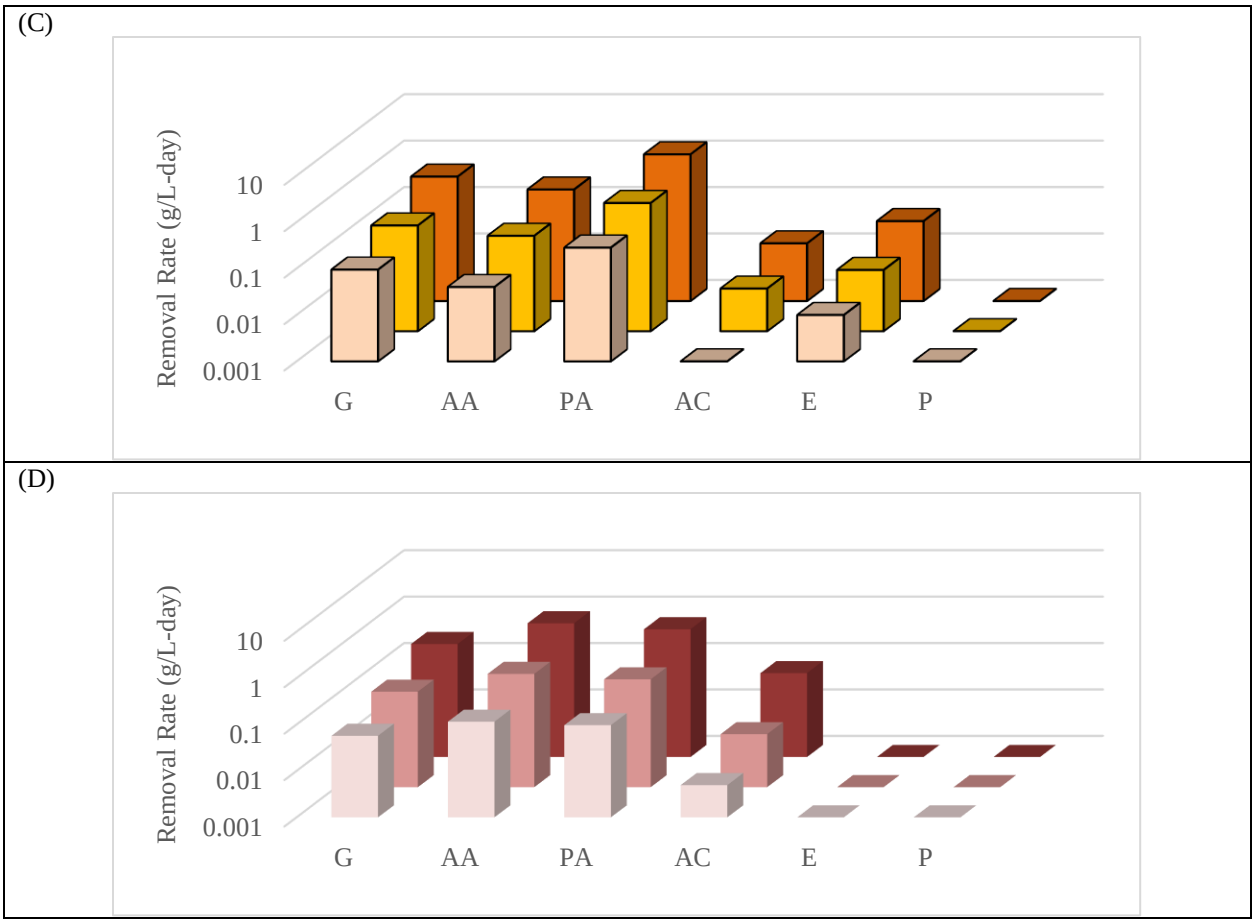

Figure 15 continued

Glycerol removal was almost 100% for all organic loading rates tested using MECs fed with HAP-C and was above 95% under the same loading rates when MECs were fed HAP-T. Similar results have been reported when it is used as a sole carbon source [52] or as a component of a complex feedstock [35]. By contrast, acetate removal was not 100% under all conditions. However, it has been established that acetate can accumulate in MECs operating on complex feedstocks, e.g., switchgrass pyrolysis aqueous phase [53]. Propionic acid was removed at a maximum rate of 1.45 and 0.56 g/L-day at 10 g/L-day when MECs were fed HAP-C and HAP-T respectively, with removal percentages exceeding 90% under all conditions tested. Acetate removal rates were highest at 10 g/L-day as well, reaching 0.25 and 0.76 g/L-day for MECs fed with HAP-C and

HAP-T respectively. HAP-C-fed MECs converted a lower percentage of acetate than when MECs were fed HAP-T under the conditions tested. MECs fed with HAP-T removed nearly all the acetate delivered, while MECs fed with HAP-C reached a maximum removal percentage of 75.9 ± 15.5% at 4 g/L-day conditions.

Acetone was shown to be degraded in MFCs recently by Wu et al. [54], who demonstrated complete removal of acetone and phenol. As shown in Figure 2, acetone was not completely removed for either of the substrates tested here. This may be because of its small concentration in the substrate, it being created as part of the breakdown of chemical species present in HAP, or due to its recalcitrance. Acetone removal will be an important factor if wastewater treatment is a primary goal. Including additional inoculum from other more unconventional sources, or selectively enriching a community on acetone in an MEC may allow for more complete acetone degradation.

Pyridine was degraded in MECs being fed HAP-C but accumulated with MECs fed with HAP-T. In MECs fed with HAP-T, pyridine increased by more than a factor of 10, and due to its low initial concentration, resulted in a large percent change of -3517 ± 1135%. This was equivalent to an accumulation rate of 1.2 ± 0.3 mg/L-day, which occurred at 10 g/L-day, several orders of magnitude less than the removal or accumulation rate of any other compound. Pyridine was completely removed in HAP-C fed MECs at loading rates of 2 and 10 g/L-day, reaching a maximum removal rate of 0.05 ± 0.00 mg/L-day at 10 g/L-day. The variance in removal could be attributed to differences in parent nitrogen compounds in the two substrates. Despite the differences observed between replications, it is unlikely that pyridine was a primary contributor to performance. The pyridine detected in both substrates represented less than 1% of the total COD delivered. Even if pyridine were fully converted, it would not result in a noticeable

increase in performance. Pyridine degradation has been documented in MFCs at higher concentrations before, using concentrations up to 500 mg/L, with more than 95% removal within 24 h [55]. Thus, it's unlikely that pyridine in the concentrations observed in this study was inhibitory or conducive to current generation.

Proton and Ammonium Transfer Results

Proton and NH_3-N accounting was carried out using the measured concentrations of proton carrying species in the anode and cathode in order to calculate separation efficiency and transfer rates. This raw data collected is found in Table 12 in the Appendix of this chapter. The proton transfer efficiency, $\eta_{p\text{-}p}$, includes the protons attributed to ammonium as well as the other sources of protons, such as monophosphate, diphosphate, carbonate, bicarbonate and free protons. The pH of the anode was near neutral, while that in the cathode was high (> 12) for both substrates, indicating ions such as ammonium were deprotonated in the cathode. Figure 16 shows the proton and NH_3-N transfer rates under continuous addition (A and B) and batch addition (C and D) for each of the substrates.

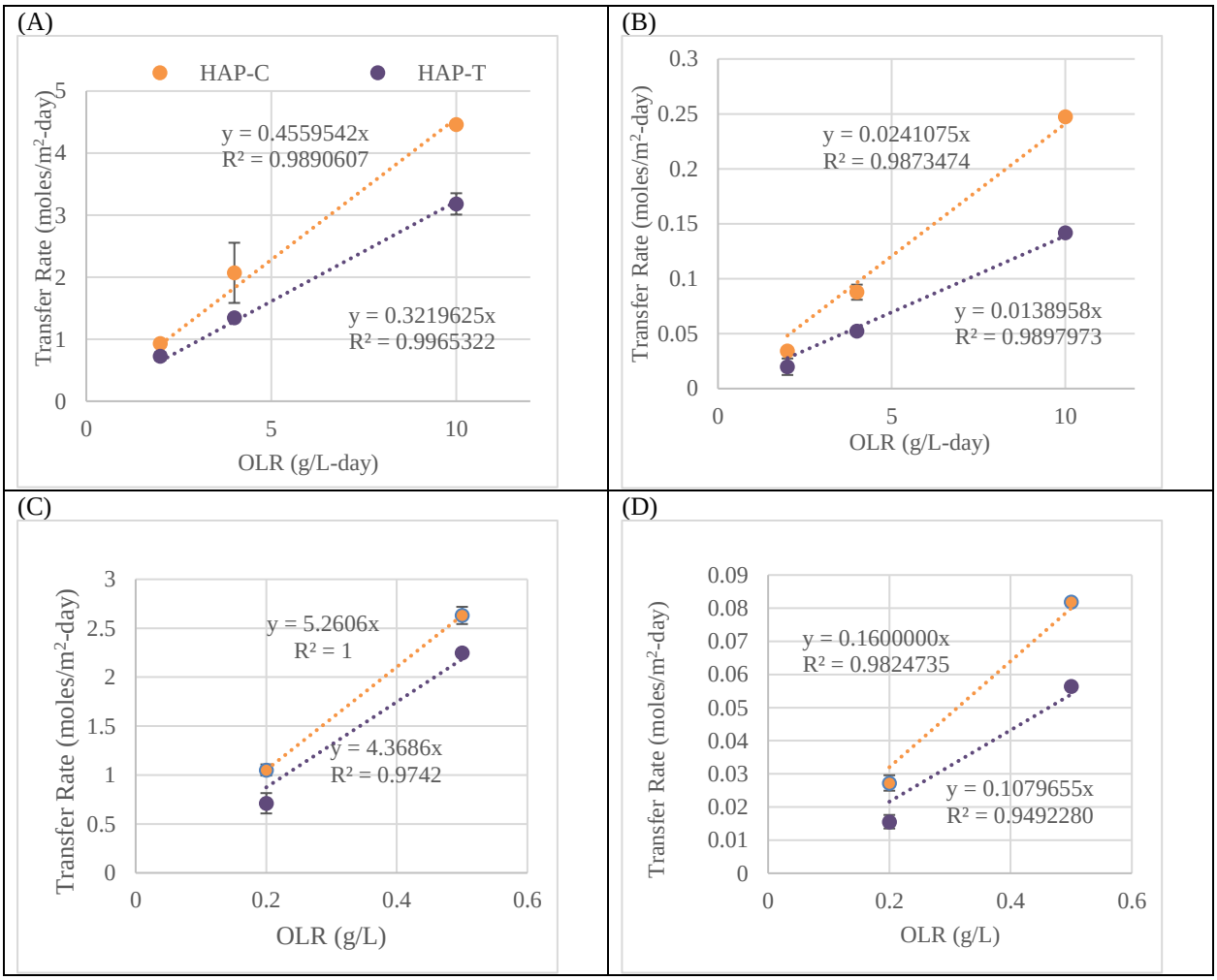

Figure 16: rate of total proton (A) and NH_3-N (B) in MECs fed HAP-C and HAP-T continuously, and rate of proton (C) and NH_3-N transfer (D) for batch experiments

The presence of multiple compounds of nitrogen in the anode, including inorganic and organic compounds, resulted in a complex set of conversions, increasing or decreasing the NH_3-N concentration, driven by the suite of reactions occurring in the anode. The conversion rate of NH_3-N ranged from -172.7 mg NH_3-N per liter of anode volume per day (mg-NH_3-N/L-day), representative of its removal to an accumulation rate of 1295.2 mg-NH_3-N/L-day. This range is larger than what was reported by Joicy et al. [21], whom showed consistent removal rates of NH_3-N averaged at 57 mg-NH_3-N/L-day. It's important to mention the differences between the reactor

used by Joicy et al. and the one used here, as they are not perfectly comparable. The authors only applying 0.6V to the whole reactor using two electrodes in a single chamber, contrasted with the two chamber MEC used in this study. Joicy et al. also only tested one loading rate of nitrogen species, using a fed-batch addition at 500 mg/L of NH_3-N and 300 mg/L of NO_2-N, while the MECs in this study were fed five different organic loading rates and two different substrates. The time period Joicy et al. used was also much longer, lasting more than 80 days, whereas each experiment conducted by the MECs in this study was only three days long at most. The comparison between their reactor and the ones used here would be more analogous if only one organic loading rate was tested in multiple reactors more than once. Despite these differences between the studies, NH_3-N removal and accumulation was consistent amongst replicates. Thus, even though there are additional complexities present in our MECs and the substrate being used, this further supports the explanation that NH_3-N may have been oxidized in MECs during operation by electrochemical or microbial activity.

The relationship between proton transfer and NH_3-N transfer scaled linearly with organic loading rate under all test conditions. As shown in Figure 16, proton and NH_3-N transfer rates were higher in MECs fed HAP-C than MECs fed with HAP-T. The rates were also proportional to the organic loading rate, and the highest proton transfer rate of 4.5 ± 0.05 moles/m^2-day was achieved during 10 g/L-day for HAP-C fed MECs. The NH_3-N transfer rate was also highest at 10 g/L-day at 0.24 ± 0.002 moles/m^2-day in HAP-C fed MEC. As more charge is created, more protons need to be transferred in order to create hydrogen and complete the reaction. However, when compared to similarly configured MECs, some interesting observations can be made. Under identical organic loading rates, MECs showed lower proton transfer rates using a different complex feedstock and lower operating voltages [23]. One might be inclined to attribute this

difference to the availability of ammonium as an alternate charge carrier. However, NH_3-N transfer balanced with only a small percentage of the current generated, representing less than 6% of the moles of charge for the cases tested. Figure 17 illustrates the fraction of cations that balanced with charge produced, including protons and NH_3-N.

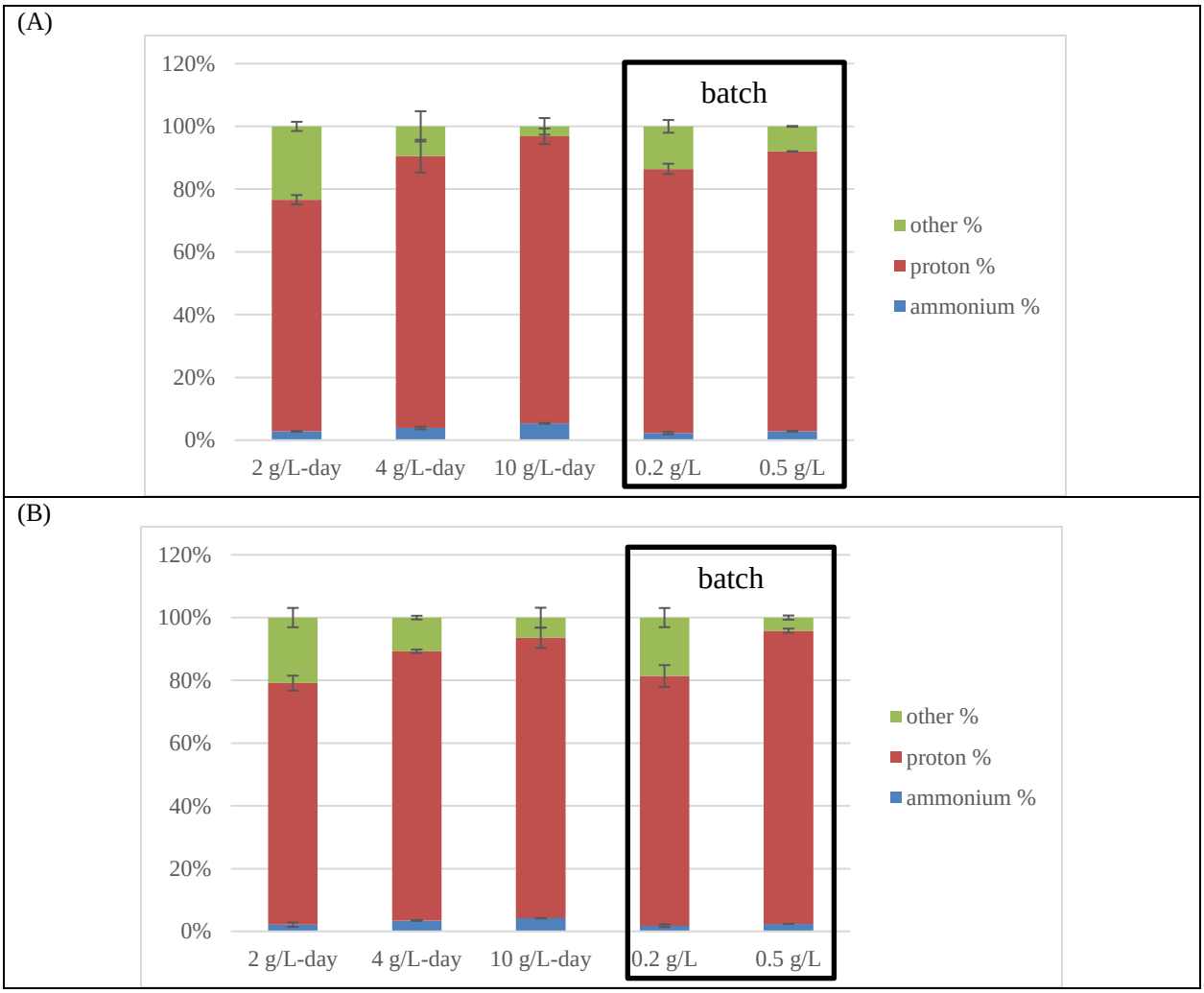

Figure 17: Percentages of moles of cations transferred corresponding to moles of charge generated using HAP-C (A) and HAP-T (B) at all organic load conditions tested. Cations included ammonium, protons, and other cations. NH_3-N was assumed to have transferred as ammonium before deprotonating. Notice that at higher organic loading conditions, higher percentages of charge transfer are attributed to ammonium and protons, not other cations.

This suggests that the rate of proton transfer was only slightly improved by the presence of NH_3-N. In the absence of a buffer in the cathode to draw protons from, hydrogen production was entirely dependent on protons made available in the cathode via proton transfer or dissociation of water from the anode. Once protons are depleted at the cathode, hydroxide ions are left. This was evident from the high pH developed in the cathode. It was also observed that at higher organic loading rates, the potential difference between the anode and cathode, under anode-poising conditions implemented in this study, also increased slightly (see Figure 21 in the Appendix of this chapter). This likely resulted in larger cation and proton transfer to the cathode, supporting the observed hydrogen production rates.

Tracking the NH_3-N and proton transfer efficiency, $\eta_{(NH3\text{-}NH3)}$ and $\eta_{(P\text{-}P)}$ respectively, may provide some additional insight, even if some of the NH_3-N may have been oxidized as a result of MEC operation. Shown in the Figure 18, $\eta_{(NH3\text{-}NH3)}$ was always larger than the percent of NH_3-N that balanced with charge.

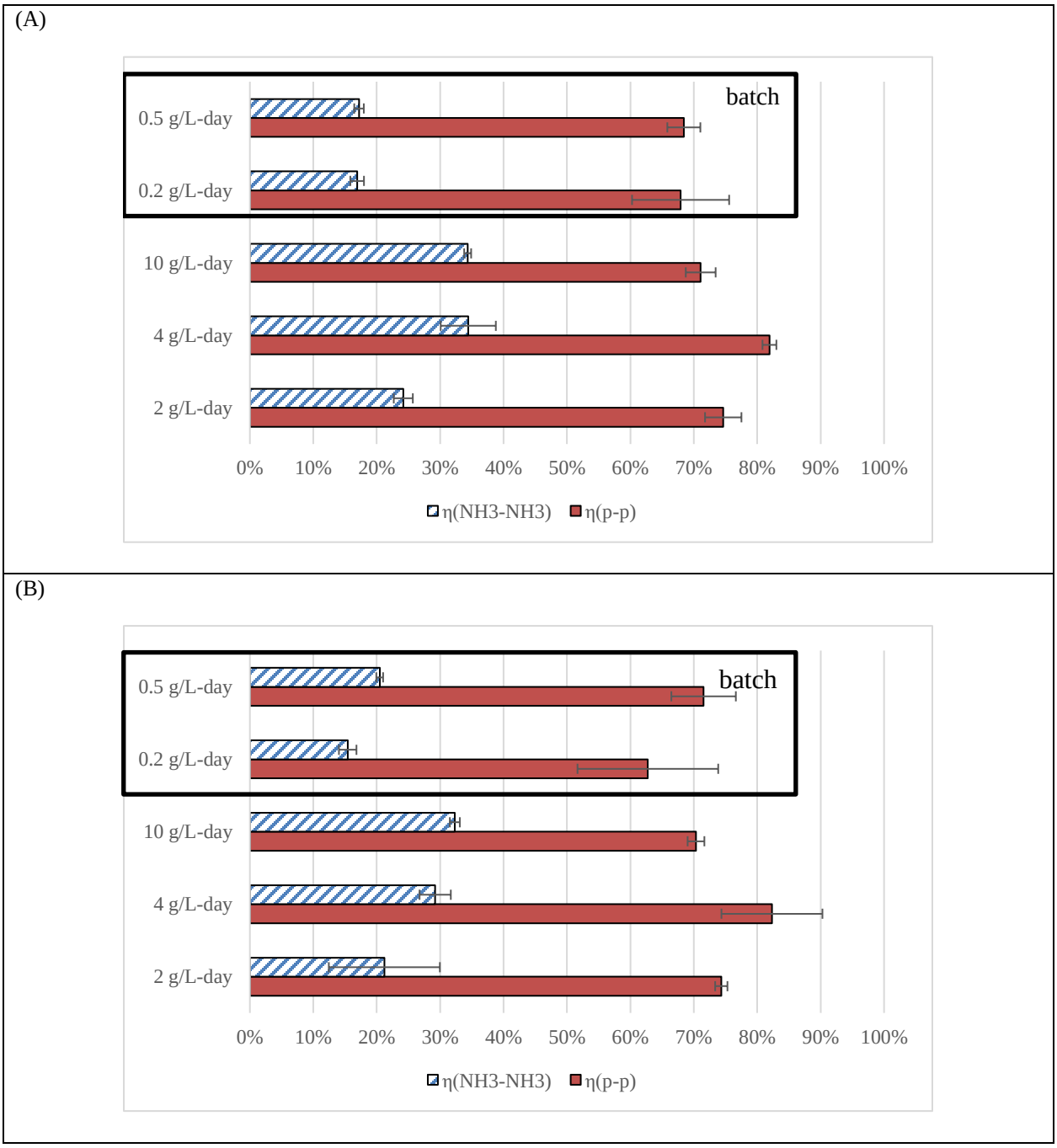

Figure 18: NH_3-N ($\eta_{(NH3-NH3)}$) and proton ($\eta_{(p-p)}$) transfer efficiency as a function of organic loading conditions for MECs fed with HAP-C (A) and HAP-T (B).

The lowest $\eta_{(NH3-NH3)}$ occurred at 0.2 g/L batch addition for each substrate, reaching values of 16.9 ± 1.07% for HAP-C-fed MECs and was 15.4 ± 1.38% for MECs fed with HAP-T. The

highest values for this efficiency occurred at 10 g/L-day for both substrates and were 34.3 ± 0.55% for HAP-C-fed MECs and 32.3 ± 0.79% when MECs were fed HAP-T. The data here shows that a larger fraction of delivered NH_3-N transferred when organic loading rates were high, and when substrate was delivered continuously. Additionally, more total moles of protons were available than NH_3-N, and despite this, a significant fraction of the added NH_3-N was transferred during electrolysis. Lower concentrations of buffers like phosphate used here may therefore drive a higher percentage of NH_3-N due to the unavailability of additional charge carriers. Removal efficiencies in other BESs have been observed previously. One of the highest NH_3-N removal efficiencies reaching above 80% by Cord-Ruwisch et al. in non-buffered MFCs, but this required a regular addition of NH_4OH in order to maintain neutral anode pH [56]. Reducing the buffer concentration in the anode liquid media in MECs may promote more NH_3-N transfer. A pH drop in the anode still occurs when running MECs, and therefore the amount of anode buffer used in order to maintain performance will need to be optimized with improved NH_3-N removal rates.

Algae Regrowth Experiments

Algae regrowth and nutrient removal was analyzed using the nutrient data before and after regrowth experiments. Growth beyond the initial OD was observed, however, both strains grew less than the control experiments that had no added organic carbon. Figure 19 shows the results of optical density (A and B), TN (C and D), and TOC (E and F) where *C. Vulgaris* results are shown in the left-hand side of the column, and *Tetraselmis* sp. results are shown in the right-hand column of the Figure panel.

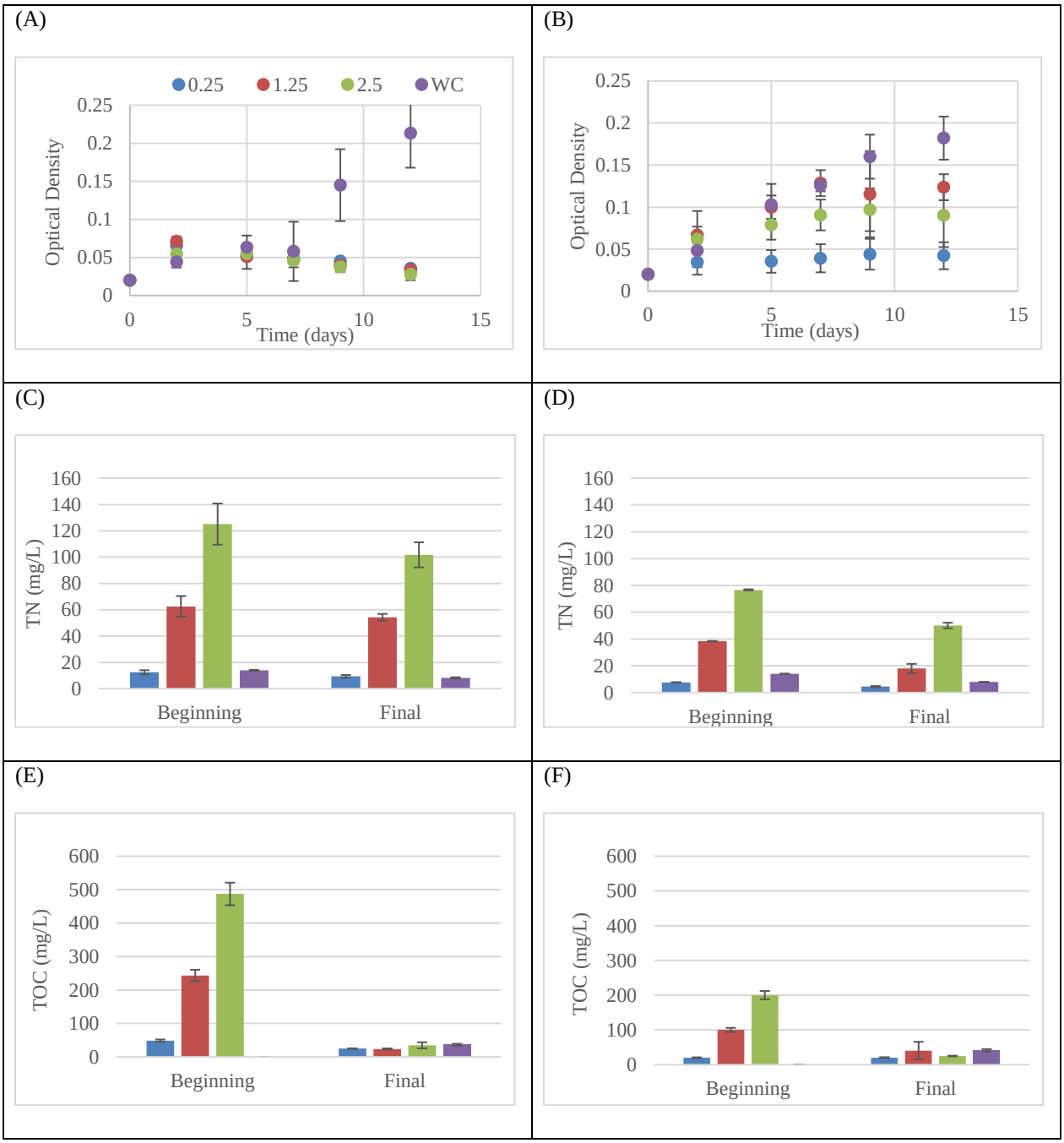

Figure 19: algae growth on MEC effluent results, including optical density (OD) (A and B), total nitrogen (TN) (C and D), total organic carbon (TOC) (E and F) for C. Vulgaris and Tetraselmis sp. regrowth experiments, respectively. Experiments used the same algae for regrowth from which the HAP was derived. Figures 5(A),(C),(E) represent results from C. Vulgaris, and Figures 5(B)(D)(F) represent Tetraselmis sp. Dilution percentages of 0.25, 1.25, and 2.5 are shown, along with the control media (WC) for comparison.

This suggests that these algae species did not grow as efficiently under heterotrophic conditions as they normally do under strictly autotrophic conditions in the WC. This is consistent with some of the results from Biller et al., who showed that algal growth using *Chlorella* HAP peaked early and followed by a loss in total biomass over time, and also that the control nutrient media lead to larger overall algal growth than when using diluted HAP [16]. As shown in prior literature, HAP can be used for microalgae regrowth but can still be inhibitory compared to control media [27-29]. Based on the results shown in this study, along with the COD removal percentages shown in Figure 14(F), MEC effluents were not completely devoid of inhibitory compounds. It was assumed that NH_3-N would contribute to the inhibited growth, specifically found with *C. Vulgaris*. However, Tam and Wong showed that *C. vulgaris* was largely unaffected by ammonium concentrations below 750 mg NH_3-N/L [40], which is a higher concentration than all of the nitrogen delivered in any of the regrowth studies used in this study. More resistant strains have also been observed to have an EC_{50} to NH_3-N up to 1.6 g/L [57]. Therefore, other chemical species not quantified here must have contributed to growth inhibition.

Despite lower growth yields, TOC removal proved promising. TOC was substantially reduced for all HAPs and dilution percentages tested, where final amounts of TOC for all trials were all below 42 mg/L. Shown in Figure 6(E), the largest TOC removal occurred using HAP-C at a dilution percentage of 2.5% MEC effluent, decreasing from 487.2 mg/L to 34.6 mg/L over the span of 11 days. Contrasted to the control media, in which the TOC increased from 0 mg/L to above 35 mg/L for both substrates, the drop in TOC to about the same level in the non-control experiments suggests that hazardous organic materials were sufficiently eliminated using this process. However, as shown by the other nutrient profiles, other inorganics that require removal remain in the growth media.

Total nitrogen did not seem to change as much by comparison to TOC but did decrease at all dilution fractions. The largest reduction occurred with HAP-T at the highest concentration of the effluent, dropping from 76.7 mg/L to 50.1 mg/L after 12 days. Combined with the TOC measurements and optical density, and two conclusions may be drawn. It is most likely that the nitrogen containing carbon compounds converted primarily into inorganic nitrogen species, and much of these were not taken up by either microalgae strain. The nitrogen removal using MEC effluent should be equivalent to what was observed in the control if growth was equivalent, however more nitrogen was removed using diluted HAP than the control despite lower growth. Ultimately, MEC pretreatment was not sufficient for removing inhibitory compounds. The removal of TOC despite the lower growth and continued presence of TN suggests that algae may better grow on MEC effluent if inhibitory compounds can be identified and removed before HAP is used for algae regrowth. The results shown here suggest that algae growth was impeded by HAPs, but nutrient uptake still occurred.

Conclusions

MECs fed HAPs proved to be able to remove significant fractions of nitrogen and organics from feed streams, while efficiently producing hydrogen. Charge balancing was primarily dominated by proton transfer, suggesting that cations of other types were not separated from the anode. However, this comes with its own limitations. Voltages continued to rise as HAP-C loading rates increased, and recalcitrant compounds continued to affect system performance. Further, MEC effluent was still not as effective as the control media when algae regrowth was attempted. It is apparent that algae can be used for effluent treatment but will require additional compound identification and removal before being a practical feedstock for

algae growth. Similarly, MECs exhibited effective removal of some organics, but not of others. Additional organic removal downstream, as demonstrated by Davidson et al. [11], may be used in conjunction with the technologies used here for improved effluent clean up. Ultimately, clean water and waste valorization may prove to be an effective motive for further additions to this framework here.

MECs continue to be plagued by charge and mass transfer limitations, where cations that do not contribute to hydrogen evolution transfer to balance charge. For MECs that are constructed to separate NH_3-N from feedstocks, that problem seems to be overcome partially by running the cathode dry. Still, this comes with its own problems, including MEC applied potentials above 1V, which are not desirable. Additionally, the NH_3-N removal efficiency was not 100%, and it is unlikely to improve beyond this without removing buffers used in the anode. Ideal MECs may not require buffers, but as stated previously in this study, oxidation of NH_3-N may lead to drops in pH that would need to be accounted for either by very precise pH control or buffering. However, because NH_3-N is also potentially created by microbial metabolism of nitrogen containing organics, losses in pH may be overcome. Balancing the generation, oxidation, and transfer of NH_3-N by identifying ideal feedstocks that can establish pH neutrality will be essential for new MECs that are fed nitrogen rich feedstocks.

Removing the compounds still present after algae growth remains a problem even with MEC pretreatment, but this is not entirely a problem. From an extraction perspective, the water used here may be more capable of being recycled into HTL for longer periods of time than previously demonstrated [7-10], as organics no longer accumulate using both of the processes described here . Inorganic removal may be possible using other methods, such as distillation or

reverse osmosis. Ultimately the results here expand on the potential to reuse the HTL wastewater provided.

References

1. Davis, R.; Aden, A.; Pienkos, P. T., Techno-economic analysis of autotrophic microalgae for fuel production. *Applied Energy* **2011,** *88*, (10), 3524-3531.
2. Thilakaratne, R.; Wright, M. M.; Brown, R. C., A techno-economic analysis of microalgae remnant catalytic pyrolysis and upgrading to fuels. *Fuel* **2014,** *128*, 104-112.
3. Gollakota, A. R. K.; Kishore, N.; Gu, S., A review on hydrothermal liquefaction of biomass. *Renewable and Sustainable Energy Reviews* **2018,** *81*, 1378-1392.
4. Chisti, Y., Chapter 1 - Introduction to algal fuels. In *Biofuels from Algae (Second Edition)*, Pandey, A.; Chang, J.-S.; Soccol, C. R.; Lee, D.-J.; Chisti, Y., Eds. Elsevier: 2019; pp 1-31.
5. López Barreiro, D.; Prins, W.; Ronsse, F.; Brilman, W., Hydrothermal liquefaction (HTL) of microalgae for biofuel production: State of the art review and future prospects. *Biomass and Bioenergy* **2013,** *53*, (Supplement C), 113-127.
6. Maddi, B.; Panisko, E.; Wietsma, T.; Lemmon, T.; Swita, M.; Albrecht, K.; Howe, D., Quantitative characterization of the aqueous fraction from hydrothermal liquefaction of algae. *Biomass and Bioenergy* **2016,** *93*, 122-130.
7. Biller, P.; Madsen, R. B.; Klemmer, M.; Becker, J.; Iversen, B. B.; Glasius, M., Effect of hydrothermal liquefaction aqueous phase recycling on bio-crude yields and composition. *Bioresource Technology* **2016,** *220*, 190-199.
8. Chen, H.; He, Z.; Zhang, B.; Feng, H.; Kandasamy, S.; Wang, B., Effects of the aqueous phase recycling on bio-oil yield in hydrothermal liquefaction of Spirulina Platensis, α-cellulose, and lignin. *Energy* **2019,** *179*, 1103-1113.
9. Li, C.; Yang, X.; Zhang, Z.; Zhou, D.; Zhang, L.; Zhang, S.; Chen, J., Hydrothermal Liquefaction of Desert Shrub Salix psammophila to High Value-added Chemicals and Hydrochar with Recycled Processing Water. *2013* **2013,** *8*, (2), 17.
10. Ramos-Tercero, E. A.; Bertucco, A.; Brilman, D. W. F., Process Water Recycle in Hydrothermal Liquefaction of Microalgae To Enhance Bio-oil Yield. *Energy Fuels* **2015,** *29*, (4), 2422-2430.
11. Davidson, S. D.; Lopez-Ruiz, J. A.; Zhu, Y.; Cooper, A. R.; Albrecht, K. O.; Dagle, R. A., Strategies To Valorize the Hydrothermal Liquefaction-Derived Aqueous Phase into Fuels and Chemicals. *ACS Sustainable Chemistry & Engineering* **2019**.
12. Tommaso, G.; Chen, W.-T.; Li, P.; Schideman, L.; Zhang, Y., Chemical characterization and anaerobic biodegradability of hydrothermal liquefaction aqueous products from mixed-culture wastewater algae. *Bioresource Technology* **2015,** *178*, 139-146.
13. Gu, Y.; Zhang, X.; Deal, B.; Han, L., Biological systems for treatment and valorization of wastewater generated from hydrothermal liquefaction of biomass and systems thinking: A review. *Bioresource Technology* **2019,** *278*, 329-345.
14. Shen, R.; Liu, Z.; He, Y.; Zhang, Y.; Lu, J.; Zhu, Z.; Si, B.; Zhang, C.; Xing, X.-H., Microbial electrolysis cell to treat hydrothermal liquefied wastewater from cornstalk and recover hydrogen: Degradation of organic compounds and characterization of microbial community. *International Journal of Hydrogen Energy* **2016,** *41*, (7), 4132-4142.
15. Shen, R.; Jiang, Y.; Ge, Z.; Lu, J.; Zhang, Y.; Liu, Z.; Ren, Z. J., Microbial electrolysis treatment of post-hydrothermal liquefaction wastewater with hydrogen generation. *Applied Energy* **2018,** *212*, 509-515.

16. Biller, P.; Ross, A. B.; Skill, S. C.; Lea-Langton, A.; Balasundaram, B.; Hall, C.; Riley, R.; Llewellyn, C. A., Nutrient recycling of aqueous phase for microalgae cultivation from the hydrothermal liquefaction process. *Algal Research* **2012,** *1*, (1), 70-76.
17. Hydrogen Production and Distribution. https://afdc.energy.gov/fuels/hydrogen_production.html (5/9/2019),
18. Kelly, P. T.; He, Z., Nutrients removal and recovery in bioelectrochemical systems: A review. *Bioresource Technology* **2014,** *153*, 351-360.
19. Jadhav, D. A.; Ghangrekar, M. M., Effective ammonium removal by anaerobic oxidation in microbial fuel cells. *Environmental Technology* **2015,** *36*, (6), 767-775.
20. He, Z.; Kan, J.; Wang, Y.; Huang, Y.; Mansfeld, F.; Nealson, K. H., Electricity Production Coupled to Ammonium in a Microbial Fuel Cell. *Environmental Science & Technology* **2009,** *43*, (9), 3391-3397.
21. Joicy, A.; Song, Y.-C.; Lee, C.-Y., Electroactive microorganisms enriched from activated sludge remove nitrogen in bioelectrochemical reactor. *J. Environ. Manage.* **2019,** *233*, 249-257.
22. Kim, H.-W.; Nam, J.-Y.; Shin, H.-S., Ammonia inhibition and microbial adaptation in continuous single-chamber microbial fuel cells. *Journal of Power Sources* **2011,** *196*, (15), 6210-6213.
23. Borole, A. P.; Lewis, A. J., Proton transfer in microbial electrolysis cells. *Sustainable Energy Fuels* **2017,** *1*, (4), 725-736.
24. Torres, C. I.; Kato Marcus, A.; Rittmann, B. E., Proton transport inside the biofilm limits electrical current generation by anode-respiring bacteria. *Biotechnology and Bioengineering* **2008,** *100*, (5), 872-881.
25. Perez-Garcia, O.; Escalante, F. M. E.; de-Bashan, L. E.; Bashan, Y., Heterotrophic cultures of microalgae: Metabolism and potential products. *Water Research* **2011,** *45*, (1), 11-36.
26. Huang, Y.; Huang, Y.; Liao, Q.; Fu, Q.; Xia, A.; Zhu, X., Improving phosphorus removal efficiency and Chlorella vulgaris growth in high-phosphate MFC wastewater by frequent addition of small amounts of nitrate. *International Journal of Hydrogen Energy* **2017,** *42*, (45), 27749-27758.
27. Leng, L.; Li, J.; Wen, Z.; Zhou, W., Use of microalgae to recycle nutrients in aqueous phase derived from hydrothermal liquefaction process. *Bioresource Technology* **2018,** *256*, 529-542.
28. Jena, U.; Vaidyanathan, N.; Chinnasamy, S.; Das, K. C., Evaluation of microalgae cultivation using recovered aqueous co-product from thermochemical liquefaction of algal biomass. *Bioresource Technology* **2011,** *102*, (3), 3380-3387.
29. Das, P.; AbdulQuadir, M.; Thaher, M.; Khan, S.; Chaudhary, A. K.; Al-Jabri, H., A feasibility study of utilizing hydrothermal liquefaction derived aqueous phase as nutrients for semi-continuous cultivation of Tetraselmis sp. *Bioresource Technology* **2020,** *295*, 122310.
30. Kumar, V.; Kumar, S.; Chauhan, P. K.; Verma, M.; Bahuguna, V.; Joshi, H. C.; Ahmad, W.; Negi, P.; Sharma, N.; Ramola, B.; Rautela, I.; Nanda, M.; Vlaskin, M. S., Low-temperature catalyst based Hydrothermal liquefaction of harmful Macroalgal blooms, and aqueous phase nutrient recycling by microalgae. *Scientific Reports* **2019,** *9*, (1), 11384.
31. Edmundson, S.; Huesemann, M.; Kruk, R.; Lemmon, T.; Billing, J.; Schmidt, A.; Anderson, D., Phosphorus and nitrogen recycle following algal bio-crude production via continuous hydrothermal liquefaction. *Algal Research* **2017,** *26*, 415-421.

32. Elliott, D. C.; Schmidt, A. J.; Hart, T. R.; Billing, J. M., Conversion of a wet waste feedstock to biocrude by hydrothermal processing in a continuous-flow reactor: grape pomace. *Biomass Conversion and Biorefinery* **2017,** *7*, (4), 455-465.
33. Elliott, D. C.; Hart, T. R.; Schmidt, A. J.; Neuenschwander, G. G.; Rotness, L. J.; Olarte, M. V.; Zacher, A. H.; Albrecht, K. O.; Hallen, R. T.; Holladay, J. E., Process development for hydrothermal liquefaction of algae feedstocks in a continuous-flow reactor. *Algal Research* **2013,** *2*, (4), 445-454.
34. Lewis, A. J.; Ren, S.; Ye, X.; Kim, P.; Labbe, N.; Borole, A. P., Hydrogen production from switchgrass via an integrated pyrolysis–microbial electrolysis process. *Bioresource Technology* **2015,** *195*, 231-241.
35. Satinover, S. J.; Schell, D.; Borole, A. P., Achieving high hydrogen productivities of 20 L/L-day via microbial electrolysis of corn stover fermentation products. *Applied Energy* **2020**, 114126.
36. Wolin, E. A.; Wolin, M. J.; Wolfe, R. S., Formation of Methane by Bacterial Extracts. *Journal of Biological Chemistry* **1963,** *238*, (8), 2882-2886.
37. Satinover, S. J.; Elkasabi, Y.; Nuñez, A.; Rodriguez, M.; Borole, A. P., Microbial electrolysis using aqueous fractions derived from Tail-Gas Recycle Pyrolysis of willow and guayule. *Bioresource Technology* **2019,** *274*, 302-312.
38. Lu, L.; Hou, D.; Wang, X.; Jassby, D.; Ren, Z. J., Active H2 Harvesting Prevents Methanogenesis in Microbial Electrolysis Cells. *Environmental Science & Technology Letters* **2016,** *3*, (8), 286-290.
39. Snoeyink, V. L.; Jenkins, D., *Water Chemistry*. 1 edition ed.; Wiley: New York, 1980; p 480.
40. Tam, N. F. Y.; Wong, Y. S., Effect of ammonia concentrations on growth of Chlorella vulgaris and nitrogen removal from media. *Bioresource Technology* **1996,** *57*, (1), 45-50.
41. Chen, S. Y.; Pan, L. Y.; Hong, M. J.; Lee, A. C., The effects of temperature on the growth of and ammonia uptake by marine microalgae. *Botanical Studies* **2012,** *53*, 125-133.
42. Mandal, S.; Shurin, J. B.; Efroymson, R. A.; Mathews, T. J., Heterogeneity in Nitrogen Sources Enhances Productivity and Nutrient Use Efficiency in Algal Polycultures. *Environmental Science & Technology* **2018,** *52*, (6), 3769-3776.
43. Shurin, J. B.; Mandal, S.; Abbott, R. L., Trait diversity enhances yield in algal biofuel assemblages. *Journal of Applied Ecology* **2014,** *51*, (3), 603-611.
44. Guillard, R. R. L.; Lorenzen, C. J., Yellow-green algae with 590 chlorophyllide. *Journal of Phycology* **1972,** *8*, (1), 10-14.
45. Brooks, V.; Lewis, A. J.; Dulin, P.; Beegle, J. R.; Rodriguez, M.; Borole, A. P., Hydrogen production from pine-derived catalytic pyrolysis aqueous phase via microbial electrolysis. *Biomass and Bioenergy* **2018,** *119*, 1-9.
46. Vitse, F.; Cooper, M.; Botte, G. G., On the use of ammonia electrolysis for hydrogen production. *Journal of Power Sources* **2005,** *142*, (1), 18-26.
47. Nisman, B., The Stickland reaction. *Bacteriol Rev* **1954,** *18*, (1), 16-42.
48. Watson, G. K.; Cain, R. B., Microbial metabolism of the pyridine ring. Metabolic pathways of pyridine biodegradation by soil bacteria. *Biochem J* **1975,** *146*, (1), 157-172.
49. Park, L. K.-E.; Satinover, S. J.; Yiacoumi, S.; Mayes, R. T.; Borole, A. P.; Tsouris, C., Electrosorption of organic acids from aqueous bio-oil and conversion into hydrogen via microbial electrolysis cells. *Renewable Energy* **2018,** *125*, 21-31.

50. Hari, A. R.; Venkidusamy, K.; Katuri, K. P.; Bagchi, S.; Saikaly, P. E., Temporal Microbial Community Dynamics in Microbial Electrolysis Cells – Influence of Acetate and Propionate Concentration. *Front Microbiol* **2017,** *8*, (1371).
51. Hari, A. R.; Katuri, K. P.; Gorron, E.; Logan, B. E.; Saikaly, P. E., Multiple paths of electron flow to current in microbial electrolysis cells fed with low and high concentrations of propionate. *Applied Microbiology and Biotechnology* **2016,** *100*, (13), 5999-6011.
52. Selembo, P. A.; Perez, J. M.; Lloyd, W. A.; Logan, B. E., High hydrogen production from glycerol or glucose by electrohydrogenesis using microbial electrolysis cells. *International Journal of Hydrogen Energy* **2009,** *34*, (13), 5373-5381.
53. Lewis, A. J.; Campa, M. F.; Hazen, T. C.; Borole, A. P., Unravelling biocomplexity of electroactive biofilms for producing hydrogen from biomass. *Microb. Biotechnol.* **2018,** *11*, (1), 84-97.
54. Wu, H.; Fu, Y.; Guo, C.; Li, Y.; Jiang, N.; Yin, C., Electricity generation and removal performance of a microbial fuel cell using sulfonated poly (ether ether ketone) as proton exchange membrane to treat phenol/acetone wastewater. *Bioresource Technology* **2018,** *260*, 130-134.
55. Zhang, C.; Li, M.; Liu, G.; Luo, H.; Zhang, R., Pyridine degradation in the microbial fuel cells. *J. Hazard. Mater.* **2009,** *172*, (1), 465-471.
56. Cord-Ruwisch, R.; Law, Y.; Cheng, K. Y., Ammonium as a sustainable proton shuttle in bioelectrochemical systems. *Bioresource Technology* **2011,** *102*, (20), 9691-9696.
57. Wang, J.; Zhou, W.; Chen, H.; Zhan, J.; He, C.; Wang, Q., Ammonium Nitrogen Tolerant Chlorella Strain Screening and Its Damaging Effects on Photosynthesis. *Front Microbiol* **2019,** *9*, (3250).

Chapter III Appendix

MEC Charge Transfer Tracking

The protons that belong to each species were calculated using information described by Snoeyink and Jenkins [1]. Phosphate species were determined using 50 mM of Phosphate ($C_{T,PO4}$) as the starting and final concentration in the cathode for all experiments, and the pH was measured before and after experiments to adjust individual species' concentrations. Carbonate was assumed to be zero in the anode at the initial condition and was measured in the anode at the final time point of the experiments. Total ammoniacal nitrogen was measured at the beginning and end of experiments in the anode and cathode. The equations used to determine the species concentrations were:

Free protons

$$[H^+] = 10^{-pH}$$

From the pH measured before and after the experiments, the concentration of free protons can be used to determine the concentrations of the various subspecies of phosphate, carbonate, and ammonium, if the total concentration of those compounds are known, otherwise they must be calculated. In this study, the total concentrations of these compounds are either known or are measured directly. They include total phosphates ($C_{t,PO4}$), total inorganic carbon ($C_{t,CO3}$), and total NH_3-N ($C_{t,NH3\text{-}N}$), all in units of M. The subspecies concentrations are then calculated using alpha notation. Below are the mathematical formulas used to derive the subspecies concentrations affiliated with each major species.

Phosphate

Phosphate can protonate three times. $C_{t,PO4}$ is added to the liquid media directly, so its concentration is assumed to be that value.

$$C_{T,PO_4} = 50\ mM$$

From here, alpha notation is used to find the concentrations of the subspecies of phosphate, namely H_3PO_4, $H_2PO_4^-$, HPO_4^{2-}, and PO_4^{3-}.

$$\alpha_{0,P} = \frac{[H^+]^3}{D_p} = \frac{[H_3PO_4]}{C_{T,PO_4}} \qquad \alpha_{1,P} = \frac{K_{a,1}[H^+]^2}{D_p} = \frac{[H_2PO_4^-]}{C_{T,PO_4}} \qquad \alpha_{2,P} = \frac{K_{a,1}K_{a,2}[H^+]}{D_p}$$

$$= \frac{[HPO_4^{2-}]}{C_{T,PO_4}} \qquad \alpha_{3,P} = \frac{K_{a,1}K_{a,2}K_{a,3}}{D_p} = \frac{[PO_4^{3-}]}{C_{T,PO_4}}$$

The brackets indicate that the subspecies is in units of M. The expression Dp is defined by using the equilibrium constants of the phosphate subspecies and the concentration of free protons.

$$D_p = [H^+]^3 + K_{a,1}[H^+]^2 + K_{a,1}K_{a,2}[H^+] + K_{a,1}K_{a,2}K_{a,3}$$

The species in brackets represent that species concentration in units of M. The equilibrium constants used are:

$$K_{a,1} = 10^{-2.1} \qquad K_{a,2} = 10^{-7.2} \qquad K_{a,3} = 10^{-12.3}$$

Carbonate

Carbonate is measured by measuring total inorganic carbon. It is assumed to be zero at the beginning of the experiment and is measured at the end of the experiment.

$$C_{T,CO_3} = determined\ by\ measurement$$

Carbonate can protonate twice. Its alpha notation is therefore defined by:

$$\alpha_{0,C} = \frac{[H^+]^2}{D_c} = \frac{[H_2CO_3^*]}{C_{T,CO_3}} \qquad \alpha_{1,C} = \frac{[H^+]K_{a,1}}{D_c} = \frac{[HCO_3^-]}{C_{T,CO_3}} \qquad \alpha_{2,C} = \frac{K_{a,1}K_{a,2}}{D_c}$$

$$= \frac{[CO_3^{2-}]}{C_{T,CO_3}}$$

And the expression for Dc is defined as:

$$D_c = [H^+]^2 + [H^+]K_{a,1} + K_{a,1}K_{a,2}$$

The equilibrium constants used were:

$$K_{a,1} = 10^{-6.33} \qquad K_{a,2} = 10^{-10.33}$$

Ammonia and Ammonium

Much like carbonate, NH_3-N is measured during the experiments, however it is measured using the kits described in the Methods section. The total amount of NH_3-N is therefore:

$$C_{T,NH_3-N} = determined\ by\ measurement$$

Ammonia can only protonate once. Its alpha notation is therefore:

$$\alpha_{0,N} = \frac{[H^+]}{D_N} = \frac{[NH_4^+]}{C_{T,NH_3-N}} \qquad \alpha_{1,N} = \frac{K_a}{D_N} = \frac{[NH_3]}{C_{T,NH_3-N}}$$

$$D_N = [H^+] + K_a$$

From the expressions above, subspecies can be calculated. Total protons were accounted for by summing each species that was capable of donating protons, scaling for the amount of protons they store. Total protons, in moles, stored in the anode were determined by the following expression calculated before (subscript i) and after (subscript f) the experiment for the anode (subscript a) and cathode (subscript c):

$$H_{a,i}^+ = (3[H_3PO_4] + 2[H_2PO_4^{2-}] + [HPO_4^{3-}] + [NH_4^+] + [H^+])_i(liquid\ volume)$$

$$= \left(3\alpha_{0,P}C_{T,PO_4} + 2\alpha_{1,P}C_{T,PO_4} + \alpha_{3,P}C_{T,PO_4} + \alpha_{0,N}C_{T,NH_3-N} + [H^+]\right)_i(liquid\ volume)$$

$$H_{a,f}^+ = (3[H_3PO_4] + 2[H_2PO_4^{2-}] + [HPO_4^{3-}] + 2[H_2CO_3^*] + [HCO_3^-] + [NH_4^+] + [H^+] + [NaOH]_{added})_f(liquid\ volume)$$

$$= \left(3\alpha_{0,P}C_{T,PO_4} + 2\alpha_{1,P}C_{T,PO_4} + \alpha_{3,P}C_{T,PO_4} + 2\alpha_{0,C}C_{T,CO_3} + \alpha_{1,C}C_{T,CO_3} + \alpha_{0,N}C_{T,NH_3-N} + [H^+] + [NaOH]_{added}\right)_f(liquid\ volume)$$

Total moles of protons stored in the cathode before and after the experiment were determined by:

$$H_{c,i}^+ = (10^{-7})(catholyte\ volume) = 0$$

$$H_{c,f}^{+} = ([NH_4^+] + [H^+])(catholyte\ volume) + \frac{2(H_2\ volume\ in\ ml)}{24.3}$$

The above equation was then scaled to the projected surface area in order to calculate the rate of transfer. The amount of protons transferred was therefore determined as:

$$H_{transferred}^{+} = H_{c,f}^{+} - H_{c,i}^{+}$$

$$NH_{3_{transferred}} = \left(C_{T,NH_3-N}\right)_{c,f} - \left(C_{T,NH_3-N}\right)_{c,i}$$

The moles of charge created was determined by the average current produced, and calculating the equivalent amount of moles of charge produced.

$$n_{moles\ e^-} = \frac{I_{avg}t}{F}$$

Where I_{avg} is the average current of the experiment, t is the time of the experiment, and F is Faraday's constant. The cathodic proton transfer ratio over charge is therefore:

$$\eta_{p-e} = \frac{H_{c,f}^{+} - H_{c,i}^{+}}{n_{moles\ e^-}} = \frac{H_{transferred}^{+}}{n_{moles\ e^-}}$$

The same formula can be used for finding the NH_3-N to charge transfer ratio:

$$\eta_{[NH_3-N]_c} = \frac{([NH_4^+]_{c,f} + [NH_3]_{c,f} - [NH_4^+]_{c,i} - [NH_3]_{c,i})}{n_{moles\ e^-}} = \frac{NH_{3_{transferred}}}{n_{moles\ e^-}}$$

To avoid accounting for the charge contributed by NH_3-N more than once, the proton transfer percentage that was plotted in the main body of the text does not include the charge transferred due to ammonium, despite this contributing to overall proton transfer. The plotted value is therefore the difference between the two ratios described above. This difference therefore accounts for any protons that may have deprotonated from ammonium to form hydrogen.

Efficiencies were calculated by taking the total final and initial concentrations of protons:

$$H_i^+ = H_{c,i}^+ + H_{a,i}^+$$

$$H_f^+ = H_{c,f}^+ + H_{a,f}^+$$

And then dividing this by the calculated amount transferred for both protons and ammonium:

$$\eta_{p-p} = \frac{H_{transferred}^+}{H_f^+ - H_i^+}$$

$$\eta_{NH_3-NH_3} = \frac{NH_{3_{transferred}}}{(NH_3)_e - (NH_3)_i}$$

Progressive Evolution Results

After the MECs were operated and swapped, the current densities and hydrogen productivities using a batch of 0.5 g/L of HAP-C were applied and compared. The graphs shown below indicate that longer exposure did not necessarily improve performance.

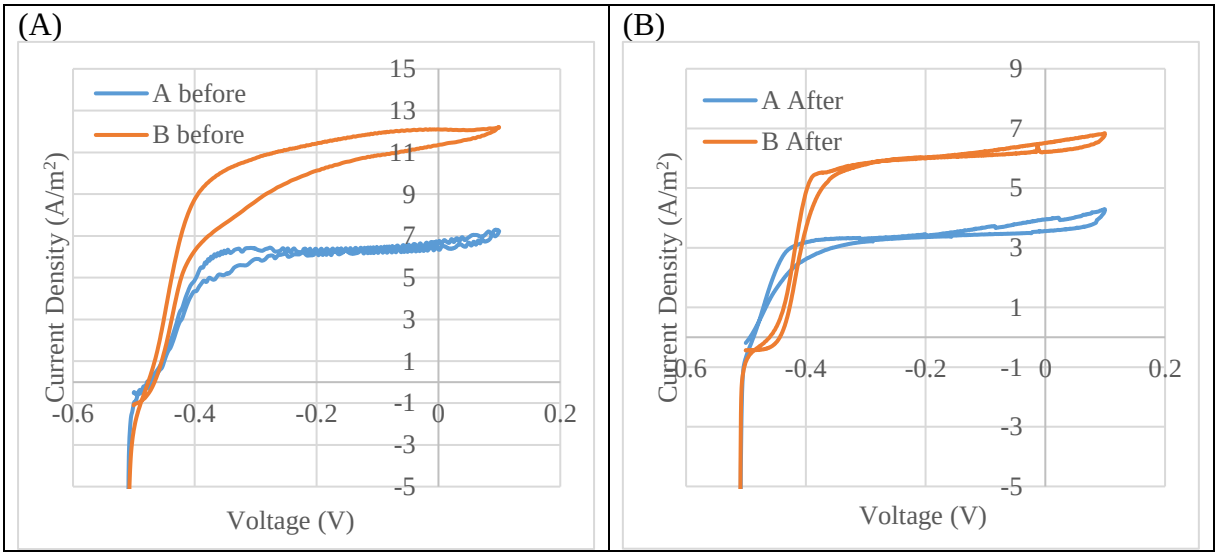

Figure 20: Cyclic voltammetry results before (A) and after (B) regrowth and attempted evolution. Notice that current densities did not necessarily improve after progressive evolution using HAP-C.

Table 10: Current densities and hydrogen productivities before and after regrowth sequences. Notice that average current densities and productivities remained unchanged despite prolonged adaptation and exposure.

Average	**0.5 g/L Before**	**0.5 g/L After**
Hydrogen productivity (L/L-day)	2.4 ± 0.0	2.4 ± 0.1
Current Density (A/m^2)	3.1 ± 0.4	2.4 ± 0.0

Table 11: COD composition each identified compound contributes to the total COD of the substrate for HAP-C (A) and HAP-T (B).

(A)

Compound	**COD %**
glycerol	5.8%
acetate	4.0%
propionate	22.3%
acetone	1.8%
ethanol	1.1%
pyridine	0.001%
Total	35.0%

(B)

Compound	**COD %**
glycerol	3.4%
acetate	8.9%
propionate	8.8%
acetone	3.8%
ethanol	0.0%
pyridine	0.001%
Total	24.9%

Additional Electrochemistry Results

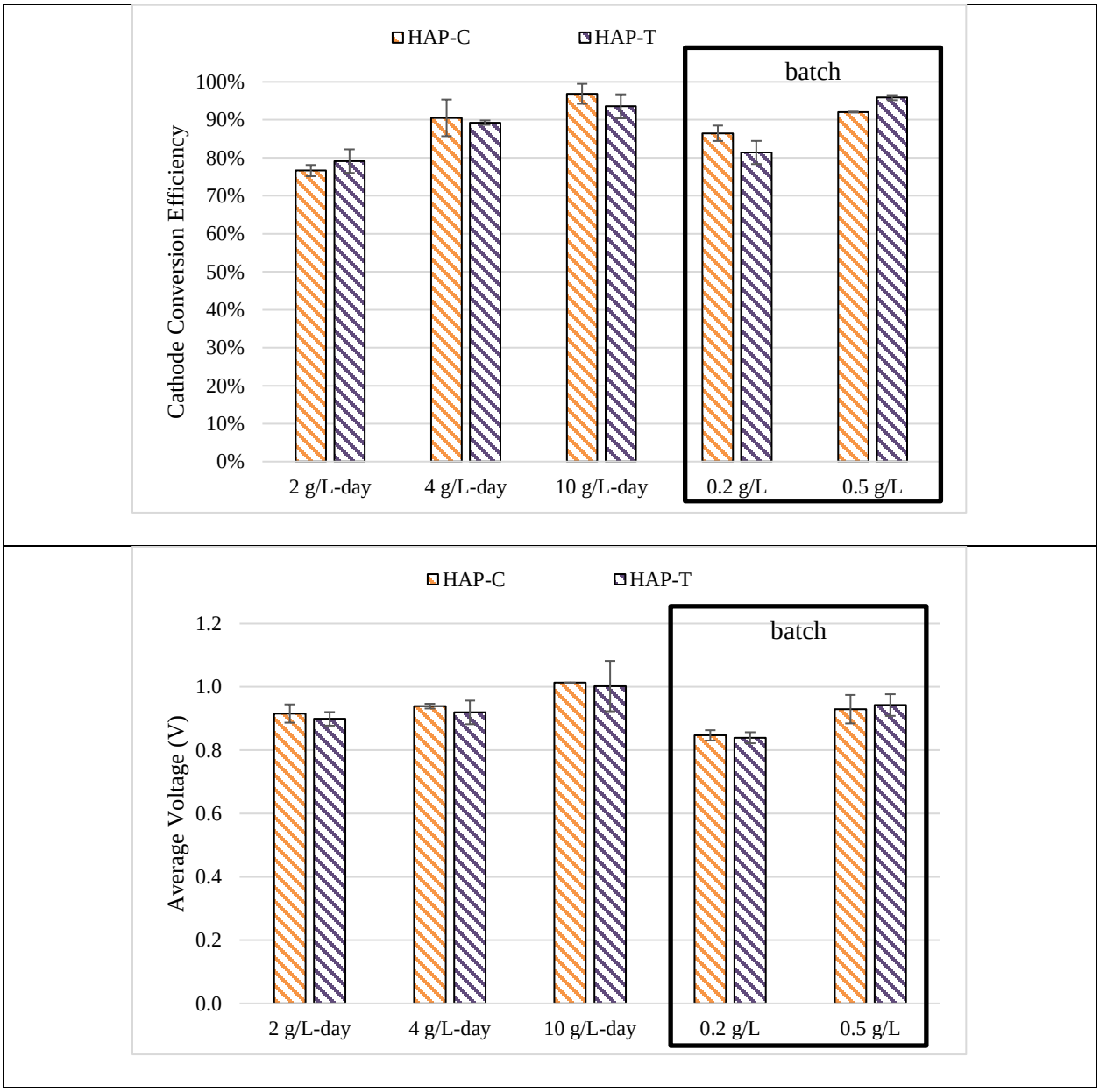

Figure 21: Cathode conversion efficiency and average voltage of MECs that were fed HAP-C and HAP-T.

Charge Transfer Data

Below is the raw data associated with the proton transfer accounting. This includes hydrogen gas produced, the inorganic carbon, the NH_3-N, added NaOH, and the operating conditions including organic loading (OL) and substrate type. Measurements made before and after experiments from the anode and cathode are shown.

Table 12: Raw data for proton transfer tracking calculations before experiments ((A) and (C)) and after experiments ((B) and (D))

(A) Anode Initial Concentrations

reactor	**TIC (mg/L)**	**NH_3-N (mg/L)**	**pH**	**H_2 (mL)**	**NaOH (mL)**	**OL (g/L-day)**	**Substrate**
80A	0	3.497764	7.04	0	0	2	HAP-C
80B	0	3.008077	7.09	0	0	2	HAP-C
80A	0	3.987451	6.91	0	0	4	HAP-C
80B	0	1.364128	6.99	0	0	4	HAP-C
80A	0	8.849343	7.12	0	0	10	HAP-C
80B	0	5.316601	7.1	0	0	10	HAP-C
80A	0	2.553368	7.12	0	0	0.2 g/L	HAP-C
80B	0	3.25292	7.09	0	0	0.2 g/L	HAP-C
80A	0	3.497764	7.1	0	0	0.5 g/L	HAP-C
80B	0	1.888793	7.1	0	0	0.5 g/L	HAP-C
80A	0	1.504038	7.14	0	0	2	HAP-T
80B	0	0.314799	7.02	0	0	2	HAP-T
80A	0	2.168614	7.04	0	0	4	HAP-T
80B	0	2.343502	7.08	0	0	4	HAP-T
80A	0	2.693278	7.18	0	0	10	HAP-T
80B	0	1.399106	7.09	0	0	10	HAP-T
80A	0	2.763233	7.36	0	0	0.2 g/L	HAP-T
80B	0	1.993725	7.26	0	0	0.2 g/L	HAP-T
80A	0	1.294173	6.99	0	0	0.5 g/L	HAP-T
80B	0	2.168614	6.99	0	0	0.5 g/L	HAP-T

Table 12 continued

(B) Anode Final Concentrations

reactor	TIC (mg/L)	NH_3-N (mg/L)	pH	H_2 (mL)	NaOH (mL)	OL (g/L-day)	Substrate
80A	4.354	34.62786	6.91	0	0	2	HAP-C
80B	4.53	34.66284	6.93	0	0	2	HAP-C
80A	0.5748	49.17856	6.58	0	0	4	HAP-C
80B	4.66	54.56512	6.83	0	0	4	HAP-C
80A	15.866	150.7536	7.05	0	1	10	HAP-C
80B	11.376	140.6101	7.23	0	1	10	HAP-C
80A	6.152	15.70496	7.01	0	0	0.2 g/L	HAP-C
80B	2.418	16.47447	7.04	0	0	0.2 g/L	HAP-C
80A	10.23	44.35165	6.89	0	0	0.5 g/L	HAP-C
80B	11.94	39.94446	6.96	0	0	0.5 g/L	HAP-C
80A	4.038	21.47627	7.01	0	0	2	HAP-T
80B	2.088	25.00901	6.9	0	0	2	HAP-T
80A	6.592	37.77585	7.01	0	0	4	HAP-T
80B	2.8	42.46285	6.88	0	0	4	HAP-T
80A	15.59	88.14365	7.03	0	0.6	10	HAP-T
80B	9.078	91.99119	6.94	0	0.6	10	HAP-T
80A	4.906	11.40271	7.23	0	0	0.2 g/L	HAP-T
80B	5.008	10.98298	7.23	0	0	0.2 g/L	HAP-T
80A	7.418	23.99466	6.78	0	0	0.5 g/L	HAP-T
80B	3.541	23.47	6.86	0	0	0.5 g/L	HAP-T

Table 12 continued

(C) Cathode Initial Concentrations

reactor	TIC (mg/L)	NH_3-N (mg/L)	pH	H_2 (mL)	NaOH (mL)	OL (g/L-day)	Substrate
80A	0	0	7	0	0	2	HAP-C
80B	0	0	7	0	0	2	HAP-C
80A	0	0	7	0	0	4	HAP-C
80B	0	0	7	0	0	4	HAP-C
80A	0	0	7	0	0	10	HAP-C
80B	0	0	7	0	0	10	HAP-C
80A	0	0	7	0	0	0.2 g/L	HAP-C
80B	0	0	7	0	0	0.2 g/L	HAP-C
80A	0	0	7	0	0	0.5 g/L	HAP-C
80B	0	0	7	0	0	0.5 g/L	HAP-C
80A	0	0	7	0	0	2	HAP-T
80B	0	0	7	0	0	2	HAP-T
80A	0	0	7	0	0	4	HAP-T
80B	0	0	7	0	0	4	HAP-T
80A	0	0	7	0	0	10	HAP-T
80B	0	0	7	0	0	10	HAP-T
80A	0	0	7	0	0	0.2 g/L	HAP-T
80B	0	0	7	0	0	0.2 g/L	HAP-T
80A	0	0	7	0	0	0.5 g/L	HAP-T
80B	0	0	7	0	0	0.5 g/L	HAP-T

Table 12 continued

(D) Cathode Final Concentrations

reactor	TIC (mg/L)	NH_3-N (mg/L)	pH	H_2 (mL)	NaOH (mL)	OL (g/L-day)	Substrate
80A	0	114.7267	13.1	44.22017	0	2	HAP-C
80B	0	103.8836	12.96	41.09311	0	2	HAP-C
80A	0	295.9108	13.26	110.4261	0	4	HAP-C
80B	0	265.1305	13.07	79.02471	0	4	HAP-C
80A	0	795.7413	13.56	205.4765	0	10	HAP-C
80B	0	785.248	13.47	202.555	0	10	HAP-C
80A	0	27.63233	12.59	16.86261	0	0.2 g/L	HAP-C
80B	0	30.95521	12.26	15.51508	0	0.2 g/L	HAP-C
80A	0	89.19298	12.94	42.06122	0	0.5 g/L	HAP-C
80B	0	89.54276	12.77	40.14934	0	0.5 g/L	HAP-C
80A	0	82.19745	12.44	35.95943	0	2	HAP-T
80B	0	47.56959	12.72	31.60077	0	2	HAP-T
80A	0	174.1886	12.66	63.99023	0	4	HAP-T
80B	0	165.794	13.07	61.3524	0	4	HAP-T
80A	0	456.4582	13.27	141.5302	0	10	HAP-T
80B	0	459.956	13.33	152.7602	0	10	HAP-T
80A	0	15.91483	12.44	12.6772	0	0.2 g/L	HAP-T
80B	0	19.2377	12.16	10.3121	0	0.2 g/L	HAP-T
80A	0	62.2602	13.17	35.70251	0	0.5 g/L	HAP-T
80B	0	61.21087	13.07	34.81717	0	0.5 g/L	HAP-T

Chapter III Appendix References

1. Snoeyink, V. L.; Jenkins, D., *Water Chemistry*. 1 edition ed.; Wiley: New York, 1980; p 480.

CHAPTER IV

ACHIEVING HIGH HYDROGEN PRODUCTIVITIES OF 20 L/L-DAY VIA MICROBIAL ELECTROLYSIS OF CORN STOVER FERMENTATION PRODUCTS

This chapter was originally published as:

Satinover, S. J.; Schell, D.; Borole, A. P., Achieving high hydrogen productivities of 20 L/L-day via microbial electrolysis of corn stover fermentation products. *Applied Energy* **2019**, 114126.

Only minor grammatical and formatting changes have been made to this chapter from the version in print. Satinover, S. conducted the microbial electrolysis work, as well as performed the analysis, wrote the chapter, and made revisions as suggested by coauthors. Schell, D. and his team provided the High-Performance Liquid Chromatography measurements used in the chapter. Borole A. provided guidance and feedback on experiments, data analysis, manuscript preparation, editing the drafts, and submitted the final version for journal publication.

Abstract

Microbial electrolysis cells have the potential to generate renewable hydrogen from underutilized waste streams, however current devices have not reached very large productivity targets using real waste products at any scale. This study used a waste from fermented corn stover known as corn stover fermentation product to reach performance metrics that could be commercialized, if adequately scaled. Average current densities in MECs with mature biofilms reached 17.9 ± 1.6 A/m^2 at an organic loading rate of 30 grams of chemical oxygen demand per liter of anode volume per day (g/L-day), reaching a maximum current density of 27.2 ± 2.9 A/m^2. Hydrogen productivities reached 20.2 ± 2.0 L of H_2 per L anode volume per day (L/L-day). These represent the highest current densities and highest hydrogen productivities using a complex feedstock in a microbial electrolysis cell. Organic acids and sugars present in untreated substrate were converted at high percentages in MECs, with most above 90% conversion, at

organic loading rates of 10, 20, and 30 g/L-day. The effect of periodic high liquid flow rates through the anode on performance was assessed. These tests, called pulsing, showed that hydrogen productivities and current densities increased most dramatically as flow was pulsed every hour at a baseline flow rate of 0.3 mL/min. These productivities show promise for high performance systems, if adequate scale up can be achieved.

Introduction

Hydrogen offers tremendous value as a feedstock for chemical processes as well as an energy carrier and a storage medium as a carbon-free energy source. One of the major limitations to growth of more widespread hydrogen use is the inability to produce it in enough quantities from renewable sources. Currently, most hydrogen is produced from natural gas via steam reforming [1], which is not sustainable. Additionally, the infrastructure needed for a central hydrogen distribution network does not exist yet. These issues have led to scrutiny of the hypothetical hydrogen energy economy. To support widespread adoption of hydrogen, the United States Department of Energy (DOE) has started a H_2@Scale initiative as part of its Fuel Cell Technologies Office, addressing the need for advancing technologies that can produce hydrogen and usher in widespread adoption [2]. Today, there are still significant bottlenecks in scale up of renewable technologies, which need to be overcome to ensure that the proposed hydrogen economy becomes a reality.

In the quest for finding a more economical, scalable, and efficient source of renewable hydrogen that may also treat waste products, scientists and engineers have rigorously investigated microbial electrolysis cells (MECs). MECs compose a subset of a more general class of reactors called bioelectrochemical systems (BESs) that harvest the electrons produced by

microbial metabolism [3]. Traditionally, a microbially colonized electrode known as an anode degrades organics, while respiring via direct electron transfer to the anode electrode material. In an MEC, these electrons combine with protons to form hydrogen gas at another electrode known as a cathode. Many new products could be generated using the captured electrons if the thermodynamic energy requirements of the desired reaction are met via catalysis or other alternatives. Not all BES products are thermodynamically favorable, including hydrogen. Therefore, MECs use an applied voltage across the cell to drive hydrogen evolution.

While many simple and complex substrates have been used in these reactors, the best source of substrate for these devices are renewable wastes. Biomass and agricultural wastes have gained recent interest for MEC development for this reason. Wastes from biomass or agricultural sources used in MECs have included those derived from cheese whey [4], potato [5], cornstalk [6], corn cob [7], switch grass [8], pine [9], guayule [10], and willow [10]. Other isolated compounds commonly found in biomass, such as cellulose [11], have also been used with MECs. Raw biomass and agricultural wastes may also be processed to further extract valuable energy products, resulting in additional wastes that can be used in BESs. The methods that have generated these wastes include hydrothermal liquefaction [12],[13], pre-fermentation [14], and pyrolysis [8],[9],[10]. The wastes from these processes have little value on their own, resulting in process efficiency losses that may be reduced using MECs. MECs therefore provide a unique capability to valorize waste to generate or improve other products. These include hydrocarbon fuels, which use hydrogen for upgrading intermediates of biomass processing, e.g. bio-oils. Additionally, ethanol has been proposed as a potential feedstock for hydrogen creation by steam reforming [15],[16]. MECs may therefore increase total hydrogen yields of biomass-based ethanol fermentation by using the fermentation effluent as a feedstock.

Corn stover has been investigated as a feedstock for renewable ethanol production, with large scale stover-to-ethanol plants beginning operation as early as 2014 [17]. Corn stover has also found applications in BESs, where pre- and post-fermented corn stover have been used in MFCs and MECs previously [18-21]. Of interest to this study, ethanol production using corn stover generates a byproduct from the fermentation process, which is the aqueous phase after ethanol recovery. This product is referred to as corn stover fermentation product (CFP) here. As with the biomass sources discussed earlier in this section, pretreatment is often used to release sugars prior to fermentation. Pretreatment of corn stover, like many lignocellulosic biomass sources, results in the production of microbial inhibitors, including short chain fatty acids such as acetate, furans, and phenolics [22],[23],[24]. While acetate is not an inhibitor in BESs, furans and phenolics have been shown to inhibit BESs [25]. Not all CFPs contain high concentrations of these inhibitory compounds. One of the CFPs generated by Pannell et al. was able to achieve a current density of 10.7 A/m^2 in an MFC [20], and this performance could be partially attributed to low concentrations of inhibitors 2-furfural and 5-hydroxymethylfurfural. Thus, further investigation using CFPs could be valuable for generation of products used in MECs.

Increasing MEC productivity for all potential substrates remains a point of inquiry. Perhaps one of the highest performing MECs was by Jeremiasse et al., who achieved hydrogen productivity rates exceeding 50 liters per liter MEC volume per day at a current density of 22.8 A/m^2 using acetate as the carbon source, though performance diminished with time [26]. High hydrogen productivity has also been achieved by abiotic enzymatic non-BES systems. Rollin et al. utilized xylose and glucose derived from corn stover and achieved a hydrogen productivity of 54 mmol H_2/L-hr, equal to roughly 31 liters of hydrogen per liter of anode volume per day (L/L-day) at standard atmospheric pressure and temperature [27]. Complex feedstock fed BESs, by

comparison, have not performed as well. Studies using biomass derived complex substrates in MECs, including those derived from corn stover, rarely if ever exceed 6 L/L-day hydrogen productivity [5],[6],[12],[28] for any size of reactor. One exception to high performing MECs using biomass derived waste came from Lewis and Borole, who recently published a study that reached a hydrogen productivity of 7.9 L/L-day and a current density of 9.2 A/m^2 using a pyrolysis byproduct known as bio-oil aqueous phase (BOAP) [29]. The authors further claimed that this was the highest reported hydrogen productivity using a complex substrate. Comparisons between simple and complex substrates using the same reactor configuration and anode community also suggest that complex feedstocks produce lower productivities. Lewis et al. (2017) recently made a comparison between batch experiments using acetate and BOAP in MECs and found that the acetate outperformed the complex feedstock by more than twice the productivity at the same organic concentrations as measured by chemical oxygen demand (COD) [30]. In all cases, these productivities are not sufficient for economic feasibility in real biorefineries. Another loss in performance can also be contributed by methanogenesis. Methanogens are particularly troublesome, as they rob the system of electrons and protons, decreasing operating efficiencies. For commercial systems, methanogenesis must be sufficiently inhibited in order to assure high purity hydrogen is created by MECs at sufficient productivities. Today, methanogens continue to play a role in MECs, and numerous studies have been conducted that attempt to inhibit methanogen activity and growth [31].

Commercial requirements of MECs varies across studies, but often focus on system cost and related performance by normalizing the performance metrics to reactor size. Escapa et al. estimated productivity as a function of cost, and found that MECs would need to operate at a current density of 5 A/m^2, consuming 0.9 Wh/g-COD, and a cost of 1220 Euros/(m^3-anode

volume) [32]. Sleutels et al. also outlined a framework that established such a target based purely on performance, and estimated that MECs would need to reach 20 A/m^2 in order for MECs to achieve profitability [33]. More recently, Aiken et al. used a different approach by focusing on the hydrogen productivity and current density associated with effluent flow-rates and organic loading density, finding that target current densities would need to reach 15.6 A/m^2 for the highest 20-year net present value scenario estimated [34], though higher current densities may be desirable if scenarios were combined. Aiken et al. further suggested that the studies by Sleutels et al. and Escapa et al. may have overestimated material costs and operating temperatures of the systems assumed. Together, there is an important take away; if materials will continue to be expensive, current densities will need to be high, as will efficiencies, using real waste products. The range of current densities discussed is clearly broad, with Sleutels et al.'s being the most ambitious. Using the equation described by Logan et al., the 20 A/m^2 target established by Sleutels et al. is equivalent to a maximum hydrogen productivity that varies between 18.9 and 21 L/L-day for the systems used in this study depending on temperatures of the systems [35]. 20 L/L-day was identified as an appropriate target productivity based on this range, with motivation being provided by the initiative started by the US Department of Energy Fuel Cell Technology Office [2]. Even with expensive reactor materials, few studies have reached this level of performance using any substrate [36, 37], and no studies have reached this level of performance using a complex feedstock, even using a small laboratory scale reactor.

In addition to identifying worthy complex feedstocks and reaching higher performances, performance of cells may also be improved by minimizing the operational energy required and documenting the effect of process conditions on performance. Anode liquid flow rate and retention time are such parameters of importance. Traditionally, efficiencies are determined by

documenting the electrical energy consumed and accounting for the chemical energy supplied. While the electrical energy used contributes to overall energy demands of MECs, the effect of flow rates and pumping regimes on MEC energy efficiency using complex substrates is not entirely understood. Lewis and Borole described the effect of continuous anode liquid flow rate on MEC performance, determining that higher flow rates would achieve higher productivities in MECs operated on a complex substrate [38], but did not consider varying the flow rate in other ways. To date, no studies have documented the effect that irregular, staggered, or pulsed flow can have on MEC performance, which may be a necessary component to determining the optimal anode media flow rate schedules in MECs.

Identifying suitable feedstocks and process conditions is essential to achieve high rates of hydrogen productivity, bridging the gap between research productivities and commercially feasible targets in MECs. Thus, the goal of this work is to investigate hydrogen productivities, current densities, and organic degradation in a mature MEC using a biomass waste substrate that had previously reached high performance metrics in MFCs [20]. CFP derived from acid and enzyme hydrolysis and ethanol fermentation was used as the substrate and organic loading rate was increased until reaching the desired hydrogen productivity target of 20 L/L-day established by Sleutels et al. [33] was reached in continuously-fed lab-scale MECs. Additionally, the effect of pulsing the anode liquid flow rate on MEC performance was also investigated.

Materials and Methods

Production of Corn Stover Fermentation Product

The CFP was created by acidification, enzymatic hydrolysis, and ethanol fermentation of corn stover using processes described previously [19]. Briefly, corn stover was fed at a rate of 5

kg/h to a continuous-horizontal screw reactor operated at National Renewable Energy Laboratory (NREL). The reactor was operated at 158 ºC where the untreated biomass was mixed with sulfuric acid, where this mixture was held for 5 minutes. The slurry was then diluted and cooled, and the pH was adjusted before cellulase was added at a loading concentration of 20 mg protein/g dry biomass for four days. After hydrolysis by cellulase, the slurry was further cooled and pH was adjusted again. Fermentation cultures composed of *Zymomonas mobiliz* were added to the slurry for an initial cell concentration of 0.5 g dry cell mass/L, along with nutrients to facilitate fermentation. Fermentation was conducted for three days before the slurry was sterilized by autoclave. Ethanol was removed by vacuum, and the samples representing the left-over CFP were sent to Oak Ridge National Laboratory (ORNL). CFP samples were filtered using a 0.2 μm filter before use in MECs and were stored at 4 ºC until used in experiments. Lower substrate delivery rate experiments used CFP that was diluted with deionized water.

Chemical Oxygen Demand Measurements

COD of samples collected before and after MEC treatment was determined using the protocol provided by the manufacturer [39]. Raw CFP COD was determined by diluting with deionized water 100- and 500-fold before measurement, which were then averaged. For all measurements, 2 mL of diluted or undiluted sample were used and run in a Hach DRB 200 using high range Hach COD vials (Hach Company, Loveland, CO). These samples were run for 2 h at 150 ºC. Absorbance was recorded using a Spectronic Genesys 20 Spectrophotometer (Thermo Fisher, Waltham, Massachusetts) at a wavelength of 620 nm. The absorbance was correlated using a standard curve obtained using COD standards from potassium hydrogen phthalate.

MEC Design, Enrichment, and Set Up

Reactors were used from a previous study [10], without any alterations to the enclosure and biofilm beyond the change in substrate. Briefly, a two chamber MEC was used, composed of a carbon felt anode in 3.81 cm (1.5 in) diameter PVC pipe. This chamber was separated by a Nafion membrane, where the cathode was a 0.5 mg Pt/cm^2 deposited carbon disc that was flushed with a stainless steel wire mesh current collector. The anode was pressed flush with the Nafion membrane, using a rubber gasket between the membrane and the anode pipe to create a tight seal. Hydrogen produced by the cathode was collected by inverted graduated cylinder in a water bath. Two reactors were run in parallel for all experiments. An acclimation period of four days on the existing MECs was conducted before experiments began, where reactors were initially fed 2 grams of COD per liter of anode volume per day (g/L-day) of the CFP. In the following set of experiments, reactors were run in continuous-fed fashion at substrate concentrations of 2, 4, 10, 20, and 30 g/L-day. The reactor volume was calculated at 83% of the 16 mL measured of the reactor volume from manufacturer specifications. The anode recirculation liquid media was composed of 200 mL of phosphate buffered nutrient solution using 2.5 mL of Wolfe's mineral and vitamin solutions previously described [8, 40]. Anode liquid media was sparged with nitrogen for 30 minutes to create the necessary anaerobic environment for the cell. 40 mL of clean liquid media was flushed through the anode before each experiment. For continuously-fed experiments, 12 mL of 200 mM potassium phosphate buffer was used, however the pulsing experiments only used an anaerobic gas cathode. In both sets of experiments, the cathode was sparged for 15 minutes with nitrogen, where the gas collection volume was then reset using a syringe. Initial gas composition of the anode and cathode was

recorded using Gas Chromatography (GC) on samples collected from a septum attached to a tee in the anode and cathode.

MEC Calculations

Current density, Coulombic efficiency, cathode conversion efficiency, hydrogen recovery, electrical energy efficiency, and overall energy efficiency were calculated using methods reported previously [10]. To determine if sufficient energy had been recovered efficiently from the MECs, energy efficiency was calculated using the formulas described by Logan et al. [35]. To summarize, electrical energy efficiency is defined as:

$$\eta_E = \frac{-W_{H_2}}{W_E}$$

Where W_{H2} is the energy produced as a function of the volume of energy produced and the heat of combustion energy of hydrogen, and W_E is the electrical energy provided as a result of the applied voltage and current produced over the length of the experiment. Overall energy efficiency incorporates the energy contained in the unconverted substrate into the previous equation to make the following expression:

$$\eta_E = \frac{-W_{H_2}}{W_E - W_s}$$

Where Ws is the energy delivered by the substrate. Operational conditions were assumed to be at room temperature (23 ºC) at atmospheric pressure (101.3 kPa). The heating value of hydrogen used was -285.8 kJ/mol, and the energy content for the substrate was estimated at -14.955 kJ/g-COD, as used previously [8],[10].

MEC Operation

For substrate loadings of 2, 4, and 10 g/L-day, anode liquid samples were collected every 24 h. For 20 and 30 g/L-day experiments, samples were collected every four h for a total of 12 h

due to resultant pH imbalance and gas accumulation rates. Cathode gas and anode gas for GC was sampled and analyzed at the same time intervals as liquid samples. Cells were operated using a three electrode assembly. A Bio-Logic VSP potentiostat (Bio-Logic USA, Knoxville, TN) was used to poise the anode at -0.2 V versus Ag/AgCl reference electrode. Anode liquid was circulated through the cells using a peristaltic pump (Cole Parmer, Vernon Hills, Il), where it was held at 3.5 mL/min for all continuously-fed experiments. Batch experiments were conducted by pulsing the anode liquid flow rate at specified intervals to be discussed in the section 2.6. These batch experiments did not use cathode buffer in order to increase potential mass transfer and kinetic limitations in the cell, using a dry anaerobic cathode instead. 100 µL of gas sample was acquired for each measurement. Two GC protocols were used for the experiments. The first used a Thermo Focus GC (ThermoFisher, Waltham, MA) instrument. The column was a HP Plot Molecular Sieve 5A (Agilent technologies Santa Clara, CA). The GC was operated at an initial oven temperature of 30 ºC for 1 minute, and ramped to 72 ºC at a rate of 5 ºC/min. The final temperature was held for 30 seconds. The inlet temperature, block temp, and transfer temp were all held at 50 ºC for each run. Helium gas was used as the carrier gas and was applied to the GC at a fixed relative pressure of 30 kPa. Four gases were detected. These include hydrogen, oxygen, nitrogen, and methane. Cathode gas composition was used to adjust hydrogen amounts measured in the graduated cylinder. The second protocol used a HP 5890 Series II (Agilent technologies Santa Clara, CA) instrument. The column was a HP Plot Q (Agilent technologies Santa Clara, CA). Like the previous protocol, helium gas was used as the carrier gas and was applied to the GC at a fixed relative pressure of 30 kPa. The inlet temperature was held at 125 ºC. The initial oven temperature was 26 ºC, and this was held for 4 minutes. The temperature was

then ramped to 45 ºC at a rate of 8 ºC/min. The final temp was held for 1 minute. Only CO_2 was detected but was not quantified using this GC.

Effect of Increased Flow Rate via Fluid Flow Pulsing Experiments

To increase mass transfer without applying continuously high flow rates, anode liquid flow pulsing was attempted. Anode liquid flow pulsing, known from here on out as simply pulsing, can be accomplished by aggressively flushing the anode with a specified volume of recycled anode liquid media at fixed time intervals, where the flow rate during pulsing is much higher than the continuous flow rate used otherwise. The hypothesis was that the increased pressure differential across the anode would carry accumulated gas out of the anode while also convectively supplying the cathode with protons, resulting in increased hydrogen evolution. Pulsing was tested using three liquid flow rates: 3.5 mL/min, 1 mL/min, and 0.3 mL/min. Pulsing was performed by increasing the flow from the baseline flow rate to about 200 mL/min for a brief period of 3 seconds. This was done using a 10 mL syringe to rapidly drawing 10 mL of liquid from the top of the cell within 3 seconds. During this time, the MEC was still being operated by potentiostat. Prior to each experiment, anode liquid media was changed as described in section 2.3, and cathodes were drained of any residual liquid and sparged with nitrogen for 15 minutes. A batch of CFP substrate was added to each cell at a loading of 0.2 g-COD/L. Pulsing was performed every 2 h at flow rates of 3.5, 1, and 0.3 mL/min, and experiments were performed with clean anode liquid media over the course of 8 h. An additional experiment was conducted at a flow rate 0.3 mL/min where pulsing was performed every hour for 8 h. Cells were depleted of useable organics by waiting 24 h before anode liquid media changes were conducted and fresh substrate was introduced.

Compound Identification and Degradation Rates

High-Performance Liquid Chromatography (HPLC) was used to identify organic acids, alcohols/polyols, furans, and sugars present in end point samples of 10, 20, and 30 g/L-day runs and in the untreated substrate. Two protocols were used for HPLC. For sugar and carbohydrate detection, a Shodex SP0810 column (Showa Denko K.K., Tokyo, Japan) was used. The mobile phase was deionized water at a flow rate of 0.6 mL/min, and the column temperature was 85 ºC. Samples were run for 20 minutes followed by a 15-minute post run. A Bio-Rad (Bio-Rad, Hercules, CA) cation and anion de-ashing guard column was used. The carbohydrates and simple sugars identified were cellobiose, glucose, xylose, galactose, arabinose, and fructose. The other protocol used a Bio-Rad (Bio-Rad, Hercules, CA) HPX-87H column, using a mobile phase of 0.01 N sulfuric acid at a flow rate of 0.6 mL/min. The column temperature was run at 55 ºC, and samples were run for 50 minutes. A Bio-Rad (Bio-Rad, Hercules, CA) cation de-ashing guard column was also used. Organic acids included lactic acid and acetic acid. Alcohols/polyols included glycerol and ethanol. Furanic compounds included 5-hydroxymethylfurfural (HMF) and furfural. Both protocols used a refractive index detector. Standards for compounds were combined in a single sample and analyzed at different concentrations to establish a standard curve for sample calibration.

Results and Discussion

Characterization of Corn Stover Fermentation Product

The COD of the CFP was found to be 72.2 g-COD/L. Table 13 shows the percentage of the compounds investigated that corresponded to the total COD.

Table 13: Compounds investigated as a percentage of total COD. The glucose peak was shifted in the chromatograph past the standard, and as a result confidence in its prevalence was not established. Acronyms include: 5-hydroxymethylfurfural (HMF), and Below Detectable Limits (BDL).

Compound	COD percentage
Cellobiose	BDL
Glucose	N/A
Xylose	18.5%
Galactose	5.2%
Arabinose	10.5%
Fructose	BDL
Lactic acid	0.4%
Glycerol	0.7%
Acetic acid	14.0%
Ethanol	BDL
HMF	BDL
Furfural	BDL
Total	49.3%

No cellobiose, fructose, ethanol, HMF, or furfural were detected in the raw substrate. The proportions of the chemicals detected are mostly consistent with Pannell et al., who used the same substrate in their studies [20]. Still, it is possible that some of these compounds were present in very small quantities, or some of which may have degraded while stored at 4 ºC, until used in this study. additional transformation was halted once samples were filter sterilized.

CFP is primarily made as a byproduct of ethanol fermentation by the process described in section 2.1. Pannell et al. showed that a non-vacuum distilled version of this product had upwards of 25.98 g/L ethanol [20], however none was found in our sample. While it is possible that ethanol was present in amounts that were below detectable limits, the results here confirm that ethanol was effectively removed via vacuum distillation after fermentation. The identified fraction of the CFP's COD appeared to be simple sugars and volatile fatty acids, totaling at

49.33% of measured COD. Inhibitory compounds such as HMF or furfural were not detected in the substrate. This suggests that at least half of the substrate should be easily converted by fermenters and exoelectrogenic microbes present in the biofilm, resulting in fast degradation rates and, therefore, higher current densities and hydrogen productivities.

Current Density and H_2 Production from Continuous Experiments

Figure 22(A) shows the average and maximum current density and the overall hydrogen productivity for the continuous experiments, while Figure 22(B) shows the calculated efficiencies, which include Coulombic efficiency, hydrogen recovery, electrical efficiency, and overall energy efficiency for each of the experiments conducted. The largest average current density and hydrogen productivity observed occurred at the loading rate of 30 g/L-day, corresponding to 17.9 ± 1.6 A/m^2 and 20.1 ± 2.1 L/L-day. The maximum current density reached was also during 30 g/L-day and was found to be 27.2 ± 2.9 A/m^2. The last 4 h of the 30 g/L-day experiments also produced sustained average current densities and hydrogen productivities that did not decrease before the experiment was ended, reaching average current densities of 22.4 ± 2.1 A/m^2 and hydrogen productivities of 25.0 ± 2.8 L/L-day. It was suspected that these performance metrics would have been sustained if more sophisticated methods to monitor and adjust pH we available, as pH was adjusted manually but dropped rapidly at the organic loading rates tested. The productivities in the last 4 h of the experiment corresponded to the end in the ramp up in performance observed at the beginning. The current density plots at 30 g/L-day are shown in Figure 25 in the Appendix of this chapter.

(A)

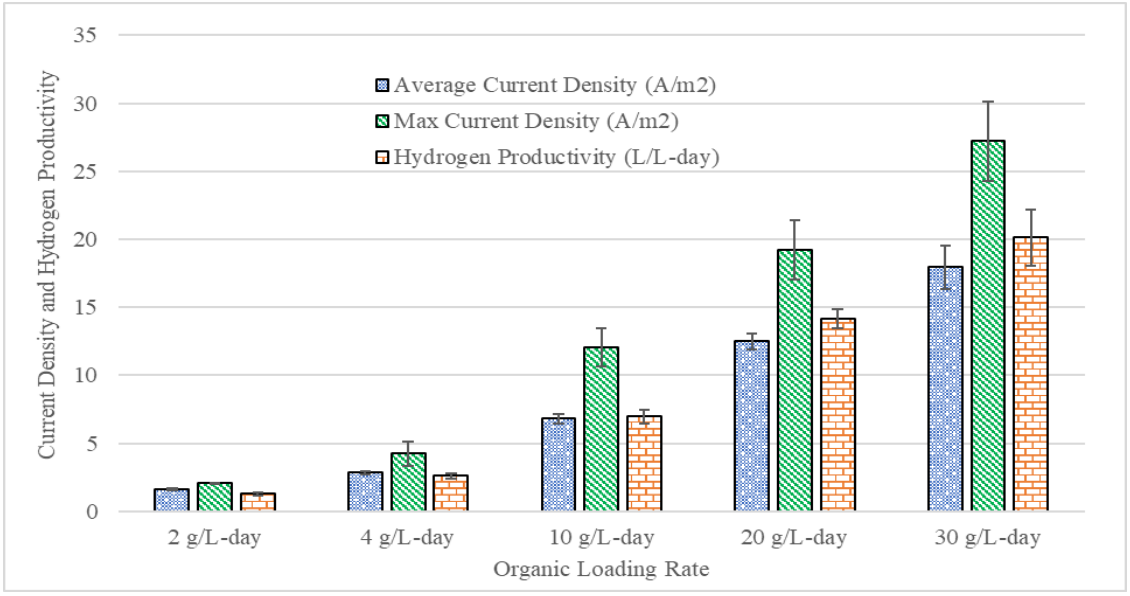

(B)

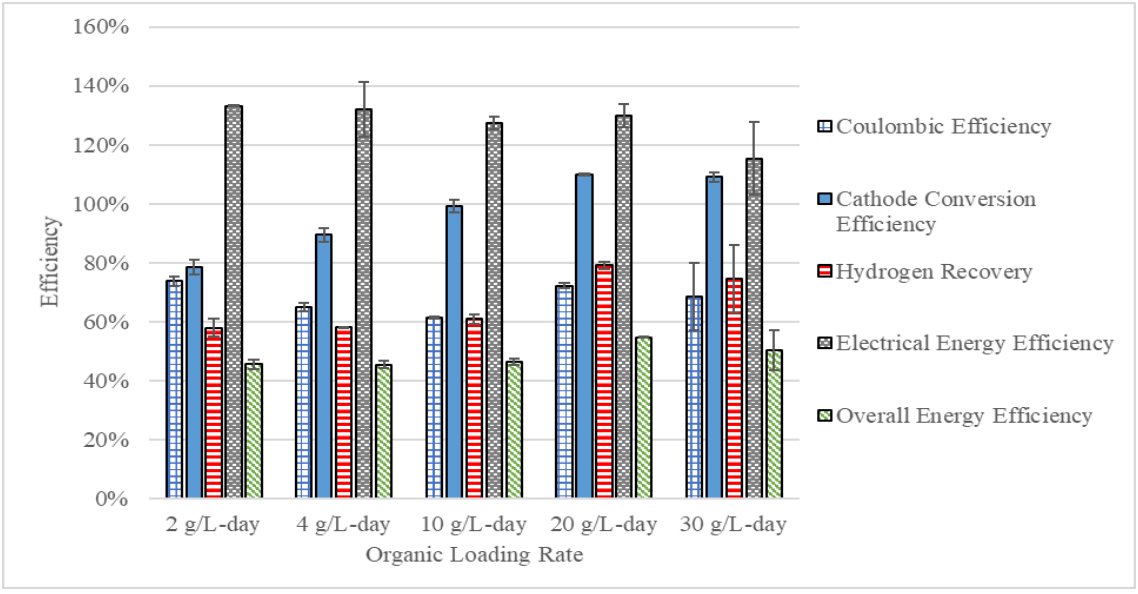

Figure 22: Average and maximum current density, and overall hydrogen productivity as a function of loading rate (A), and efficiencies associated with MEC operation at different loading rates (B).

Table 14 compares the performance of biomass-derived complex feedstocks at 10 g/L-day organic loading rate.

Table 14: comparison of performance using biomass derived feedstocks. The top five examples use the same configuration and organic loading rate, at 10 g/L-day. The other values correspond to the maximum reported values in the referenced studies, which can be the result of different applied voltages, organic loadings, etc.

Substrate	**Organic Loading**	**COD removal**	**Current Density (A/m^2)**	**Hydrogen Productivity (L/L-day)**	**Anode Coulombic Efficiency**	**Hydrogen Recovery**	**Reference**
Switchgrass BOAP	10 g/L-day	52.0%	4.5	4.3	54%	50%	[8]
Pine pyrolysis aqueous product	10 g/L-day	63.9%	4.2	2.7	45%	30%	[9]
Willow pyrolysis aqueous product	10 g/L-day	66.8%	5.0	5.0	50.7%	49.5%	[10]
Guayule pyrolysis aqueous product	10 g/L-day	39.5%	1.8	1.5	32.8%	27.0%	[10]
Neutralized switchgrass BOAP	10 g/L-day	60.8%	5.3	4.3	59.9%	51.5%	[41]
CFP	10 g/L-day	75.8%	6.8	7.0	61.3%	60.8%	This study
CFP	30 g/L-day	60.4%	17.9	20.1	68.5%	74.6%	This study
Other Reactor Configurations							
Cheese whey	1-2 g/L	assumed 100%	< 0.06	0.8	120%		[4]
Potato wastewater	1.9-2.5 g/L	79.0%	6.4	0.74	80%		[5]
Dark fermented cornstalk	12.0 - 3.0 g/L	44.0%	340 A/m^3	3.43	71.0%	64.0%	[6]
Hydrothermal liquefied cornstalk wastewater	2	80.2%	< 6 mA/m^3	0.00392	7.0%		[12]
Dark fermentation effluent	0.4 -1.2 g/L	85%		0.081			[14]
Cornstalk fermentation effluent	0.398 g	71%	480 A/m^3	4.52	76%	0.87 L/g-COD	[28]

Many of the studies performed previously used an organic loading rate of 10 g/L-day under continuously-fed conditions. The MEC design and configuration used the upper half of this table are the same, so a direct comparison can be made. As shown, the CFP-fed MECs exceeded current density, COD removed, and hydrogen productivity compared to the other studies using the same configuration. Different configurations were also compared; however, the metrics are often reported differently. Of the reactors listed, this reactor configuration outcompeted other MEC configurations using biomass derived substrates. This is likely attributed to the composition of this feedstock, which contains substrates more suitable for exoelectrogenic conversion, unlike the other feedstocks, which contained higher concentration of comparatively recalcitrant or inhibitory compounds [9, 10, 42], as well as the MEC design and starting inoculum, which had been adapted to these more recalcitrant feedstocks. Further evidence of the substrate's relative recalcitrance will be discussed in Section 3.4. The design and operation of the reactor also promotes effective microbial biofilm formation for several reasons. Neutral pH's were maintained throughout the operation of the MEC using a buffered media and manual pH adjustment, and lower pH's would cause product inhibition. The anode electrode, a porous carbon felt, was used that therefore allowed for large biofilm formation with the available surface area. Shear induced by flow of liquid medium in the anode has been shown to increase biofilm performance and microbial cell density in MFCs [43]. Anode flow also promotes convective mass transfer of cations to the cathode, a feature that can limit performance in batch devices without flow. The distance between electrodes is also close, as both electrodes are pressed flush against the Nafion membrane, creating a distance that is roughly the thickness of the Nafion membrane and the gasket separators (approximately 2 mm). Shorter distances between electrodes have been shown to improve BES current production when cross flow was

applied [44]. Anode poising has also been shown to increase hydrogen productivities compared to whole cell voltages [45], which was also used in this design. Overall, our design allowed microbial communities to effectively create and transfer charge to the cathode.

These productivities would be less promising if the gas produced was impure. However, the purity of hydrogen produced at the cathode was confirmed via GC analysis. In all runs, the hydrogen produced in the cathode exceeded 95% of the gas generated, while methane was less than 3%. The observed purity may be explained by a few operational considerations in our system. In single chamber MECs, these purities are not regularly observed. Lee et al. confirmed that the hydrogen gas produced by MECs in up flow reactors converted to methane over time, and attributed this conversion to hydrogenotrophic methanogens on the cathode [46]. Lee et al.'s findings support a more general trend discussed in review by Karthikeyan et al., which concluded that methane production was always present in single chamber MECs without a membrane and hydrogen yields were therefore lower [31]. By contrast, a two-chamber MEC with no added carbon to the cathode using a Nafion membrane limits crossover of a carbon source, preventing cathode-based methanogenesis. Additionally, the pH at the cathode becomes high (approximately 13) further preventing microbial activity on the cathode. MEC methanogenesis inhibition has also been demonstrated by poising the anode compared to applying a whole cell voltage [45], a strategy deployed in the MECs used here. The membrane also helped prevent diffusion of anode methane generated, a capability that would be lost in single chamber MECs. Another process control used to further prevent methanogenesis included active H_2 harvesting by replicating the experimental set up used by Satinover et al. using an inverted graduated cylinder to apply a small amount of negative pressure to the cathode [10]. Active H_2 harvesting using a negative pressure on the cathode of a two-chamber MEC has been shown to prevent

methanogenesis by Lu et al. [47]. Additionally, Lewis and Borole showed that high amounts of organic loading using a different complex feedstock could result in less methanogenic losses compared to lower organic delivery rates with the same reactor configuration [29].

What microbes were responsible for fermentation and exoelectrogenesis while limiting methanogenesis were not determined, however prior studies using this consortia and device design may provide insight into potential contributors. A community structure function has been proposed by Lewis et al. (2017), where fermenters degrade higher order compounds (sugars, phenolics, furans, etc.), which then either exchange products to other fermenters or produce acetic acid for exoelectrogenic consumption [30], though the specifics of the pathway remain unknown. Some additional insight may also be gained from understanding the inoculum used and discussing other BESs that have used the same substrate. The starting inoculum, originally enriched by Lewis et al. (2015), determined that *Geobacteraceae* contributed no more than 10% of the relative OTUs detected, and that families such as *Flavobacteriaceae* and *Sphingobacteriaceae* also flourished [8]. Additionally, Pannell et al. found that the majority of the microbes operated in continuously fed- fashion using CFP in MFCs belonged to the class Clostridia, with some of the Clostridia belonging to known exoelectrogens, and a very small percentage of community belonged to methanogens [20]. Thus, it is likely that only small amounts of methane were detected in the anode and cathode due to selective enrichment of a highly cooperative fermentative and exoelectrogenic community, in part contributed by substrate feeding regime and system design. Thus, while further experiments will be required to determine if methanogenesis can be suppressed at longer operating times before media changes, it was suspected that this would be possible with proper pH adjustment and monitoring given the starting community and design configuration. Additionally, Lewis and Borole determined that

these reactors could be operated for at least two weeks using continuously fed operation of a complex feedstock without a significant loss in performance at 20 g/L-day [29]. Altogether, this design demonstrates that adequate process and biological controls can be used for producing high purity hydrogen gas at a laboratory scale with minimal methanogenesis. The MEC efficiencies described in the next section further support the direct conversion of organics to hydrogen in this design.

Efficiencies of MECs in Continuous Addition Experiments

Efficiencies of the MECs operating at the various continuous addition rates are shown in Figure 22(B). The anode Coulombic efficiency was largest at 20 g/L-day and reached 72.0 ± 0.9%. By comparison to the other complex feedstocks, the anode Coulombic efficiency was higher than for the other substrates tested in this reactor design in Table 14, however it was still not 100%. Certainly, some of the efficiency losses occur due to fermentation, which often releases CO_2 as a byproduct, preventing potential electrons from being captured by the electrodes. CO_2 was detected in the anode headspace of all trials, although it was not quantified. Dark fermentation may have occurred in the anode, however; this did not result in hydrogen accumulation in the anode headspace. That being said, methane was detected in the anode but was effectively separated away from the cathode due to the two-chamber design used. Still, the presence of some methane was indicative of some electron diversion away from current, reducing anode Coulombic efficiencies below 100%, even though methanogensis remained limited in this MEC design.

Cathode conversion efficiency increased as substrate delivery rate was increased up to 20 g/L-day, reaching a value of 109.8 ± 0.3%. Hydrogen diffusion to the anode was assumed to be negligible due to these high efficiencies and because no hydrogen was observed in the anode

headspace as mentioned earlier, suggesting that these values are representative of high cathode conversion efficiencies occurring. The efficiency being higher than theoretical expectation is an anomaly, but several studies have reported cathode conversion efficiencies above 100% previously [48],[49]. The exact cause of this remains unknown, as prior studies were unable to determine the cause of this. One study by Siegert et al. demonstrated above 100% cathode conversion efficiency in a methane generating BES, and suggested that these efficiencies were caused by microbially induced corrosion of the cathode [50], but this mechanism would not be possible for an abiotic hydrogen producing cathodes used in our study. In order for cathode conversion efficiency to be higher than 100%, charge must be transferred through some other mechanism than by current. It may be possible that other chemical species that migrate from the anode to the cathode through the Nafion membrane are being transformed into hydrogen at the cathode. While this has not been determined, additional work using these MECs has found that the cathode buffer can gradually change color while the system is operating. The cause of this color change is unidentified; however, it may be indicative of organics that have migrated from the anode to the cathode. It is possible that at high pH, these organics are further reduced by chemical catalysis at the cathode, resulting in larger hydrogen volume than theoretically expected. This may also contribute to lower Coulombic efficiencies found in these systems than in other studies shown in Table 14. In addition, fouling regularly occurred on the Nafion membranes used in this study, resulting in dark colored membranes, although MEC performance reached a steady state and did not worsen over time of the experiments. From a performance perspective, fouled cation exchange membranes have been shown to operate at lower Coulombic efficiencies compared to new membranes, although this is not necessarily attributed to biofouling [51]. Further investigation of the morphology of Nafion biofilms and physiochemical

characteristics of biofouling in high performance MECs may be needed to explain the discrepancies in efficiency found in this study.

Not all of the trends observed with cathode conversion efficiency are unusual. Our findings show that the cathode conversion efficiency increased with loading rate, which is consistent with previous studies [8],[41], which also achieved high cathode conversion efficiencies. These high values can be attributed to design. The distance between the electrodes was minimized, where MECs with high cathode conversion efficiencies have been demonstrated with devices using small electrode separation [52]. Thus, even though the efficiencies demonstrated exceed 100%, high efficiency due to design considerations were expected. Further, platinum, a commonly used catalyst in MECs, allowed for ready and easy conversion of hydrogen at these efficiencies, though platinum is not always necessary for high or comparable performance to other catalysts [37]. While fabricating smaller distance between electrodes is feasible for commercial systems, platinum use remains a limitation for future designs, as platinum is expensive. Finding more affordable cathode catalysts that can facilitate high productivities remains a critical point of inquiry.

Hydrogen recovery increased as loading increased up to 20 g/L-day, where it was highest at 79.1 ± 1.2%. These high values for hydrogen recovery suggest that much of the contributed COD was directly converted to hydrogen via electrons, which can be credited to the exoelectrogenic population's ability to convert the diverse compounds present in CFP into current and the adequately catalyzed cathode, without scavenging in the anode or cathode. Table 14 shows that both anode Coulombic efficiency and hydrogen recovery were higher than the equivalent organic loading using other substrates, where the CFP operated MECs achieved an

anode Coulombic efficiency and hydrogen recovery of 61.3 ± 0.3% and 60.8 ± 1.7% respectively at 10 g/L-day.

Electrical efficiency was highest at 2 g/L-day at 133.1 ± 0.09%, while overall energy efficiency was highest at 20 g/L-day, equal to 54.7 ± 0.2%. Table 14 does not include these metrics because not all the studies referenced calculated them. However, some comparison will be useful here. Lewis et al. achieved electrical efficiencies approximately 161% and overall energy efficiencies just above 60% at 2 g/L-day [8]. It is likely the electrical efficiency and overall efficiency are largely governed by mass transfer limitations, as the applied voltage was consistently higher in the cells operating on CFP than on BOAP. Here, the applied voltage reached a maximum of 1.41 ± 0.17 V at 30 g/L-day, and the other voltages can be found in the Appendix of this chapter. Because the MECs operated here are anode-poised, the high cell voltage indicates rising energy requirements of the cathode to continue the reaction that cannot be attributed to anode limitations. The cathode's increased energy demands can be explained a few ways. Insufficient cathode catalysis will increase the cathode operating potential; however, this can be effectively ruled out in this study because a platinum-deposited carbon catalyst was used. The other possibility is a lack of protons at the cathode caused by insufficient proton transfer from the anode to the cathode. Proton transfer limitations in MECs has been reported previously, first demonstrated to be influenced by membrane selection by Rozendal et al. [53] and later by Torres et al., who showed that increased anode buffer concentration and pH could alleviate limitations caused by proton transfer, thereby improving current densities while maintaining a constant anode potential [54]. Cathode limitations become more apparent as the current densities and hydrogen productivities increase. A recent study identified proton transfer as a major limitation at high loading conditions using a complex substrate and the same reactor

configuration used in this study [55]. In our study, the highest organic loading rate used resulted in the highest operating voltage and lowest electrical efficiency. Improvements in cathode conversion efficiency would also increase electrical efficiency, however cathode conversion efficiency peaked at 20 g/L-day, and voltage continued to rise past 20 g/L-day, being responsible for the loss in efficiency past 20 g/L-day. Deployed systems can use applied cell potential vs. poised anode potential to manage efficiency, but it is possible that this drop in electrical efficiency is explained by the changes in cathode efficiency and applied voltages observed. While no study has reached this level of performance using a complex substrate, most cells in literature have not reached high voltages. Even Jeremiasse et al. used only an applied cell voltage of 1V to their system to reach the performance discussed earlier [26]. Further work is needed on optimizing energy requirements to achieve high overall electrical efficiency without sacrificing hydrogen productivity.

Conversion of Compounds Determined by HPLC

Figure 23 shows the percent removal of compounds (A) and the rate of removal of those compounds (B) for 10, 20, and 30 g/L-day experiments.

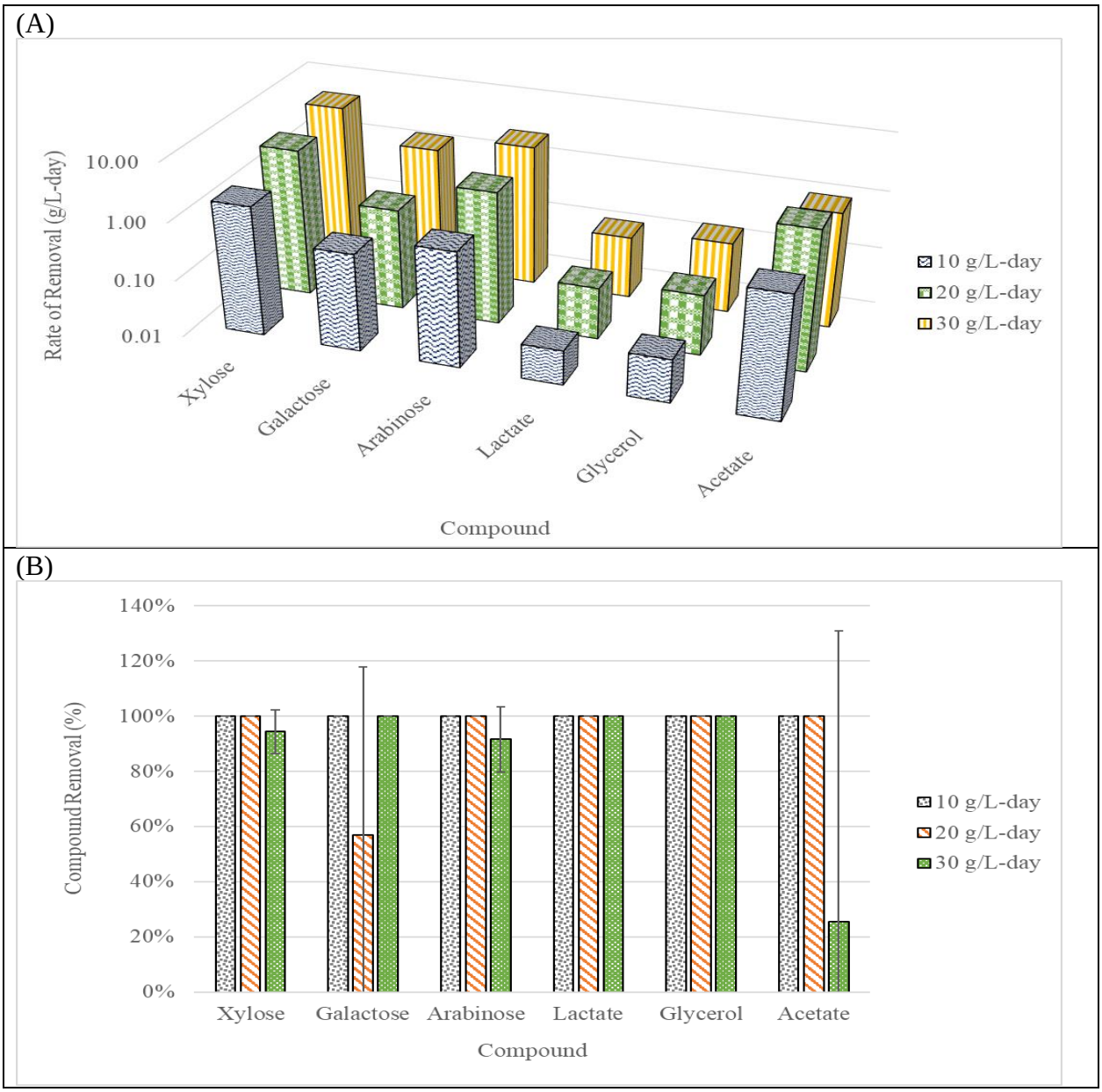

Figure 23: Removal rate (A) as a function of substrate loading at 10, 20, and 30 g/L-day for detected compounds, and percentage removal under the same conditions (B). Other compounds not listed but investigated were below detectable limits before and after use in MECs.

In general, the compounds identified were removed to the point of being below detectable limits for all trials except for xylose, arabinose, and acetate at 30 g/L-day, and galactose at 20 g/L-day. As shown in Figure 23(B), the highest removal rate among all compounds was that for xylose,

equal to 4.92 ± 0.41 g/L-day obtained at a loading rate of 30 g/L-day. Besides acetate, which is regularly used in BES studies, the detected compounds have all been used in BESs in the past with high percent removal, exceeding 80% for most compounds. [56-59]. Therefore, this level of removal is not surprising, but the ability to convert almost 100% of the variety of sugars and their fermentation products regularly found in complex substrates is important from a commercial standpoint. These results suggest that MECs can be used to generate relatively clean effluent while also effectively producing high value products such as hydrogen. Such high level of conversion into hydrogen is not possible by other methods like dark fermentation, which can only produce four moles of hydrogen per mole of glucose by the following reaction [60]:

$$C_6H_{12}O_6 + 2H_2O \rightarrow 2CH_3COOH + 2CO_2 + 4H_2$$

Dark fermentation produces unutilized secondary organic metabolites, including acetate shown above. For MECs, the number of electrons credited to the COD of glucose is equal to six moles of chemical oxygen demand per mole of glucose, creating a theoretical maximum of 12 moles of hydrogen per mole of glucose. Thus, MECs should be able to convert more organic material to hydrogen than dark fermentation. Further, secondary metabolites produced such as acetate are also consumed in MECs for hydrogen production. The acetate produced in the equation above will yield a maximum of 8 moles of hydrogen in an MEC. For this reason, dark fermentation has been used in conjunction with MECs [6, 11].

These findings can also help elucidate some important mechanisms that may be taking place that explain the high conversion rates and large hydrogen production. None of the furanic compounds that have been previously identified in other biomass substrates used in MECs like furfural and HMF [8, 9, 41] were detected in this substrate, suggesting that substrate inhibition may be less of a contributing factor to performance. However, it is still likely that recalcitrant

chemicals exist, as not all the organic content was removed according to COD measurements. Using the 10 g/L-day experiment as an example, 24.2% of the COD remained unconverted, as shown in Table 14. Correctly identifying these remaining compounds will be the first step in uncovering the recalcitrance of these substrates

From the chemicals that were successfully detected, the variance in degradation of acetate may seem peculiar. Acetate accumulated in one of the replicates at the end of the 30 g/L-day experiment, resulting in significant variability shown in Figure 23(B) illustrated by the error bars, most likely contributing to the lower COD conversion percentage than what was observed at 10 g/L-day. This may be explained by acetate's role in other MECs operating on complex feedstocks. Lewis et al. 2017 determined that acetate is an intermediate product in MECs operating on BOAPs, where it accumulated under open circuit conditions during a batch experiment of 0.5 g/L [30]. At the high organic loading rates used in this study, it is possible that acetate was not consumed as quickly as it was generated in the second replicate, while the first replicate converted all the supplied and generated acetate. This is further shown by the second replicate's lower current density and hydrogen productivity, reflected in the variability of the efficiencies shown in Figure 22(B). Why and how acetate was not effectively converted in the second replicate at 30 g/L-day could be answered by several explanations. The community structure may not be the same in both cells, where one cell may contain more exoelectrogens than the other, while fermenters dominate in the underperforming cell. Detecting community structure differences between anodes at such high performances, and identifying the pathways used by the consortia, would help explain these discrepancies. The MECs may also have different operational limitations due to anode flow profile dissimilarity, membrane fouling, or other mechano-chemical structural nuances in the cell. These differences can exacerbate

performance changes at high organic loading conditions otherwise not found at lower organic loading. These issues will be worth consideration for future designs. Commercially viable MECs will require large absolute hydrogen production rates not demonstrated in lab scale experiments, while using high organic loading such as the loading rates used here. As shown by the increased variability at 30 g/L-day, such discrepancies will likely be prevalent in larger systems. Thus, commercially viable MECs will require much more precise design and engineering that may not be obvious when operating at lower organic loading rates. Currently, few if any studies have incorporated design changes to improve acetate consumption at such high organic loading rates using complex substrates.

Results from Pulsing Experiments

Because flow rate has been shown to alleviate proton transfer limitations and improve hydrogen production [38, 55], it was thought that increases in flow rate through pulsed flow would promote proton transfer and therefore, increase current and hydrogen productivity. Figure 24 shows the current density response as a function of pulsing at flow rates of 0.3 mL/min (A), 1 mL/min (B) and 3.5 mL/min (C).

(A)

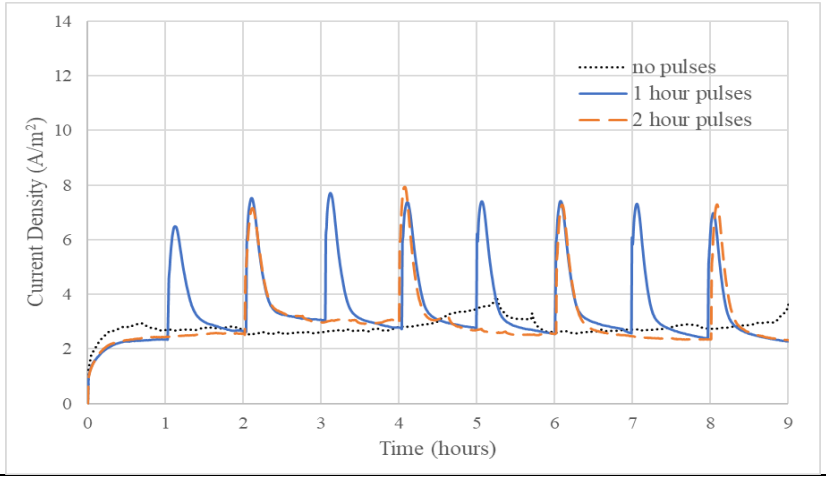

(B)

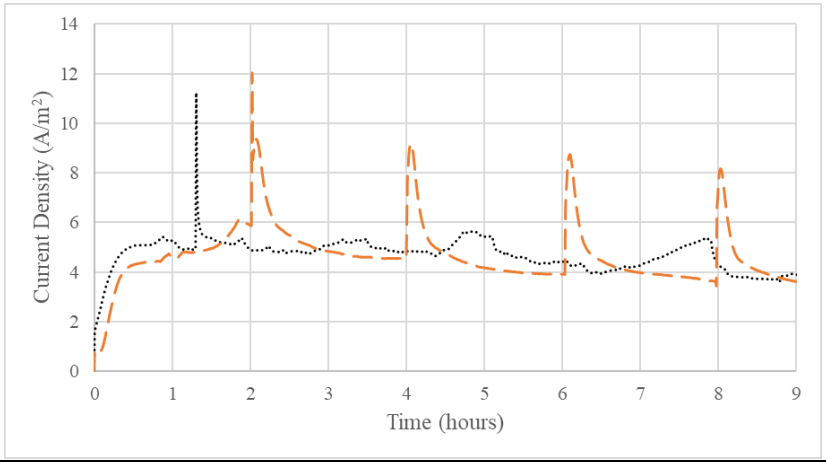

(C)

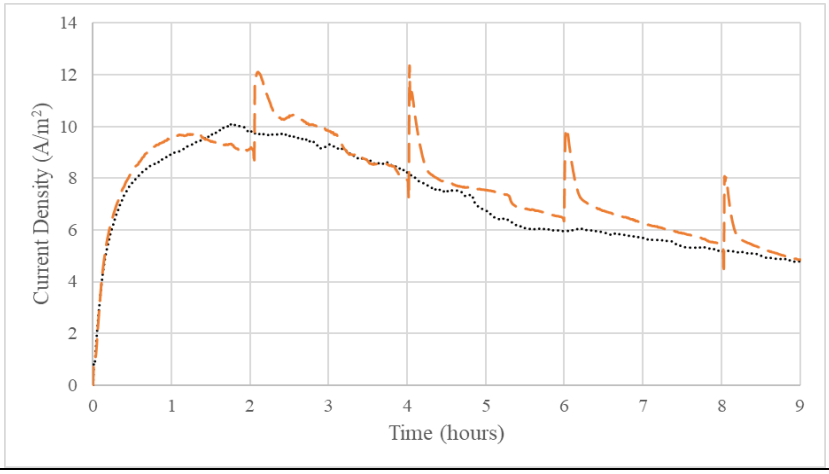

Figure 24: Current density of pulsing experiments using 0.2 g-COD/L CFP at different flow rates 0.3 mL/min (A), 1 mL/min (B), and 3.5 mL/min (C). Notice the spike in current density at every surge and the higher current densities at 3.5 mL/min, indicating the importance of flow rate on current production. The second replicate charts are included in the Appendix of this chapter.

In all cases, current increased sharply after pulsing anode liquid through the anode before returning to baseline current gradually over a period of 30 minutes. Average current density increased substantially as flow rate was increased but did not necessarily increase as much when the anode was pulsed. Table 15 shows the performance comparisons of pulsing, including average current density, hydrogen productivity, and electrical efficiency.

Table 15: current density, hydrogen productivity, average and electrical efficiency associated with pulsing experiments at different flow rates and pulsing frequencies.

Media flow rate (mL/min)	**Pulse Frequency**	**Current Density (A/m^2)**	**Hydrogen Productivity (L/L-day)**	**Average voltage (V)**	**Electrical Efficiency**
3.5	none	8.2 ± 1.0	9.1 ± 1.1	1.2 ± 0.03	136.0 ± 4.1%
3.5	every 2 h	8.8 ± 1.1	10 ± 1.4	1.2 ± 0.02	136.8 ± 1.0%
1	none	6.7 ± 2.6	7.3 ± 2.7	1.2 ± 0.1	136.8 ± 15.2%
1	every 2 h	6.2 ± 2.1	6.7 ± 2.2	1.2 ± 0.09	134.9 ± 10.5%
0.3	none	3.6 ± 1.1	3.7 ± 1.1	1.1 ± 0.07	138.5 ± 9.5%
0.3	every 2 h	3.8 ± 1.2	4.3 ± 1.3	1.1 ± 0.05	146.4 ± 9.7%
0.3	every hour	4.2 ± 1.1	4.8 ± 1.1	1.1 ± 0.04	149.2 ± 8.6%

The largest average current density observed was 8.8 ± 1.1 A/m^2 while pulsed flow was performed at 3.5 mL/min operated MECs. However, the non-pulsed cells at the same flow rate had an average current density of 8.2 ± 1.0 A/m^2, indicating only a marginal difference in current density. The increase in current density did not necessarily appear more pronounced at lower flow rates either. At 0.3 mL/min, the average current density was 3.6 ± 1.1 A/m^2, while pulsing every hour increased it to 4.2 ± 1.1 A/m^2. Thus, continuous flow rates appeared to be much more capable of establishing higher current densities than pulses.

A separate metric, hydrogen productivity, increased after pulsing for all flow rates except 1 mL/min. The maximum hydrogen productivity was 10.0 ± 1.4 L/L-day at 3.5 mL/min flow rate

with 2 h pulses, versus 9.1 ± 1.1 L/L-day at the same flow rate without pulses. The lowest observed hydrogen productivity corresponded to non-pulsed samples at 0.3 mL/min flow rates, reaching only 3.7 ± 1.1 L/L-day. Hourly pulsed samples at the same flow rate achieved hydrogen productivities of 4.8 ± 1.1 L/L-day. These further confirm the idea that increased flow rate in cross flow systems can improve hydrogen productivity as discovered earlier [38, 55], despite this being a novel flow regime change. In high performing two chamber MECs like those used here, gases produced by the anode can accumulate at the interface of the anode and the membrane, further impeding mass transfer and increasing cell resistance. To ensure hydraulic conductivity between the electrodes, these gases should be purged, with increasing frequency of accumulation as the substrate delivery rate increases and anode gases are produced. Pulsing provides this benefit by creating the necessary fluid pressure differential to remove these gases.

Pulsing did not necessarily decrease the operating voltage. MEC operating voltage remained at 1.1V at 0.3 mL/min regardless of pulsing, and was highest at both 1 mL/min and 3.5 mL/min at 1.2 V. Pulsing did not also appear to increase electrical efficiency at higher flowrates, however this difference was pronounced at 0.3 mL/min. Pulsing every hour at 0.3 mL/min anode liquid flow rates reached an electrical efficiency of 149.2 ± 8.6%, but without pulsing the same anode liquid media flow rates achieved an electrical efficiency of only 138.5 ± 9.5%. This increase in electrical efficiency is significant because it also corresponds with a higher current density and hydrogen productivity. With pulsing at the lowest flow rate, all of the performance metrics improved due to frequency of pulsing. This suggests that pulsing could be used as an alternative means of producing more current and hydrogen along with increasing anode liquid flow rates. However, the current densities and hydrogen productivities are still higher at higher flow rates than at 0.3 mL/min at all pulsing frequencies. Thus, if the goal of MECs is to generate

the highest hydrogen productivity, then high flow rates may be the most effective way to accomplish this goal. Operators may decide to balance maximizing hydrogen productivity with electrical efficiency. This added option to adjust electrical efficiency by running dynamic anode liquid flow schedules may prove to be valuable based on owner preferences. Owners that want to save operation costs but are willing to sacrifice hydrogen production rates may opt to run their systems with lower flow rates and pulsing. More rigorous pulsed flow studies that vary the duty cycle of the liquid flow rate between high and lower flow rates may also be required. In this study, the average flow rates were changed only marginally as pulses were applied. For example, the average flow rate was estimated to increase by 0.16 mL/min with hourly pulses, and 0.07 mL/min for pulses conducted every two h. Further pulse studies should be conducted that change average flow more significantly, randomly, or by ramping flow rate. Increasing anode liquid media flowrates has been shown to increase hydrogen productivity by alleviating mass transfer limitations [38], however alternative pumping schedules, such as flowrate pulsing, had not been tested until here. Other flow regimes rather than strictly continuous flow rates commonly discussed, may increase hydrogen productivities while also reducing MEC electrical energy demands and therefore cost of operation. While this study did not determine the energy use of anode liquid pumps used, the findings support further study.

Within the context of flow profiles in BESs, modeling and optimizing flow in BESs has seen some interest. Massaglia et al. analyzed the fluid flow created by an MFC enclosure and the amount of anode area exposed to liquid the cells experienced using computational fluid dynamics on three different cell geometries [61]. The authors concluded that longer chamber "drop" style anodes would produce more exposed anode area and therefore higher power densities, confirming performance with acetate fed experiments in the reactors modeled. More

recently, finite element methods have been used to characterize perpendicular flow through a porous carbon fabric versus parallel flow over an anode [62]. The authors found that perpendicular flow enhanced convective mass transfer in microbial fuel cells compared to more traditional parallel flow. These same insights can be useful for MECs, despite this kind of modeling not being regularly conducted on MECs. For both studies, the models did not calculate the possible flow regime changes associated with the biofilm formation in a porous electrode. The biofilm on the anode continuously changes, which changes the tortuous pathway of the fluid in ways that can be difficult to predict. This phenomenon of continuously changing biofilm structure is qualitatively evident by the turbidity of the media, discoloration of the anode material, and increased resistance to fluid flow when the MEC anode is flushed with new liquid media as it is maintained. To truly optimize MEC anode flow modeling, these affects will need to be considered. As new modeling constraints are incorporated, models will continue to improve future enclosure designs and aid in the discovery of anode liquid pump operational strategies that reduce total costs. Further computational fluid dynamics modeling of MECs will be useful, if not necessary, for improving MEC performance.

Implications for Future MEC Applications

The work presented here indicates that complex feedstocks can be used to reach potentially commercial targets in MECs using laboratory-scale systems. As mentioned in the introduction, MECs have been estimated to require current densities as high as 20 A/m^2 for economic feasibility by Sleutels et al. [33] corresponding to a hydrogen productivity of 20.7 L/L-day. This hydrogen productivity was achieved by the MECs used in this study. Additionally, substrates that are complex can still be degraded at high percentages, and multiple compounds

can be degraded simultaneously and effectively in MECs. Current densities and hydrogen productivities can also be modified by using irregular or pulsed flow rates instead of continuous anode liquid media flow, which may be beneficial to purge gas accumulation and also reduce pump requirements. However, continuous liquid flow rates and pulsed flow rates seems to both increase hydrogen productivity more than pulsing exclusively. These findings show promise for future systems. If the productivities demonstrated here can be successfully sustained in systems at scale, then biorefineries will benefit from incorporating MECs into their design. Additionally, CFP has been shown to be a useful substrate that can be produced regularly and easily. Today, CFP is primarily considered as a waste product, and therefore acts as a deterrent for more widespread adoption of corn stover-derived fuel. The potential to produce hydrogen from this resultant waste product adds value to corn stover as a fuel producing biomass, potentially incorporating MEC technology in biorefineries that now can be used to make even greater yields of hydrogen than by ethanol production alone. With the demonstrated productivities used here, corn stover wastes may also find itself as part of a feedstock for additional energy applications beyond ethanol, being used to create hydrogen even as a standalone product.

While the productivities demonstrated here are promising, several other challenges will need to be overcome for enabling commercial feasibility. Buffered media was required to help maintain pH, which may be impractical for real world systems from a cost and operational perspective. MECs will need to be capable of using real waste streams without buffers. Additionally, MEC scale up is still a significant issue, which so far has not been solved. While the systems used here achieved normalized productivity targets on a laboratory scale, this is traditionally not true for larger systems. A pilot study using a 100 L system operated on domestic wastewater documented by Heidrich et al. [63] reached an average productivity of only 0.007 L/L

reactor volume -day, several orders of magnitude less than the MECs used in this study. Larger MECs almost always have lower productivities than smaller MECs, though this difference is not always significant. A study by Cotterill et al. produced 0.003 liters of H_2 per tank volume per day with a total anode tank volume 175 L, and produced 0.004 liters of H_2 per tank volume per day with an anode tank volume 30 L at ambient winter temperatures [64]. The authors concluded that this difference was negligible. Ultimately, these productivities are also still several orders of magnitude less than the commercial targets identified earlier in the introduction. Additionally, MECs will require improved charge transfer and reduced cost of cathode catalysts to reach commercial feasibility. Even with the addition of a platinum deposited carbon catalyst, voltages were still high, resulting in lower electrical efficiency at 30 g/L-day. This may be alleviated by directly transferring protons to the cathode without a membrane, however; this strategy has shown to encourage cathode colonization of methanogens in many studies [31]. Inhibiting methanogenesis while improving hydrogen yields and lowering operating voltages remains a problem that future MECs must solve before commercial deployment. Finally, changing flow regimes rather than steady state flow rates must be better understood for large scale systems. While the pulsed rates were 200 mL/min, proportionally large flow rates may not be possible in larger systems. What larger flow rates are allowed will need to be studied further. All of the issues described here remain and will require innovative solutions not demonstrated here. However, with the demonstration of 20 L/L-day productivity using a complex feedstock, researchers can be assured that such high productivities are possible.

Commercial systems will need to demonstrate the productivities at larger overall scales. To determine appropriate scaling, accounting for the volume of the system is necessary, as it is important in determining the capital expense (CapEx) of the system. Necessary reactor volumes

and productivities rely on the systems using hydrogen, which can include larger systems used in transportation or materials handling needs, or smaller systems such as fuel cell driven forklifts. For the former, hydrogen production was estimated to be at least 100 kg/day, while the latter would require 10-50 kg/day. Based on the lowest demand, the required MEC volume will be at least 6 m^3 of anode volume, assuming the productivities mentioned are achieved. As mentioned in the introduction, Escapa et al. estimated that a CapEx of \$1500/m^3-anode (€1220/m^3-anode) would make MEC technology economically feasible if a current density of 5 A/m^2 were reached [32]. At current densities of 20 A/m^2, a 4-fold higher cost of MEC (\$6000/m^3-anode) would be acceptable, assuming that the MEC cost is the dominant contributor to the CapEx. By contrast, Aiken et al. used a reverse approach. They determined CapEx based on material costs, and then estimated current density needed to achieve breakeven point. Based on the reduction in materials costs they suggested, the CapEx for our MEC design would be \$4000/m^3-anode. Aiken et al. indicated that a current density of 3 A/m^2 would make their system reach breakeven point [34]. Thus, the higher current density achieved using corn stover-derived waste feedstock suggests that the MEC technology can be economically feasible. However, this performance must be demonstrated in larger scale reactors. The compact design of the MEC used in this study has potential to be scaled-up to demonstrate such performance. It is expected that the aspect ratio of the reactor may change as it is scaled-up, however, other design and process parameters such as anode-cathode distance, high electrode area to anode volume ratio, and flow-through operation need to be maintained. The materials to be used at a larger scale will need to be of lower cost, as platinum and Nafion are still cost prohibitive for scaled commercial systems. Thus, while much of the design remains the same, the effect of change in materials used, such as the use of a stainless-steel cathode vs. platinum as the cathode catalyst, will need to be examined. However,

it should be noted that the key factor in achieving the performance obtained in this study was the anode biocatalyst and process design. This should not be affected by scale. Application of the concepts derived from our optimized MEC design and process parameters, along with suitable lower cost materials, to study scale-up is needed to move towards a successful demonstration of commercially feasible MEC technology. Given the ability of the anode consortia to utilize complex substrates and generate the hydrogen productivities reported here, the chances of successful demonstration of this novel bioenergy technology at larger scales appear to be on the horizon.

Conclusions

Microbial electrolysis cells are a novel technology that can convert a wide variety of biomass substrates into renewable hydrogen. This study confirms that corn stover derived substrates can be used to generate high productivities in these reactors at high organic loading rates. Conversion of residual organics found in fermentation effluents can be converted at high percentages and rates at high organic loading rates. Additionally, pulsed anode liquid flow regimes can contribute to increased hydrogen productivities and electrical efficiencies. The findings conducted in this study further support the viability of complex feedstocks used in microbial electrolysis cells for biomass derived hydrogen production, reaching normalized commercial targets for the first time, in microbial electrolysis cells operated at a laboratory scale. However, future biorefineries and commercial reactors will require additional considerations, including proportional scale up, lowering operational energy usage, lowering electrical energy applied to the electrodes, optimizing anode liquid media pumping schedules, and further understanding of the effects of flow on larger systems.

References

1. Hydrogen Production and Distribution. https://afdc.energy.gov/fuels/hydrogen_production.html (5/9/2019),
2. Pivovar, B., H2@Scale Overview. In *2018 DOE Hydrogen and Fuel Cells Program Review*, National Renewable Energy Laboratory: 2018.
3. Borole, A.; Reguera, G.; Ringeisen, B.; Wang, Z.-W.; Feng, Y.; Hong Kim, B., Electroactive biofilms: Current status and future research needs. *Energy & Environmental Science* **2011,** *4*, (12), 4813-4834.
4. Rago, L.; Baeza, J. A.; Guisasola, A., Bioelectrochemical hydrogen production with cheese whey as sole substrate. *Journal of Chemical Technology & Biotechnology* **2017,** *92*, (1), 173-179.
5. Kiely, P. D.; Cusick, R.; Call, D. F.; Selembo, P. A.; Regan, J. M.; Logan, B. E., Anode microbial communities produced by changing from microbial fuel cell to microbial electrolysis cell operation using two different wastewaters. *Bioresource Technology* **2011,** *102*, (1), 388-394.
6. Li, X.-H.; Liang, D.-W.; Bai, Y.-X.; Fan, Y.-T.; Hou, H.-W., Enhanced H2 production from corn stalk by integrating dark fermentation and single chamber microbial electrolysis cells with double anode arrangement. *International Journal of Hydrogen Energy* **2014,** *39*, (17), 8977-8982.
7. Zhao, Y.; Cao, W.; Wang, Z.; Zhang, B.; Chen, K.; Ouyang, P., Enhanced succinic acid production from corncob hydrolysate by microbial electrolysis cells. *Bioresource Technology* **2016,** *202*, 152-157.
8. Lewis, A. J.; Ren, S.; Ye, X.; Kim, P.; Labbe, N.; Borole, A. P., Hydrogen production from switchgrass via an integrated pyrolysis–microbial electrolysis process. *Bioresource Technology* **2015,** *195*, 231-241.
9. Brooks, V.; Lewis, A. J.; Dulin, P.; Beegle, J. R.; Rodriguez, M.; Borole, A. P., Hydrogen production from pine-derived catalytic pyrolysis aqueous phase via microbial electrolysis. *Biomass and Bioenergy* **2018,** *119*, 1-9.
10. Satinover, S. J.; Elkasabi, Y.; Nuñez, A.; Rodriguez, M.; Borole, A. P., Microbial electrolysis using aqueous fractions derived from Tail-Gas Recycle Pyrolysis of willow and guayule. *Bioresource Technology* **2019,** *274*, 302-312.
11. Wang, A.; Sun, D.; Cao, G.; Wang, H.; Ren, N.; Wu, W.-M.; Logan, B. E., Integrated hydrogen production process from cellulose by combining dark fermentation, microbial fuel cells, and a microbial electrolysis cell. *Bioresource Technology* **2011,** *102*, (5), 4137-4143.
12. Shen, R.; Liu, Z.; He, Y.; Zhang, Y.; Lu, J.; Zhu, Z.; Si, B.; Zhang, C.; Xing, X.-H., Microbial electrolysis cell to treat hydrothermal liquefied wastewater from cornstalk and recover hydrogen: Degradation of organic compounds and characterization of microbial community. *International Journal of Hydrogen Energy* **2016,** *41*, (7), 4132-4142.
13. Shen, R.; Jiang, Y.; Ge, Z.; Lu, J.; Zhang, Y.; Liu, Z.; Ren, Z. J., Microbial electrolysis treatment of post-hydrothermal liquefaction wastewater with hydrogen generation. *Applied Energy* **2018,** *212*, 509-515.
14. Rivera, I.; Buitrón, G.; Bakonyi, P.; Nemestóthy, N.; Bélafi-Bakó, K., Hydrogen production in a microbial electrolysis cell fed with a dark fermentation effluent. *Journal of Applied Electrochemistry* **2015,** *45*, (11), 1223-1229.

15. Sharma, Y. C.; Kumar, A.; Prasad, R.; Upadhyay, S. N., Ethanol steam reforming for hydrogen production: Latest and effective catalyst modification strategies to minimize carbonaceous deactivation. *Renewable and Sustainable Energy Reviews* **2017,** *74*, 89-103.
16. Mattos, L. V.; Jacobs, G.; Davis, B. H.; Noronha, F. B., Production of Hydrogen from Ethanol: Review of Reaction Mechanism and Catalyst Deactivation. *Chemical Reviews* **2012,** *112*, (7), 4094-4123.
17. Kemp, L. *Cellulosic Ethanol From Corn Stover: Can We Get it Right?*; Natural Resrouces Defense Council: November 2015, 2015; p 26.
18. Speers, A. M.; Reguera, G., Consolidated Bioprocessing of AFEX-Pretreated Corn Stover to Ethanol and Hydrogen in a Microbial Electrolysis Cell. *Environmental Science & Technology* **2012,** *46*, (14), 7875-7881.
19. Borole, A. P.; Hamilton, C. Y.; Schell, D., Conversion of residual organics in corn stover-derived biorefinery stream to bioenergy via microbial fuel cells. *Environ Sci Technol.* **2013,** *47*, 642-8.
20. Pannell, T. C.; Goud, R. K.; Schell, D. J.; Borole, A. P., Effect of fed-batch vs. continuous mode of operation on microbial fuel cell performance treating biorefinery wastewater. *Biochemical Engineering Journal* **2016,** *116*, 85-94.
21. Borole, A. P., Chapter 9 - Opportunities for Electricity and Hydrogen Production in Bioelectrochemical Systems. In *Ethanol*, Basile, A.; Iulianelli, A.; Dalena, F.; Veziroğlu, T. N., Eds. Elsevier: 2019; pp 231-255.
22. Varga, E.; Klinke, H. B.; Réczey, K.; Thomsen, A. B., High solid simultaneous saccharification and fermentation of wet oxidized corn stover to ethanol. *Biotechnology and Bioengineering* **2004,** *88*, (5), 567-574.
23. Cao, G.; Ren, N.; Wang, A.; Lee, D.-J.; Guo, W.; Liu, B.; Feng, Y.; Zhao, Q., Acid hydrolysis of corn stover for biohydrogen production using Thermoanaerobacterium thermosaccharolyticum W16. *International Journal of Hydrogen Energy* **2009,** *34*, (17), 7182-7188.
24. He, Y.; Zhang, L.; Zhang, J.; Bao, J., Helically agitated mixing in dry dilute acid pretreatment enhances the bioconversion of corn stover into ethanol. *Biotechnology for Biofuels* **2014,** *7*, (1), 1.
25. Zeng, X.; Borole, A. P.; Pavlostathis, S. G., Inhibitory Effect of Furanic and Phenolic Compounds on Exoelectrogenesis in a Microbial Electrolysis Cell Bioanode. *Environmental Science & Technology* **2016,** *50*, (20), 11357-11365.
26. Jeremiasse, A.; Hamelers, H.; Saakes, M.; Buisman, C., Ni foam cathode enables high volumetric H2 production in a microbial electrolysis cell. *International Journal of Hydrogen Energy* **2010,** *35*, (23), 12716-12723.
27. Rollin, J. A.; Martin del Campo, J.; Myung, S.; Sun, F.; You, C.; Bakovic, A.; Castro, R.; Chandrayan, S. K.; Wu, C.-H.; Adams, M. W. W.; Senger, R. S.; Zhang, Y. H. P., High-yield hydrogen production from biomass by in vitro metabolic engineering: Mixed sugars coutilization and kinetic modeling. *Proceedings of the National Academy of Sciences of the United States of America* **2015,** *112*, (16), 4964-4969.
28. Li, X.; Zhang, R.; Qian, Y.; Angelidaki, I.; Zhang, Y., The impact of anode acclimation strategy on microbial electrolysis cell treating hydrogen fermentation effluent. *Bioresource Technology* **2017,** *236*, 37-43.

29. Lewis, A. J.; Borole, A. P., Microbial electrolysis cells using complex substrates achieve high performance via continuous feeding-based control of reactor concentrations and community structure. *Applied Energy* **2019,** *240*, 608-616.
30. Lewis, A. J.; Campa, M. F.; Hazen, T. C.; Borole, A. P., Unravelling biocomplexity of electroactive biofilms for producing hydrogen from biomass. *Microb. Biotechnol.* **2018,** *11*, (1), 84-97.
31. Karthikeyan, R.; Cheng, K. Y.; Selvam, A.; Bose, A.; Wong, J. W. C., Bioelectrohydrogenesis and inhibition of methanogenic activity in microbial electrolysis cells - A review. *Biotechnology Advances* **2017,** *35*, (6), 758-771.
32. Escapa, A.; Gómez, X.; Tartakovsky, B.; Morán, A., Estimating microbial electrolysis cell (MEC) investment costs in wastewater treatment plants: Case study. *International Journal of Hydrogen Energy* **2012,** *37*, (24), 18641-18653.
33. Sleutels, T. H. J. A.; Ter Heijne, A.; Buisman, C. J. N.; Hamelers, H. V. M., Bioelectrochemical Systems: An Outlook for Practical Applications. *ChemSusChem* **2012,** *5*, (6), 1012-1019.
34. Aiken, D. C.; Curtis, T. P.; Heidrich, E. S., Avenues to the financial viability of microbial electrolysis cells [MEC] for domestic wastewater treatment and hydrogen production. *International Journal of Hydrogen Energy* **2019,** *44*, (5), 2426-2434.
35. Logan, B. E.; Call, D.; Cheng, S.; Hamelers, H. V. M.; Sleutels, T. H. J. A.; Jeremiasse, A. W.; Rozendal, R. A., Microbial Electrolysis Cells for High Yield Hydrogen Gas Production from Organic Matter. *Environmental Science & Technology* **2008,** *42*, (23), 8630-8640.
36. Lu, L.; Ren, Z. J., Microbial electrolysis cells for waste biorefinery: A state of the art review. *Bioresource Technology* **2016,** *215*, 254-264.
37. Escapa, A.; Mateos, R.; Martínez, E. J.; Blanes, J., Microbial electrolysis cells: An emerging technology for wastewater treatment and energy recovery. From laboratory to pilot plant and beyond. *Renewable and Sustainable Energy Reviews* **2016,** *55*, 942-956.
38. Lewis, A. J.; Borole, A. P., Understanding the impact of flow rate and recycle on the conversion of a complex biorefinery stream using a flow-through microbial electrolysis cell. *Biochemical Engineering Journal* **2016,** *116*, (Supplement C), 95-104.
39. Oxygen Demand, Chemical. In Hach: 2014.
40. Borole, A. P.; Hamilton, C. Y.; Vishnivetskaya, T. A.; Leak, D.; Andras, C.; Morrell-Falvey, J.; Keller, M.; Davison, B., Integrating engineering design improvements with exoelectrogen enrichment process to increase power output from microbial fuel cells. *Journal of Power Sources* **2009,** *191*, (2), 520-527.
41. Park, L. K.-E.; Satinover, S. J.; Yiacoumi, S.; Mayes, R. T.; Borole, A. P.; Tsouris, C., Electrosorption of organic acids from aqueous bio-oil and conversion into hydrogen via microbial electrolysis cells. *Renewable Energy* **2018,** *125*, 21-31.
42. Ren, S.; Ye, X. P.; Borole, A. P.; Kim, P.; Labbé, N., Analysis of switchgrass-derived bio-oil and associated aqueous phase generated in a semi-pilot scale auger pyrolyzer. *Journal of Analytical and Applied Pyrolysis* **2016,** *119*, 97-103.
43. Pham, H. T.; Boon, N.; Aelterman, P.; Clauwaert, P.; De Schamphelaire, L.; Van Oostveldt, P.; Verbeken, K.; Rabaey, K.; Verstraete, W., High shear enrichment improves the performance of the anodophilic microbial consortium in a microbial fuel cell. *Microb. Biotechnol.* **2008,** *1*, (6), 487-496.

44. Cheng, S.; Liu, H.; Logan, B. E., Increased Power Generation in a Continuous Flow MFC with Advective Flow through the Porous Anode and Reduced Electrode Spacing. *Environmental Science & Technology* **2006,** *40*, (7), 2426-2432.
45. Nam, J.-Y.; Tokash, J. C.; Logan, B. E., Comparison of microbial electrolysis cells operated with added voltage or by setting the anode potential. *International Journal of Hydrogen Energy* **2011,** *36*, (17), 10550-10556.
46. Lee, H.-S.; Torres, C. I.; Parameswaran, P.; Rittmann, B. E., Fate of H2 in an upflow single-chamber microbial electrolysis cell using a metal-catalyst-free cathode. *Environmental Science & Technology* **2009,** *43*, (20), 7971-7976.
47. Lu, L.; Hou, D.; Wang, X.; Jassby, D.; Ren, Z. J., Active H2 Harvesting Prevents Methanogenesis in Microbial Electrolysis Cells. *Environmental Science & Technology Letters* **2016,** *3*, (8), 286-290.
48. Call, D. F.; Wagner, R. C.; Logan, B. E., Hydrogen Production by Geobacter Species and a Mixed Consortium in a Microbial Electrolysis Cell. *Appl Environ Microbiol* **2009,** *75*, (24), 7579-7587.
49. Yossan, S.; Xiao, L.; Prasertsan, P.; He, Z., Hydrogen production in microbial electrolysis cells: Choice of catholyte. *International Journal of Hydrogen Energy* **2013,** *38*, (23), 9619-9624.
50. Siegert, M.; Yates, M. D.; Call, D. F.; Zhu, X.; Spormann, A.; Logan, B. E., Comparison of Nonprecious Metal Cathode Materials for Methane Production by Electromethanogenesis. *ACS sustainable chemistry & engineering* **2014,** *2*, (4), 910-917.
51. Choi, M.-J.; Chae, K.-J.; Ajayi, F. F.; Kim, K.-Y.; Yu, H.-W.; Kim, C.-w.; Kim, I. S., Effects of biofouling on ion transport through cation exchange membranes and microbial fuel cell performance. *Bioresource Technology* **2011,** *102*, (1), 298-303.
52. Call, D.; Logan, B. E., Hydrogen Production in a Single Chamber Microbial Electrolysis Cell Lacking a Membrane. *Environmental Science & Technology* **2008,** *42*, (9), 3401-3406.
53. Rozendal, R. A.; Hamelers, H. V. M.; Molenkamp, R. J.; Buisman, C. J. N., Performance of single chamber biocatalyzed electrolysis with different types of ion exchange membranes. *Water Research* **2007,** *41*, (9), 1984-1994.
54. Torres, C. I.; Kato Marcus, A.; Rittmann, B. E., Proton transport inside the biofilm limits electrical current generation by anode-respiring bacteria. *Biotechnology and Bioengineering* **2008,** *100*, (5), 872-881.
55. Borole, A. P.; Lewis, A. J., Proton transfer in microbial electrolysis cells. *Sustainable Energy Fuels* **2017,** *1*, (4), 725-736.
56. Huang, L.; Logan, B. E., Electricity production from xylose in fed-batch and continuous-flow microbial fuel cells. *Applied Microbiology and Biotechnology* **2008,** *80*, (4), 655.
57. Selembo, P. A.; Perez, J. M.; Lloyd, W. A.; Logan, B. E., High hydrogen production from glycerol or glucose by electrohydrogenesis using microbial electrolysis cells. *International Journal of Hydrogen Energy* **2009,** *34*, (13), 5373-5381.
58. Catal, T.; Li, K.; Bermek, H.; Liu, H., Electricity production from twelve monosaccharides using microbial fuel cells. *Journal of Power Sources* **2008,** *175*, (1), 196-200.
59. Kim, H. J.; Park, H. S.; Hyun, M. S.; Chang, I. S.; Kim, M.; Kim, B. H., A mediator-less microbial fuel cell using a metal reducing bacterium, Shewanella putrefaciens. *Enzyme and Microbial Technology* **2002,** *30*, (2), 145-152.

60. Viswanathan, B., Chapter 15 - Biochemical Routes for Energy Conversion. In *Energy Sources*, Viswanathan, B., Ed. Elsevier: Amsterdam, 2017; pp 357-368.
61. Massaglia, G.; Gerosa, M.; Agostino, V.; Cingolani, A.; Sacco, A.; Saracco, G.; Margaria, V.; Quaglio, M., Fluid Dynamic Modeling for Microbial Fuel Cell Based Biosensor Optimization. *Fuel Cells* **2017,** *17*, (5), 627-634.
62. Krieg, T.; Wood, J. A.; Mangold, K.-M.; Holtmann, D., Mass transport limitations in microbial fuel cells: Impact of flow configurations. *Biochemical Engineering Journal* **2018,** *138*, 172-178.
63. Heidrich, E. S.; Edwards, S. R.; Dolfing, J.; Cotterill, S. E.; Curtis, T. P., Performance of a pilot scale microbial electrolysis cell fed on domestic wastewater at ambient temperatures for a 12month period. *Bioresource Technology* **2014,** *173*, 87-95.
64. Cotterill, S. E.; Dolfing, J.; Jones, C.; Curtis, T. P.; Heidrich, E. S., Low Temperature Domestic Wastewater Treatment in a Microbial Electrolysis Cell with 1 m2 Anodes: Towards System Scale-Up. *Fuel Cells* **2017,** *17*, (5), 584-592.

Chapter IV Appendix

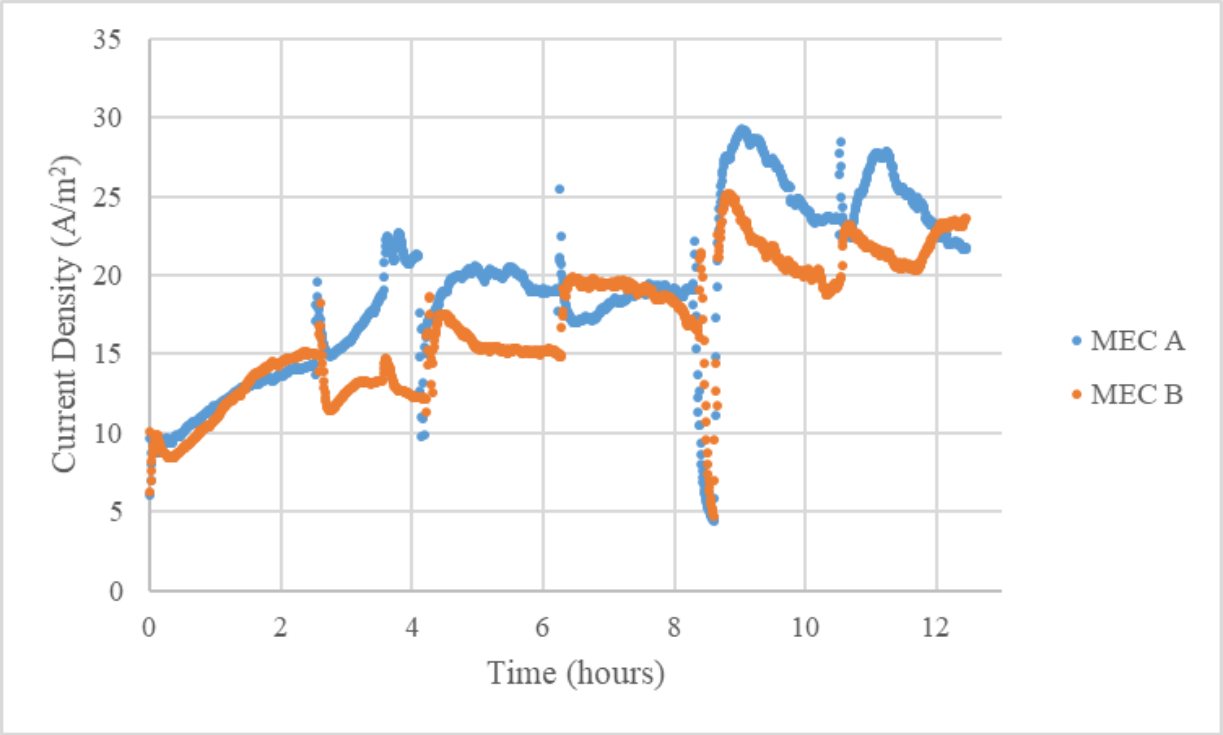

Figure 25: Corn Stover current densities at substrate loading at 30 g/L-day, displaying replicates A and B.

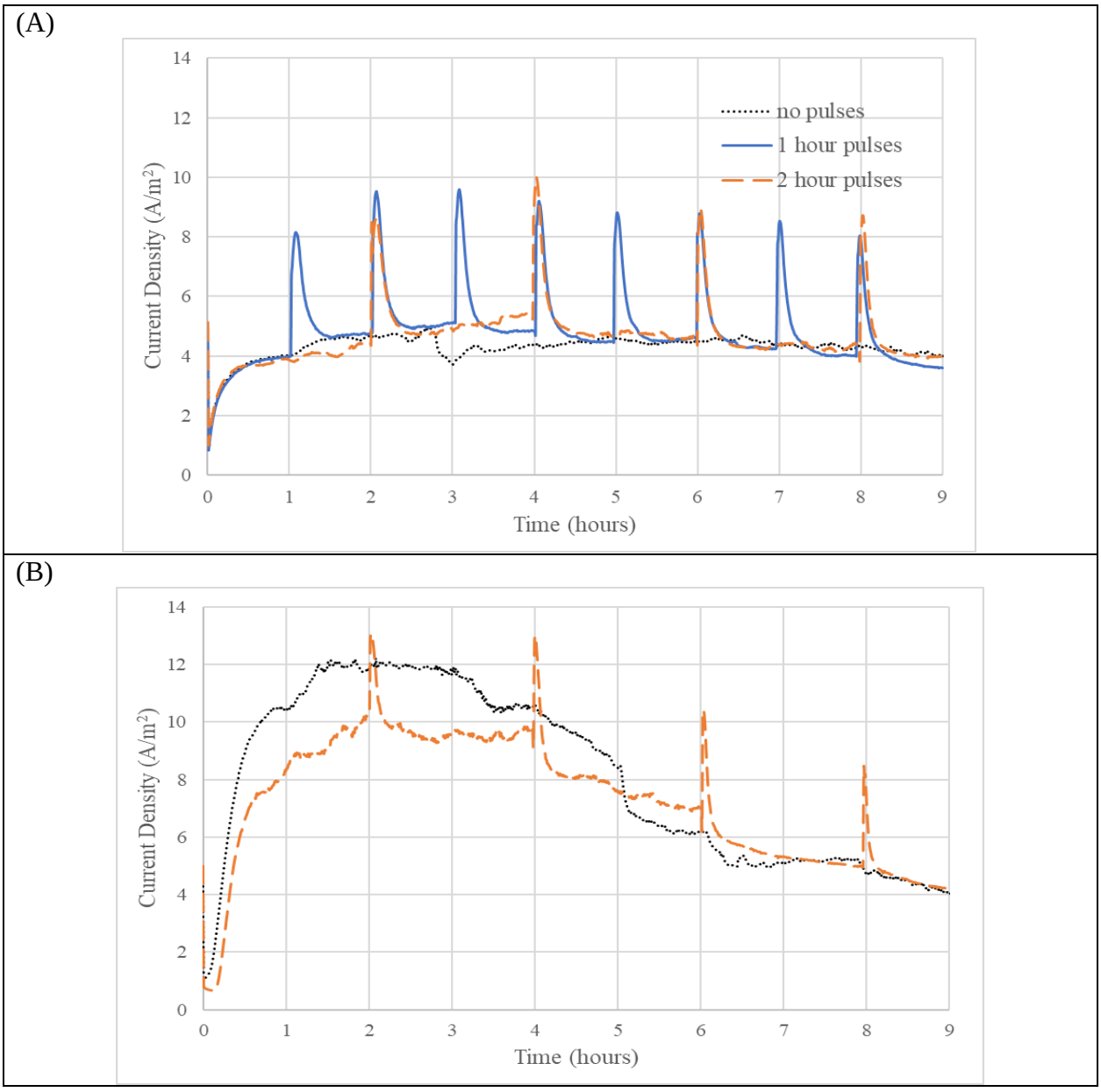

Figure *26*: Current density of pulsing experiments of secondary replicate using 0.2 g-COD/L CFP at different flow rates 0.3 mL/min (A), 1 mL/min (B), and 3.5 mL/min (C).

(C)

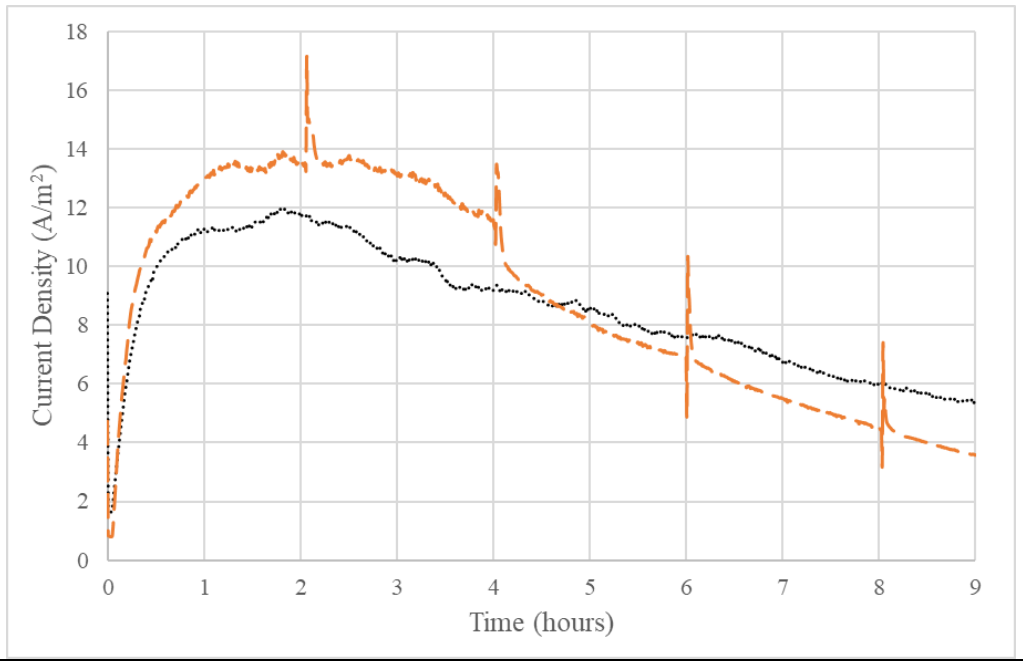

Figure 26 continued

Table 16: voltage data for 2, 4, 10, 20, and 30 g/L-day experiments

Organic Loading Rate (g/L-day)	**Average Voltage (V)**
2	0.87 ± 0.03
4	1.01 ± 0.05
10	1.16 ± 0.01
20	1.25 ± 0.04
30	1.41 ± 0.17

CHAPTER V

ADDITIONAL HYDROGEN PRODUCTION DEMONSTRATIONS IN MICROBIAL ELECTROLYSIS CELLS FROM OTHER BIOMASS PYROLYSIS WASTES

This chapter contains data published as part of the manuscript:

Park, L. K.-E.; Satinover, S. J.; Yiacoumi, S.; Mayes, R. T.; Borole, A. P.; Tsouris, C., Electrosorption of organic acids from aqueous bio-oil and conversion into hydrogen via microbial electrolysis cells. *Renewable Energy* **2018,** *125*, 21-31.

Much, but not all, of the content found in this manuscript have been used in this dissertation, which includes portions of the introduction, methods and materials, data from the electrochemical results and analytical chemistry run after microbial electrolysis cell operation, and written content from the results and discussion on MECs. Satinover, S. conducted all of the microbial electrolysis work and High-Performance Liquid Chromatography (HPLC), as well as performed the analysis and wrote the associated sections of the manuscript. Park L.K.E., Yiacoumi S. and Tsouris C. produced the neutralized aqueous product used in the experiments and wrote the other sections of the manuscript. Borole A. provided guidance and feedback on experiments, data analysis, and content for the manuscript. The remaining data using the other feedstock in this chapter remains unpublished and unsubmitted. Satinover S. conducted the experiments and analytical chemistry, as well as wrote the portion associated with those experiments in this dissertation. Borole A. provided guidance on experiments, data analysis, and feedback on the written content.

Abstract

The data presented in this chapter was derived from two sources: a neutralized bio oil aqueous phase (BOAP) from switch grass, and a BOAP derived from red oak. Red Oak BOAP (ROBOAP) and Neutralized BOAP (NBOAP) performed similarly. Average current for ROBOAP and NBOAP was found to be highest at organic loading rates of 10 g/L-day at 4.61 ± 0.07 A/m^2 and 5.27 ± 0.15 A/m^2 respectively. Major compounds in the water phase included organic acids, sugar derivatives, furanic and phenolic compounds and were degraded between 80 – 90% in both substrates. Performance was similar to other biomass wastes discussed earlier. Additional rigor for these substrates would include voltage measurement, further chemical compound identification analytical chemistry techniques such as mass spectroscopy, and batch addition experiments.

Introduction

Biomass pyrolysis can be extended to a variety of other feedstocks, and processing conditions can alter the composition of pyrolysis end products significantly. So far, only two pyrolysis products have been demonstrated for microbial electrolysis cells (MECs) in this dissertation, which is hardly exhaustive. While this dissertation does not intend on demonstrating pyrolysis biomass as the sole feedstock, additional pyrolysis byproducts are worth discussing. MEC capability with complex wastes can continue to be expanded upon using other bio-oil aqueous phases (BOAPs). However, pyrolysis processing can vary considerably, and feedstocks with different processing techniques should not be ignored entirely. Additional demonstrations of substrate utilization will provide meaningful insight and justification for future study and the

remaining chapters of this dissertation despite differences in process conditions used on the feedstocks discussed.

This chapter focuses on the results associated with microbial electrolysis cells (MECs) using two additional pyrolysis waste products originating from different sources and BOAP processing. For one feedstock, capacitive deionization (CDI) was used after the bio-oil was neutralized and harvesting the CDI rinse water for use in MECs. CDI can be used to capture acidic ions from the neutralized bio-oil contacted water phase, where the rinse water can contain significant amounts of these separated organics. Acid removal is important for ensuring bio-oils are not corrosive, and therefore harvesting the separated organics becomes an important consideration that MECs may be able to solve. Thus, the findings shown here demonstrate the performance associated with using such a CDI rinse water and characterization of the waste.

Other feedstocks may not necessarily be neutralized but may come from different sources of biomass. Much like other woody biomass sources like guayule and willow as discussed in Chapter I, red oak tree can also be used as a feedstock for pyrolysis [1], though the bio-oil it creates suffers from the same issues as bio-oil derived from other sources [2]. Many of the organics found from red oak pyrolysis are water soluble, can be recovered in multiple stages of separation [1] and can also depend on the temperature of the operating pyrolysis reactor [3]. BOAP from a water-heavy stage fraction after pyrolysis should also contain organic acids and sugars.

Prior studies by the MEC community made comparison between performances of any kind less meaningful due to varying operating conditions, reactor designs, and differences in electrochemical analysis. Further, complex feedstocks can vary so wildly that meaningful comparison between unrelated feedstocks can be difficult. Because both sources discussed here originate from biomass pyrolysis, comparing the performance of the MECs and degradation of

the substrates can be made with greater ease. Thus, the goal of this chapter was to compare the performance of MECs fed BOAPs from other sources and techniques from switch grass used prior [4] using the same reactor configuration, electrochemical characterization, and starting community, using similar, but different, waste sources to switch grass BOAP first demonstrated by Lewis et al. [4]. By using a mature biofilm and using identical MEC operating conditions, the findings produced here further expand on similarities between substrates and introduce some of the nuances associated with the types and effectiveness of complex substrate degradation in MECs.

Methods and Materials

Substrate Creation

Both substrates were characterized by COD analysis discussed earlier in this dissertation, however the processes to create the substrates varied. The details of switchgrass composition and the auger pyrolysis system can be found in previous studies [5-8]. The pH neutralization of bio-oil was performed as described in previous studies [6]. In brief, crude switchgrass bio-oil obtained from the University of Tennessee was centrifuged using a Beckman Coulter Avanti J-E centrifuge with a JLA 10.500 rotor at 3000 rpm (1673 *g*) for 30 minutes to obtain aqueous bio-oil before neutralization experiments. Then, NaOH (aq, 50%) was added to aqueous bio-oil to reach a pH 6.0. The neutralized bio-oil mixture was centrifuged after reaching equilibrium to separate aqueous and organic phases that were formed during neutralization. Once separated, NBOAP was filter sterilized before use in capacitive deionization. Batch electrosorption/CDI was performed using a laboratory-scale CDI cell with a pair of carbon aerogel electrodes. Carbon aerogels were obtained from Marketech (Port Townsend, WA). Details on the carbon aerogels

can be found in Ying et al. [9]. The two sheets of carbon aerogel electrodes were in contact with titanium sheets, which were used as current collectors. The edges of the carbon sheets were taped on the titanium sheets to ensure sufficient contact. A plastic mesh was placed in between the two electrodes to prevent any shortage. The distance between the two electrodes, which were separated by a central hollow piece of Viton gasket, was 0.6 cm. The titanium sheets were connected to a direct-current (DC) power supply (Hewlett Packard E3630A Triple output DC power supply) with a voltage range of 0 to 15 V and a current range of 0 to 7 A.

Approximately 11–14 mL of the initial solution was placed in the CDI reactor using a syringe. After initializing the CDI cell by allowing the electrodes to reach equilibrium with the initial solution, a potential of 1.4 V was applied between the two electrodes. The electric field was applied for at least 20 minutes and until the current reached 0.02 A. While the electric field was on, the CDI-treated solution was removed from the CDI cell using a syringe. Then, the electrical potential was turned off to 0 V, and deionized water was introduced into the CDI cell to recover desorbed ions and regenerate the electrodes. Finally, after at least 2 h of regeneration, the rinsing water phase was collected for use in MECs, referred to as neutralized BOAP (NBOAP).

The ROBOAP was prepared as described previously [1]. Briefly, red oak wood chips were ground by hammer mill. The ground biomass was then fed into a fluidized bed fast pyrolysis reactor that was operated at 500 C, fluidized with nitrogen, and was fed biomass at a rate of 8 kg/hr. Particular matter was then cylconed off before distillation. Five stages of seperation followed pyrolysis to effectively seperate vapors, oils, and water. Each stage was used for collection of different compounds and different retention times. At the fifth stage, water was seperated from the bio-oil, with the additional intent of removing volatile organic acids such as

acetic acid. The water extracted from this stage, the red oak BOAP (ROBOAP), was cooled, centrifuged, and filter sterilized before using in MECs. Both substrates were then stored in a 4 ºC refirdgerator until used in MECs.

Microbial Electrolysis Experiments

The experimental set up was the same as Chapter I of this dissertation. Substrate injection was performed at 2, 4, and 10 gld COD to both replicates and substrates, with cathode buffer and media being replaced before each experiment. NBOAP was used in MECs first, followed by an adaptation period using ROBOAP that lasted no more than one month. Experiments using 2 gld NBOAP were run for 67.3 h, experiments using 4 gld were run for 112 h, and experiments using 10 gld were run for 79.3 h. For ROBOAP, experiments using 2 gld were run for 94.5 h, experiments using 4 gld were run for 67.8 h, and experiments using 10 gld were run for 73.4 h. COD analysis of media was completed using high range Hach COD vials. The last sample of the 10 gld loading experiment was used for HPLC measurements. Standards for 10 notable compounds were also measured out with concentrations of 1, 0.1, and 0.02 g/L. Those compounds were, furfural, 5-hydroxymethylfurfural, vanillic acid, syringic acid, catechol, phenol, acetic acid, propionic acid, levoglucosan, and 4-hydroxybenzaldehyde. Each sample and standard were measured out in 250 µL samples and acidified prior to being analyzed on HPLC. The HPLC column was an Aminex HPX-87H produced by Bio-Rad (Bio-Rad, Hercules, CA). The column oven was run at 60 °C. A refractive index detector (RID), Shimadzu RID-20 and a photo diode array (PDA) detector, Shimadzu SPD-m20, were both used to identify compounds, and both ran at 50 °C. The PDA captured wavelengths from 190-800 nm. All samples and standards were run for 2 h each, using 5 mM H_2SO_4 as the mobile phase, at a flow rate of 0.5 m/min. Current and poise potential were recorded in order to calculate hydrogen cathode

conversion efficiency, current density, and anodic Coulombic efficiency over the period the experiments were conducted, as calculated previously [4].

Results and Discussion

Electrochemical Performance of MECs

Electrochemical performance was similar across both substrates. Figure 27 shows the average current density (A), hydrogen productivity (B), Coulombic efficiency (C), cathode conversion efficiency (D), COD removal % (E), and hydrogen recovery (F) for each substrate.

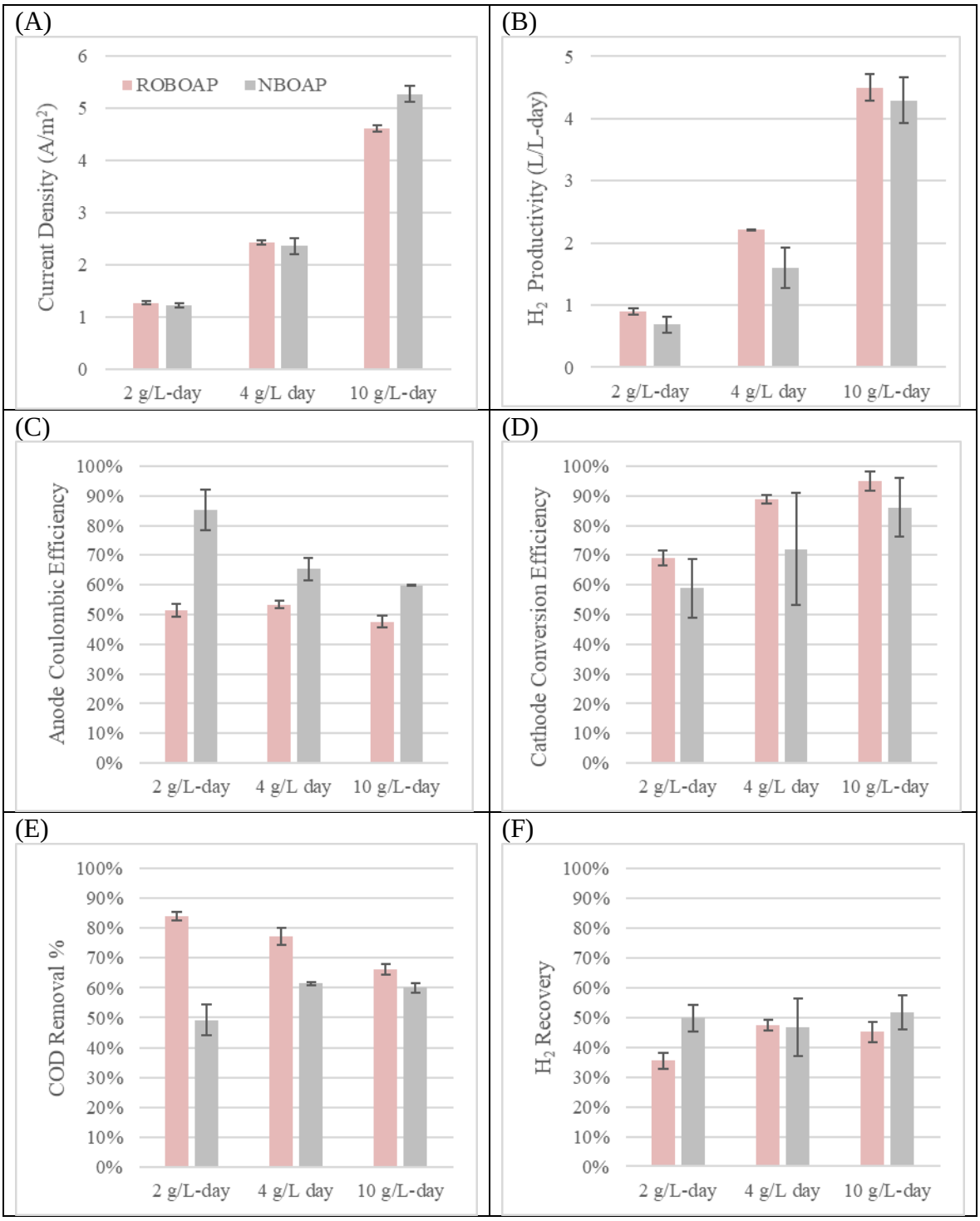

Figure 27: Electrochemical performances of ROBOAP and NBOAP fed MECs under 2, 4, and 10 g/L-day organic loading conditions.

The average current density for ROBOAP and NBOAP-fed MECs was highest at 10 g/L-day, reaching 4.6 ± 0.03 A/m^2 and 5.3 ± 0.03 A/m^2 respectively. Compared to the results from Lewis et al., these results are similar, where Lewis et al. reported an average current density of 4.5 A/m^2 [4]. The average hydrogen productivities between both substrates was also similar, with ROBOAP slightly edging out NBOAP with averages of 4.5 ± 0.22 L/L-day and 4.3 ± 0.37 L/L-day respectively. COD conversion for ROBOAP was considerably higher than NBOAP, with the highest removal percentage of 83.9 ± 1.34% at 2 g/L-day for ROBOAP, while NBOAP only had a removal percentage of 49.2 ± 5.20%. However, ROBOAP had some characteristics that NBOAP did not when diluting for use in MECs. ROBOAP has significantly higher initial COD concentration, more than an order of magnitude larger than NBOAP. Thus, it required more dilution than NBOAP. For both substrates, precipitation occurred during storage, which may have resulted in a loss of trackable COD. Additionally, precipitation occurred when stock COD was diluted. Both instances of precipitation may have resulted in injected stock COD that may have been overestimated as a result of organic losses during dilution that were not accounted for. This would also explain the trends observed with anode Coulombic efficiency for ROBOAP, where anode Coulombic efficiency traditionally decreases in this reactor configuration as continuous substrate loading increases (shown in the previous chapters). Additional MEC analysis in this dissertation that uses ROBOAP accounts for this loss by filtering the diluted stock and reanalyzing COD from the used stock.

The takeaway is the same, even with unaccounted organics potentially being lost, high performance can be achieved from two similar but independent feedstocks with minimal adaptation time. This concept was shown with more rigor in Chapter II (which occurred

chronologically later), however this further supports the notion discussed there. To further confirm that the design was suitable as a high performing lab scale system, comparisons to other tests are useful. Table 17 shows additional performance comparisons to other feedstocks for relevant productivities at the time these two substrates were tested.

Table 17: MEC performance for studies using complex substrates as feed. The units for current density are A/m^2, unless specified otherwise. CE: Coulombic efficiency

Substrate	**Current density,[#] A/m^2**	**Hydrogen productivity, L/L-day**	**Operating conditions and efficiency**	**Reference**
Sugar beet fermentation effluent	3.6	0.24	Batch study, substrate loading ~ 8 g/L	[10]
Milk	150 A/m^3	0.93	Batch study, CE = 52%	[11]
Cellulose				[12]
Vinasse residue from sugar beet	3.85	0.066	Batch study, MEC substrate derived from fermentation effluent, CE = 74.1%	[13]
Papermill wastewater	2.2	0.0096	Batch study, MEC substrate derived from fermentation effluent, CE = 32.3%	[13]
Spent yeast with ethanol	222 A/m^3	2.2	Batch study, Ethanol necessary as a co-substrate	[14]
Pig manure	2.5	N/A	MEC coupled to anaerobic digester, CE = 8%	[15]
BOAP	4.5	4.3	Continuous loading, 10 g/L-day	[4]
Corn stalk fermentation effluent	480 A/m^3	4.5	Batch study, substrate loading = 8.84 g/L	[16]
NBOAP	5.3	4.3	Continuous loading, 10 g/L-day	This work
ROBOAP	4.6	4.5	Continuous loading, 10 g/L-day	This work

As shown in the Table 17, the literature at the time showed that this MEC outperformed many other systems reported for both preliminary substrates tested, including those using complex substrates such as biomass-derived liquids or biomass polymers. Since then, MECs using corn stover fermentation effluent have achieved larger current densities [17], but that substrate is exceptional for biomass feedstocks and is not the norm. Further comparisons were

also made in Chapter IV, which suggested that this MEC configuration outperformed other substrate types used in other configurations. The same conclusion can be drawn here. Most of the references in the table report hydrogen productivities below 1 L/L-day. One exception was a study conducted using corn stalk-derived substrate (fermenter effluent) which reported a hydrogen productivity of 4.52 L/L-day [16]. Li et al.'s study was, however, conducted under batch operating conditions with a high substrate loading of 8.84 g COD/L, of which approximately 3.1 g/L was acetate. In comparison, this study was conducted as a semi-continuous operation with continuous feeding of the substrate. This resulted in the total substrate concentration fed into the MEC being much lower, which eventually increased to about 0.86 g/L after 3 days of operation for both substrates. Despite the significantly lower substrate loading, the hydrogen productivity obtained in this study was almost similar to that reported by Li et al. [16]. The total substrate conversion achieved in the MEC is an important factor, if the end goal is to efficiently achieve water treatment in addition to hydrogen production. The use of spent yeast as a solid/slurry feed has been reported recently, which yielded a hydrogen productivity of 2.2 L/L-day [14]. This is an important advancement considering that a pretreatment was not used, and the spent yeast cells were directly fed into the MEC. Addition of a co-substrate (ethanol) was, however, reported to be necessary to achieve this high productivity, functioning as a quasi-pretreatment. By comparison, none of the substrates used in the MECs described here required pretreatment beyond filtration.

Compound Degradation in MECs

Removal percentages for nearly all the compounds were quite high, exceeding or being close to 80% in most instances. Figure 28 shows the individual compound degradation determined by HPLC associated with each substrate.

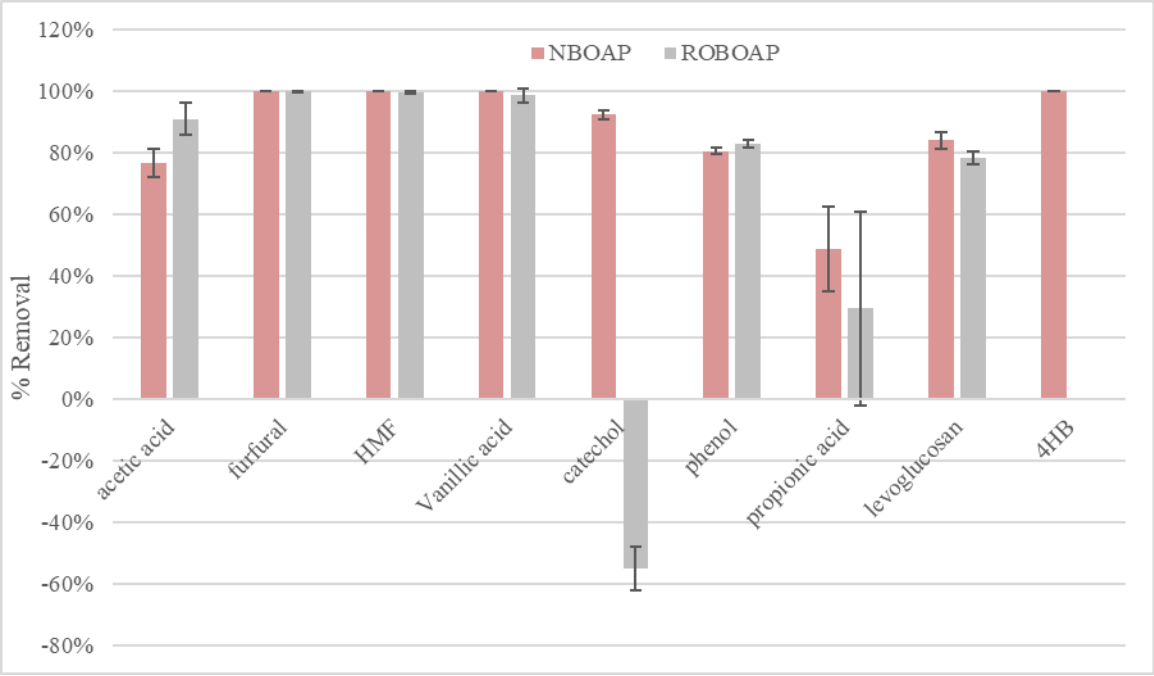

Figure 28: Compound degradation percentages associated with MEC operated on NBOAP and ROBOAP at 10 g/L-day. Note that catechol accumulated in ROBOAP but did not for NBOAP. Abbreviations include 5-hydroxymethylfurfural (HMF) and 4-hydroxybenzaldehyde (4HB).

However, there are a few observations and differences that are worth discussion. First, while precipitation occurred for these substrates while in storage and for dilution, none of the compounds identified would precipitate upon dilution, suggesting that the concentrations delivered, and the degradation percentages remained unchanged. Of the percentages removed, there are some instances that may appear unusual. Removal of acetic acid for NBOAP was lower than for ROBOAP, where NBOAP reached a removal percentage of 76.4 ± 4.58% versus 90.9 ± 5.31% for ROBOAP. Even though NBOAP's removal rate for acetate appears low, this is still comparable to the removal rates shown previously with TGRP PyAPs and switch grass BOAP [4, 18], as well as prior chapters. As discussed in Chapter II, acetate is an intermediate product in MECs, including those found in MECs, so it not being completely degraded is expected. The

same can also be said for several of the other compounds detected here, specifically notably catechol and phenol, which are not only intermediates, but can be inhibitory to MEC performance [19, 20]. Much like switch grass BOAP, the substrate recalcitrance is most likely the cause of the less than ideal performance. However, Coulombic efficiencies for both of these substrates suggest that a significant fraction of COD was diverted elsewhere. The next chapter will expand on one cause for this loss in efficiency: compound adsorption.

Pretreatment is not desirable, but may be a necessity for use in MECs, where waste products must be solubilized or neutralized first. Here, the substrates contained primarily water-soluble fractions, but this is largely untrue for other wastes. More porous anode materials may allow for substrates with insolubilized fractions to be used in MECs without risk of clogging the reactor, although additional porosity may compromise total biofilm forming potential, limiting degradation rates. Further, insoluble compound degradation rates are contingent on available organic particle surface area, an additional constraint regularly solubilized organics do not have. Emulsification of insolubilized wastes may also be a useful strategy; however emulsified substrates are rarely tested in MEC systems despite this strategy being deployed regularly in other bioremediation practices, such as with dispersants for use in oil spills. Improving substrate accessibility by using energy efficient pretreatment, or by identifying renewable complex sources that do not require pretreatment before MEC introduction, will be necessary to improve MEC technology viability.

Conclusions

This Chapter outlines conversion of additional substrates from Red Oak BOAP and a Neutralized BOAP. These substrates that were processed using the same starting inoculum. Red

Oak BOAP-fed had an average current density of 4.6 ± 0.03 A/m^2 and NBOAP-fed MECs had an average current density of 5.3 ± 0.03 A/m^2 at 10 g/L-day Compared to the MECs fed substrates in previous chapters, these MECs produced similar average current densities at 10 g/L-day to the pyrolysis aqueous phase from willow, and also the HTL effluent from *Chlorella* sp. Thus, the performance was similar between these substrates. Unfortunately, the tests conducted on these two substrates did not include voltage data, which would have been useful for further investigation. Regardless of this shortcoming, the preliminary findings here will be necessary for selecting substrates in the following Chapter.

References

1. Pollard, A. S.; Rover, M. R.; Brown, R. C., Characterization of bio-oil recovered as stage fractions with unique chemical and physical properties. *Journal of Analytical and Applied Pyrolysis* **2012,** *93*, 129-138.
2. Mohan, D.; Pittman, C. U.; Steele, P. H., Pyrolysis of wood/biomass for bio-oil: a critical review. *Energy & fuels* **2006,** *20*, (3), 848-889.
3. Rover, M. R.; Johnston, P. A.; Whitmer, L. E.; Smith, R. G.; Brown, R. C., The effect of pyrolysis temperature on recovery of bio-oil as distinctive stage fractions. *Journal of Analytical and Applied Pyrolysis* **2014,** *105*, 262-268.
4. Lewis, A. J.; Ren, S.; Ye, X.; Kim, P.; Labbe, N.; Borole, A. P., Hydrogen production from switchgrass via an integrated pyrolysis–microbial electrolysis process. *Bioresource Technology* **2015,** *195*, 231-241.
5. Kim, P.; Johnson, A.; Edmunds, C. W.; Radosevich, M.; Vogt, F.; Rials, T. G.; Labbé, N., Surface Functionality and Carbon Structures in Lignocellulosic-Derived Biochars Produced by Fast Pyrolysis. *Energy & Fuels* **2011,** *25*, (10), 4693-4703.
6. Park, L. K.-E.; Ren, S.; Yiacoumi, S.; Ye, X. P.; Borole, A. P.; Tsouris, C., Separation of Switchgrass Bio-Oil by Water/Organic Solvent Addition and pH Adjustment. *Energy & Fuels* **2016,** *30*, (3), 2164-2173.
7. Ren, S.; Ye, X. P.; Borole, A. P., Separation of chemical groups from bio-oil water-extract via sequential organic solvent extraction. *Journal of Analytical and Applied Pyrolysis* **2017,** *123*, 30-39.
8. Mikhaylin, S.; Bazinet, L., Fouling on ion-exchange membranes: Classification, characterization and strategies of prevention and control. *Advances in Colloid and Interface Science* **2016,** *229*, 34-56.
9. Ying, T.-Y.; Yang, K.-L.; Yiacoumi, S.; Tsouris, C., Electrosorption of ions from aqueous solutions by nanostructured carbon aerogel. *Journal of colloid and interface science* **2002,** *250*, (1), 18-27.
10. Dhar, B. R.; Elbeshbishy, E.; Hafez, H.; Lee, H.-S., Hydrogen production from sugar beet juice using an integrated biohydrogen process of dark fermentation and microbial electrolysis cell. *Bioresource Technology* **2015,** *198*, 223-230.
11. Montpart, N.; Rago, L.; Baeza, J. A.; Guisasola, A., Hydrogen production in single chamber microbial electrolysis cells with different complex substrates. *Water Research* **2015,** *68*, 601-615.
12. Lusk, B. G.; Colin, A.; Parameswaran, P.; Rittmann, B. E.; Torres, C. I., Simultaneous fermentation of cellulose and current production with an enriched mixed culture of thermophilic bacteria in a microbial electrolysis cell. *Microbial Biotechnology* **2017**.
13. Marone, A.; Ayala-Campos, O. R.; Trably, E.; Carmona-Martinez, A. A.; Moscoviz, R.; Latrille, E.; Steyer, J.-P.; Alcaraz-Gonzalez, V.; Bernet, N., Coupling dark fermentation and microbial electrolysis to enhance bio-hydrogen production from agro-industrial wastewaters and by-products in a bio-refinery framework. *International Journal of Hydrogen Energy* **2017,** *42*, (3), 1609-1621.
14. Sosa-Hernandez, O.; Popat, S. C.; Parameswaran, P.; Aleman-Nava, G. S.; Torres, C. I.; Buitron, G.; Parra-Saldivar, R., Application of microbial electrolysis cells to treat spent yeast from an alcoholic fermentation. *Bioresource Technology* **2016,** *200*, 342-349.

15. Cerrillo, M.; Viñas, M.; Bonmatí, A., Unravelling the active microbial community in a thermophilic anaerobic digester-microbial electrolysis cell coupled system under different conditions. *Water Research* **2017,** *110*, 192-201.
16. Li, X.; Zhang, R.; Qian, Y.; Angelidaki, I.; Zhang, Y., The impact of anode acclimation strategy on microbial electrolysis cell treating hydrogen fermentation effluent. *Bioresource Technology* **2017,** *236*, 37-43.
17. Satinover, S. J.; Schell, D.; Borole, A. P., Achieving high hydrogen productivities of 20 L/L-day via microbial electrolysis of corn stover fermentation products. *Applied Energy* **2020**, 114126.
18. Satinover, S. J.; Elkasabi, Y.; Nuñez, A.; Rodriguez, M.; Borole, A. P., Microbial electrolysis using aqueous fractions derived from Tail-Gas Recycle Pyrolysis of willow and guayule. *Bioresource Technology* **2019,** *274*, 302-312.
19. Zeng, X.; Borole, A. P.; Pavlostathis, S. G., Inhibitory Effect of Furanic and Phenolic Compounds on Exoelectrogenesis in a Microbial Electrolysis Cell Bioanode. *Environmental Science & Technology* **2016,** *50*, (20), 11357-11365.
20. Zeng, X.; Borole, A. P.; Pavlostathis, S. G., Biotransformation of Furanic and Phenolic Compounds with Hydrogen Gas Production in a Microbial Electrolysis Cell. *Environmental Science & Technology* **2015,** *49*, (22), 13667-13675.

CHAPTER VI

MICROBIAL ELECTROLYSIS ADAPTABILITY AND TAXONOMY ASSOCIATED WITH COMPLEX FEEDSTOCKS

This chapter has been derived from a manuscript in preparation for publication. Satinover, S. conducted the microbial electrolysis work, DNA extractions, 16S rRNA sequencing, as well as performed the analysis and wrote the chapter, making revisions suggested by coauthors. Rodriguez, M. Jr. assisted with High-Performance Liquid Chromatography. Campa, M.F. aided with DNA extraction, and sequencing. Hazen, T. provided equipment and supplies for 16S rRNA sequencing. Borole A. provided guidance and feedback on experiments, planning, data analysis, assisted in manuscript preparation and editing the drafts.

Abstract

Microbial electrolysis cells (MECs) are promising technologies because of their ability to convert aqueous wastes into hydrogen. However, the correlation between substrate composition intermediates generated and community structure has not been well established. Substrate adaptability is an important feature, seldom documented in MEC studies. This study used a high performing MEC capable of reaching over 10 L/L-day of hydrogen productivity using switchgrass-derived bio-oil aqueous phase, a complex feedstock. The four other substrates included a bio-oil aqueous phase from red oak, a corn stover fermentation product, an equal parts-by-COD mixture of phenol and acetate, and acetate. MECs were acclimated the substrates in sequence using a 1-week long adaptation period at an organic loading rate of 10 grams of Chemical oxygen demand (COD) per Liter of anode volume per day (g/L-day). The highest performing MEC fed with complex feedstock was the one using corn stover fermentation product, producing an average current density of 7.3 ± 0.51 A/m^2, although acetate-fed MEC outperformed the other conditions. 16S rRNA sequencing showed that community structure and community diversity were not predictive of performance, and replicate community structures

diverged despite identical inoculum and enrichment procedure. However, there were some qualitative trends that were common among replicates when substrates were transitioned, including an increase in the relative abundance of *Desulfovibrio* when red oak bio-oil aqueous phase was fed to MECs. *Geobacter* was the most dominant genus across all of the samples tested, but its abundance did not correlate strongly to current density. High-Performance Liquid Chromatography (HPLC) showed that acetate accumulated during open circuit conditions when MECs were fed with complex feedstocks and was quickly degraded once closed-circuit conditions were applied. The largest net acetate removal rate occurred when MECs were fed red oak bio-oil aqueous phase, at a rate of 2.93 ± 0.00 g/L-day. Principal component analysis found that MEC performance metrics such as current density, hydrogen productivity, and COD removal % were closely correlated. Net acetate removal was also found to correlate with performance. However, no genus correlated to performance metrics, and the analysis suggested that less than 70% of the variance was accounted for by the two components. This study demonstrates the robustness of microbial communities to adapt to a range of feedstocks, generating hydrogen at high productivities. MECs have potential to play a central role in the 21st century bioeconomy as factories producing a zero emission fuel.

Introduction

Microbial electrolysis cells (MECs) may pave the way for renewable hydrogen production, and have recently grown in popularity as a point of research. MECs have been applied to a number of different feedstocks, ranging from simple organic materials to complex wastes from industrial sources [1, 2]. Complex feedstocks will represent the most valuable substrates for MEC development, but MECs fed with complex feedstocks generally

underperform compared to those fed with simple substrates. While most of the biological understanding is gained via MECs fed with simple substrates, the role of biological specificity and functionality in MECs fed with a complex feedstock largely remains unknown. This can be important for understanding limitations of MECs using complex substrates and help develop new strategies for designing MECs.

Practical deployment of MECs will benefit from using a mature high performance community and simply adapting the community to new substrates, rather than regrowing the anode on new substrates. Few studies compare the changes in microbial performance associated with a mature anode felt that has adapted to a new substrate, and few studies show the differences in community structure that occur when MECs are transitioned from one substrate to another. Regardless of feeding regime, the body of knowledge on studies that compare the community and performance development when fed different substrates does not have a strong consensus. Chae et al., tested acetate, butyrate, propionate, and glucose in a microbial fuel cell (MFC). The authors concluded that *β-Proteobacteria* dominated acetate, butyrate, and glucose-fed MFCs, but *Firmicutes* dominated propionate-fed reactors [3]. The authors also showed that acetate-fed reactors produced less power density than glucose-fed reactors, but also had higher Coulombic efficiencies (72.3% when fed with acetate vs 15.0% when fed with glucose). Kiely et al. (2011a) showed that more diverse communities in MECs being fed dairy manure preformed worse than MECs fed with potato wastewater, which were less diverse [4]. Another study by Kiely et al. (2011b) investigated 1-year operated MFCs, and found that simple substrates including acetic acid, formic acid, lactic acid, succinic acid, and ethanol caused significant differences in community structure based on substrate [5]. Kiely et al. (2011b) also determined that succinic acid-fed MFCs had the highest diversity determined by Shannon index but also had the second worst

power density, reaching a maximum power density of 444 ± 12.5 mW/m^2. Sun et al. showed that the starting feeding regime can affect community diversity, as acetate-fed MFCs had less diversity and higher performance than MFCs that were fed with bioethanol effluent, even after acetate-fed MFCs transitioned to bioethanol effluent [6]. The authors also found that MFCs had more exoelectrogenic bacteria when fed with acetate than with bioethanol effluent.

Community structure may not be predictive of performance, as conflicting data exists. One of the earliest studies that tracked community development was conducted by Ruiz et al., claimed that starting inoculum plays a major role, but that it was not completely predictive [7]. The authors also mentioned that even with the same substrate concentrations and types (acetate and propionate) as well as the same starting inoculum, significantly different microbial communities developed. Miceli et al. showed that starting inoculum and the resulting community structure could result in high performance despite containing very different community members [8]. Sampling errors may also be playing a larger role in these studies, as community structure can be dependent on where the community is sampled in the reactor. Kim et al. used a tubular MFC fed with sucrose and found 80–90% similarity in species composition across replicates, but showed that significant changes in community structure occurred between the beginning and the end of the tubular MEC [9]. Using a compact MEC fed with complex feedstocks and starting with a selectively enriched community may produce more consistent results, although special differences will exist depending on substrate concentration and complexity. More recently, Lesnik and Liu used an artificial neural network to predict the community structure and performance by first inoculating MFCs, feeding them acetate, and then growing the reactors on different simple and complex substrates [10]. Cai et al then reversed this approach by predicting the substrate fed to reactors from identified community structures using different machine learning

algorithms, and found over 80% accuracy for four of the six algorithms [11]. The drive towards more automated design has been outlined by a review by Gadkari et al., who suggests that modeling bioelectrochemical systems (BESs) like MECs and MFCs will be necessary for more streamlined development [12]. This approach needs to be combined with recovering additional biochemical data on previously uncharacterized substrates, and further exploring the relationships between these input and output variables.

Complex wastes can be composed of hundreds of individual compounds with individual degradation pathways. There are some key compounds of importance, however. Starting compounds and intermediates in complex feedstocks' treatment often include volatile fatty acids (VFAs) and other organic acids. Acetic acid has been most often identified as a precursor to anaerobic digestion via acetoclastic methanogenesis. VFAs are also important commodity chemicals and reagents, which can be derived from lignocellulosic fermentation [13]. Because MECs often contain a consortium of microbes, organic acids can be produced *in-situ* in MECs fed with complex feedstocks, in addition to being delivered directly via the substrate. Perhaps the most desirable organic acid for MECs is acetate, as it is commonly used as a model substrate. It may be key to high performance. Recently, Lewis et al. showed that acetate accumulated in open circuit conditions for MECs operating on a complex feedstock [14]. Once closed-circuit conditions were applied, acetate quickly degraded. Other VFAs, like propionic acid, can be degraded in MECs but do so less efficiently [15, 16]. If acetate and other organic acids are critical to current production in MECs, then higher performing MECs should accumulate and degrade these compounds at faster rates, with acetate being the most important of the organic acids. However, compound transformation is not entirely represented by organic acids in MECs either. Phenol and catechol can accumulate as a result of biotransformation of other phenolics and furans in

MECs [17, 18]. Thus, documenting the utilization of the parent compounds as well as identification of intermediates must both be done to better understand the microbial metabolism at work.

MEC performance is highly dependent on the process parameters, which in turn dictates the biology in the anode. Optimizing operating parameters is essential to developing high performance MECs [19]. Early studies by Liu et al. showed that the applied voltage was integral to higher hydrogen productivities, where an applied voltage of 0.7 V produced nine times more hydrogen than at 0.3 V [20]. The authors also showed that MECs that had been operated as MECs from the start outperformed those that had been operated as MFCs before transitioning to an MEC. Providing sufficient energy to exoelectrogens in MECs is critical, as anode poising has been shown to improve MEC performance over applying a whole cell potential [21]. Hari et al. further supported this notion using MECs fed with propionate by poising the anode, where anode potentials of 0 V vs SHE produced the highest hydrogen yields, current density, and Coulombic efficiency [22]. Mass transfer limitations must also be minimized. Improved mass transfer can be achieved by increasing the anode liquid flow rate in flow-through systems [23]. Finally, closing the distance between electrodes has also shown to improve MEC performance [24]. In order to advance MEC technology, integration of effective strategies discovered thus far is necessary. High performance systems can be developed by combining as many of the design and operating parameters as possible into one system [25, 26].

An advanced MEC incorporated with previously identified key design and operating parameters is important to obtain information relevant with any new study parameter. The goal of this study is to investigate the microbial diversity of MECs fed with complex feedstocks using MECs with previously demonstrated high performance. Thus, an MEC which previously reported a hydrogen productivity of17.9 L/L-day using a complex substrate derived from corn

stover [26] was used. The MECs were inoculated with the pre-developed community, grown to maturity, and adapted to five different substrates in a specific sequence and using a fixed adaptation period. Five substrates were selected that range from complex wastes to simple compound solutions. Electrochemical performance associated with the substrates, as well as chemical characterization, was determined to track utilization of key compounds and accumulation of intermediates. 16S rRNA sequencing was used to track the MEC community structure developed using each substrate. Finally, exploratory statistical analysis was used to find similarities associated with taxonomical classification, performance metrics, and compound removal/accumulation.

Methods

MEC Construction and Operation

MECs were constructed using two chamber designs elements previous described [26]. Two duplicate MECs were used in the experiments. Briefly, 1.5 in PVC pipe cut to 0.5 in was used for both anode and cathode chambers, which were pressed against polycarbonate plates and screwed tight to form a gas-tight seal. The anode was made of steam sterilized carbon felt prior to inoculation. A 1/8in stainless steel rod was used as the current collector and came in direct contact with the carbon felt. A Nafion 115 membrane separated the two chambers. 0.5 mg/cm^2 Pt deposited carbon was used as the cathode catalyst, which contacted a stainless-steel mesh for current collection. Cathode gas was collected using Viton hosing exiting the chamber into to a 250 mL inverted graduated cylinder. Anode media included trace vitamins and minerals originally described by Wolin et al. [27], more commonly known as Wolfe's mineral and vitamin solutions. In addition to vitamins, 5.8 mM ammonium chloride, 1.7 mM potassium chloride, was

added to media, along with 50 mM of phosphates using NaH_2PO_4 and Na_2HPO_4 to buffer the media to a pH of 7.25. Anode liquid media was replaced before every experiment. The media was recycled and flown through the anode using a peristaltic pump at a flow rate of 3.5 mL/min, where a total anode liquid media volume was 180 mL. Prior to experiments, cathodes were drained of accumulated catholyte and rinsed with deionized anaerobic water. No cathode buffer was used in any of the MECs, and accumulated catholyte was recycled back into the anode liquid media every 24 h.

MECs were operated by a Bio-Logic (Bio-Logic, Knoxville, TN) VSP potentiostat, and were operated as a three electrode assembly. Anodes voltages were poised using an Ag/AgCl reference electrode that was inserted into the anode chamber, contacting the anode liquid media and close to the anode for good contact between electrodes. MEC anodes were poised at -0.2 V versus standard hydrogen electrode for all experiments. Reference electrodes were changed bi-monthly in order to maintain proper poising potential. Whole cell voltage was recorded using a DATAQ (DATAQ Instruments, Akron, Ohio) DI-1100, which recorded the whole MEC voltage every minute. WinDAQ software provided by DATAQ using a Microsoft Windows operated computer was used to log the voltage applied to the reactors.

MECs were inoculated with a starting felt sample from a community that had been previously operated on switch grass BOAP described previously [28]. Felt inoculum was inserted in the anode chamber as a ¼ in core. Two cores from the BOAP-fed MECs, were inserted into the sterile felt in the new reactors by using a flame sterilized coring bit to remove felt from the mature anode felt and cut sterile felt for replacement. Inoculation was first conducted by opening the MECs in an anaerobic chamber. Additional inoculum from other operating reactors was supplemented to MECs by injecting anode nutrient media from other reactors into the entry port

of the anode. The reactors were fed a batch of 0.2 g/L glucose and acetate, and then 2 g/L-day BOAP. The organic loading was increased by an additional 2 g/L-day every 24 h until current no longer increased, or organic loading rate reached 10 g/L-day, representing a carbon ramp. Once current plateaued, anode liquid media was changed, and the ramp in organic loading was started again. Acetate and glucose were added in batches of 0.2 g/L sparingly to both reactors when current rise stalled, but was stopped once MECs reached 10 g/L-day.

Experiments were performed using 10 grams of chemical oxygen demand (COD) per liter of anode volume per day (g/L-day) for each substrate tested. The five substrates tested included a pyrolysis bio oil aqueous phase (BOAP) from switch grass [28], a pyrolysis bio oil aqueous phase from red oak (ROBOAP) [29], a corn stover fermentation product (CFP) [26, 30, 31], a blend of equal parts acetate and phenol by grams of COD (phe/ace), and acetate. Experiments were conducted over the span of 72 h for all substrates tested. 5 mL of sample was collected every 24 h for analysis. Following the 10 g/L-day experiments, MEC anode liquid media was tested for compound accumulation by operating the reactors in open circuit conditions for eight h. Closed circuit conditions discussed earlier in this section followed and were applied for the remaining 40 h for a total experiment time of 48 h. MECs fed with phe/ace were tested under an additional condition, where 2.3 g/L of phenol was added to the media before continuous experiments started. This concentration was shown to inhibit current production by 36% in MECs reported previously [18]. After 2.3 g/L, MECs were regrown using BOAP, and then transitioned to acetate using the carbon ramp described earlier in this section.

MEC Electrochemical Analysis

Electrochemical analysis was performed as previously described [26, 32]. Briefly, the performance metrics calculated included average current density, in units of Amps per meter of

projected surface area squared (A/m^2), Hydrogen productivity in units of liters of H_2 per liter of anode volume per day (L/L-day), and average voltage in V. Efficiency metrics included anode Coulombic efficiency, cathode conversion efficiency, the multiplication of these efficiency metrics to calculate hydrogen recovery, electrical efficiency, and overall energy efficiency. Hydrogen production rates were adjusted based on measurements from Gas Chromatography. COD used to calculate the electrochemical performance was measured using Hach high range COD vials and digested in a Hach DRB 200 for two h (Hach Company, Loveland, CO). Gas Chromatography (GC) was performed using a Thermo Focus GC (ThermoFisher, Waltham, MA) using a method described previously [26]. Samples were run on the instrument for 8 minutes using a HP-PLOT (Agilent Technologies, Santa Clara, CA) Molesieve 5A column. For continuous addition experiments, these metrics were calculated every 24 h and cumulatively. For open circuit experiments, these metrics were calculated for the first 8 h, the next 16 h during closed circuit conditions, and then the following 24 h, as well as cumulatively. For continuous addition experiments, an electron balance was conducted using the gas accumulated in the cathode and anode and the gas composition determined by GC. Henry's law was used to estimate the amount of methane present in the anode liquid media.

Analytical Chemistry of Substrates in MECs

High-Performance Liquid Chromatography (HPLC) was used to quantify compounds of interest using methods that have been previously described [32]. Briefly, two detectors and one column were used to detect compounds. A Shimadzu (Shimadzu, Torrance, CA) photo diode array (PDA) and a refractive index detector (RID) were used to detect compounds. The model for the PDA was an SPD-M20A, and the model number for the RID was a RID-20A. Both detectors were operated at 50 ºC. The RID was only operated under a single detection

wavelength, and the PDA was operated to detect the maximum value between 190-330 nm to represent the chromatograph. A Bio-Rad (Bio-Rad, Hercules, CA) Animex-87H was used as the HPLC column and was operated at 60 ºC for all samples and standards. 5 mM H_2SO_4 was used as the mobile phase, which was pumped at a flow rate of 0.5 mL/min for all samples. A 10% isopropyl rinse was used with every sample and a 5 mM acid blank was used every 5-6 samples in order to keep the instrument lines clean. Compound standards were prepared for each fresh batch of mobile phase at three different concentrations.

Compounds of interested were influenced from prior work [26, 32]. Compound classes included organic acids, phenolics, and furans. The PDA was used to identify furans and phenolics, while the RID was used to identify organic acids. Organic acids included acetic acid, propionic acid, and lactic acid. Phenolics included phenol, catechol, vanillic acid, and 4-hydroxybenzaldehyde. Furans included furfural and 5-hydroxymethylfurfural. All substrates were tested along with standard concentrations of compounds in order to determined starting and ending concentration of compounds. Removal was determined by calculating the amount added by syringe pump and recording the difference in concentration from what was expected to what was found in the anode media. Ion chromatography was also performed on all of the substrates to detect sulfate.

During closed circuit conditions, acetate gains and losses did not contribute to electricity production, while acetate removal during closed circuit conditions would have contributed to current production. To account for the total removal of acetate more accurately, either as it is delivered or created by biological transformation, a “total-removal” metric was established that took the difference of the rates of acetic acid removal observed during open circuit ($R_{A,CC}$) and closed circuit ($R_{A,OC}$) conditions:

$$R_T = R_{A,CC} - R_{A,OC}$$

Microbial Community Characterization

After each 10 g/L-day experiment for each substrate, a core was extracted from each reactor, and was replaced with a sterile felt core for the open circuit experiments. The faceplate on the anode had a hole and a rubber stopper press fit using a bracket and stainless-steel screws to allow easy access to the felt for sampling. When sampling occurred, the faceplate and rubber stoppers were removed in an anaerobic chamber. This core was then replaced again with another sterile felt core before transitioning to the next substrate. Felt samples for sequencing were stored at -75 ºC before DNA extraction. DNA extraction was performed using a QIAGEN (QIAGEN, Hilden, Germany) Powersoil Pro kit, following the procedure described with the kit. Prior to use in the kit, felt was thawed and cut into small pieces using a flame and ethanol sterilized blade before cell lysis. Quality assurance, quality control (QA/QC), and sequencing was then performed in line with previous studies [33-35]. The DNA was initially quantified and confirmed for sufficiency using a Nanodrop (ThermoFisher Scientific, Waltham, MA) Spectrophotometer. Once DNA was confirmed to be successfully extracted, Polymerase Chain Reaction (PCR) was then performed on 1-10 μL of extracted DNA. Amplicons were then initially visualized using a 1% agarose electrophoresis gel, which was operated at 60V for 60 minutes. This was followed by analyzing the amplicons using a Agilent Bioanalyzer (Agilent technologies Santa Clara, CA). Amplicons were then quantified using a Qubit fluorometer (ThermoFisher Scientific, Waltham, MA), and DNA was then run on a micro kit and using an Illumina MiSeq (Illumina, San Diego, CA). Digitized sequence data from the MiSeq was processed using Qiime2 [36] installed on a Linux Server. Genera level identification of sequences was determined using the Silva database [37-39].

Statistical Analysis

Linear regression was used to identify the correlation between current density and key organic acid removal rates, including acetic and propionic acid. Pearson correlations were also calculated in order to compare the average current density of the MECs with alpha diversity metrics: Choa1, Shannon, and Simpson indices. Principal component analysis (PCA) was used to track the similarity between variables documented, including relative OTU abundance of key microbes, current density, hydrogen productivity, COD removal, methane efficiency, and net acetate removal. PCA was conducted using SPSS software (IBM Corporation, Armonk, NY), and was rotated using Oblimin rotation.

Results and Discussion

Substrate Characterization

The three complex feedstocks tested contained some similar characteristics despite the differences in pretreatment used. All three complex feedstocks contained significant fractions of VFAs. The largest compound present in the complex feedstocks was acetic acid, which accounted for 16.2, 24.8 and 15.7% of the COD in BOAP, ROBOAP, and CFP respectively, as determined by HPLC. Propionic acid also represented a significant fraction of the feedstocks, at percentages of 3.2, 3.7, and 1.0% of the COD in BOAP, Red Oak BOAP, and CFP, respectively. Phenol was also detected between the substrates, where the concentration varied between 0.035 – 0.33% of the COD. However, there were also some differences among the substrates. CFP contained vanillic acid and lactic acid which represented 0.013% and 1.6% of the COD, respectively, and did not contain any furfural. HPLC was unable to confirm if lactic acid or vanillic acid were present. A more detailed characterization on the substrates is shown in the Appendix of this chapter. These differences are best explained by the treatment. The stage

fraction the ROBOAP was extracted from was designed to remove water and light oxygenated compounds [29], explaining the high concentration of acetic acid found in the substrate. In contrast, BOAP was extracted from a pyrolysis process that used only one fractionation [28], which did not select for any particular compounds. CFP, being a fermentation product of enzyme and acid hydrolysis, can have significant fractions of furans and phenolics [40-42]. However, the method used to prepare the CFP in this study did not demonstrate this previously [30, 31]. For this reason, the pretreatments were deemed sufficient to create different substrates from biomass.

Electrochemical Performance of Closed Circuit Conditions

CFP-fed MECs resulted in highest performance among complex substrates, producing an average current density of 7.3 ± 0.51 A/m^2, while the lowest performance came from BOAP-fed MECs, generating 4.7 ± 0.18 A/m^2. Correspondingly, CFP-fed MECs also had the highest hydrogen productivity of 7.3 ± 0.45 L/L-day, while BOAP-fed MECs produced the lowest hydrogen productivity of 4.7 ± 0.18 L/L-day. These findings agree with prior studies. where Lewis et al. reported a current density of 4.5 ± 0.22 A/m^2 and a hydrogen productivity of 4.3 ± 0.05 L/L-day with BOAP [28] while Satinover et al. reported achieving current densities of 6.8 ± 0.33 A/m^2 and a hydrogen productivity of 7.0 ± 0.50 L/L-day with CFP [26]. Figure 29 shows the trends associated with all the substrates tested.

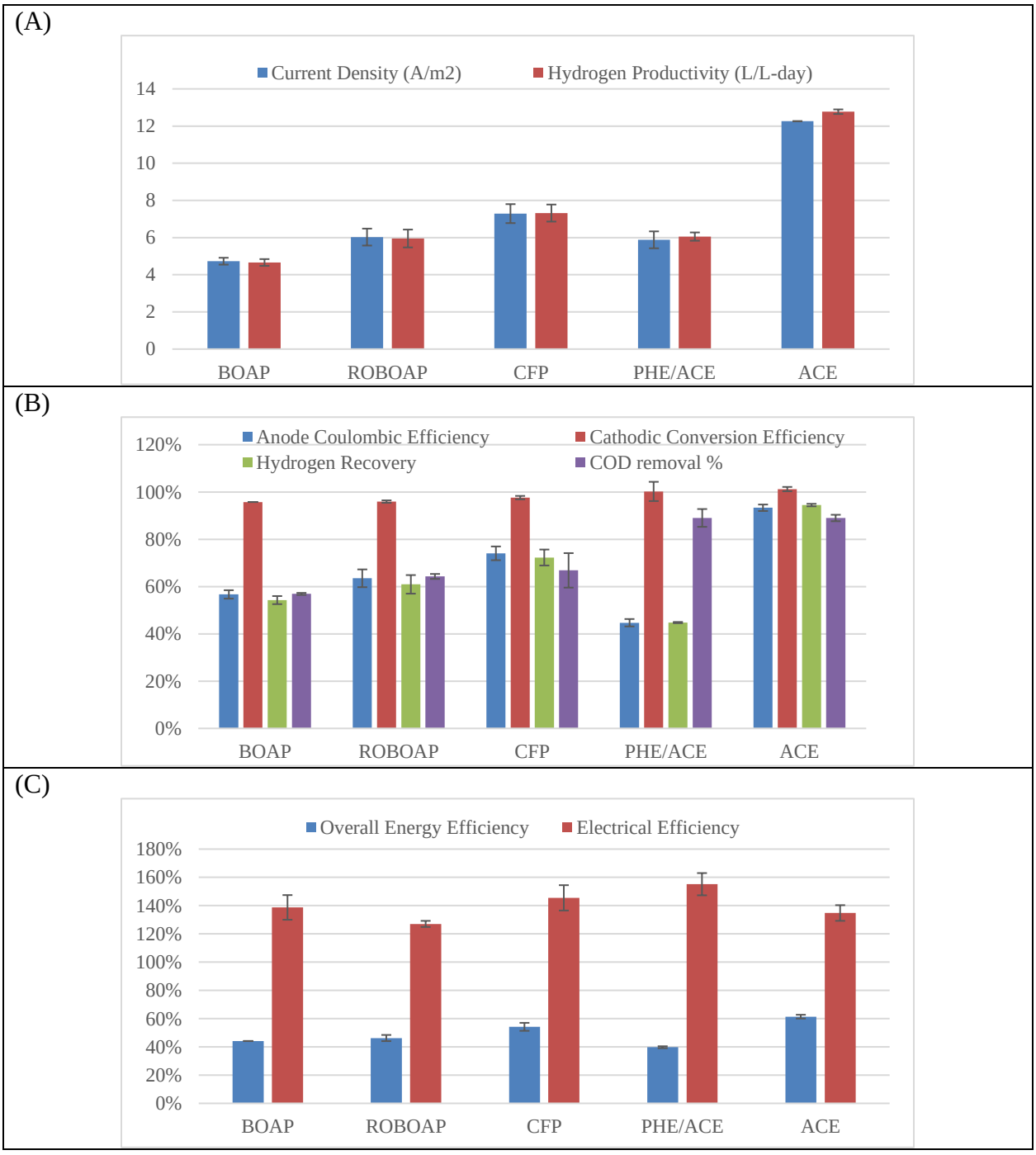

Figure 29: Electrochemical performance of MECs fed 10 g/L-day of each substrate. Substrates includes BOAP, Red Oak BOAP (ROBOAP), Corn stover fermentation product (CFP), equal fractions by COD of phenol and acetate (PHE/ACE) and acetate (ACE).

Acetate-fed MECs achieved the highest current density among all, reaching 12.3 ± 0.007 A/m^2 and a hydrogen productivity of 12.8 ± 0.12 L/L-day. Current density and hydrogen productivity were observed to be linearly correlated with organic loading rate. The linear relationship between current density and hydrogen productivity is shown in the Appendix of this chapter. Prior studies have shown similar correlations between organic loading and hydrogen productivity up to an organic loading rate of 10 g/L-day using biomass pyrolysis aqueous phase [28, 43, 44], and up to 30 g/L-day using corn stover fermentation product [26]. This relationship occurred despite unique characteristics of the substrates, which will be discussed in the next section, and rapid adaptation times.

Anode Coulombic efficiency varied more considerably from substrate to substrate, which was lowest when phe/ace was fed to MECs, reaching 44.7 ± 1.56%. Coulombic efficiency was highest for acetate-fed MECs, reaching 94.5 ± 1.37%. Of the complex feedstocks, CFP-fed MECs produced the highest Coulombic efficiency, while BOAP-fed MECs produced the lowest. This likely caused the variance in hydrogen productivity observed as well (Figure 29(B)). Overcoming all the complexities of the substrate delivered in order to produce current represents a challenge. Because cathode conversion efficiency was less effected by substrate used here, cathode catalysis was not the largest limiting factor in MEC performance, but rather the anode's ability to efficiently degrade organics.

Because the catholyte was regularly recycled back into the anode, pH adjustment was not required for acetate-fed MECs. Interestingly, NaOH addition was required for all other substrates in addition to catholyte recycling. Addition ranged from 0.2 mL every 24 h to 0.5 mL of 5M NaOH, equivalent to adding approximately 14 mM/day of NaOH in order to maintain neutral pH. Substrate conversion therefore contributed to proton accumulation that cannot be used for

hydrogen production, even with ideal mass transfer. Using an example, anaerobic acetogenic fermentation from glucose follows the overall reaction:

$$C_6H_{12}O_6 \rightarrow 3CH_3COOH$$

Similarly, dark fermenters that convert glucose to acetate perform the following reaction:

$$C_6H_{12}O_6 + H_2O \rightarrow 2CH_3COOH + 2CO_2 + 4H_2$$

The acetate produced by dark fermentation is then metabolized via the exoelectrogens and MEC cathode to drive the reaction:

$$CH_3COOH + 2H_2O \rightarrow 2CO_2 + 4H_2$$

Without a buffer, CO_2 reacts with water to form carbonic acid, which continues to lower the pH of the anode liquid media. The drop in pH caused by carbonic acid accumulation can be overcome partially by degassing the anode liquid media, which was not performed during the experiments, only at the beginning. However, while glucose can convert perfectly to CO_2 and H_2O in MECs, other metabolic processes may be occurring in MECs that do not oxidize perfectly. For these metabolic processes, protons will accumulate even if perfect proton transfer and conversion to hydrogen occurs. Buffer use and pH control in MECs will be a necessity for complex feedstocks for substrates that acidify upon degradation. For the complex feedstocks used here, pH adjustment would still be required for MECs even with ideal mass transfer.

Methane was also detected in the headspace of the anode ranging from 1.5 to 14.4%. The electron balance determined that methane accumulation was largest in MECs fed with ROBOAP, representing 14.4 ± 1.93% of the electrons extracted from COD. These results are shown in Figure 30.

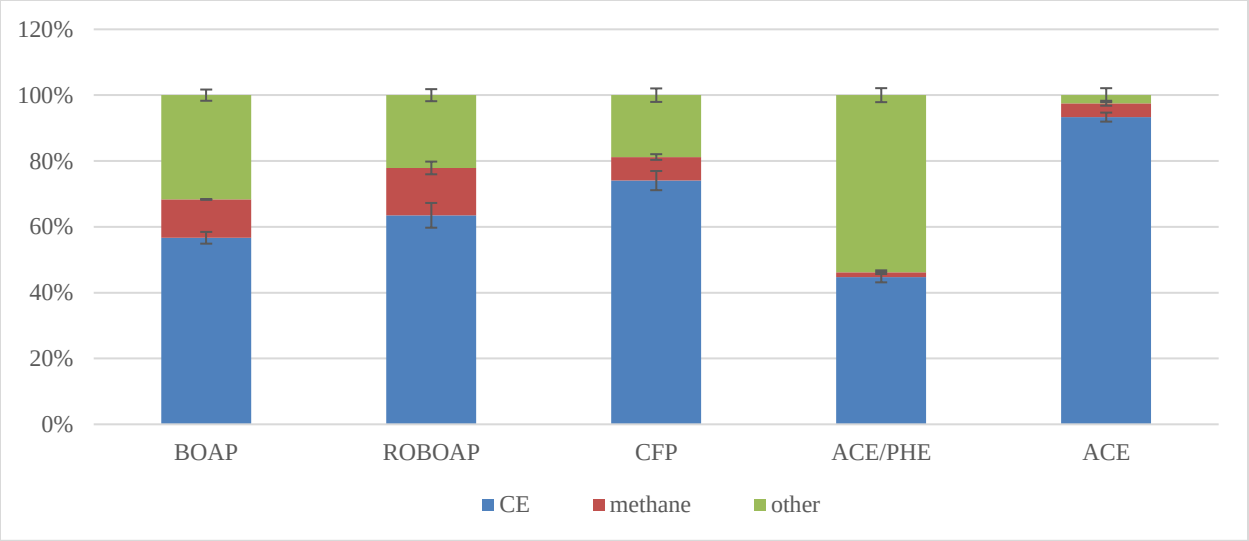

Figure 30: Electron balance results showing the percentage of COD that corresponded to electrons that contributed to current (CE), methane, or other sinks.

The phe/ace-fed MECs showed the largest diversion of electrons to unknown sinks, representing 53.8 ± 2.13% of the total converted COD. Acetate-fed reactors would had very little of the substrate diverted to other sinks (2.5 ± 2.12% towards other electron sinks). Undefined sinks have been attributed to extracellular storage by Freguia et al. by pulsed substrate addition [45]. It is possible that phe/ace fed MECs diverted more of the substrate to storage. However, HPLC showed that another mechanism was taking place: substrate adsorption. This will be discussed in the following section. Acetate-fed reactors also diverted less of the of the degraded COD's electrons to methane (4.2 ± 0.75%) than any of the complex feedstocks. This is further demonstrated by the high Coulombic efficiencies obtained in acetate-fed MECs. This suggests that acetate was minimally converted to methane via acetoclastic methanogenesis. The results from the taxonomical classification and the analytical chemistry will help improve the understanding on where this methane may have originated from for the complex feedstock fed MECs.

Electrical efficiency ranged between 127.1 – 155.2% for all of the substrates tested, with ROBOAP-fed MECs producing the lowest electrical efficiency, and phe/ace-fed MECs producing the highest. By contrast, overall efficiency was highest for acetate-fed MECs at 61.4 ± 1.34%, and lowest for phe/ace-fed MECs at 39.8 ± 0.67%. This difference in overall energy efficiency is largely determined by the COD removal percentage and the anode Coulombic efficiency. Because the Coulombic efficiency of the phenol acetate experiments was also lowest despite high COD removal percentages (89.0 ± 3.76%), this translated to a smaller overall energy efficiency. Acetate-fed MECs not only converted high percentages of total COD (89.9 ± 3.77%) but also had higher Coulombic efficiencies as discussed earlier. Combined with the results discussed in the electron balance (Figure 30), it is apparent that the substrate conversion efficiency largely dictated the overall energy efficiency of the MECs.

High-Performance Liquid Chromatography of Closed Circuit Conditions

Nine different compounds were quantified via HPLC to understand the conversion of the substrates. Acetate was removed above 75% for all substrates tested, and removal percentage increased with time. Figure 31 shows these trends for each of the compounds tested.

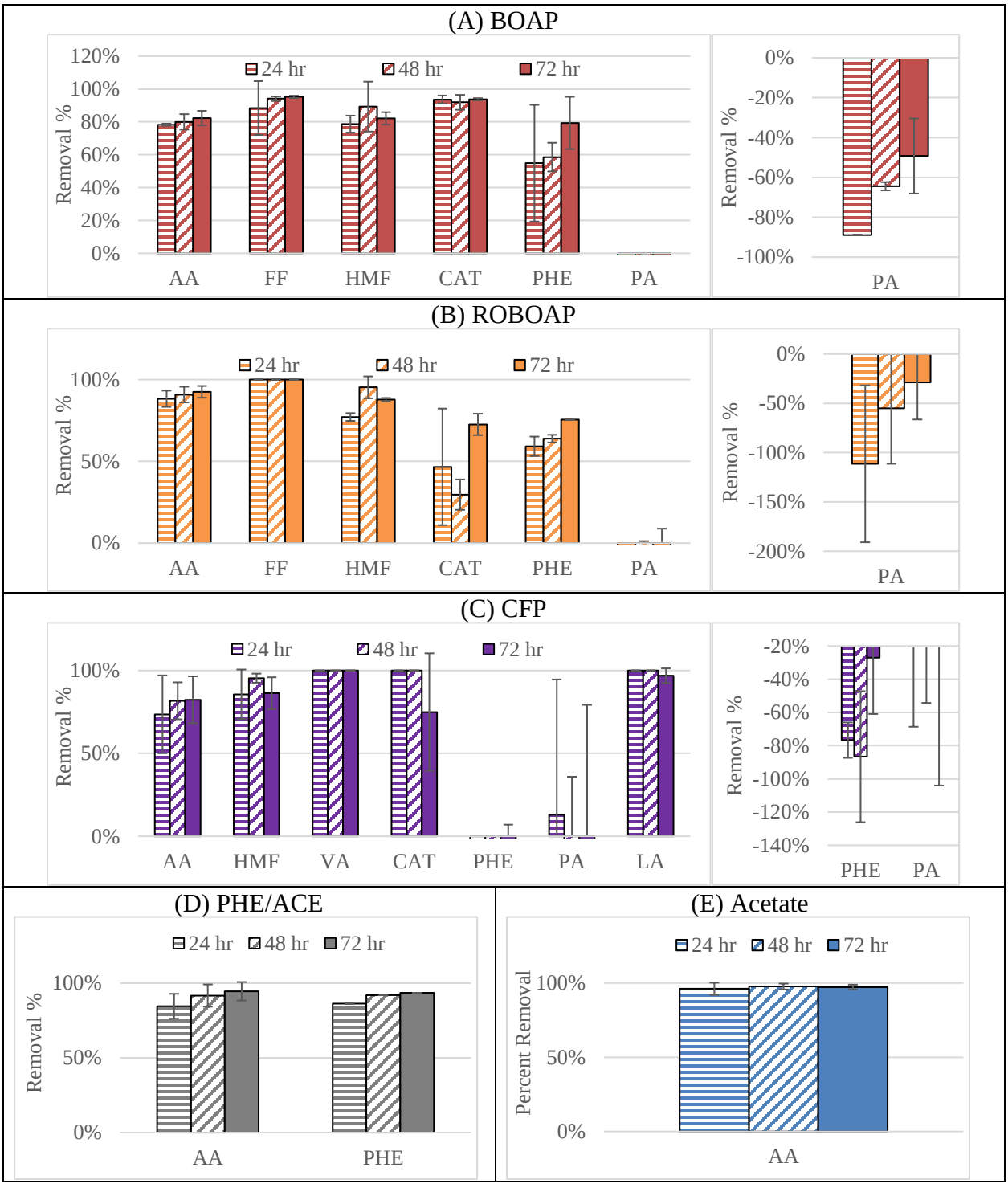

Figure 31: Compound removal of MECs fed 10 g/L-day of each substrate. Substrates includes BOAP, Red Oak BOAP (ROBOAP), Corn stover fermentation effluent (CFP), equal fractions by COD of phenol and acetate (PHE/ACE) and acetate (ACE). Compounds include Acetic acid (AA), Furfural (FF), 5-hydroxymethylfurfural (HMF), Catechol (CAT), Phenol (PHE), Propionic Acid (PA), and Lactic Acid (LA).

Propionic acid accumulated for the substrates tested, with the lowest percentage of removal being -111.3 ± 79.6% for ROBOAP-fed MECs after the first 24 h. Its accumulation decreased to -28.8 ± 37.6% as the experiment progressed. A similar trend was observed with BOAP-fed MECs, while in CFP-fed MECs the accumulation decreased only after 72 h. Propionic acid is a potential intermediate in the metabolism of complex substrates. The initial accumulation of propionic acid indicates that there was a delay in starting its metabolism in these MECs. Further, the communities also did not have as high a capacity to degrade propionic acid as reported in prior studies. Lewis et al. reported propionic acid degradation percentages above 60% using the same switchgrass BOAP feedstock [28]. How it accumulates or degrades in MECs operated on complex feedstocks is not well understood. These results show that propionic acid accumulation is largely contingent on the substrate type and the community. Microbes found in our MECs might be more prone to produce propionic acid for ROBOAP than for BOAP, for instance, but the compounds and microbes that are responsible for these differences have not been determined.

During acetate closed-circuit experiments, phenol appeared in anode liquid media of acetate-fed MECs in concentrations of 5.29, 7.64, and 9.98 mg/L at 24, 48, and 72 h in the anode liquid media respectively. Because no phenol was added to the MEC during this experiment, this finding suggests that phenol adsorbed to the felt, which systematically removed it from the liquid media without converting it directly to electrons. Much of this adsorbed phenol likely came from the 2.3 g/L phenol batch addition experiment conducted before the experiments with acetate. Even with a recovery period afterwards that was more than three weeks long, and conducted with three anode liquid medium replacements, phenol was still apparent in the anode liquid media. Scaled to the anode volume, this represents an approximate maximum desorption rate of 43.8 mg/L-day. Phenolic compound adsorption to porous carbon materials like activated carbon is

well documented [46], and is not unheard of in BESs. Hejazi et al. capitalized on phenol adsorption for use in a granular activated carbon anode in an MFC, and achieved a removal efficiency of 95% after 72 h, and reached a Coulombic efficiency of 45.77% [47]. Zhang et al. also suggested that phenol adsorption occurred when fed to their BES, which achieved more than 95% removal of phenol and Coulombic efficiencies as high as 27.3% [48]. While the MECs used here did not use activated carbon, we did observe a similar removal percentage of phenol with the phe/ace-fed MECs, reaching a removal percentage of 93.5 ± 0.08% in 72 h. Other studies that have experimented with phenol-fed BESs have found Coulombic efficiencies lower than 10% [49, 50]. In this study, the Coulombic efficiency for phe/ace-fed MECs was below 45% despite HPLC suggesting that more than 90% of the phenol and acetate was removed after the experiment. Assuming acetic acid was the only compound that contributed to current in the phe/ace blend fed to the MECs, the acetic acid would have generated a Coulombic efficiency of 84.2 ± 1.00%. The MECs fed with acetate had higher Coulombic efficiencies than this, reaching 93.3 ± 1.37%. Thus, a significant fraction of phenol that was removed may not have contributed to current or was not degraded biologically.

It is also possible that other compounds that are removed at large percentages may also be adsorbing. Large removal percentages for some compounds, including vanillic acid, 5-hydroxymethylfurfural, and furfural, were observed for all substrates tested, exceeding 75%. Adsorption is electrode dependent. Furfural, 5-hydroxymethylfurfural, and vanillic acid, did not adsorb to carbon felt in MECs according to Zeng et al. (2015) [17]. By contrast, furans and phenolics have been shown to adsorb to activated charcoal that follow Langmuir and Freundlich isotherm models (R^2 > 80%) [51]. Adsorption without conversion would partially explain the lower Coulombic efficiencies in the complex feedstocks compared to acetate-fed MECs. It is possible

that the compounds detected besides phenol contributed to current only minimally regardless of the mechanism of removal. Zeng et al. (2018) performed an electron balance on MECs using phenolics including syringic acid, vanillic acid, 5-hydroxybenzoic acid, and found that only vanillic acid and hydroxybenzoic acid had electron equivalents that did not contribute primarily to current [52]. The compounds analyzed Zeng et al. (2018) would probably not be the only adsorbing compounds, as the total COD contributed by the phenolic compounds detected in the complex substrates represented less than 6% of the substrate COD according to HPLC. Even if they did not convert effectively, these compounds would not have a significant impact on performance. Other compounds present in these complex feedstocks were not tested but will need to be in future studies, as the implications for the functionality of the electrode material on BES performance are significant. Fermentation has been deemed limiting in MECs fed with BOAP [14], and this apparent limitation may be contributed by the immobilization of compounds adsorbed to the carbon felt.

16S rRNA Sequencing Results

The most dominant microbe genus on average was *Geobacter*, however the relative abundance of *Geobacter* was inconsistent when comparing replicates. Replicate B had significantly more *Geobacter* than replicate A under the substrates tested. In particular, when MECs were fed with acetate, replicate B had more than 84.97% of the population represented by *Geobacter*. Figure 32 shows the bar charts for the 16S rRNA sequencing.

*Figure 32:*16S rRNA sequencing of reactor replicates A and B. Reactor A and B had very different microbial compositions despite coming from the same inoculum source and being grown under identical conditions.

Geobacter is a commonly known exoelectrogenic genus, and while dominant in replicate B, it was not present at the same quantities in replicate A during complex feedstock operation despite observing similar performance between the replicates. The average relative abundance of

Geobacter in replicate A across all substrates tested was 14.3%, while it was 42.1% in replicate B. When fed with phenol and acetate, both replicates had significant *Geobacter* populations, reaching 34.6% of the OTUs in A and 25.4% of the OTUs in B. Based on these results, the current density was not found to correlate strongly with relative abundance of *Geobacter* (R^2 = 0.20). The results suggest that *Geobacter* is not entirely necessary for high performance MECs using complex substrates. Other OTUs were also not found to correlate to current density. Thus, the community composition is not a strong deterministic factor for electrochemical performance exclusively.

Similar conclusions were reported by Ruiz et al. [7] and Miceli et al. [8], which are now expanded to complex feedstocks using only a single inoculum source. The work here also suggests that the extent of diversity is not a good predictor of performance either, as relative OTU abundance did not correlate with performance for either reactor using any of the diversity metrics (Shown in Table 19 in the Appendix of this chapter). Low correlation between diversity and performance have been reported by Stratford et al., who showed that R values were consistently below 0.65 when correlating diversity and power density in MFCs fed with glucose [53]. The work here showed weak negative correlation coefficients using Shannon, Simpson, and Chao1 indices versus current density. Pearson correlation (R) values across both replicates were -0.28, -0.53, and -0.48 respectively. Data from acetate-fed MECs was seen to skew these results due to the high current density and variability between the replicates. When acetate fed MEC data was omitted, Pearson correlation coefficients changed to 0.05, 0.71, and 0.84 for Shannon, Simpson, and Chao1 indices respectively. Acetate results should not be ignored, as device performance was similar across the replicates despite their differences in community structure.

Therefore, these results suggest that alpha diversity is only marginally (if at all) predictive of current density in MECs fed with complex feedstocks, and therefore performance.

Even though the correlations between community structure and performance are not very strong, the 16S rRNA sequencing can still be useful in explaining the observations. Besides *Geobacter* sp., there are presence of other microbes that are worth discussion. *Robinsoniella* was present in significant quantities for both replicates and was largest represented when MECs were fed BOAP and CFP. The sequencing allowed for species identification of this genus, indicating that the *Robinsoniella* sp. was actually *R. peoriensis. R. peoriensis* has been shown to grow on several poly and monosaccharides, including, "amygdalin, arabinose, cellobiose, fructose, glucose, maltose, lactose, raffinose, starch, trehalose, xylan and xylose," according to Cotta et al. [54]. CFP had been shown previously to contain significant fractions of xylose and arabinose, and this microbe was also found in MFCs fed with the same substrate previously [26, 30, 31]. Lachnospiraceae, the family that *R. peoriensis* belongs to, was also found in MECs fed with BOAP [28]. Thus, these results are consistent with prior reports. Interestingly, *R. peoriensis* declined when MECs were fed ROBOAP, phe/ace, and acetate, to less than 2% of the relative OTUs. For acetate and/or phenol – fed MECs, this is expected, as there is little or no evidence to suggest that *R. peoriensis* is capable of using either phenol or acetate. None of the substrates were investigated for sugar content, and this suggests that ROBOAP did not have the sugars needed for *R. peoriensis* enrichment.

The next most abundant microbe was an unknown genus of *Paludibacteraceae*. The only identified genus of *Paludibacteraceae* is *Paludibacter,* which contains species that are fermenters that produces propionic acid and acetic acid [55, 56]. *Paludibacter* was also found in long tubular MFCs being fed sucrose [9]. This may explain the propionic acid accumulation

observed from the complex substrates in open circuit conditions. However, the final products of *Paludibacteraceae* are not the same as other fermenters found in these MECs. Dark fermentation, in particular, may also be taking place. Potential dark fermenters were also present in MECs. A strain of *Sphaerochaeta*, has been found to contain species that produce hydrogen from glucose fermentation, while it could also grow on other sugars including glucose, maltose, ribose, and xylose [57]. Sun et al. also determined that *Sphaerochaeta* was enriched (6% relative abundance) in MFCs fed with a phenol-rich complex feedstock, pyroligneous liquor, which removed 84% of the phenol delivered [58]. Together, this suggests that the *Sphaerochaeta* sp. found in the MECs used in this study may have produced hydrogen as a result of some of the phenolic degradation observed while consuming other sugars not detected here. Another potential dark fermenter is *Eubacterium* sp., which was also found in the highest abundances during ROBOAP feeding. Wallace et al. suggested that a species of *Eubacterium*, *E. pyrovativorans*, produced hydrogen from pyruvate and lactate, although growth on lactate was limited [59]. It has also been shown to use amino acids, as it is not saccharolytic [60]. For any of the dark fermenters detected, the MECs could enrich a co-culture of hydrogenotrophic organisms.

While *Geobacter* was the dominant exoelectrogenic genus observed, it was not the only exoelectrogenic genus detected. *Desulfovibrio* was also determined in significant quantities in this study, where it was more prominent when MECs were fed ROBOAP, exceeding 15% of the relative abundance among the replicates. Traditionally *Desulfovibrio* is a sulfate reducing bacteria, however a species of this microbe has been shown be exoelectrogenic without the need for sulfate [61]. Further, none of the fractions of the pyrolysis oil that the ROBOAP came from had high sulfur concentrations according to the study it was created from, where sulfur represented only 0.03% of the weight percentage as g/g-fraction of the oil [29]. The reason for this microbe's

enrichment likely stems from the source of carbon, where *Desulfovibrio* was preferentially enriched due to the carbon available.

Methanogens were also present in significant relative abundance but were not primarily represented by acetoclastic methanogens. *Methanobrevibacter* was found to be the most abundant methanogenic genus across all substrates tested, and whose population varied considerably depending on the replicate observed. In replicate A, *Methanobrevibacter* was most prominent in MECs fed with acetate (21.2% relative abundance) as well as when fed phe/ace, while in B *Methanobrevibacter* represented 7.4% during acetate and phenol feeding, but less than 2% when fed with acetate. *Methanobrevibacter* has species that produce methane from hydrogen, such as *M. smithii*, which is often studied due to its presence in humans [62]. The source of this hydrogen could come from several places but is unlikely to be primarily from back diffusion from the cathode. The cathode conversion efficiency exceeded 95% across substrates, so only a small fraction of produced hydrogen would have been scavenged if this mechanism occurred. According to the electron balance (Figure 30), methane represented a much larger electron sink than what could be attributed to losses in cathode conversion efficiency (Figure 29(B)). Therefore, it is unlikely that hydrogen back diffusion was the primary cause of hydrogen scavenging. Rather, dark fermentation likely contributed to its enrichment. *Methanobrevibacter*'s presence is also unusual for acetate-fed MECs given how little methane was created from COD removal. For acetate-fed MECs, we would not expect such high abundances as seen in replicate A. It is possible that compounds such as phenol, which adsorbed to the felt, continued to contribute to the enrichment of this microbe even without additional carbon sources being provided.

Candidatus Methanoplasma was also found in large relative abundance, but only when MECs were fed ROBOAP. Unlike *Methanobrevibacter*, it is unlikely that *Candidatus Methanoplasma* can make methane from CO_2 and H_2 alone. This genus belongs to a group of microbes known as seventh order methanogens, which have been reported to be hydrogen dependent methylotrophs [63]. Methylotrophs consume compounds such as methanol, which was not investigated for any of the substrates or MEC effluents , however other methylated compounds have been reported in the oils the stage fraction the BOBOAP came from previously [29]. Thus, if methanol was created that promoted *Candidatus Methanoplasma* enrichment, it was likely an intermediate from higher order methylated compound degradation.

Operational effects were the same for all of the conditions tested, except for during the regrowth after the 2.3 g/L phenol addition experiments. During regrowth after the phenol addition, Replicate B struggled to recover. Several attempts to solve this included providing Replicate B with an addition of 0.2 g/L of acetate while being fed BOAP. Effluent and replicate A felt scrapings using a sterile wire was also injected into replicate B to supplement the underperforming community. Finally, the anode enclosure on replicate B was replaced during the carbon source ramp on acetate at 10 g/L-day, and only this caused current to be restored. It was possible that the connection between the stainless-steel electrode and the felt was compromised by the phenol addition. By replacing the stainless-steel rod, communities may have gained improved ability to respire on the anode, as current spiked above 30 mA once the anode closure was restored, before dropping to the current observed in replicate A after 24 h. The large representation of *Geobacter* during acetate feeding in replicate B may have been caused by some of these operation differences used to regrow the anode communities after batch phenol addition.

However, these differences in *Geobacter*'s relative abundance would not explain the other differences in community structure observed when MECs were fed the other substrates.

The results from the 16S rRNA sequencing demonstrate that the substrate has a definite impact on community composition, but it is not co-related with performance. The differences observed amongst replicates which were fed the same carbon source could be attributed to subtle differences in the MECs that are not well understood, as the initial growth procedures were identical amongst both replicates and the inoculum source was also the same. Gene expression is likely to be more important than community structure, but this requires more sophisticated 'omics techniques to reveal the function-based co-relations. The lack of necessity of a specific community composition to achieve a target performance could be a boon for advancing the MEC technology. Process conditions and design of MECs could be sufficient to achieve target performance utilizing the diversity of microbial communities without requiring the presence of a specific defined community.

Electrochemical Performance of Open/Closed Circuit Experiments

When the MECs were operated under open circuit conditions, only negligible amounts of hydrogen were produced, as expected. Performance after closed circuit conditions were reinstated were greater than the performance of the 72 h experiments but were similar to the 72 h experiments when the entire 48 h period of operation was analyzed. These trends are shown in Figure 33(A) and in Figure 33(B) respectively.

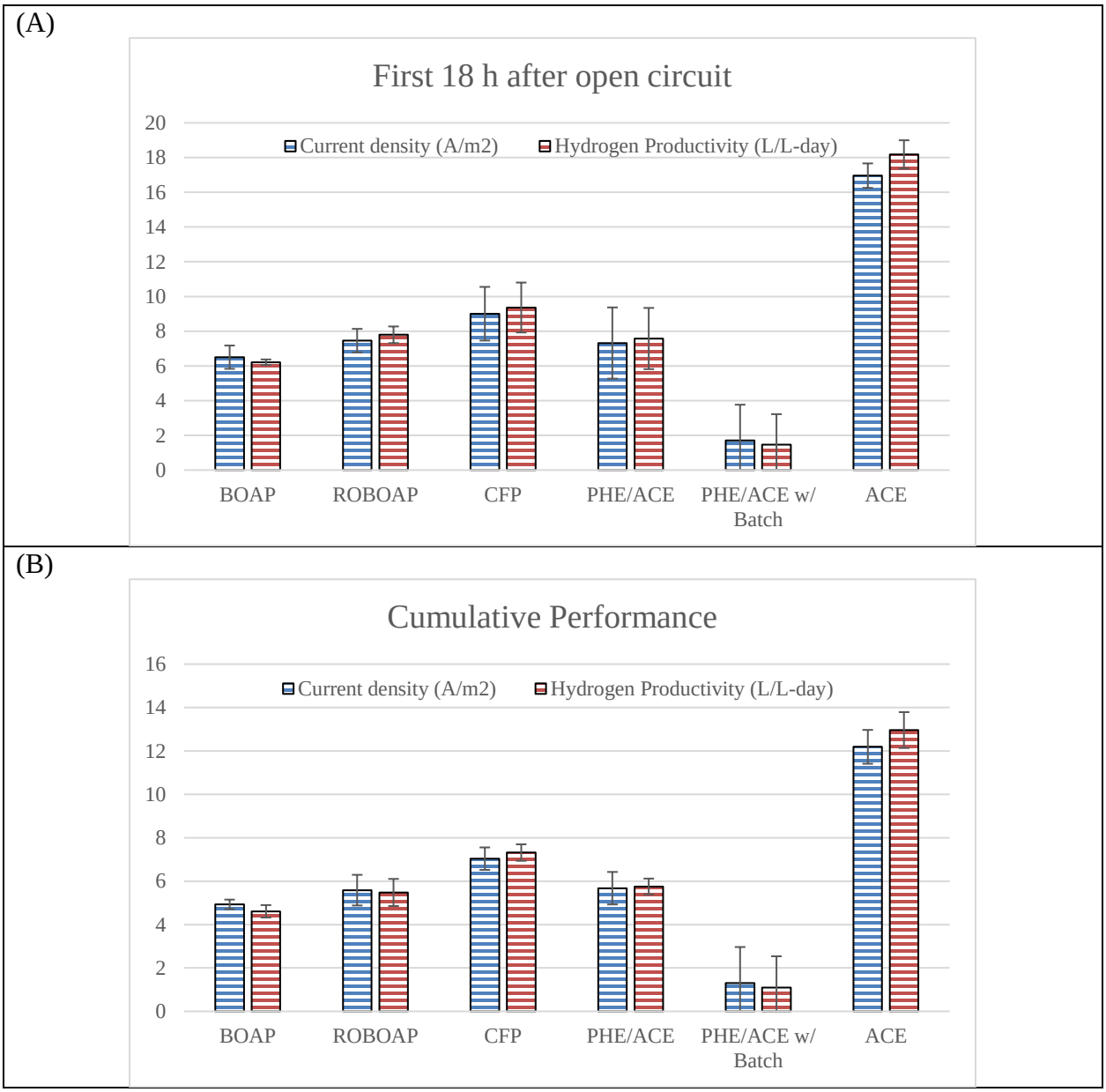

Figure 33: Electrochemical performance of MECs fed 10 g/L-day of each substrate 18 h after open circuit conditions (A), and the cumulative performance including the open circuit data (B). Substrates includes BOAP, Red Oak BOAP (ROBOAP), Corn stover fermentation effluent (CFP), equal fractions by COD of phenol and acetate (PHE/ACE), equal fractions by COD of phenol and acetate fed 2.3 g/L batch phenol and acetate (ACE).

Acetate-fed MECs had the largest performance, having an average current density of 12.2 ± 0.78 A/m^2 and an average hydrogen productivity of 13.0 ± 0.83 L/L-day, which is similar to the performances found in purely closed-circuit conditions. The worst performing occurred with

BOAP-fed MECs, which had an average current density and hydrogen productivity of 4.9 ± 0.22 A/m^2 and 4.6 ± 0.29 L/L-day. While the current density was slightly larger for BOAP, the error associated with the measurements suggests that the difference between the average current density and hydrogen productivity were not statistically different ($p > 0.05$). This was found to be true for the substrates tested. Therefore, upon applying closed circuit conditions, MECs continued to perform similarly.

Current density and hydrogen productivity were larger for the first 16 h of closed-circuit conditions than the average over the entire length of the experiment. The largest current density and hydrogen productivity was demonstrated by acetate-fed MECs at 17.0 ± 0.70 A/m^2 and 18.2 ± 0.81 L/L-day respectively. The lowest was demonstrated by BOAP-fed MECs, at 6.5 ± 0.67 A/m^2 and 6.2 ± 0.15 L/L-day for current density and hydrogen productivity respectively. This suggests that fermentation continued in the MECs without exoelectrogenesis of the intermediates generated, under the open circuit conditions. Once closed-circuit conditions were applied, exoelectrogenesis resumed removing the accumulated compounds, and generated current.

Fed-batch conditions were implemented to understand the phenol utilization in MECs. These MECs performed the worst of all the conditions tested after closed circuit conditions were applied, reaching average current densities and hydrogen productivities of 1.3 ± 1.66 A/m^2 and 1.1 ± 1.44 L/L-day, respectively. This is more than the 50% decrease in performance originally discussed by Zeng et al. (2016) at the same organic loading rate used here [18]. No improvement in performance was observed until an active recovery period with three media changes was conducted. The residual COD also did not decrease as much while operating, reaching a removal percentage of only 45.9 ± 3.9%. For comparison, phe/ace-fed MECs with phenol batch addition had a COD removal % of 84.6 ± 7.41%. Coulombic efficiency also suffered after 2.3 g/L batch

addition, dropping to 3.9 ± 4.83%. In these inhibited systems, neither phenol nor acetate contributed to current. Phenol most likely occurred and was observed in the following experiments due to the dosage used here. Phenol may have prevented a conductive pathway to the electrode as a result of adsorbance, which would further prevent exoelectrogenic metabolism. Alternatively, phenol may have simply inhibited the metabolism of exoelectrogens. Identifying the mechanisms of phenolic inhibition in MECs will improve MEC designs and operation of the future.

HPLC Results of Open/Closed Circuit Experiments

Acetic acid was the most represented compound in the complex substrates tested, and therefore deserves the most attention. The largest accumulation rate of acetic acid occurred when MECs were fed CFP, which accumulated at a rate of 1.7 ± 0.10 g/L-day, while ROBOAP-fed MECs accumulated the least amount of acetate at 0.8 ± 0.10 g/L-day. Figure 34 shows the additional results of this analysis.

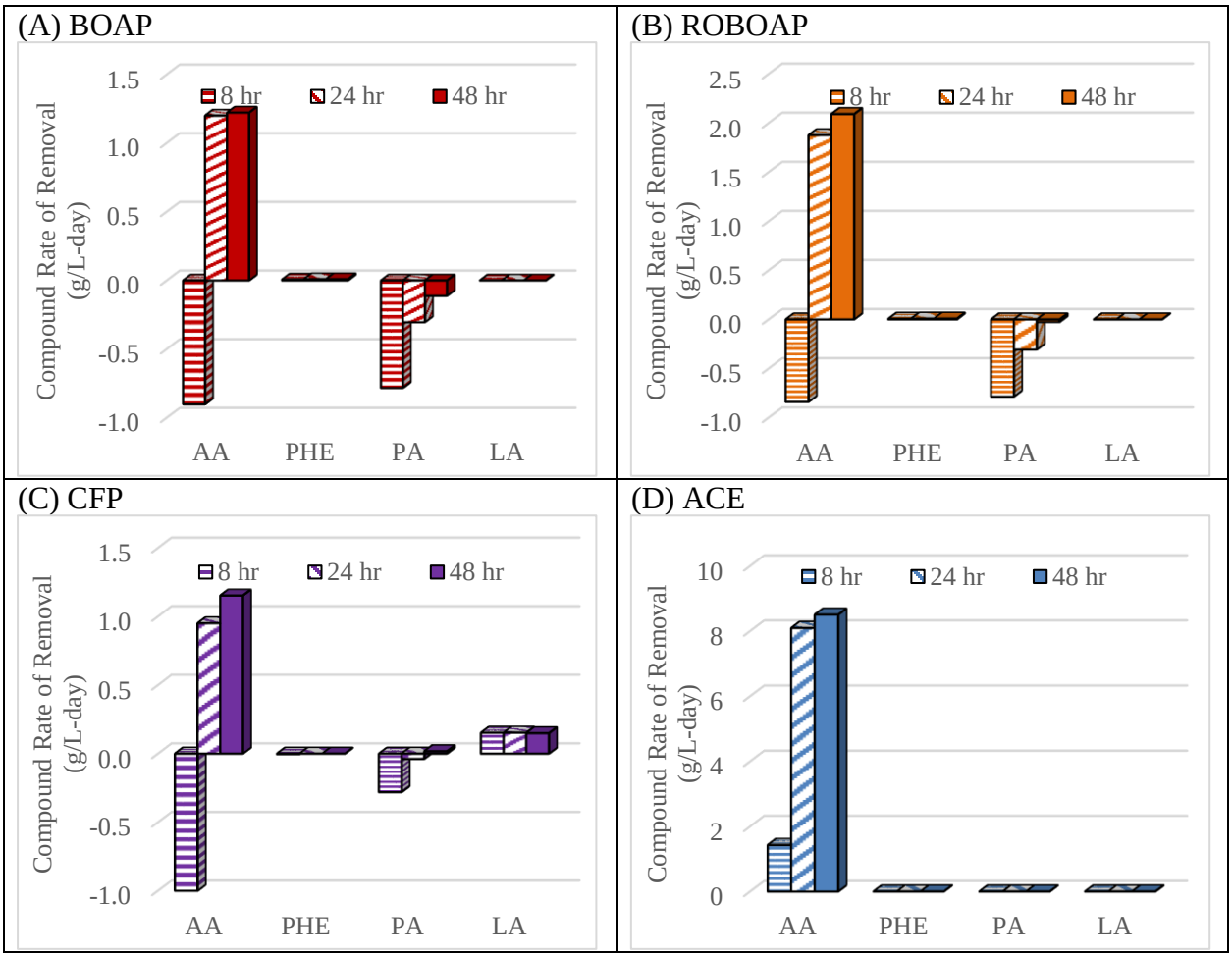

Figure 34: Compound accumulation and removal during open circuit conditions (8 hr) and during closed circuit conditions at 24 h and 48 h time points. Compounds tracked included acetic acid (AA), phenol (PHE), propionic acid (PA), and lactic acid (LA). Substrates documented included BOAP (A), ROBOAP (B), CFP (C), Acetate (D), and phe/ace blend (E). Figure 34(E) also includes the conditions where 2.3 g/L of phenol were added, labeled as batch.

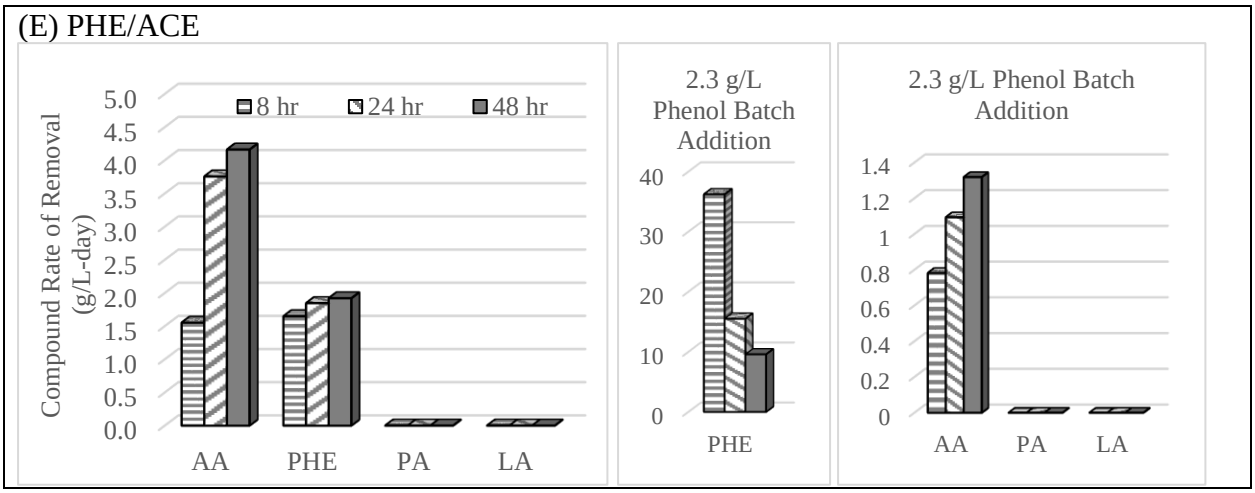

Figure 34 continued

The analysis performed here is not all encompassing, as not all the fermentable compounds were detected. As mentioned previously, the CFP used in this study was found previously to contain significant fractions of sugars such as galactose, xylose, and arabinose [26, 30, 31], which were not quantified here. Similarly, the BOAP was also found to contain levoglucosan, which was removed from anode liquid media in high percentages (above 90%) in a previous study [28]. The findings here suggest a much wider range of carbon sources that were not quantified in this study may have also contributed directly to exoelectrogenesis. However, acetate accumulation was clearly an important factor towards current production that cannot be dismissed. When MECs were switched to closed circuit conditions, acetic acid removal percentages returned to values that were similar to closed circuit conditions after 24 and 48 h. Net acetic acid removal, taking the difference between the closed circuit and open circuit removal rates, was largest for ROBOAP at 2.93 ± 0.0004 g/L-day. Acetate was therefore rapidly consumed. This supports the idea that fermentation is limiting for complex feedstocks [14], generalizing this finding to other types of complex feedstocks.

As mentioned in the introduction, acetic acid is not the only intermediate product, even if it may be easily converted to electrons as is coveted in MECs. First, the correlation between average net acetate consumption and current density was also found to have an R^2 value of 0.79 However, R^2 decreased without the acetate-fed MEC data to a value of 0.61. While somewhat correlated, there are other compounds that are contributing directly to anode respiration. The other VFA tested was propionic acid, which accumulated more in open circuit conditions that the closed-circuit conditions. The largest accumulation rate for propionic acid was with MECs fed with ROBOAP, which accumulated propionic acid at a rate of 0.6 ± 0.14 g/L-day. Interestingly, CFP-fed MECs accumulated the least amount of propionic acid during open circuit conditions, reaching an accumulation rate of only 0.27 ± 0.012 g/L-day. This percent accumulation is proportionally large and represented more than a 400% increase in propionic acid accumulation from what was delivered. Comparing the total accumulation rates of both organic acids, and CFP accumulated the most organic acid at a combined rate of 1.95 g/L-day, while ROBOAP accumulated the least at 1.63 g/L-day. Because CFP-fed MECs performed better than ROBOAP-fed MECs, other carbon sources in the substrate must have been channeled directly to exoelectrogenesis or other intermediates contributed to exoelectrogenesis that are not quantified here. Accumulation percentages of some compounds not traditionally considered substrates for exoelectrogens, such as catechol and phenol, were also observed at larger accumulation percentages during open circuit conditions than closed circuit conditions when fed with CFP. However, as discussed earlier in this study, the quantities of these compounds delivered were small enough that they likely did not contribute to current as prominently as acetic acid or other compounds not determined here. Here, it is unlikely that exoelectrogens were the only microbes that consumed lactic acid, as CFP-fed reactors (the only substrate where lactic acid was detected)

did not accumulate lactic acid when operated in open circuit conditions. Fermenters, representing a much larger taxonomy, metabolize even more compounds. Microbial flexibility is supported by the 16S data shown earlier. The replicates showed similar performance across substrates despite the differences in community structure. Thus, the microbes present may have exhibited different roles as the substrates were changed.

Although acetate is not the only intermediate product, it is clearly an important one. Batch addition of phenol in phe/ace-fed MECs reduced the acetic acid removal rate to 1.3 ± 0.98 g/L-day, down from 4.2 ± 0.48 g/-day that was observed when no batch of phenol was added. The phenol that was added was removed rapidly from the MEC, averaging a removal rate of 9.58 ± 0.3 g/L-day after 48 h. This represented a removal percentage of 53.8 ± 1.69%, which was lower than the non-batch added carbon source. The significant rates of removal did not correspond well to current, as the Coulombic efficiency was low as previously mentioned. This supports the idea that phenol is most likely adsorbing in these MECs more than it is being biochemically converted to current.

Acetic acid was also removed initially when fed to reactors in open circuit conditions for both phe/ace mixes and acetate-fed MECs. This implies that acetate was either transformed or other organics desorbed in the process. While phenol was a detected adsorbate, it is also possible that acetate adsorbed to MECs in open circuit conditions. Lee and Park determined adsorbance isotherm curves for acetate using activated charcoal [51]. Further, there may be some acetoclastic methanogenesis taking place, as methane was detected in acetate fed reactors (Figure 30) despite high cathode conversion efficiencies. However, to reiterate, acetoclastic methanogenesis were unlikely to be the dominant cause of methane production, as methane production was larger in

MECs fed with complex feedstocks than those fed pure acetate. A combination of mechanisms may therefore be taking place.

Principal Component Analysis (PCA) Loading Plot Results

PCA was carried out using the five most dominant microbe genera across all of the systems. These included: *Geobacter*, *Robinsoniella*, *Paludibacteraceae – unknown*, *Methanobrevibacter*, and *Desulfovibiro*. Key performance metrics were also included. The loading plot from PCA is shown in Figure 35(A) for all of the data collected.

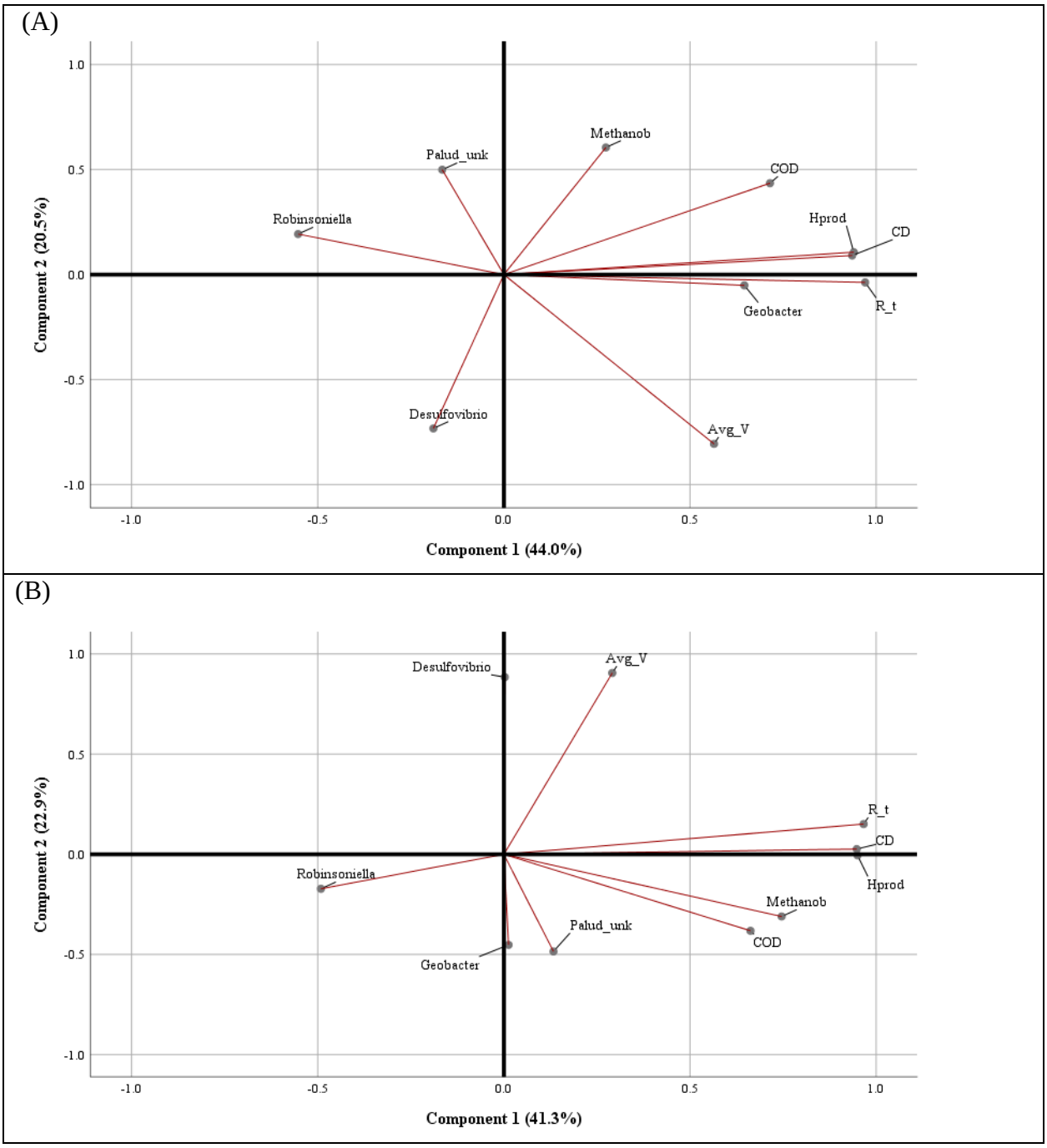

Figure 35: PCA loading plot with all data (A) and without replicate B - acetate-fed MECs (B). Variables used in the analysis include current density (CD), hydrogen productivity (Hprod), net acetate removal, R_t (R_t), average applied whole cell voltage (Avg_V), COD removal % (COD), and relative abundances of the following microbe genera: *Geobacter*, *Robinsoniella*, Paludibacteraceae – unknown (Palud_unk), *Methanobrevibacter* (Methanob), and *Desulfovibiro*.

As shown, *Geobacter* was the strongest correlated genus with the electrochemical performance metrics (current density, hydrogen productivity), which were otherwise tightly grouped when all of the data was included. *Geobacter*'s correlation was most likely skewed due to the high abundance in replicate B when fed with acetate. When the same analysis was performed without the data from replicate B – acetate-fed MECs (Figure 35(B)), the results were much different. Microbes and performance do not seem to be strongly correlated. *Robinsoniella* seemed to be negatively correlated to performance. Whether or not this means that *Robinsoniella* would be present only on poorly converted substrates is unknown. However, it may be fair to assume that some fermenters such as *Robinsoniella* are not as active as others that may contribute to faster conversion of organics to current or the MEC efficiency. Alternatively, there may be compounds present in complex substrates that are inherently recalcitrant that only *Robinsoniella* is capable of degrading. If MECs are fed with recalcitrant substrates, which may be the case since BOAP contains many such compounds like phenolics and furans [14, 28], microbes that poorly contribute to current or substrate degradation may be enriched.

Performance metrics including current density, net acetate removal rate, and hydrogen productivity were grouped closely together. By contrast, COD removal % and average voltage were not, as they appear to be anti-correlated to each other. This is surprising considering the organic loading rate was equal for all of the substrates used. As more COD was removed, current densities should increase, and average voltages should rise. This analysis shows that the relationships between community structure and substrate degradation are much more complex and require further investigations. Accumulation of various intermediates shown in this study indicate that the fermentation and exoelectrogenesis are not always in balance and are dynamic in nature. This could lead to the unexpected co-relations observed via PCA. Modeling of

fermentation, exoelectrogenesis, and the growth rate of the two class of organisms is required at a minimum to understand the dynamics.

Interestingly, *Methanobrevibacter* was associated with both components shown in both analyses, indicating that it had somewhat of a grouping with performance. This can be explained by product inhibition. Given the presence of dark fermenters, *Methanobrevibacter* may have assisted in accelerating higher order compound degradation, consuming accumulated hydrogen that might have otherwise caused product inhibition. Similarly, *Desulfovibrio* seems more strongly related to the second component than the first in both loading plots, which suggests that it is not correlated with MEC performance. This suggests that its presence was not necessary to achieve high performance but must be serving a different function, specifically related to conversion of ROBOAP.

The PCA results are not all encompassing, as the total variance represented by the plots is quite low, accounting for only 64.5% of the dataset's variance with all of the data (Figure 35(A)), and only 64.2% of the variance when the acetate-fed replicate B data was excluded (Figure 35(B)). As shown, when individual samples were pulled from the analysis, the loading plots changed dramatically. This analysis therefore does not define the relationships between variables as strongly as it would if the components represented more of the variance. This further supports the idea that community structure cannot be used to accurately predict performance. Using only duplicate MECs, the inferences made are limited. To further test this idea, additional sampling and MEC replicates may be used, which may reduce the observations in variance. More rigor would be required for more detailed exploratory statistics and to further support the findings here. While the performance did not correlate with community structure, the study clearly demonstrated the impact of feedstock on the microbial community.

Conclusions

MECs demonstrated here could convert a wide variety of substrates, including complex feedstocks, yielding high performance with fast adaptation time. The results suggest that MECs can rapidly transition from one complex feedstock to another without the need for new inoculation or mechanical disruption of the biofilm. 16S rRNA sequencing showed that community structure was also not correlated to performance, however, transitioning between substrates changed the communities. Differences were observed in the two replicates with respect to the community structure, indicating that specific composition of community is not necessary for any of the five substrates examined, to achieve a target high performance. Utilization of acetate could be correlated with performance, however, conversion of complex substrates in MECs was not found to be directly correlated with any specific compound. Fermentable compounds were removed by microbial action with or without dynamic coupling to exoelectrogenesis observed via variable accumulation of intermediates. Some compounds like phenol were observed to be adsorbed in MECs, leading to abiotic removal. PCA showed that electrochemical performance metrics of MECs were more tightly correlated across substrates than the community structure. Further understanding for the cause of the behavior will need to come from more rigorous ‘omics approaches, or by identifying additional key compounds of substrates that heavily influence MEC performance.

References

1. Pant, D.; Singh, A.; Van Bogaert, G.; Irving Olsen, S.; Singh Nigam, P.; Diels, L.; Vanbroekhoven, K., Bioelectrochemical systems (BES) for sustainable energy production and product recovery from organic wastes and industrial wastewaters. *RSC Adv.* **2012,** *2*, (4), 1248-1263.
2. Kadier, A.; Simayi, Y.; Kalil, M. S.; Abdeshahian, P.; Hamid, A. A., A review of the substrates used in microbial electrolysis cells (MECs) for producing sustainable and clean hydrogen gas. *Renewable Energy* **2014,** *71*, 466-472.
3. Chae, K.-J.; Choi, M.-J.; Lee, J.-W.; Kim, K.-Y.; Kim, I. S., Effect of different substrates on the performance, bacterial diversity, and bacterial viability in microbial fuel cells. *Bioresource Technology* **2009,** *100*, (14), 3518-3525.
4. Kiely, P. D.; Cusick, R.; Call, D. F.; Selembo, P. A.; Regan, J. M.; Logan, B. E., Anode microbial communities produced by changing from microbial fuel cell to microbial electrolysis cell operation using two different wastewaters. *Bioresource Technology* **2011,** *102*, (1), 388-394.
5. Kiely, P. D.; Rader, G.; Regan, J. M.; Logan, B. E., Long-term cathode performance and the microbial communities that develop in microbial fuel cells fed different fermentation endproducts. *Bioresource Technology* **2011,** *102*, (1), 361-366.
6. Sun, G.; Thygesen, A.; Meyer, A. S., Acetate is a superior substrate for microbial fuel cell initiation preceding bioethanol effluent utilization. *Applied Microbiology and Biotechnology* **2015,** *99*, (11), 4905-4915.
7. Ruiz, V.; Ilhan, Z. E.; Kang, D.-W.; Krajmalnik-Brown, R.; Buitrón, G., The source of inoculum plays a defining role in the development of MEC microbial consortia fed with acetic and propionic acid mixtures. *J Biotechnol* **2014,** *182-183*, 11-18.
8. Miceli, J. F.; Parameswaran, P.; Kang, D.-W.; Krajmalnik-Brown, R.; Torres, C. I., Enrichment and Analysis of Anode-Respiring Bacteria from Diverse Anaerobic Inocula. *Environmental Science & Technology* **2012,** *46*, (18), 10349-10355.
9. Kim, J. R.; Beecroft, N. J.; Varcoe, J. R.; Dinsdale, R. M.; Guwy, A. J.; Slade, R. C. T.; Thumser, A.; Avignone-Rossa, C.; Premier, G. C., Spatiotemporal development of the bacterial community in a tubular longitudinal microbial fuel cell. *Applied Microbiology and Biotechnology* **2011,** *90*, (3), 1179-1191.
10. Lesnik, K. L.; Liu, H., Predicting Microbial Fuel Cell Biofilm Communities and Bioreactor Performance using Artificial Neural Networks. *Environmental Science & Technology* **2017,** *51*, (18), 10881-10892.
11. Cai, W.; Lesnik, K. L.; Wade, M. J.; Heidrich, E. S.; Wang, Y.; Liu, H., Incorporating microbial community data with machine learning techniques to predict feed substrates in microbial fuel cells. *Biosensors and Bioelectronics* **2019,** *133*, 64-71.
12. Gadkari, S.; Gu, S.; Sadhukhan, J., Towards automated design of bioelectrochemical systems: A comprehensive review of mathematical models. *Chemical Engineering Journal* **2018,** *343*, 303-316.
13. Baumann, I.; Westermann, P., Microbial Production of Short Chain Fatty Acids from Lignocellulosic Biomass: Current Processes and Market. *Biomed Res Int* **2016,** *2016*, 8469357-8469357.

14. Lewis, A. J.; Campa, M. F.; Hazen, T. C.; Borole, A. P., Unravelling biocomplexity of electroactive biofilms for producing hydrogen from biomass. *Microb. Biotechnol.* **2018,** *11*, (1), 84-97.
15. Hari, A. R.; Katuri, K. P.; Gorron, E.; Logan, B. E.; Saikaly, P. E., Multiple paths of electron flow to current in microbial electrolysis cells fed with low and high concentrations of propionate. *Applied Microbiology and Biotechnology* **2016,** *100*, (13), 5999-6011.
16. Shao, Q.; Li, J.; Yang, S.; Sun, H., Effects of different substrates on microbial electrolysis cell (MEC) anodic membrane: biodiversity and hydrogen production performance. *Water Science and Technology* **2019,** *79*, (6), 1123-1133.
17. Zeng, X.; Borole, A. P.; Pavlostathis, S. G., Biotransformation of Furanic and Phenolic Compounds with Hydrogen Gas Production in a Microbial Electrolysis Cell. *Environmental Science & Technology* **2015,** *49*, (22), 13667-13675.
18. Zeng, X.; Borole, A. P.; Pavlostathis, S. G., Inhibitory Effect of Furanic and Phenolic Compounds on Exoelectrogenesis in a Microbial Electrolysis Cell Bioanode. *Environmental Science & Technology* **2016,** *50*, (20), 11357-11365.
19. Borole, A.; Reguera, G.; Ringeisen, B.; Wang, Z.-W.; Feng, Y.; Hong Kim, B., Electroactive biofilms: Current status and future research needs. *Energy & Environmental Science* **2011,** *4*, (12), 4813-4834.
20. Liu, W.; Wang, A.; Cheng, S.; Logan, B. E.; Yu, H.; Deng, Y.; Nostrand, J. D. V.; Wu, L.; He, Z.; Zhou, J., Geochip-Based Functional Gene Analysis of Anodophilic Communities in Microbial Electrolysis Cells under Different Operational Modes. *Environmental Science & Technology* **2010,** *44*, (19), 7729-7735.
21. Nam, J.-Y.; Tokash, J. C.; Logan, B. E., Comparison of microbial electrolysis cells operated with added voltage or by setting the anode potential. *International Journal of Hydrogen Energy* **2011,** *36*, (17), 10550-10556.
22. Hari, A. R.; Katuri, K. P.; Logan, B. E.; Saikaly, P. E., Set anode potentials affect the electron fluxes and microbial community structure in propionate-fed microbial electrolysis cells. *Scientific reports* **2016,** *6*, 38690-38690.
23. Lewis, A. J.; Borole, A. P., Understanding the impact of flow rate and recycle on the conversion of a complex biorefinery stream using a flow-through microbial electrolysis cell. *Biochemical Engineering Journal* **2016,** *116*, (Supplement C), 95-104.
24. Cheng, S.; Liu, H.; Logan, B. E., Increased Power Generation in a Continuous Flow MFC with Advective Flow through the Porous Anode and Reduced Electrode Spacing. *Environmental Science & Technology* **2006,** *40*, (7), 2426-2432.
25. Borole, A. P.; Hamilton, C. Y.; Vishnivetskaya, T. A.; Leak, D.; Andras, C.; Morrell-Falvey, J.; Keller, M.; Davison, B., Integrating engineering design improvements with exoelectrogen enrichment process to increase power output from microbial fuel cells. *Journal of Power Sources* **2009,** *191*, (2), 520-527.
26. Satinover, S. J.; Schell, D.; Borole, A. P., Achieving high hydrogen productivities of 20 L/L-day via microbial electrolysis of corn stover fermentation products. *Applied Energy* **2020**, 114126.
27. Wolin, E. A.; Wolin, M. J.; Wolfe, R. S., Formation of Methane by Bacterial Extracts. *Journal of Biological Chemistry* **1963,** *238*, (8), 2882-2886.

28. Lewis, A. J.; Ren, S.; Ye, X.; Kim, P.; Labbe, N.; Borole, A. P., Hydrogen production from switchgrass via an integrated pyrolysis–microbial electrolysis process. *Bioresource Technology* **2015,** *195*, 231-241.
29. Pollard, A. S.; Rover, M. R.; Brown, R. C., Characterization of bio-oil recovered as stage fractions with unique chemical and physical properties. *Journal of Analytical and Applied Pyrolysis* **2012,** *93*, 129-138.
30. Pannell, T. C.; Goud, R. K.; Schell, D. J.; Borole, A. P., Effect of fed-batch vs. continuous mode of operation on microbial fuel cell performance treating biorefinery wastewater. *Biochemical Engineering Journal* **2016,** *116*, 85-94.
31. Borole, A. P.; Hamilton, C. Y.; Schell, D., Conversion of residual organics in corn stover-derived biorefinery stream to bioenergy via microbial fuel cells. *Environ Sci Technol.* **2013,** *47*, 642-8.
32. Satinover, S. J.; Elkasabi, Y.; Nuñez, A.; Rodriguez, M.; Borole, A. P., Microbial electrolysis using aqueous fractions derived from Tail-Gas Recycle Pyrolysis of willow and guayule. *Bioresource Technology* **2019,** *274*, 302-312.
33. Ritalahti, K. M.; Amos, B. K.; Sung, Y.; Wu, Q.; Koenigsberg, S. S.; Löffler, F. E., Quantitative PCR Targeting 16S rRNA and Reductive Dehalogenase Genes Simultaneously Monitors Multiple Dehalococcoides Strains. *Appl Environ Microbiol* **2006,** *72*, (4), 2765-2774.
34. Campa, M. F.; Techtmann, S. M.; Gibson, C. M.; Zhu, X.; Patterson, M.; Garcia de Matos Amaral, A.; Ulrich, N.; Campagna, S. R.; Grant, C. J.; Lamendella, R.; Hazen, T. C., Impacts of Glutaraldehyde on Microbial Community Structure and Degradation Potential in Streams Impacted by Hydraulic Fracturing. *Environmental Science & Technology* **2018,** *52*, (10), 5989-5999.
35. Harms, G.; Layton, A. C.; Dionisi, H. M.; Gregory, I. R.; Garrett, V. M.; Hawkins, S. A.; Robinson, K. G.; Sayler, G. S., Real-Time PCR Quantification of Nitrifying Bacteria in a Municipal Wastewater Treatment Plant. *Environmental Science & Technology* **2003,** *37*, (2), 343-351.
36. Bolyen, E.; Rideout, J. R.; Dillon, M. R.; Bokulich, N. A.; Abnet, C.; Al-Ghalith, G. A.; Alexander, H.; Alm, E. J.; Arumugam, M.; Asnicar, F.; Bai, Y.; Bisanz, J. E.; Bittinger, K.; Brejnrod, A.; Brislawn, C. J.; Brown, C. T.; Callahan, B. J.; Caraballo-Rodríguez, A. M.; Chase, J.; Cope, E.; Da Silva, R.; Dorrestein, P. C.; Douglas, G. M.; Durall, D. M.; Duvallet, C.; Edwardson, C. F.; Ernst, M.; Estaki, M.; Fouquier, J.; Gauglitz, J. M.; Gibson, D. L.; Gonzalez, A.; Gorlick, K.; Guo, J.; Hillmann, B.; Holmes, S.; Holste, H.; Huttenhower, C.; Huttley, G.; Janssen, S.; Jarmusch, A. K.; Jiang, L.; Kaehler, B.; Kang, K. B.; Keefe, C. R.; Keim, P.; Kelley, S. T.; Knights, D.; Koester, I.; Kosciolek, T.; Kreps, J.; Langille, M. G. I.; Lee, J.; Ley, R.; Liu, Y.-X.; Loftfield, E.; Lozupone, C.; Maher, M.; Marotz, C.; Martin, B. D.; McDonald, D.; McIver, L. J.; Melnik, A. V.; Metcalf, J. L.; Morgan, S. C.; Morton, J.; Naimey, A. T.; Navas-Molina, J. A.; Nothias, L. F.; Orchanian, S. B.; Pearson, T.; Peoples, S. L.; Petras, D.; Preuss, M. L.; Pruesse, E.; Rasmussen, L. B.; Rivers, A.; Robeson, I. I. M. S.; Rosenthal, P.; Segata, N.; Shaffer, M.; Shiffer, A.; Sinha, R.; Song, S. J.; Spear, J. R.; Swafford, A. D.; Thompson, L. R.; Torres, P. J.; Trinh, P.; Tripathi, A.; Turnbaugh, P. J.; Ul-Hasan, S.; van der Hooft, J. J. J.; Vargas, F.; Vázquez-Baeza, Y.; Vogtmann, E.; von Hippel, M.; Walters, W.; Wan, Y.; Wang, M.; Warren, J.; Weber, K. C.; Williamson, C. H. D.; Willis, A. D.; Xu, Z. Z.; Zaneveld, J. R.; Zhang, Y.; Zhu, Q.; Knight, R.; Caporaso, J. G., QIIME 2: Reproducible, interactive, scalable, and extensible microbiome data science. *PeerJ Preprints* **2018,** *6*, e27295v2.

37. Quast, C.; Pruesse, E.; Yilmaz, P.; Gerken, J.; Schweer, T.; Yarza, P.; Peplies, J.; Glöckner, F. O., The SILVA ribosomal RNA gene database project: improved data processing and web-based tools. *Nucleic Acids Research* **2012,** *41*, (D1), D590-D596.
38. Yilmaz, P.; Parfrey, L. W.; Yarza, P.; Gerken, J.; Pruesse, E.; Quast, C.; Schweer, T.; Peplies, J.; Ludwig, W.; Glöckner, F. O., The SILVA and "All-species Living Tree Project (LTP)" taxonomic frameworks. *Nucleic Acids Research* **2013,** *42*, (D1), D643-D648.
39. Glöckner, F. O.; Yilmaz, P.; Quast, C.; Gerken, J.; Beccati, A.; Ciuprina, A.; Bruns, G.; Yarza, P.; Peplies, J.; Westram, R.; Ludwig, W., 25 years of serving the community with ribosomal RNA gene reference databases and tools. *J Biotechnol* **2017,** *261*, 169-176.
40. Varga, E.; Klinke, H. B.; Réczey, K.; Thomsen, A. B., High solid simultaneous saccharification and fermentation of wet oxidized corn stover to ethanol. *Biotechnology and Bioengineering* **2004,** *88*, (5), 567-574.
41. Cao, G.; Ren, N.; Wang, A.; Lee, D.-J.; Guo, W.; Liu, B.; Feng, Y.; Zhao, Q., Acid hydrolysis of corn stover for biohydrogen production using Thermoanaerobacterium thermosaccharolyticum W16. *International Journal of Hydrogen Energy* **2009,** *34*, (17), 7182-7188.
42. He, Y.; Zhang, L.; Zhang, J.; Bao, J., Helically agitated mixing in dry dilute acid pretreatment enhances the bioconversion of corn stover into ethanol. *Biotechnology for Biofuels* **2014,** *7*, (1), 1.
43. Park, L. K.-E.; Satinover, S. J.; Yiacoumi, S.; Mayes, R. T.; Borole, A. P.; Tsouris, C., Electrosorption of organic acids from aqueous bio-oil and conversion into hydrogen via microbial electrolysis cells. *Renewable Energy* **2018,** *125*, 21-31.
44. Brooks, V.; Lewis, A. J.; Dulin, P.; Beegle, J. R.; Rodriguez, M.; Borole, A. P., Hydrogen production from pine-derived catalytic pyrolysis aqueous phase via microbial electrolysis. *Biomass and Bioenergy* **2018,** *119*, 1-9.
45. Freguia, S.; Rabaey, K.; Yuan, Z.; Keller, J., Electron and Carbon Balances in Microbial Fuel Cells Reveal Temporary Bacterial Storage Behavior During Electricity Generation. *Environmental Science & Technology* **2007,** *41*, (8), 2915-2921.
46. Dąbrowski, A.; Podkościelny, P.; Hubicki, Z.; Barczak, M., Adsorption of phenolic compounds by activated carbon—a critical review. *Chemosphere* **2005,** *58*, (8), 1049-1070.
47. Hejazi, F.; Ghoreyshi, A. A.; Rahimnejad, M., Simultaneous phenol removal and electricity generation using a hybrid granular activated carbon adsorption-biodegradation process in a batch recycled tubular microbial fuel cell. *Biomass and Bioenergy* **2019,** *129*, 105336.
48. Zhang, M.; Wang, Y.; Liang, P.; Zhao, X.; Liang, M.; Zhou, B., Combined photoelectrocatalytic microbial fuel cell (PEC-MFC) degradation of refractory organic pollutants and in-situ electricity utilization. *Chemosphere* **2019,** *214*, 669-678.
49. Luo, H.; Liu, G.; Zhang, R.; Jin, S., Phenol degradation in microbial fuel cells. *Chemical Engineering Journal* **2009,** *147*, (2), 259-264.
50. Moreno, L.; Nemati, M.; Predicala, B., Biodegradation of phenol in batch and continuous flow microbial fuel cells with rod and granular graphite electrodes. *Environmental Technology* **2018,** *39*, (2), 144-156.
51. Lee, S. C.; Park, S., Removal of furan and phenolic compounds from simulated biomass hydrolysates by batch adsorption and continuous fixed-bed column adsorption methods. *Bioresource Technology* **2016,** *216*, 661-668.

52. Zeng, X.; Borole, A. P.; Pavlostathis, S. G., Processes and electron flow in a microbial electrolysis cell bioanode fed with furanic and phenolic compounds. *Environmental Science and Pollution Research* **2018,** *25*, (36), 35981-35989.
53. Stratford, J. P.; Beecroft, N. J.; Slade, R. C. T.; Grüning, A.; Avignone-Rossa, C., Anodic microbial community diversity as a predictor of the power output of microbial fuel cells. *Bioresource Technology* **2014,** *156*, 84-91.
54. Cotta, M. A.; Whitehead, T. R.; Falsen, E.; Moore, E.; Lawson, P. A., Robinsoniella peoriensis gen. nov., sp. nov., isolated from a swine-manure storage pit and a human clinical source. *International Journal of Systematic and Evolutionary Microbiology* **2009,** *59*, (1), 150-155.
55. Ueki, A.; Akasaka, H.; Suzuki, D.; Ueki, K., Paludibacter propionicigenes gen. nov., sp. nov., a novel strictly anaerobic, Gram-negative, propionate-producing bacterium isolated from plant residue in irrigated rice-field soil in Japan. *International Journal of Systematic and Evolutionary Microbiology* **2006,** *56*, (1), 39-44.
56. Qiu, Y.-L.; Kuang, X.-Z.; Shi, X.-S.; Yuan, X.-Z.; Guo, R.-B., Paludibacter jiangxiensis sp. nov., a strictly anaerobic, propionate-producing bacterium isolated from rice paddy field. *Arch Microbiol* **2014,** *196*, (3), 149-155.
57. Miyazaki, M.; Sakai, S.; Ritalahti, K. M.; Saito, Y.; Yamanaka, Y.; Saito, Y.; Tame, A.; Uematsu, K.; Löffler, F. E.; Takai, K.; Imachi, H., Sphaerochaeta multiformis sp. nov., an anaerobic, psychrophilic bacterium isolated from subseafloor sediment, and emended description of the genus Sphaerochaeta. *International Journal of Systematic and Evolutionary Microbiology* **2014,** *64*, (12), 4147-4154.
58. Sun, G.; Kang, K.; Qiu, L.; Guo, X.; Zhu, M., Electrochemical performance and microbial community analysis in air cathode microbial fuel cells fuelled with pyroligneous liquor. *Bioelectrochemistry* **2019,** *126*, 12-19.
59. Wallace, R. J.; Chaudhary, L. C.; Miyagawa, E.; McKain, N.; Walker, N. D., Metabolic properties of Eubacterium pyruvativorans, a ruminal 'hyper-ammonia-producing' anaerobe with metabolic properties analogous to those of Clostridium kluyveri. *Microbiology* **2004,** *150*, (9), 2921-2930.
60. Wallace, R. J.; McKain, N.; McEwan, N. R.; Miyagawa, E.; Chaudhary, L. C.; King, T. P.; Walker, N. D.; Apajalahti, J. H. A.; Newbold, C. J., Eubacterium pyruvativorans sp. nov., a novel non-saccharolytic anaerobe from the rumen that ferments pyruvate and amino acids, forms caproate and utilizes acetate and propionate. *International Journal of Systematic and Evolutionary Microbiology* **2003,** *53*, (4), 965-970.
61. Eaktasang, N.; Kang, C. S.; Ryu, S. J.; Suma, Y.; Kim, H. S., Enhanced Current Production by Electroactive Biofilm of Sulfate-Reducing Bacteria in the Microbial Fuel Cell. *Environmental Engineering Research* **2013,** *18*, (4), 277-281.
62. Miller, T. L.; Wolin, M. J.; de Macario, E. C.; Macario, A. J., Isolation of Methanobrevibacter smithii from human feces. *Appl Environ Microbiol* **1982,** *43*, (1), 227-232.
63. Lang, K.; Schuldes, J.; Klingl, A.; Poehlein, A.; Daniel, R.; Brune, A., New Mode of Energy Metabolism in the Seventh Order of Methanogens as Revealed by Comparative Genome Analysis of "Candidatus Methanoplasma termitum". *Appl Environ Microbiol* **2015,** *81*, (4), 1338-1352.

Chapter VI Appendix

Table 18: Compound concentration as a percent of the COD of substrate. 4-hydrozybenzaldehyde (4HB) was not detected in any of the substrates.

	BOAP	**ROBOAP**	**CFP**
Acetic Acid	16.2%	24.8%	15.7%
Furfural	0.91%	2.0%	ND
5-hydroxymethylfurfural	0.31%	0.2%	0.10%
Vanillic Acid	ND	ND	0.013%
Catechol	0.85%	0.2%	0.009%
Phenol	0.33%	0.3%	0.035%
Propionic Acid	3.2%	3.7%	1.0%
4HB	ND	ND	ND
lactic acid	ND	ND	1.6%
total	21.8%	31.2%	18.5%

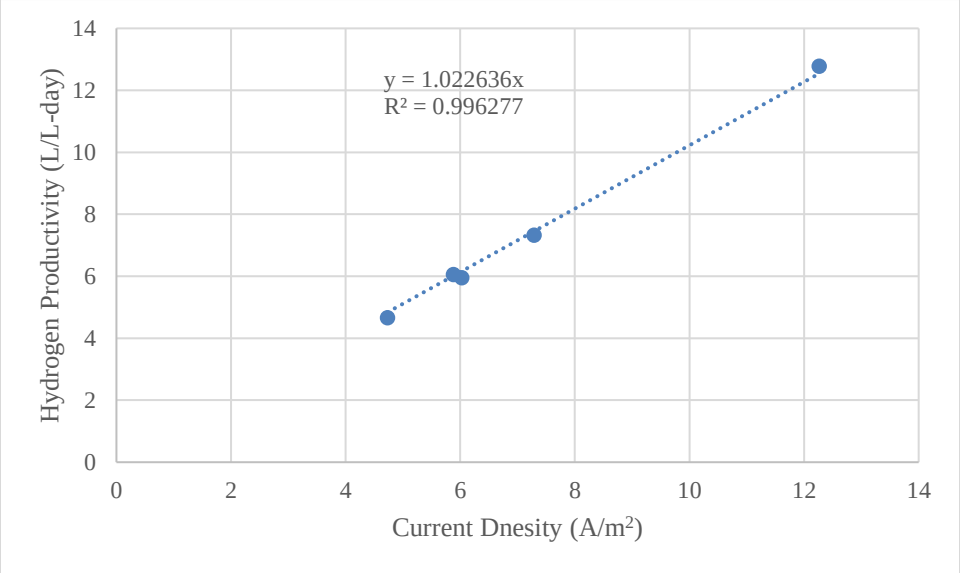

Figure 36: Correlation between current density and hydrogen productivity across all substrates tested.

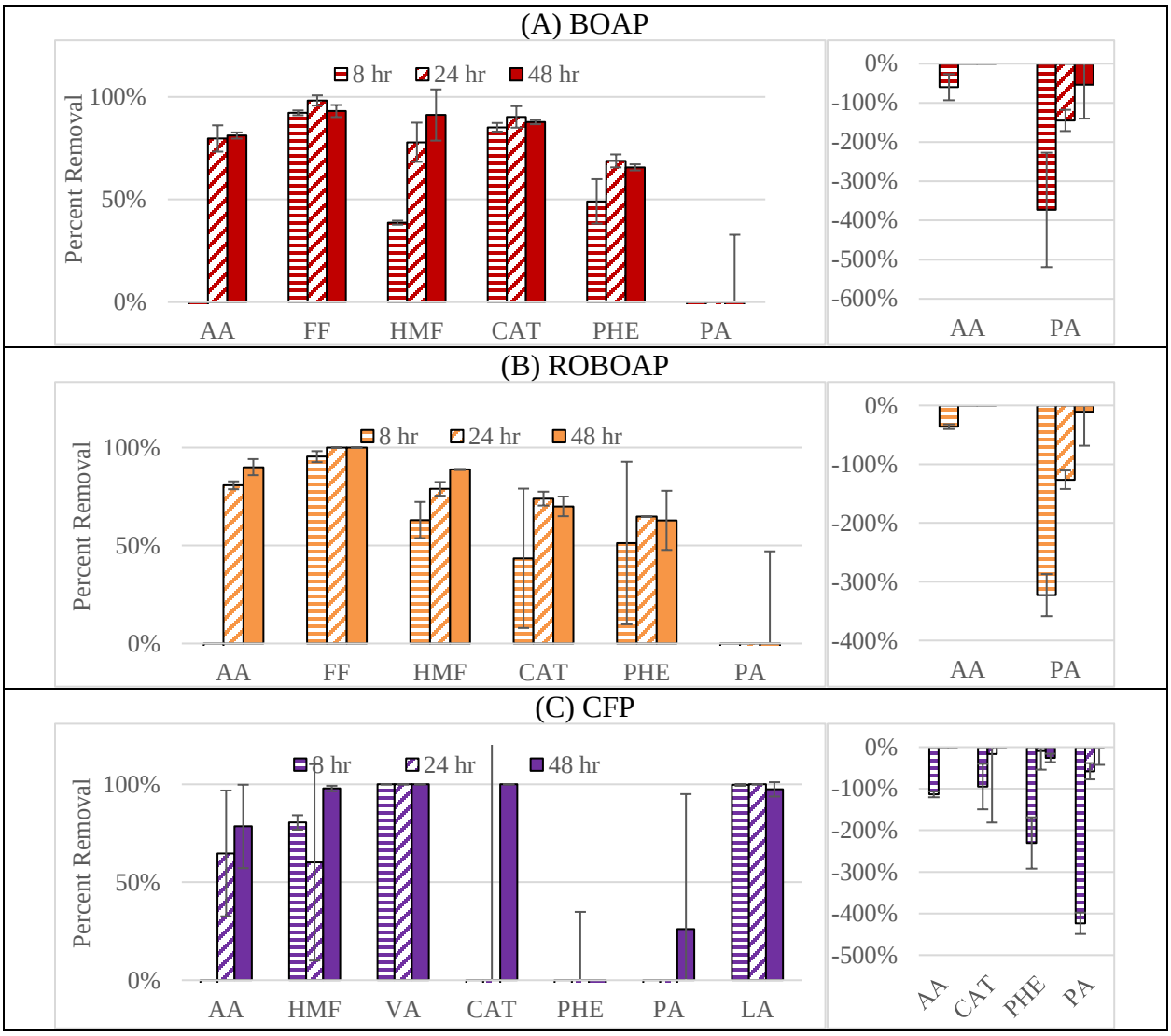

Figure 37: Compound removal of MECs fed 10 g/L-day of each substrate dur open circuit and closed circuit conditions. Substrates includes BOAP, Red Oak BOAP (ROBOAP), Corn stover fermentation product (CFP), equal fractions by COD of phenol and acetate (PHE/ACE) and acetate (ACE). Compounds include Acetic acid (AA), Furfural (FF), 5-hydroxymethylfurfural (HMF), Catechol (CAT), Phenol (PHE), Propionic Acid (PA), and Lactic Acid (LA).

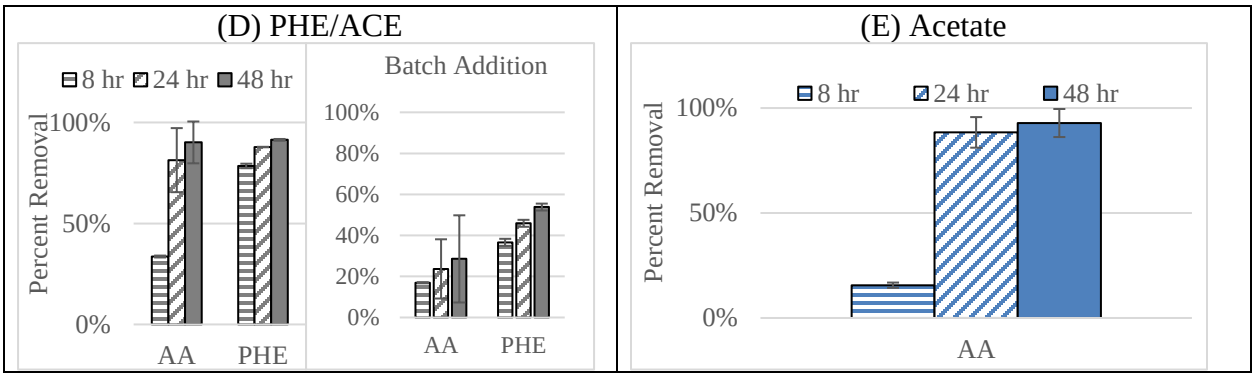

Figure 37 continued

Table 19: diversity indices calculated from rarified 16S rRNA data. Pearson correlation coefficients between diversity indices and current density were low (<0.5)

Replicate	Substrate	Chao1	Simpson	Shannon
A	**BOAP**	87.0	0.817	3.78
A	**ROBOAP**	79.0	0.889	4.14
A	**CFP**	71.0	0.915	4.61
A	**ACE_PHE**	91.8	0.914	4.25
A	**ACE**	102.4	0.899	4.37
B	**BOAP**	79.0	0.802	3.84
B	**ROBOAP**	87.7	0.906	4.16
B	**CFP**	112.4	0.889	4.23
B	**ACE_PHE**	87.0	0.913	4.38
B	**ACE**	44.0	0.383	1.58

CHAPTER VII

FINAL COMPARISONS ACROSS SUBSTRATES

The previous chapters discussed the findings from a set of electrochemical data using different substrates under similar operating conditions. Nine different substrates with unique chemical properties were tested on MECs. They showed individual discrepancies that resulted in differences in performance, which were discussed in detail in each chapter. The common elements between these substrates that correlate with device performance, as well as how MEC performance metrics relate to one another when an MEC is fed an arbitrary substrate, can only be understood by analyzing this data together. Principle Component Analysis (PCA) is a tool that can be used to find the correlations between variables in the dataset.

Principle Component Analysis for Continuously-Fed MECs

For this data set, results used in Chapter I are excluded, as the substrate used in that chapter was only fed to reactors via batch addition. Additionally, because the data from chapter V did not include voltage data, it could not be used for PCA. Otherwise, seven of the nine substrates were included at the organic loading conditions they were tested at. Lastly, the substrates used in Chapter III did not have phenol quantified. A previous report that investigated the composition of algal HTL aqueous effluents did not find phenol in either substrate [1]. When GC-MS was performed on the substrates in Chapter III, phenol was not detected in the effluent from *Chlorella* sp., but was detected in the effluent from *Tetraselmis* sp. The phenol concentration was therefore estimated using the response factor for pyridine observed in Chapter III, producing an estimated phenol concentration of 0.48 mg/L. The performance metrics analyzed included current density, hydrogen productivity, and average voltage. Other metrics included the substrate delivery rate of acetic acid, propionic acid, and phenol, as well as the COD removal % and organic loading rate.

PCA indicated that performance metrics were grouped together closely, suggesting that they were tightly correlated across any substate. Namely, if current density increased, a rise in hydrogen productivity and average voltage would occur regardless of substrate type. These trends are shown in Figure 38.

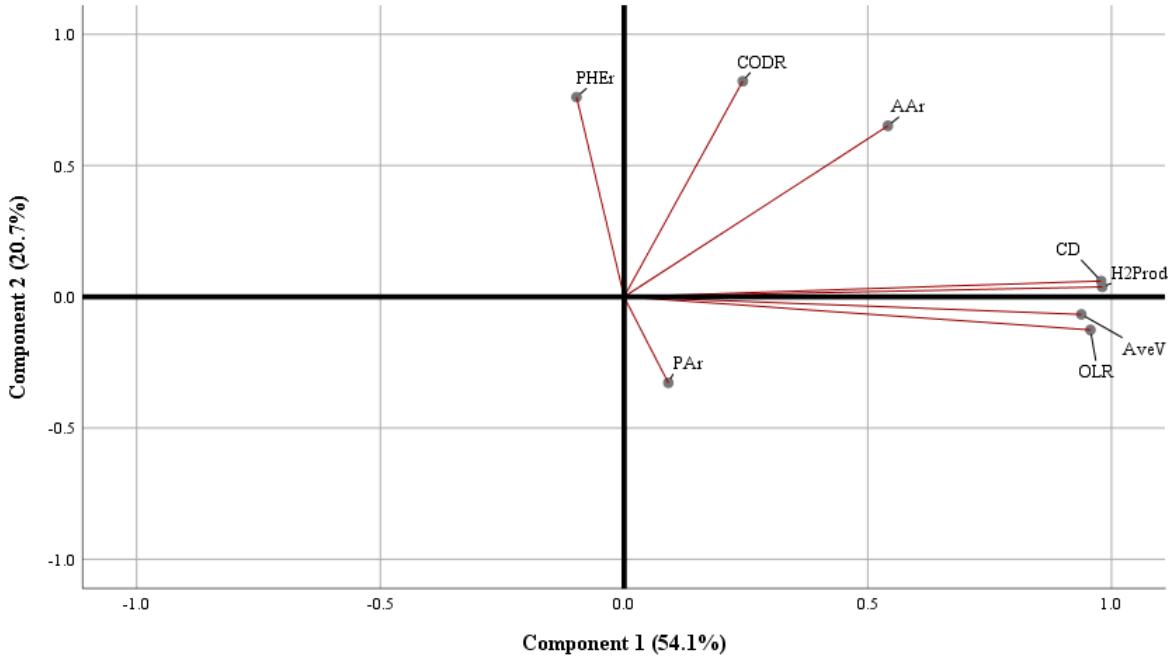

Figure 38: PCA loading plot of data set from continuously fed reactors. Variables included Propionic Acid Delivery Rate (PAr), Organic Loading Rate (OLR), Average Voltage (AveV), Hydrogen Productivity (H2Prod), Current Density (CD), Acetic Acid Delivery Rate (AAr), Phenol Delivery Rate (PHEr), and Chemical Oxygen Demand Removal Percentage (CODR).

The loading plot also shows tight grouping of performance metrics with organic loading rate. This is expected, as organic loading rate provides more carbon needed for more current production. Here, Organic loading rate represents the sole independent variable tested, while the chemical delivery rates (acetic acid, propionic acid, and phenol delivery rate) are quasi-independent, since they are controlled by organic loading rate but were also substrate dependent.

As shown in Figure 38, organic loading rate was strongly correlated with current density and hydrogen productivity for the continuous addition experiments. Therefore, this cause and effect relationship can be extended to arbitrary substrates used in these MECs. Additionally, because the cathode conversion efficiencies in the prior chapters were high at higher organic loading rates (above 75%), it is safe to assume that hydrogen productivity would have scaled with current density for any substrate as the organic loading rate increases. Organic loading therefore drives the variables in this grouping.

One might be tempted to assume that MECs have no limit on the maximum organic loading rate delivered and the hydrogen they produce as a result. However, this prediction may fall apart at higher organic loading rates than what was tested here. Brooks et al. showed that current density did not scale linearly with organic loading rate past 10 g/L-day when using a Pine wood-based pyrolysis aqueous product [2]. Further study at higher organic loading rates across the same substrates would confirm the strength of this correlation. The PCA plot also illuminates a limitation to the current design. Whole cell voltage, and the energy requirements needed to run the system, also increases as performance goes up across substrates. This idea was alluded to in Chapter IV, where mass transfer limitations were explored using a pulsed anode liquid media technique. While mass transfer limitations in two chamber designs are well established, the results here support the conclusion that higher organic loading rates may contribute to additional mass transfer limitations.

Interestingly, propionic acid delivery rate was inversely correlated to COD removal % and was only weakly correlated to performance. Propionic acid is degradable in MECs according to the findings in this dissertation and elsewhere [3, 4], but perhaps the community used here was simply ill-equipped to degrade propionic acid efficiently. Chapter VI showed accumulation of

this compound when MECs were fed 10 g/L-day. The loading plot therefore reflects these findings. The loading plot suggests that substrate composition may be useful for two roles. Either MEC operators may want to remove more total organics, or they may be more interested in recovering more energy. The application desired by the owner will be substrate dependent. However, in order to find the right substrates for the desired application, further comparisons between additional compounds and performance will need to be made.

Phenol delivery rate is somewhat correlated to COD removal but was not correlated to performance. Because of the adsorption observed in Chapter VI, the PCA loading plot supports the idea that phenol adsorption may be occurring for all of the substrates tested in this study. If not, phenol transformation is inefficient in substrates, as was also directly demonstrated in Chapter VI. Therefore, substrates rich in phenol may make for poor MEC substrates if the intent is to produce high volumes of hydrogen.

Principle Component Analysis for Batch-fed MECs

Performing the same analysis on the data from the batch fed experiments may provide additional insight. Unfortunately, several of the substrates were not fed to MECs in batch experiments, including the Red Oak BOAP, the CFP, or phenol acetate blend. Thus, the data set was not as comprehensive as the previous data. Unlike continuous experiments, which were all run for 72 h, batch experiments were operated on a variety of time scales ranging from 24 h to 72 h. To eliminate time an additional variable, only the first 24 h of each batch experiment data was used. The data still indicates some similar trends despite the difference in operational mode. Figure 39 shows the PCA loading plot for these experimental conditions and substrates.

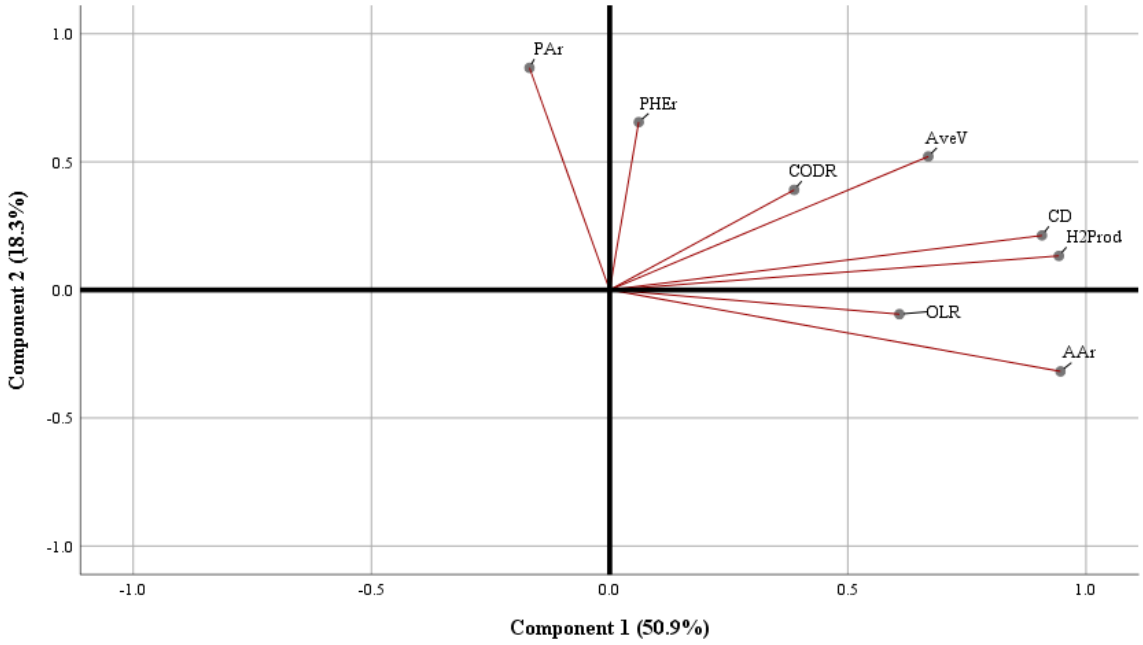

Figure 39: PCA loading plot of data set from batch fed reactors. Variables included Propionic Acid Delivery Rate (Par), Organic Loading Rate (OLR), Average Whole Cell Voltage (AveV), Hydrogen Productivity (H2Prod), Current Density (CD), Acetic Acid Delivery Rate (AAr), Phenol Delivery Rate (PHEr), and Chemical Oxygen Demand Removal Percentage (CODR).

Average voltage was not as closely correlated to the other performance variables (current density, hydrogen productivity, and organic loading rate) as it was in the continuously fed reactors. This may be affected by the data from the produced water experiments, which increased in salinity as the organic loading increased. Additional salinity would decrease ohmic losses in the MEC, which would affect the operating voltage beyond what can be described by the variables used in PCA. The other substrates changed conductivity of the anode liquid media negligibly. The other process problems observed in Chapter I, such as the formation of films and poor COD conversion, may also have influenced the correlations between the variables in ways that were not observed in the continuously fed reactors. These differences may explain why the

variance represented by the two components is slightly less for batch experiments than for continuous experiments.

The other trends observed with continuously fed reactors, such as the relationship between propionic acid feeding rate and phenolic feeding rate as they correspond with the second component also appears to be true for batch fed reactors. Propionic acid concentration may therefore be a good proxy for determining the capability of an MEC to degrade total organics in either feeding regime, and less of a proxy for determining potential performance. Phenol delivery also appears to be unrelated to performance for batch fed reactors as well, further supporting the notion that its removal does not effectively result in conversion. As established in Chapter VI, this mechanism may be primarily due to rapid adsorption without subsequent biochemical conversion.

The PCA shown here indicates that more of the variance can be accounted for by substrate composition and performance than when biological composition is included (See Chapter VI). Thus, it appears that substrate composition can be used to more accurately predict performance than community structure. These results depend on the community present in the MEC, even when using a fixed MEC design, even though community structure does not fully represent the microbial dynamics at work. The extent at which these relationships can be predicted across arbitrary MECs must be confirmed. Because of this, the PCA demonstrated here is conditional, but it may be useful for fully developed anode communities in MECs of the future.

References

1. Maddi, B.; Panisko, E.; Wietsma, T.; Lemmon, T.; Swita, M.; Albrecht, K.; Howe, D., Quantitative characterization of the aqueous fraction from hydrothermal liquefaction of algae. *Biomass and Bioenergy* **2016,** *93*, 122-130.
2. Brooks, V.; Lewis, A. J.; Dulin, P.; Beegle, J. R.; Rodriguez, M.; Borole, A. P., Hydrogen production from pine-derived catalytic pyrolysis aqueous phase via microbial electrolysis. *Biomass and Bioenergy* **2018,** *119*, 1-9.
3. Hari, A. R.; Venkidusamy, K.; Katuri, K. P.; Bagchi, S.; Saikaly, P. E., Temporal Microbial Community Dynamics in Microbial Electrolysis Cells – Influence of Acetate and Propionate Concentration. *Front Microbiol* **2017,** *8*, (1371).
4. Shao, Q.; Li, J.; Yang, S.; Sun, H., Effects of different substrates on microbial electrolysis cell (MEC) anodic membrane: biodiversity and hydrogen production performance. *Water Science and Technology* **2019,** *79*, (6), 1123-1133.

FINAL CONCLUSIONS

Hydrogen is a critical energy carrier and product that sees use in many industrial sectors today and may see even more use as part of the proposed hydrogen economy. This dissertation investigated the conversion of nine different substrates in MECs to hydrogen and investigated each of their properties and their effects on performance. Compound removal for up to nine compounds found in the substrates were investigated, along with the performance metrics current density, hydrogen productivity, and COD removal percentage. This was then coupled with a brief exploratory approach to the biology at work using these different substrates. The work in this dissertation then used the behavior observed with each substrate to identify key criteria, being either substrate composition or MEC behavior, and if those could be used to predict MEC properties.

Chapter Specific Conclusions

MECs were first shown to be able to shift easily between produced water and acetate, while simultaneously achieving the largest hydrogen productivity and Coulombic efficiency of any MEC fed with produced water to date. Coulombic efficiency at anode liquid media conductivities varying between 20-40 mS/cm was above 80% when fed with acetate, and was above 30% when fed with produced water. The highest Coulombic efficiency for produced water-fed MECs was 81.9 ± 10.4% at 40 mS/cm, which corresponded to a current density of 0.71 ± 0.02 A/m^2 After an acclimation period of one week, 16S rRNA sequencing showed that the community structure changed as a result of the shift towards the new different substrates tested. *Geobacter* dominated all of the samples tested, and the relative abundance of *Geobacter*

increased for most of the samples once the MECs were fed acetate. Alpha diversity was also smaller for acetate-fed MECs than produced water-fed MECs. The differences in community behavior and structure were largely attributed to the composition of the substrate, where produced water is much more complex and recalcitrant than acetate. Salt and organic loading did not have a noticeable effect on community structure. However, produced water also posed additional problems, namely precipitation, film adsorption, and high salinity. Na_2HPO_4 pretreatment alleviated the calcium-based precipitation but did not solve the additional problems. Produced water is therefore not an ideal substrate for this kind of MEC. New device architecture will need to be made in order to improve sustain waste treatment, however the results suggest that using the techniques to enrich a high-performance community and reactor can lead to improved performance on this substrate. The remaining substrates avoided these problems.

The difference between substrate composition and performance was further explored when two pyrolysis aqueous phase (PyAPs) from two different feedstocks were tested under identical organic loading rates. One aqueous phase was made from guayule and the other was from willow. The results showed that willow PyAP-fed MECs outperformed the guayule MECs under all of the organic loading conditions tested. The highest average current density was 5.0 ± 0.7 A/m^2 for willow fed MECs, and was 1.8 ± 0.2 A/m^2 for guayule PyAP-fed MECs. When the substrates were analyzed for compounds by High-Performance Liquid Chromatography, a larger fraction of the COD in willow PyAP was represented by acetic acid (31.0%) than what was found in the guayule PyAP (2.98%). COD removal percentage was also higher for willow PyAP-fed MECs than for guayule-fed MECs under most conditions. These results implied that substrate composition is an important metric towards achieving performance, and that composition can have a marked effect on performance despite using a previously demonstrated

high performing inoculum. Substrates that are composed of more MEC ideal compounds, such as organic acids and sugars, should degrade more easily. Guayule PyAPs contained only 9.4% of the compounds detected by HPLC, whereas 65.0% of the COD was detected by HPLC for willow PyAP. However, not all of these compounds are easily degradable. More than 20% of the willow PyAP's COD was represented by phenol. Chapter IV showed that phenol could adsorb in MECs. Thus, it is possible that the phenol removal observed in this study corresponded to more adsorption than to biochemical conversion to electrons.

The next study expanded on these comparisons with complex substrates using another untested waste product, this time from hydrothermal liquefaction (HTL). The HTL aqueous phase (HAP) was taken from an HTL process that had been used on two algae strains. The two HAPs were from *Chlorella* sp. and *Tetraselmis* sp. (HAP-C and HAP-C respectively). HAP-C fed MECs outperformed HAP-T-fed MECs. The average current density was greatest at 10 g/L-day, and was 5.1 ± 0.19 A/m^2 for HAP-C fed MECs and was 3.8 ± 0.20 A/m^2. Hydrogen productivity corresponded to current density, and was 5.1 ± 0.05 L/L-day for HAP-C-fed MECs and was 3.7 ± 0.20 L/L-day for HAP-T-fed MECs. At 2 g/L-day, Coulombic efficiency for HAP-C exceeding 100%. The data suggested that HAP-C, which contained ammoniacal nitrogen, had some of the ammoniacal nitrogen oxidized during MEC operation. This created current without removing COD. Ammoniacal nitrogen was not thought to be inhibitory in the short term operation of MECs, as it was used in the anode liquid media for all of the other substrates tested as the nitrogen source. Rather, COD removal using both substrates was low, not exceeding 50% under any of the conditions tested. The most abundant organic compound detected was propionic acid, unlike the acetic acid observed in the other substrates. It is possible that the relative recalcitrance of the HAPs therefore caused the losses in current despite NH_3-N oxidation. NH_3-N

was also shown to separate from the anode to the cathode once delivered by the substrate at separation percentages that exceeded 30%. Additionally, proton transfer percentages exceeded when cathode buffer was omitted from the cathode. Thus, cathode buffers may not be necessary for efficient proton transfer or for efficient MEC operation.

Mass transfer proved to be adequate for these kinds of MECs and substrates, and it was suspected that recalcitrance proved to be the most critical factor for MEC performance. Thus, the next set of experiments fed a less recalcitrant feedstock derived from corn stover fermentation product (CFP) to MECs in order to reach higher hydrogen productivities. CFP was fed to MECs at an organic loading rate from 2 to 30 g/L-day. This resulted in the highest current density observed across all of the substrates tested, reaching a current density of 17.9 ± 1.58 A/m^2 and a hydrogen productivity of 20.1 ± 2.06 L/L-day. However, mass transfer proved to have an increased effect at these organic loading rates, as the whole cell voltage climbed to 1.41 ± 0.17 V and the electrical efficiency was lowest at these organic loading conditions at 115.3 ± 12.2%. A strategy to alleviate mass transfer was also established by pulsing anode liquid meda flow, which showed to be most effective at the lowest steady state flow rates. New designs that can overcome mass transfer will be required, however the anode community appears capable of high productivities if the substrate allows it.

Looking at the results of the substrates tested, including the additional ones demonstrated in Chapter V, the community used in these MECs appeared to adapt to multiple substrates in rapid succession. It was believed that the community was largely responsible for this adaptation to such different substrates. However, the changes in community structure, and correlations between community structure, substrate composition, and performance, had not been established. The next study in Chapter VI investigated the relationship between those concepts using five

substrates, a switch grass bio-oil aqueous phase, a red oak bio-oil aqueous phase demonstrated in Chapter V, the corn stover fermentation product demonstrated in Chapter IV, a blend of phenol and acetate, and acetate. Volatile Fatty Acids are common degradation products, and acetate is often a model substrate in MECs. For this reason, acetate accumulation and degradation was predicted to be one of the most integral compounds related to performance. Rapid adaptation proved to occur here, as 1-week adaptation periods allowed MECs to reaching or exceed the performances observed in the prior studies of this dissertation. Net acetate removal, a metric calculated by taking the difference between the degradation rate and the accumulation rate of acetic acid, was calculated across the five substrates tested. Red Oak bio-oil aqueous phase was found to have the largest net acetate removal rate at rate of 2.9 ± 0.00 g/L-day. When MECs were fed the corn stover fermentation product discussed in Chapter IV, it resulted in the best performance of the MECs fed complex feedstocks tested despite a lower net acetate removal rate. Acetate was therefore considered an important intermediate towards current generation, but was not the only compound that converted directly to electrons in complex feedstocks. Tracking all of those compounds would be an added challenge, however identifying critical compounds commonly found in waste products, such as organic acids, may still add value for identifying worthy complex feedstocks for use in MECs.

Combining the data from the previous chapters, correlations between performance metrics and substrate composition was conducted using principal component analysis (PCA). PCA showed that continuously fed reactors could be correlated with two components within a high percentage of variance (62.5% for component 1 and 21.5% for component 2). Performance metrics, including hydrogen productivity, current density, and average voltage, were tightly grouped around the first component, however substrate composition more heavily influenced the

second component. Prominent compounds in the substrates were acetate, propionate, and phenol. Propionic acid, in particular, was found to be inversely correlated to COD removal, and phenol removal was found to be uncorrelated to performance metrics. The analysis suggests that substrate composition would be an important metric for not only performance, but also determining the capacity of MECs to effectively remove COD from an arbitrary substrate. This conclusion seems intuitive, however the prediction by the loading plot has additional value. It suggests that propionic acid and phenol could be used as a proxy for such a goal. This may be true for other compounds in complex as well. Further study would expand this analysis to other substrates with different dominant compounds than acetate, propionate, or phenol. Only then would such predictive capabilities be useful for a general class of substrates. However, the results here indicate that those relationships could exist if demonstrated in wider scope.

General Conclusions of Work

There are several main ideas that can be interpreted from this dissertation. MECs can be very robust and do not require long adaptation periods to new substrates if they have been demonstrated to effectively degrade complex substrates previously. HPLC analysis indicated sizeable fractions, often above 80% of the compounds delivered were removed from substrates. However, the pathways associated with compound degradation that is taking place must continue to be explored. Beyond compounds that contribute directly to exoelectrogenesis, adsorption properties of materials in MECs must be better characterized for complex feedstocks. Even with this in mind, there are certain performance markers, such as current density and hydrogen productivity, that are very tightly correlated regardless of the substrate used. The relationship between current density and hydrogen productivity scaled closely, and are therefore most likely

due to reactor design, and not biology. Shooting for one metric in high performance designs should therefore assure the other is reached if a high-performance reactor design is used. Performance may be accomplished at the expense of efficiency, as whole cell voltage was also shown to correlate somewhat to current density and hydrogen productivity. These performance outcomes are primarily driven by organic loading, while substrate composition plays an additional role. Select compounds in the substrate could be good indicators of the MEC's ability to convert substrates. However, the most impactful compounds may also be affected by materials used in the construction of MECs. On the biological scale, community composition is poorly predictive of performance on the taxonomical level. This implies that the community observed in these studies is malleable not just because it is composed of a diverse community, but also perhaps because the roles of the members are diverse. As a result, MEC biological dynamics while being fed complex feedstocks is not well explained by taxonomy. This does not mean that the roles of the community members are trivial either, only that there is a level of flexibility among the members in the community that is not explained by their presence alone. To understand the roles these community members play, identifying the genes that are expressed, as the MEC's microbes are consuming substrate, must be better understood as they are fed these complex substrates. For commercial applications, requiring this level of understanding before deploying an MEC is impractical. However, investigating MECs at this level of understanding may enable advancements in the technology that more accurately identify the roles of microbes present in MECs.

FUTURE WORK

There are several experiments that need to be conducted in order to more fully support the findings in this dissertation. More tests of the same nature on different substrates will certainly help advance the field. MECs fed additional wastes could also be added to the repository of data collected here to further strengthen the understanding and the correlations. Additionally, using different reactor configurations, and testing them with the same protocols used here, may also shed light on the validity of the findings here. The composition of the substrates may also play different roles on MEC behavior in different MECs, which will likely be influenced by starting anode inoculum. Deeper understanding of the compounds that are converted here will improve the technology. However, researchers will also need to be aware of overfitting to these predictions as well, as too much data and variables may result in erroneous predictions that converge poorly, adversely affecting future predictions.

Additional work would expand on the findings by verifying these findings under different operating conditions. Other process conditions that affect these MEC's behavior while fed multiple wastes will be needed. For instance, adjusting flow rate or applied anode potential while these feedstocks are fed to MECs could change community behavior in ways that were not observed at the consistent process conditions applied here. Finally, adsorption will need to be further explored for the complex feedstocks used. Using abiotic control MECs to track adsorption compared to biotic MECs should be sufficient.

EPILOGUE

SCIENCE COMMUNICATION AND OUTREACH: A PERSPECTIVE

In conjunction with my dissertation, I spent many hours firmly engaged in science communication and outreach initiatives. Much of this time was spent discussing the work in the dissertation as well as the work of others. I had always enjoyed talking about science, so it seemed like an obvious choice when I had to pick the knowledge breadth component of my PhD program. Even more appealing to me, science communication seemed starkly deficient in competent experts that were needed to give science the representation it deserved to the public. Science journalism, in particular, seemed rife with click-bait titles or complete misrepresentations of the findings. I believed this caused the rise in science denialism I'd observed while browsing the internet, either as free time or as a result of procrastinating (because we've all procrastinated, let's just best honest). As I identified this problem, I knew only a handful of PhDs that were well known for their content. Neil deGrasse Tyson, Adam Ruben and Joe Palca immediately came to mind, but otherwise there seemed to be a pretty big void between the people talking to the public about science and the people actually doing the science. I truly believed I would be a much-needed addition in a landscape where not enough of the right people were actively participating. Surely, if an actual scientist did the work that was otherwise done by non-experts, science would be better represented in media, and all the nonscientific opinions would be finally placed in obscurity. We would finally be trusted. This was clearly overly optimistic in hindsight. It feels dumb reading that now. Blinded by naiveté and motivated by the prospect, I started a column in the university newspaper *The Daily Beacon* called, "Ask a Scientist" that resulted in more than 30 publications where I was a primary author, and more that I helped supervise.

I'll preface by saying that my opinion was guided by a legitimate concern, not just my own anecdotes. Geoffrey Kabat recently wrote an article in EMBO Reports that urged scientists

to take this whole public-trust-with-science issue seriously [1]. Similarly, the book, "The Death of Expertise" suggested that public trust in expert opinion, such as with scientists, had dropped significantly within the last few decades [2]. To make matters even more grave, a study was released which found that new content made by scientists was becoming increasingly more difficult to read amongst their peers [3], not just to the public. However, denial of scientific expertise hasn't completely taken over, necessarily. The Pew Research Center published a report recently that suggested that the majority of Americans still trust and support the work of scientists, though the opinion on scientists' roles in informing government policy seems to be party dependent [4]. I was convinced that Americans had a significant science literacy and trust problem on their hands. The information provided by others was compelling at the time and stills stands true today. My column therefore attempted to solve a legitimate problem that I stand by as a worthy effort, even if the outcomes weren't always what I'd expected.

So how did my column do? Well, if you'd used my column as an indicator of trust in science, the commentary I received would paint a dark picture that, unfortunately, my work did little to fix. My most popular article represents a perfect example of this hostile landscape. The piece addressed the recent resurgence of the flat earth theory [5], which is the idea that the globe model is fraudulent. To flat earth believers, Earth's geometry is more representative of a flat disc, not a ball-like object whizzing through space around a star. The reason the globe model exists? The globe model was a conspiracy perpetrated by governmental agencies across the planet to prevent exploration and discovery of the earth's true physical form. This is all, of course, not true. Scientists virtually all agree that the earth is a spheroid. I painstakingly worked on the piece to make the scientific position on earth's shape accessible and nonconfrontational to as many people as possible. Despite my efforts, flat earth proponents emailed me and

commented on the column attacking my position, with none wavering in their opinions. Supporters of the scientific position I'd proposed, however, were quiet initially. Only after the first rush of anti-spheroid comments happened did my supporters issue their rebuttals. Both sides used my piece as an opportunity to insult one another and cast vitriol, far from civil dialog that might be considered persuasive. I found the reaction to my piece both amusing and alarming.

Through all my writing and participation with the column, I noticed some common behaviors from commenters that I saw with the flat earth piece. Science denialism, or skepticism on the scientific consensus, made appearances in the comments sections of other pieces, including GMOs [6], aluminum adjuvants in vaccines [7], calcium fluoride in water [8], and even the theory of relativity [9]. While I was not the primary author on all these pieces, I read through them quite carefully and worked to make them nonconfrontational. Despite my efforts, the content still instigated people with opposing views. The positive commentary I received that was much less frequent, and usually came from friends and acquaintances. However, there were a few occasions I received supportive emails from strangers, and that was rewarding.

The column served as a reminder that controversy sells, and perhaps the more important lesson, that the most vocal proponents of a position are often the most noticed, even if they don't represent the consensus. I believe American author Josh Billings said it best, "The squeaky wheel gets the grease." I imagine this is what exacerbates the perception we have on the mistrust with science media. A few outspoken detractors make aggressive statements, and suddenly they get more attention than the quiet agreeable readers that otherwise represent most content viewers. This also reinforced an idea known as the Pareto Principle, which has since been adopted into internet culture as "the 80/20 rule", but the concept is the same. Most of the activity is produced by the minority of participants. If the minority of the participants happen to have bad ideas, and

are inspired to say something, you'll hear more from them than others. I tell myself this, at least, because the other explanation is that the column was just not very good. Either explanation is possible, though I am inclined to believe that it's probably a combination of both. Other media outlets, including NPR's Joe's Big idea (now NPR Scicommers), have shared pieces in my column, so surely it couldn't have been too bad, even if it's not winning any Pulitzer prizes.

Regardless on if I wrote good material or not, the commentary I received showed that I'd failed at convincing detractors to accept mainstream scientific position. At the very least, I don't have any evidence that I persuaded anyone. This was frustrating, so I turned to help from an expert. When I spoke to Joe Palca at NPR last year about this problem, he made it very clear that such an effort was not worth it. He suggested that arguing with people with fringe positions actually did the actual science a disservice. By even discussing fringe ideas, I was detracting from the validity of actual scientific positions while entertaining nonscientific ones. Keep in mind, Joe Palca has been an active journalist for decades, working for the likes of NPR, Nature Publishing Group, and the American Association for the Advancement of Science. If there was ever an expert to listen to, he'd be one of them. Hearing him dismiss the possibility to fight and win against science denialism was hard, but it also firmly grounded me in the reality I'd been experiencing.

So is there really a science communication crisis? For the public, yes, if only because getting the best information into the right hands remains a challenge. Currently, there's a lot of science communication out there already that does a wonderful job being informative and entertaining, even without experts being the producers of the content. The people that support and enjoy this content do so largely without much of a stir, while the detractors are very vocal about their opposition. I believe they would be no matter who produced the content. Like all

science, there's no such thing as too much content, if it's accurate. I believe the limitation is, and always has been, accessibility. Any piece of media, small or large, may help make science more accessible, but how we make the most effective content remains an unopened question my work has yet to solve. If I've learned anything from my experiences, it's that ideal content hasn't been made yet for a very simple reason, one that is largely unsatisfying. It's difficult to make, and it isn't getting any easier.

But for me, I am not solely driven to science communication to combat science denialism. Or not anymore at least. There's more to good science communication than that. The most fun pieces to write weren't the ones that covered controversial topics. I wrote a piece about why beans caused flatulence for instance [10]. It's silly, and I don't know anyone that contests the premise either. If they do, they aren't nearly as enthusiastic about challenging it as others were for things like flat earth theory or GMOs. But while writing that piece, even though I knew I wouldn't be challenging anyone, I still enjoyed the process. The feedback I received was positive and uplifting. I believe there is still a void in expert-crafted science communication that I can fill without having to solve this much larger problem of science denialism. Competitions like Three Minute Thesis [11] and the Up-goer Five text challenge [12], of which I've participated in both [13, 14], have been made to share dissertation level work to a general audience, and the content isn't usually controversial. New materials, special microbes, medical devices, you name it, if it's a scientific topic, it fits into these formats. Clearly someone is paying attention. Afterall, these challenges wouldn't exist if people weren't interested. I plan to keep on participating in some shape or form. It just seems right. And who knows? Maybe one day I'll get really good at science communication. Maybe I'll even change some strongly held opinions. All I can do is try.

References

1. Kabat, G. C., Taking distrust of science seriously: To overcome public distrust in science, scientists need to stop pretending that there is a scientific consensus on controversial issues when there is not. *EMBO Rep* **2017,** *18*, (7), 1052-1055.
2. Nichols, T., *The Death of Expertise*. Oxford University Press: 2017.
3. The Readability Of Scientific Texts Is Decreasing Over Time | bioRxiv. **2017**.
4. Funk, C.; Hefferon, M.; Kennedy, B.; Johnson, C. *Trust and Mistrust in Americans' Views of Scientific Experts*; Pew Research Center: 2019.
5. Satinover, S.; Clark, E., Ask a Scientist: Is the Earth flat? *The Daily Beacon* **2017**.
6. Halsted, M.; Dulka, B., Ask a Scientist: What is a GMO? *The Daily Beacon* **2017**.
7. Cross, K., Ask a Scientist: Shouldn't we be worried about aluminum in vaccines? *The Daily Beacon* **2018**.
8. Satinover, S.; Dulka, B., Ask a Scientist: Is calcium fluoride a beneficial micromineral? **2017**.
9. Satinover, S.; Clark, E., Ask a Scientist: Why can't we travel at light speed? *The Daily Beacon* **2017**.
10. Satinover, S., Ask A Scientist: Why do beans make you fart? *The Daily Beacon* **2019**.
11. Three Minute Thesis. https://threeminutethesis.uq.edu.au/
12. Munroe, R. Up Goer Five. https://xkcd.com/1133/
13. Tennessee, U. o., 3MT Final Competition 2019. In 2019.
14. Satinover, S., Ask Scientists: The Up-Goer Five text challenge. *The Daily Beacon* **2019**.

VITA

Scott Satinover was born in Chicago, Illinois. He along with his twin brother were raised in Oak Park, Illinois. Upon graduating from Oak Park River Forest High School, Scott pursued a combined bachelor's and master's degree in mechanical engineering from the University of Colorado at Boulder. While at the University of Colorado, Scott was an active participant in student honor societies, academic research, and helping professors with courses as a teaching assistant. Upon graduation, Scott decided to work in industry. His first job after graduation was with Halliburton Energy Services. There, he was based in Hobbs, New Mexico, where he worked as a field engineer, more formally known as a technical professional, in hydraulic fracturing in the Permian Basin region. He worked for Halliburton for three years before returning to The University of Tennessee at Knoxville to pursue a PhD in Energy Science and Engineering.